

**NEUTROPHIL EXTRACELLULAR TRAPS IN
PRIMARY INFLUENZA PNEUMONIA
AND SECONDARY PNEUMOCOCCAL PNEUMONIA**

ANANDI NARAYANA MOORTHY

(M.Sc.)

**A THESIS SUBMITTED
FOR THE DEGREE OF DOCTOR OF PHILOSOPHY**

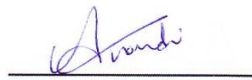
**DEPARTMENT OF MICROBIOLOGY
NATIONAL UNIVERSITY OF SINGAPORE**

2015

DECLARATION

I hereby declare that the thesis is my original work and it has been written by me in its entirety. I have duly acknowledged all the sources of information which have been used in the thesis.

This thesis has also not been submitted for any degree in any university previously.



Anandi Narayana Moorthy

6 December 2015

ACKNOWLEDGEMENTS

I wish to express my deepest gratitude to my supervisor, A./Prof. Vincent T.K. Chow, who gave me the opportunity to pursue my Ph.D. in his research laboratory. I am indebted to him for the constant guidance and encouragement throughout this period. I have learnt many things about research from him which would be immensely useful for me in the future. I thank him for entrusting me with this project and I hope that I have completed it to his satisfaction.

I wish to express my heart-felt thanks to Asst./Prof. Narasaraju, Oklahoma State University, for his constant encouragement and motivation during the course of my Ph.D. He helped me through discussions over the Skype and gave me insights into the areas of research work and manuscript writing. I appreciate his time and effort in helping me.

I am greatly thankful to A./Prof. Tan Kong Bing and Asst./Prof. Wang Shi, Dept. of Pathology, NUH, for helping me with the histopathology scoring and kindly teaching me how to do it. Many thanks for all your time and effort. I extend a special thanks to Prof. Tan for always being cheerful and ready to help.

I would also like to extend a special thanks to Asst./Prof. Zhang Yongliang and his staff, Hui Peng, for helping me with some of the qPCR and ELISA work. I wish to thank Hui Peng for his time and effort in doing these techniques for chapter 4 in this dissertation. I greatly appreciate Prof. Zhang's useful comments and suggestions during our meetings and his constant support and helpfulness.

I thank Prof. Hiroshi Watanabe, Kurume University and Prof. Andrew Camilli, Tufts University for providing the bacterial strains for experiments covered under chapter 4 in this dissertation.

I am greatly indebted to NUS and YLL School of Medicine for providing me with research scholarship and thereafter, tuition fee allowance which greatly reassured me during the final stressful period.

I would also like to thank a few people who helped me in some way or the other during this entire time - Fui Leng, Hooi Lin and Yamada (SMART-IDIRG) and the ever cheerful CRC confocal staff (NUS).

Prashant and Li Na, my colleagues from SMART, you people really helped me a lot with your time, effort and kind words. Thank you Prashant for working with me on the pneumococcal studies and good luck in your future endeavours. Thank you Li Na for always being eager to help, be it trouble shooting inconclusive data or thesis writing; good luck to you as well in your job and personal life.

I also would like to thank Mrs. Phoon and Kelly, Dept. of Microbiology for providing the virus stocks and laboratory materials. Mrs. Phoon, your presence always lights up the environment in the lab and many thanks for taking care of the details of lab safety. I would like to thank Dr. Perumal for the useful discussions.

No work can be successful without the presence of helpful colleagues. I thank all past and present HAPI/HGL lab members, especially the first set I met after joining Ph.D. – Jung Pu, Kai sen, Charlene, Fiona, Fabian, Edwin and Ivan

as well as Priscilla, Minxia and Waseem. You guys have made my life in lab very comfortable and happy throughout this journey. Kai Sen, Fabian and Edwin, thanks for teaching me animal handling and infection techniques.

Amita, Shadi, Priyanka, Madhu, Trini, Arrchana, Bipasha, Bijal & Vinod - thanks a lot for making my stay in Singapore very joyous and memorable. I will miss the fun times that we had together, the long chats in the canteen and in Utown and all that absolute craziness.

Priyanka, Madhavi, Jenny and Arun - thanks for sticking with me all these years and I sincerely wish that our friendship continues over many more decades to come.

No words can express my gratitude towards my family for the pain that they have gone through to make me reach where I am now. I am indebted to my mother for her constant prayers for my well-being, my father for his unwavering support, my brother for his affection and Lucky, who passed away a few days before I came to Singapore but still lives in our memories. I am really blessed to be a part of this family and would like to be so in every birth.

Finally, I offer my gratitude to the all-pervasive almighty for guiding me at every step, preventing me from going against my conscience by punishing me immediately whenever I do something wrong and helping me make my life choices, the full picture of which I shall see in the end.

LIST OF PUBLICATIONS

Narayana Moorthy, A., T. Narasaraju, P. Rai, R. Perumalsamy, K. B. Tan, S. Wang, B. Engelward and V.T. K. Chow. 2013. *In vivo* and *in vitro* studies on the roles of neutrophil extracellular traps during secondary pneumococcal pneumonia after primary pulmonary influenza infection. *Front. Immunol.* 4:56.

Narasaraju, T., E. Yang, R.P. Samy, K.S. Tan, **A.N. Moorthy**, M.C. Phoon, N. van Rooijen, H.W. Choi and V.T. Chow. 2014. Combination therapy with hepatocyte growth factor and oseltamivir confers enhanced protection against influenza viral pneumonia. *Curr Mol Med.* 14(5):690-702.

CONFERENCE PRESENTATIONS

Poster presentation titled “Formation of Neutrophil extracellular traps in murine lungs during secondary pneumococcal infection following influenza infection”. 12th Nagasaki-NUS joint symposium on infectious diseases, Singapore, June 2015.

Poster presentation titled “Understanding the role of lung micro-environment in neutrophil extracellular traps (NETs)-mediated lung injury during influenza

infection”. 9th Asia-pacific congress of Medical Virology, Adelaide, Australia, June 2012.

Oral presentation titled “Role of neutrophil extracellular traps in secondary pneumococcal pneumonia post-primary influenza infection”. Inaugural Microbiology Students' Symposium, Dept. of Microbiology, Yong Loo Lin School of Medicine, National University of Singapore, January 2013.

Poster presentations titled “Role of neutrophil extracellular traps in secondary pneumococcal pneumonia post-primary influenza infection”. Annual Graduate Scientific Congress, Yong Loo Lin School of Medicine, National University of Singapore, January 2015 and March 2013.

TABLE OF CONTENTS

Summary	XVII
List of figures	XX
List of tables	XXIV
List of abbreviations	XXV
Chapter One – Introduction and literature review	
1.1 INFLUENZA – A historical perspective	1
1.2 Types of Virus	2
1.3 Pandemics in the history of influenza	3
1.4 Therapy	7
1.5 Influenza A viruses	10
1.5.1 Types of influenza A Viruses	10
1.5.2 Influenza A Virus structure	10
1.5.3 Influenza A virus life cycle	12
1.6 Influenza pathophysiology	15
1.7 Secondary bacterial infections	16
1.8 Inflammation and cellular infiltration	17
1.9 Neutrophil	18
1.9.1 Neutrophil granules	18
1.9.2 Modes of bacterial killing by neutrophil	19
1.9.2.1 Phagocytosis	20
1.9.2.2 Extracellular killing of bacteria	21

1.10	Neutrophil extracellular traps	21
1.10.1	Components	21
1.10.2	Mechanism of NET formation	22
1.10.2.1	ROS are generally required for NETosis	23
1.10.2.2	NETosis is distinct from apoptosis and necrosis	23
1.10.2.3	Histone hypercitrullination mediates chromatin decondensation and NETosis	26
1.10.2.4	MPO and NE synergistically enhance chromatin decondensation	27
1.10.2.5	Other pathways involved in NETosis	28
1.10.3	Antimicrobial function of NETs	29
1.10.3.1	Bacterial infections	29
1.10.3.1.1	Secretion of nucleases	30
1.10.3.1.2	Expression of capsules	31
1.10.3.1.3	Inhibition/Repulsion of AMPs	31
1.10.3.2	Fungal and parasitic infections	32
1.10.3.3	Viral infections	34
1.10.4	NETs and tissue injury	36
1.10.5	Techniques for studying NETs	38
1.11	Aims and objectives	39

Chapter Two – Materials and methods

2.1 Propagation of influenza virus [Chapters 3-6]	41
2.2 Propagation of bacteria and fungi	41
2.2.1 <i>Streptococcus pneumoniae</i> [Chapters 3 and 4]	41
2.2.2 <i>Klebsiella pneumoniae</i> [Chapter 3]	42
2.2.3 <i>Candida albicans</i> [Chapter 3]	42
2.2.4 Estimation of CFU/ml in a culture sample [Chapters 3 and 4]	42
2.3 Bacterial assays	43
2.3.1 PCR amplification of <i>cps4D</i> gene to confirm deletion [Chapter 4]	43
2.3.2 FITC-Dextran exclusion assay to measure capsule thickness [Chapter 4]	44
2.3.3 DNase activity assay [Chapter 3]	45
2.4 <i>In vitro</i> assays using murine neutrophils	45
2.4.1 Isolation and purification of bone marrow-derived neutrophils [Chapters 3 and 4]	45
2.4.2 Stimulation of neutrophils to induce NETs [Chapters 3 and 4]	46
2.4.3 Visualisation of NETs and scoring [Chapters 3 and 4]	47
2.4.4 Effect of inhibition of redox enzymes on NETs [Chapter 3]	48

2.4.5 mRNA gene expression of bactericidal proteins during NETs generation [Chapter 3]	48
2.4.6 Estimation of bacterial entrapment by NETs [Chapter 3]	49
2.4.7 Antimicrobial activity assay using NETs generated during influenza infection [Chapter 3]	50
2.4.8 Surface killing assay [Chapter 4]	50
2.5 Animal experiments	51
2.5.1 Intratracheal instillation of pathogens [Chapters 3-6]	51
2.5.2 Harvesting and processing of tissues [Chapters 3-6]	52
2.5.3 Harvesting and processing of blood and bronchoalveolar lavage fluid [Chapters 3 and 4]	52
2.5.4 Homogenisation of frozen lung tissues for microbial load and other assays [Chapters 3-6]	52
2.5.4.1 Plaque assay [Chapters 5 and 6]	53
2.5.4.2 Amplex red hydrogen peroxide assay [Chapters 4-6]	54
2.5.4.3 Myeloperoxidase activity [Chapters 4-6]	54
2.5.4.4 Superoxide dismutase activity [Chapter 6]	55
2.5.4.5 Protein concentration [Chapters 3-6]	55
2.5.5 Extraction of RNA from lung tissues [Chapters 3 and 6]	55

2.5.6 Paraffin-embedding of tissues and Haematoxylin & Eosin staining [Chapters 3-6]	55
2.5.7 Immunohistochemistry of lung sections and NETs scoring [Chapters 3-5]	56
2.5.8 Analyses used for secondary pneumococcal study [Chapter 4]	57
2.5.8.1 RNA extraction and real-time PCR analyses	57
2.5.8.2 Enzyme-linked immunosorbant assay	58
2.5.9 Special diet course [Chapter 5]	59
2.5.9.1 Body weight and BMI	60
2.5.9.2 Food and calorie intake	60
2.5.9.3 Blood glucose level	60
2.5.9.4 Harvesting organs and tissues	60
2.6 Statistical analyses [Chapter 3-6]	61
2.7 Histopathology scoring systems	61
2.7.1 Comparison of influenza with secondary pneumococcal pneumonia [Chapter 3]	61
2.7.2 Comparison of different pneumococcal serotypes [Chapter 4]	62
2.7.3 Influenza infection [Chapters 5 and 6]	62

2.8 Buffer and media preparations	65
2.8.1 10x Tris-buffered saline	65
2.8.2 Overlay medium for plaque assay	65
2.8.3 1% crystal violet solution	65
2.8.4 1M Sodium phosphate buffer, pH 7.0	66
2.8.5 Haematoxylin and Eosin staining reagents	67
2.8.6. 10x Sodium Citrate Buffer, pH 6.0	68

Chapter Three – Secondary pneumococcal infection after influenza infection leads to higher generation of neutrophil extracellular traps in murine lungs

3.1 Background	69
3.1.1 Epidemiology	69
3.1.2 Pneumococcal respiratory infection and pneumonia	70
3.1.3 Secondary pneumococcal infection post-influenza infection.....	72
3.1.4 Treatment available	74
3.1.5 <i>Streptococcus pneumoniae</i> and NETs	75
3.2 Specific objectives of the study	77
3.3 Results and Discussion	78
3.3.1 Lethal synergism between primary influenza infection and secondary pneumococcal infection leads to increased bacterial persistence in lungs and higher lung pathology	78

3.3.2 Secondary bacterial infection with pneumococcus leads to enhanced NETs formation in the lungs	81
3.3.3 NETs induced <i>in vitro</i> representing primary influenza-secondary pneumococcal stimulation are influenced by redox enzymes	85
3.3.4 NETs are partially degraded in the presence of <i>S. pneumoniae</i>	89
3.3.5 NETs do not show any antibacterial activity but possess antifungal activity	90
3.4 Conclusion	94
Chapter Four – Capsule plays an important role in the variability amongst pneumococci in inducing neutrophil extracellular traps and lung pathology during murine pneumonia	
4.1 Background	98
4.1.1 Clinical prevalence of pneumococcal serotypes	98
4.1.2 Pneumococcal capsule biosynthesis	100
4.1.3 Capsule and pneumococcal virulence	103
4.1.4 Capsule and NETs	106
4.2 Specific objectives of the study.....	107
4.3 Results and discussion	108
4.3.1 Purified pneumococcal capsular polysaccharide induces NETs in a dose-dependent manner	108

4.3.2 Capsule thickness of pneumococci influences their susceptibility to neutrophil-mediated surface killing	109
4.3.3 Capsule thickness correlates with overall pathogenesis and pulmonary NETosis during primary pneumococcal pneumonia	113
4.3.4 Capsule thickness along with other virulence factors influences the virulence and NETs-inducing ability of <i>S. pneumoniae</i> during secondary lung infection following influenza infection	117
4.3.5 NETs induction in bone marrow-derived neutrophils by pneumococci does not reflect <i>in vivo</i> patterns of NETosis.....	129
4.4 Conclusion	132
Chapter Five – High fat diet-fed mice show a marginal increase in the formation of neutrophil extracellular traps in lungs in response to influenza infection	
5.1. Background	135
5.1.1 Epidemiology of obesity-impact of a high fat diet	135
5.1.2 Inflammation and oxidative stress during obesity	136
5.1.3 Obesity and neutrophils	137
5.1.4 Obesity and respiratory health	138
5.1.5 Obesity and influenza	139
5.2 Specific objectives of the study	141

5.3 Results and Discussion	142
5.3.1 Prolonged consumption of HFD leads to increased adiposity in mice	142
5.3.2 HFD and LFD mice show similar disease progression upon influenza A infection	145
5.3.3 HFD mice show marginal increase in NETs formation despite lower MPO activity.....	147
5.4 Conclusion	149
Chapter Six – Chemical inhibition of NADPH oxidase does not prevent influenza- induced lung injury in mice	
6.1 Background	152
6.1.1 Reactive oxygen species and oxidative stress	152
6.1.2 ROS from neutrophils and other phagocytes	152
6.1.3 ROS and tissue injury	155
6.1.4 Influenza-induced oxidative stress in lungs and antioxidant- based therapeutic approaches	157
6.1.5 Inhibitors of redox enzymes used in the study	159
6.2 Specific objectives of the study	160
6.3 Results and discussion	161
6.3.1 High cellular infiltration phase after influenza infection correlates with increased oxidative activities in the lungs	161

6.3.2 Mild improvement in the appearance of lung consolidation was observed with the inhibition of NADPH oxidase	164
6.3.3 Inhibition of NADPH oxidase by flavin-binding DPI does not improve lung pathology after lethal influenza challenge.....	166
6.3.4 Inhibition of NADPH oxidase does not improve lung pathology even with lower dose of influenza challenge	169
6.4 Conclusion	173
Chapter Seven – Concluding remarks and future scope	176
7.1 NETs and secondary pneumococcal pneumonia after influenza infection	177
7.2 High fat diet, NETs and influenza infection	181
7.3 Neutrophil NADPH oxidase and influenza-induced oxidative stress	182
7.4 Conclusion	184
Chapter Eight – Bibliography	
8.1 Journal references	187
8.2 Web references	211

SUMMARY

Neutrophils release chromatin fibres into the extracellular space upon activation by certain stimuli via an oxidative process. Structures known as neutrophil extracellular traps (NETs) are embedded with histones and other neutrophil granule proteins, and can entrap and kill a wide range of microorganisms. Since their discovery, NETs have been implicated in various conditions including severe influenza pneumonia where NETs are extensively induced in the lungs of mice infected with influenza A virus. Murine models were employed to analyse the extent of NETs formation (NETosis) during primary influenza pneumonia and secondary pneumococcal pneumonia. Compared to primary lethal influenza challenge, secondary pneumococcal infection induced greater NETosis in murine lungs. Although significantly higher in number, these NETs failed to curtail bacterial replication in the lungs. *In vitro* analyses revealed the inability of NETs (formed by stimulation with bronchoalveolar lavage fluid from influenza-infected mice) to kill *Streptococcus pneumoniae* even though significant bacterial entrapment dependent on multiplicity of infection was observed. Many degraded clusters of NETs were noticed in the lungs of dual-infected mice, which may be attributed to endonuclease generated by *S. pneumoniae*. NETs also lacked antibacterial activity against non-nuclease producing *Klebsiella pneumoniae*, thus alluding to other mechanisms of evasion such as bacterial capsule production. However, NETs exhibited significant anti-fungal activity against *Candida albicans*, thus retaining some anti-microbial

defence mechanisms. Further, the differences between certain serotypes of *S. pneumoniae* in generating NETs were compared in murine models of both primary and secondary pneumococcal pneumonia. Serotypes 19F, 3 and 4 were compared for their induction of NETosis and severity of pulmonary pathology. The role of capsule in the pathogenesis of NETosis was also evaluated using a capsule mutant of serotype 4. Clinically invasive strains (i.e. serotypes 3 and 4) possessed larger capsules and induced the most abundant NETs, lung pathology and inflammatory response compared to less invasive strain 19F. The serotype 4 capsule mutant failed to replicate in murine lungs, and generated significantly less NETs and lower pro-inflammatory cytokine response than its wild-type counterpart. These findings highlight the importance of NETs in the overall pathogenesis of influenza and pneumococcal pneumonia.

Obesity in humans confers greater susceptibility to influenza-related complications. Hence, the effect of adiposity on NETs formation in the lungs of influenza-infected mice was investigated. Mice were fed with high or low fat diets for 18 weeks, following which they were infected with a lethal challenge of influenza virus. NETs and viral titres were marginally enhanced in obese mice, thereby implicating adiposity and excessive dietary fat in influencing oxidative-inflammatory mechanisms such as NETosis during influenza pneumonia.

NETosis is an oxidative process, and NETs can inflict damage to surrounding tissues. The effects of chemical inhibition of NADPH oxidase on lung injury in influenza-infected mice were also studied. Diphenyleneiodonium chloride (DPI) inhibits reactive oxygen species (ROS) by acting on flavoenzymes.

DPI dissolved in 1% DMSO was administered either daily or on alternate days to mice challenged with low and high lethal doses of influenza virus, and their disease progression was monitored. Some reduction in the activity of redox enzymes such as myeloperoxidase and superoxide dismutase was observed with DPI treatment, but was not significant compared with the control group treated with 1% DMSO. The concentration of hydrogen peroxide was also similar between DPI and DMSO treatment groups which showed ROS reduction. For both treatment groups, there was no significant difference in body weight loss, survival patterns and lung histopathology of mice, suggesting that ROS reduction alone could not positively influence the outcome of influenza pneumonia.

The findings of these studies highlight the important contributions of NETs to host-pathogen interactions during the pathogenesis of influenza and pneumococcal pneumonia.

LIST OF FIGURES

Figure 1.1. Global occurrence of influenza positive cases as on 9 th July, 2015	9
Figure 1.2. The structure of an influenza A virus virion	11
Figure 1.3. Life cycle of influenza A virus	14
Figure 1.4. SEM micrographs showing DNA traps emerging out of stimulated neutrophils and NETs entrapping <i>Shigella flexneri</i>	22
Figure 1.5. Confocal microscopy images of neutrophils releasing NETs	24
Figure 1.6. Transmission electron micrographs of neutrophils undergoing apoptosis, necrosis and NETosis	25
Figure 1.7. Model of MPO and NE synergism during NETs formation	27
Figure 1.8. Haematoxylin and eosin stained-lung sections showing NETs present on day 10 post-infection in macrophage-depleted mice infected with influenza A virus	35
Figure 3.1. Complexity of combined viral/bacterial and post-influenza pneumonia	69
Figure 3.2. <i>S. pneumoniae</i> and virulence factors	71
Figure 3.3. Microbial replication in the lungs of dually infected mice	79
Figure 3.4. Histopathological analyses of lung sections	80
Figure 3.5. Immunofluorescence detection and quantification of NETs in the lungs of infected mice	84

Figure 3.6. Induction of NETs <i>ex vivo</i> mimicking primary influenza stimulation	87
Figure 3.7. Pneumococcal entrapment on NETs released during influenza stimulation	88
Figure 3.8. Partial degradation of NETs in the lungs of dually infected mice	90
Figure 3.9. Gene expression analyses of antibacterial proteins during NETs release	91
Figure 3.10. Microbicidal activity of NETs generated by influenza stimulation	93
Figure 4.1. World-wide type distribution of <i>S. pneumoniae</i> strains isolated from invasive clinical cases	99
Figure 4.2. Illustration of the Wzx/Wzy-dependent pathway for the biosynthesis of CPS 9A	101
Figure 4.3. Gene clusters and the repeat unit structures of the serotypes used in this study	105
Figure 4.4. Pneumococcal capsular polysaccharide induces NETs in a dose-dependent manner	109
Figure 4.5. Thicker capsule protects pneumococci from neutrophil-mediated surface killing	112
Figure 4.6. Primary infection with serotypes 19F, 3, 4 and 4cps4D-	114
Figure 4.7. NETs and neutrophil activity in lungs after primary pneumococcal infection	116
Figure 4.8. Secondary infection with serotypes 19F, 3, 4 and 4cps4D-	119

Figure 4.9. Histopathology and lung bacterial load after secondary infection	121
Figure 4.10. NETs and neutrophil activity in lungs after secondary pneumococcal infection	125
Figure 4.11 A. mRNA expression of pro-inflammatory cytokines and cytokine-regulatory proteins	128
Figure 4.11 B. Protein levels of pro- and anti-inflammatory cytokines	129
Figure 4.12. Induction of NETs <i>in vitro</i> using <i>S. pneumoniae</i> do not reflect the <i>in vivo</i> trend in primary and secondary infection model	131
Figure 5.1. Time course for mice on low and high fat diets	142
Figure 5.2. HFD mice show higher body weight gain and body mass index compared to LFD mice	143
Figure 5.3. HFD mice show increased adiposity compared to LFD mice	144
Figure 5.4. HFD and LFD mice show similar body weight loss patterns and histopathology upon influenza A infection	146
Figure 5.5. Marginal increase in ROS and decreased MPO activity in the lungs of infected HFD mice	148
Figure 5.6. Infected HFD mice have marginally higher NETs formation in the lungs	149
Figure 6.1. Assembly of NADPH complex upon activation	153
Figure 6.2. Generation of reactive oxygen-nitrogen species by activated neutrophils	154
Figure 6.3. Effects of ROS on host	156

Figure 6.4. Serial histopathology and redox mechanisms after lethal challenge with influenza A virus	163
Figure 6.5. Inhibition of NADPH oxidase, MPO and SOD in lungs of infected mice	165
Figure 6.6. DPI treatment of mice infected with 100 PFU influenza virus	167
Figure 6.7. Redox enzyme activities in the lungs after DPI treatment of lethally challenged mice	168
Figure 6.8. DPI treatment of mice infected with 20 PFU influenza virus	170
Figure 6.9. Viral titre and histopathology after DPI treatment of mice infected with low lethal dose of influenza virus	171
Figure 6.10. Redox enzyme activities in the lungs after low lethal challenge and DPI treatment	172
Figure 7.1. Schematic representation of NETs-Host-Pathogen interactions in influenza-pneumococcal pneumonia model	186

LIST OF TABLES

Table 1.1. Proteins encoded by various RNA segments of influenza A virus	12
Table 2.1. List of primers used for real time PCR	63
Table 3.1. Semi-quantitative scoring system for the evaluation of NETs in the lungs of infected mice	82
Table 3.2. Attributes and corresponding weightage used for NETs scoring	83
Table 5.1. Weights of different organs and fat pads of LFD and HFD mice after 18 weeks on diet	145

LIST OF ABBREVIATIONS

ABAH	4-amino benzoic acid hydrazide
ALI	Acute lung injury
AMPs	Antimicrobial peptides
ANA	Anti-nuclear antibodies
ANCA	Anti-neutrophil cytoplasmic antibodies
ARDS	Acute respiratory distress syndrome
ATCC	American Tissue Culture Collection
BALF	Bronchoalveolar lavage (BAL) fluid
BAT	Brown adipose tissue
BHI	Brain heart infusion
BMI	Body mass index
BPI	Bacterial permeability index
BSA	Bovine serum albumin
CaCl ₂	Calcium chloride
CAMPs	Cationic antimicrobial peptides
CAP	Community-acquired pneumonia
CFU	Colony forming units
Cps	Capsule
d.H ₂ O	Distilled water

DAD	Diffused alveolar damage
DAPI	4',6-diamidino-2-phenylindole
DEPC	Diethylpyrocarbonate
DETC	Diethyldithiocarbamate
DIO	Diet-induced obesity
DMSO	Dimethyl sulfoxide
dNTP	Deoxynucleotide triphosphates
DPI	Diphenyleneiodonium chloride
EDTA	Ethylenediaminetetraacetic acid
ELISA	Enzyme-linked immunosorbent assay
EMEM	Eagle's minimum essential medium
Eno	Enolase
ERK	Extracellular signal regulated kinases
FAD	Flavin adenine dinucleotide
FBS	Foetal bovine serum
FeLV	Feline leukemia virus
FITC	Fluorescein isothiocyanate
GalU	Glucose-1-phosphate uridyl transferase
GAS	Group A Streptococcus
Glc	Glucose
GlcUA	Glycosaminoglycan

gp91	Glycoprotein 91
GPx	Glutathione peroxidase
GTPase	Guanosine triphosphatases
H2B	Histone 2B
H ₂ O ₂	Hydrogen peroxide
H ₂ SO ₄	Sulphuric acid
HA	Haemagglutinin
HCl	Hydrochloric acid
HEF	Haemagglutinin-esterase fusion
HEPES	4-(2-hydroxyethyl)-1-piperazineethanesulfonic acid
HFD	High fat diet
HIV	Human immunodeficiency virus
HOCl	Hypochlorous acid
HPAI	High pathogenic avian influenza strains
Hyl	Hyaluronate lyase
ICAM-1	Intercellular adhesion molecule-1
IFN	Interferon
IL	Interleukin
IPD	Invasive pneumococcal disease
LB	Luria-Bertani or Lysogeny broth
LFD	Low fat diet

LPAI	Low pathogenic avian influenza strains
LPS	Lipopolysaccharide
LTA	Lipoteichoic acid
LytA	Autolysin A
M 1 and 2	Matrix proteins 1 and 2
MDCK	Madin-Darby canine kidney
MEM	Minimum essential medium
MgCl ₂	Magnesium chloride
MLD ₅₀	Mouse lethal dose
MMPs	Matrix metalloproteinases
MOI	Multiplicity of infection
MPO	Myeloperoxidase
NA	Neuraminidase
NaCl	Sodium Chloride
NADPH	Nicotinamide adenine dinucleotide phosphate
Ncf	Neutrophil cytosolic factor
NE	Neutrophil elastase
NEF	Nuclear export protein
NETs	Neutrophil extracellular traps
Nox2	Neutrophil oxidase
NP	Nucleoprotein

O.D.	Optical density
O ₂ ⁻	Superoxide
OPD	O-phenylenediamine dihydrochloride
p22phox	Phagocyte oxidase 22, Cytochrome b245-β
p40phox	Phagocyte oxidase 40, Ncf4
p47phox	Phagocyte oxidase 47, Ncf1
p67phox	Phagocyte oxidase 67, Ncf2
PA	RNA Polymerase subunit A
PAD	Peptidyl argininedeiminase
PAFr	Platelet-activating factor receptor
PAMPs	Pathogen associated-molecular patterns
PavA	Pneumococcal adhesion and virulence A
PB1 & PB2	RNA Polymerases subunit B1 and B2
PBS	Phosphate-buffered saline
PCR	Polymerase chain reaction
PCV	Pneumococcal conjugate vaccine
PFA	Paraformaldehyde
PFU	Plaque forming units
Pgm	Phosphoglucomutase
PiaA	Pneumococcal iron acquisition A
PiuA	Pneumococcal iron uptake A

PKC	Protein kinase C
Ply	Pneumolysin
PMA	Phorbol 12-myristate 13-acetate
PMN	Polymorphonuclear leukocytes
PPV	Pneumococcal polysaccharide vaccine
PR8	Influenza virus A/Puerto Rico/8/34, H1N1
PRRs	Pattern recognition receptors
PS	Polysaccharide, capsule
Psa A	Pneumococcal surface antigen A
Psp	Pneumococcal surface proteins
RA	Rheumatoid arthritis
Rac1 & Rac2	Rho GTPases 1 and 2
RANTES	Regulated on activation, normal T cell expressed and secreted
RNP	Ribonucleoprotein complex
RNS	Reactive nitrogen species
ROS	Reactive oxygen species
RPMI	Roswell park memorial institute
SDA	Sabouraud dextrose agar
SEM	Scanning electron microscopy
SLE	Systemic erythematous lupus
SOD	Superoxide dismutases

SP	<i>Streptococcus pneumoniae</i>
SP-D	Surfactant protein D
TBS	Tris-buffered saline
TIGR	The Institute for Genomic Research
TLR	Toll-like receptor
TNF- α	Tumour necrosis factor-alpha
TOD	Time of death
TPCK	Tosyl phenylalanyl chloromethyl ketone
Tregs	Regulatory T cells
UDP-Glc	Uridine diphosphate glucose
UDP-GlcUA	Uridine diphosphoglucuronic acid
vRNA	viral RNA
WAT	White adipose tissue
WHO	World Health Organization
XO	Xanthine oxidase

CHAPTER ONE

INTRODUCTION AND LITERATURE REVIEW

1.1 INFLUENZA – A historical perspective

Influenza, commonly known as ‘flu’, has been around for many centuries. The exact origin of influenza is very hard to trace given the similarity of its symptoms to many other diseases like dengue and typhoid fever. It has been speculated that influenza has zoonotic origins and it probably jumped species when humans started domesticating birds and animals (reviewed in (Hollenbeck, 2005)). The modern history of influenza begins around the early 20th century with the occurrence of the deadly ‘Spanish flu’ during the First World War which spearheaded the research in this area. In 1918, J.S. Koen, a veterinarian in the United States of America (U.S.A. or U.S.) first observed the occurrence of a similar disease in pigs; later believed to be the same as ‘Spanish flu’ (reviewed in (Hollenbeck, 2005)).

Influenza research took a giant leap in 1931 when Richard E. Shope successfully demonstrated the transmission of virus between swines by inoculating the mucous and lung filtrate of an infected swine into healthy swines that reproduced similar symptoms (Shope, 1931). Shope also isolated a bacterium, *Haemophilus influenzae suis*, from most of the cases and successfully demonstrated that injecting the virus and bacterium together results in a severe infection. This was the first ever demonstration of virus-bacterium co-operation in

a disease. Following Shope's methodology, Christopher H. Andrewes, Wilson Smith and Patrick Laidlaw first isolated the influenza virus from humans in 1933. The work, published in *The Lancet*, used the nasal washings of an influenza-infected researcher to demonstrate the occurrence of same symptoms in ferrets (Smith et al., 1933). These experiments clearly established the causative organism to be a virus. It overthrew the earlier belief that influenza is caused by a bacterium mostly assumed as 'Pfeiffer's bacillus'.

Later occurrences of influenza pandemics have been sporadic and less severe, most likely due to better awareness and technology. The most recent worldwide outbreak happened in 2009, also dubbed as 'Swine flu'. The virus was of the same lineage as the 'Spanish flu', however it had a lower mortality rate compared to the latter (reviewed in (Morens & Taubenberger, 2011; Palese, 2004)).

1.2 Types of Virus

Influenza viruses are RNA viruses belonging to three genera of the *Orthomyxoviridae* family (Centers for Disease Control and Prevention (CDC), Influenza¹). The three types differ in the composition of their nucleoproteins (NP) and matrix (M1) proteins. Influenza A and B viruses have 8 RNA segments and contain at least ten proteins whereas influenza C has 7 RNA segments and contains 9 proteins. Another prominent difference is found in the surface glycoproteins where types A and B have haemagglutinin (HA) and neuraminidase (NA) whereas type C has only haemagglutinin-esterase fusion (HEF) protein which has similar function to NA.

Influenza A viruses affect humans, mammals like pigs and horses; as well as birds. All the known influenza pandemics have been caused by this type. The virus is classified into various subtypes based on the HA and NA expressed on its surface. There are 18 known HAs and 11 known NAs (CDC, Influenza¹; Tong et al., 2013). The influenza viruses are named according to the virus type, the host of origin, geographical origin, strain number, year of isolation and for influenza A viruses, their HA and NA antigen description in in parentheses. The detail about the host is omitted for human strains, e.g. A/duck/Alberta/35/76 (H1N1) for duck origin and A/Puerto Rico (PR)/8/34 (H1N1) for human origin (CDC, Influenza¹).

Influenza B viruses are less common than A due to their limited host diversity. They infect humans and seals. Due to their limited host diversity and low mutation rate (Nobusawa & Sato, 2006), they are not successful in causing pandemics. Nevertheless, immunity to influenza B virus can decline over an extended period of time when the mutation eventually occurs and hence the strains are included in the trivalent and quadrivalent influenza vaccines (CDC, Influenza²).

Influenza C viruses are very uncommon among the three types but can cause epidemics in humans, pigs and dogs (reviewed in (Muraki & Hongo, 2010)).

1.3 Pandemics in the history of influenza

World Health Organization (WHO) describes influenza pandemics on the basis of a six-phase criterion (WHO guidelines, 2009, 2013^{3,4}). This includes phases 1-3 of predominantly animal infections which ranges from no known

human infection (phase 1) to known cases of infection in some humans (phase 2) and finally if the cases occur in small clusters within one region with no human-to-human transmission (phase 3). Phase 4 implies increased severity of the situation with human-to-human transmission being reported. The danger increases dramatically from here with phase 5 implying at least two countries from a single WHO region being affected by the same virus and phase 6 implies that the infection has spread to more than one continent and might be on its way to becoming a 'global outbreak'.

Throughout history, the virus has been linked to many outbreaks mostly occurring in waves (U.S. Department of Health & Human Services⁵). There are no precise data available to attribute influenza as a cause of outbreak prior to the 1500s; though some historians have speculated influenza to be the cause for many outbreaks since 875 CE (reviewed in ((Hollenbeck, 2005)). Scientists believe that at least two pandemics occurred near the 16th century between 1485 and 1580 (reviewed in (Morens & Taubenberger, 2011)). The latter pandemic was the first clearly documented pandemic; spreading from Europe to Asia Minor and northern Africa. The clinical signs that were taken into consideration were abrupt febrile onset, cough and general malaise for at least one week. This also corresponded with the European age of exploration that might have resulted in exporting strains of the virus to populations with no prior immunity.

The next two centuries saw the shift of pandemic origin from Europe to Asia. In the 18th century, three pandemics occurred from 1729-1730, 1732-1733 and 1781-1782 (reviewed in (Morens & Taubenberger, 2011)). It followed a 147 year

pandemic-free period with no known global spread. The pandemic in 1729 probably originated in China spreading towards the west through Russia. The 1781 pandemic was more dramatic and covered both eastern and western hemisphere. Most of the affected people were the elderly and pregnant women.

In the 19th century, two pandemics occurred from 1833-1836 and in 1889, both originating in Asia and spreading westwards (reviewed in (Morens & Taubenberger, 2011)). From 1889 onwards, incidents of outbreaks have been better documented.

The 20th century saw four pandemics with the first one occurring in 1918 being the deadliest influenza outbreak in human history (reviewed in (Morens & Taubenberger, 2011; Palese, 2004)). No clear origin has been demonstrated though the U.S.A., China or France are thought to be potential origins. The ‘Spanish flu’, caused by a highly virulent H1N1 strain, came in three waves during 1918, each time more severe than the previous ones. The unique aspect of the ‘Spanish flu’ was that it affected young adults (20-40 years) more compared to the elderly (reviewed in (Shanks & Brundage, 2012)). All other pandemics mostly affected very young children or older people. It is estimated that some 40-million deaths could be ascribed to the ‘Spanish flu’. The major cause of mortality has been attributed to a cytokine storm which ravaged the host system and to the onset of secondary bacterial infections (reviewed in (McAuley et al., 2015; Osterholm, 2005; Shanks & Brundage, 2012)).

The next pandemic occurred in 1957 originating from Hong Kong (reviewed in (Morens & Taubenberger, 2011; Palese, 2004)). Also known as the ‘Asian flu’, it was caused by the H2N2 strain of virus and spread across East Asia, the Indian subcontinent, the Middle East and eventually to Europe and the U.S.A. An estimated one to four million deaths occurred during this pandemic.

The 1968 ‘Hong Kong flu’ had comparatively lower morbidity and mortality (reviewed in (Morens & Taubenberger, 2011; Palese, 2004)). The causative strain arose due to an antigenic shift of the 1957 H2N2 virus. The new H3N2 virus differed only in the haemagglutinin and PB1 region while the neuraminidase was pretty well-conserved (Kawaoka et al., 1989). This may have provided some protection to those who were earlier exposed to the H2N2 strain. Nevertheless, it still caused about 750,000 deaths worldwide.

The last pandemic of the 20th century occurred during 1977-78 known as the ‘Russian flu’; though it was markedly milder. This strain was related to the H1N1 subtypes and mostly affected people born after 1950 (Greg et al., 1978). Scientists believe that people born before 1950 had protective immunity due to exposure to the earlier H1N1 strains (reviewed in (Palese, 2004)).

The most recent pandemic occurred in the 21st century. The 2009 ‘Swine flu’ pandemic saw the circulation of a new type of H1N1 strain that resulted from the combination of a previous triple reassortment of viruses from human, swine and avian lineages with the Eurasian pig influenza (Bastien et al., 2010). The disease was first detected in Mexico City in April 2009 and spread worldwide mostly

affecting Southeast Asia and Africa. An estimated 201,000 deaths occurred due to this strain. As of July 2015, variants of this strain continue to circulate around the world (Figure 1.1, WHO⁷). The unique feature of this pandemic is that it was evenly spread across all age groups unlike the previous pandemics which mostly affected the elderly (Dawood et al., 2012). During this pandemic, obesity emerged as an independent risk factor for influenza-related complications and mortality throwing light on the influence of underlying chronic metabolic conditions on the disease outcome (Louie et al., 2009).

1.4 Therapy

Treatment of influenza is usually provided by two classes of drugs – neuraminidase inhibitors namely oseltamivir, zanamivir and peramivir, that prevent release of viral progeny from the infected host cells and M2 ion channel inhibitors, adamantanes namely amantadine and rimantadine, that block proton transport into acidic endosomal compartments thereby preventing viral uncoating of ribonucleoprotein complex (CDC, Influenza⁶). However, widespread mutations at M2 amongst circulating human strains and the resulting drug resistance have reduced the reliability of adamantanes in the treatment of influenza (Bright et al., 2006).

Vaccinations are prescribed during seasonal influenza epidemics as well as during pandemics since they have been shown to reduce mortality during epidemics (Rothberg et al., 2008). Due to the high mutation rates of the virus, no vaccine is efficient for a prolonged period necessitating annual vaccinations

(CDC, Influenza²). As of 2015, the quadrivalent vaccine formulation contains antigens from two strains each from influenza A viruses - A/California/7/2009 (H1N1) pdm09-like virus & A/Switzerland/9715293/2013 (H3N2)-like virus; and influenza B viruses -B/Phuket/3073/2013-like virus (B/Yamagata lineage) & B/Brisbane/60/2008-like virus (B/Victoria lineage) (CDC, Influenza²).

**Percentage of respiratory specimens that tested positive for influenza
By influenza transmission zone**

Status as of 9 July 2015

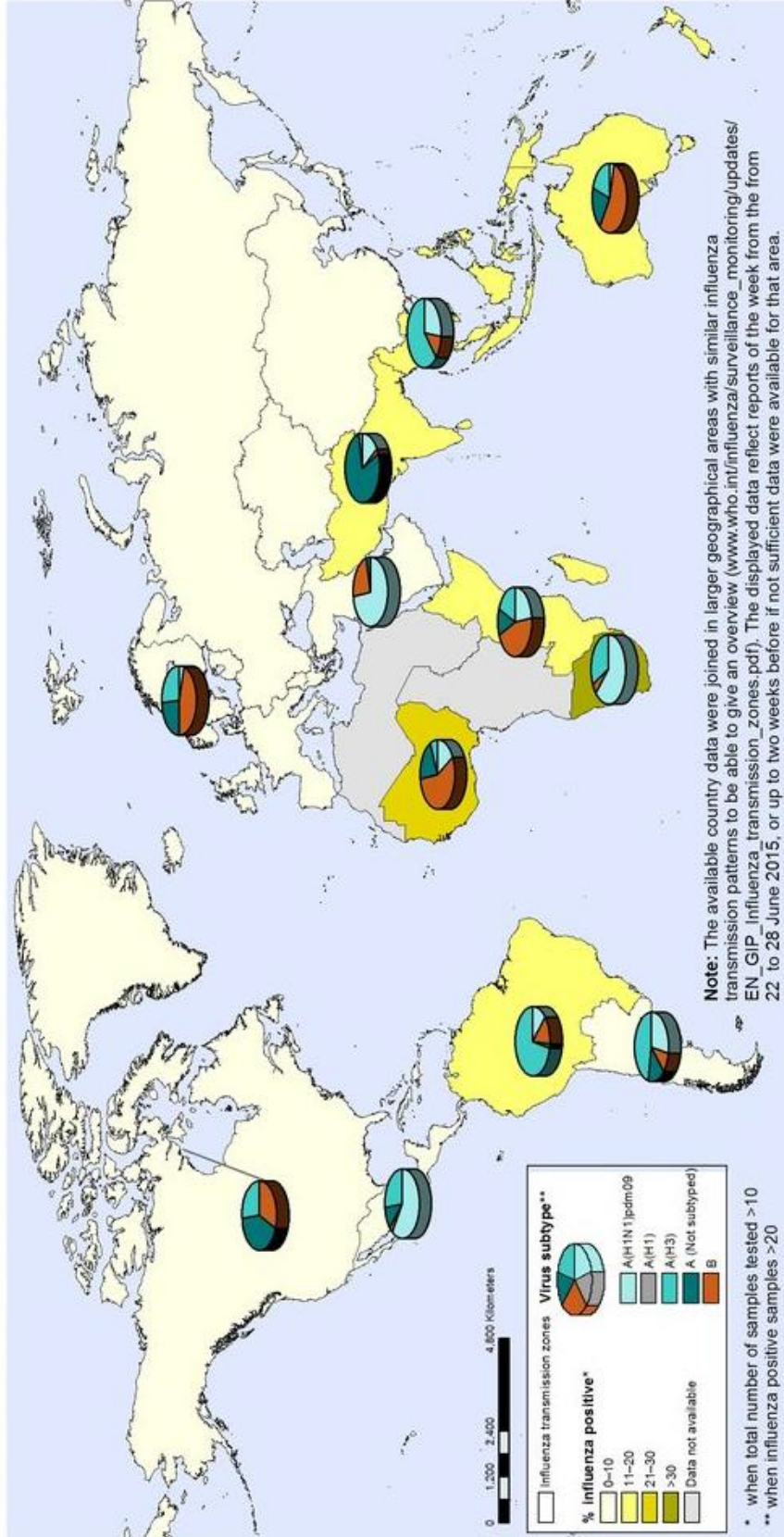


Figure 1.1. Global occurrence of influenza positive cases as on 9th July, 2015. Type A viruses of the H3N2 and H1N1pdm09 ('Swine flu') subtypes, as well as type B viruses, continue to circulate in humans. (Adapted from Global Influenza Surveillance and Response System, www.who.int/flu-net, World Health Organization July 2015⁷).

1.5 Influenza A viruses

1.5.1 Types of influenza A Viruses

Influenza A viruses are the frequent cause of epidemics in humans, birds (avian influenza), horse (equine influenza), pigs (swine influenza) and dogs (canine influenza). The avian influenza is further classified into low or high pathogenic avian influenza strains (LPAI or HPAI).

1.5.2 Influenza A Virus structure

Influenza A virions are mostly spherical and approximately 100 nm in diameter but occasionally may be found in filamentous forms too, although remaining compositionally similar. The virion comprises of a core surrounded by a lipid bilayer with glycoprotein spikes projecting from the surface (Figure 1.2). Haemagglutinin and neuraminidase are the two types of glycoprotein spikes that are found on the lipid membrane in varying ratios between strains. M2 ion channels traverse the lipid envelope and together with the HA, NA and the lipid envelope, it overlays M1 protein matrix that encloses the virion core. Inside the core is the ribonucleoprotein (RNP) complex, the nuclear export protein (NEF) and RNA-dependent RNA polymerases that comprises two basic subunits, PB1 and PB2, as well as one acidic subunit, PA. (Reviewed in (Bouvier & Palese, 2008)).

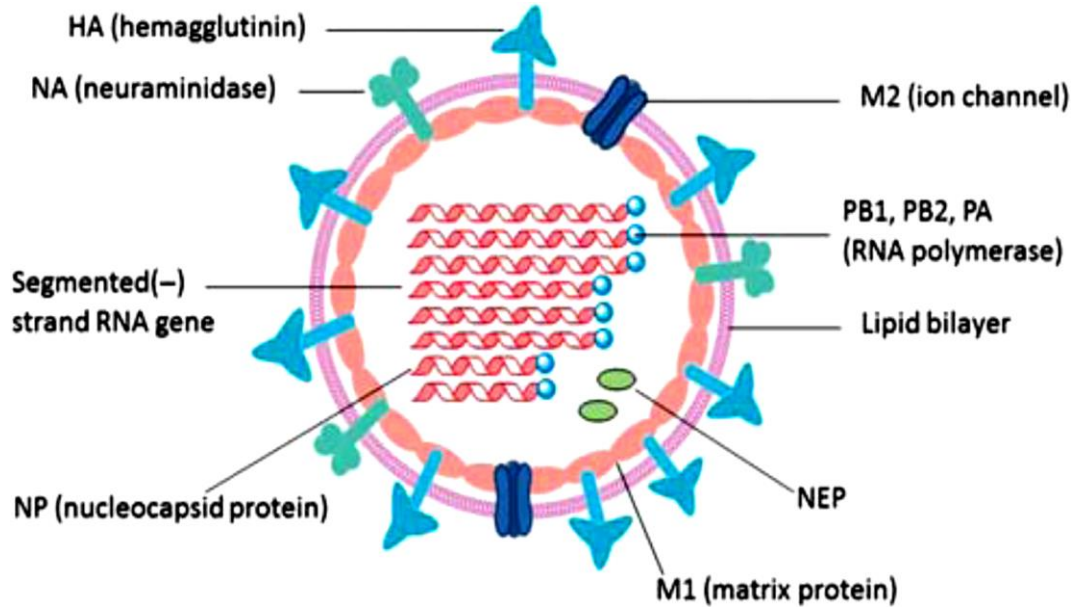


Figure 1.2. The structure of an influenza A virus virion. (Adapted from Ge et al., 2010).

The influenza genome consists of eight negative sense single-stranded RNA segments with each segment coding for one or more proteins (Table 1.1). The segmentation facilitates exchange of genes between strains leading to ‘antigenic shift’ whereby a particular strain acquires a different HA or possibly NA segment from another subtype leading to a novel strain to which population immunity is naïve. Cells infected with different viruses of human or animal lineages can generate virions of mixed lineages. The ends of viral RNA (vRNA) form helical hairpin structures that are bound with RNA polymerase and the rest is coated with arginine-rich nucleoprotein. The net positive charge binds to the negatively charged phosphate backbone of RNA. (Reviewed in (Bouvier & Palese, 2008)).

Table 1.1. Proteins encoded by various RNA segments of influenza A virus

RNA segments	Protein coded
1	PB2
2	PB1
3	PA
4	HA
5	NP
6	NA
7	M1 and through mRNA splicing M2
8	NS1 and through mRNA splicing NEP/NS2

1.5.3 Influenza A virus life cycle

The HA of influenza virus recognizes the N-acetylneuraminic (sialic) acid on the host cell surface (Couceiro et al., 1993). Sialic acids are nine carbon monossacharides that are found on many cell types. The carbon-2 of sialic acid either binds to carbon-3 or carbon-6 of galactose making α -2,3 or α -2,6 linkages which provide different steric configurations to the sialic acid. α -2,6 linkages are commonly found in the human trachea whereas α -2,3 linkages are of avian origin. However, a small amount of α -2,3 linkages are also found in the lower respiratory

tract of humans like alveoli and bronchioles (Matrosovich et al., 2004). Since the virus commonly encounters only the upper respiratory tract, avian influenza viruses very rarely cause human infections. But in case they do so, the infection spreads rapidly to pneumonia with high mortality rates.

During replication, the HA is cleaved by serine proteases into HA1 and HA2 subunits which is necessary for infectivity. HA1 contains the receptor-binding and antigenic sites whereas HA2 is involved in the fusion of viral envelope with host cell membrane. Antibody against HA can neutralize viral infectivity and hence small mutations occur at the antigenic sites of HA. Accumulation of these minor changes can cause an 'antigenic drift' in the virus which over time renders the HA immunity from neutralization by existing antibodies. (Reviewed in (Bouvier & Palese, 2008)).

After the HA attachment to sialic acid, the virus is endocytosed (Figure 1.3). The low pH in the endosome causes fusion of viral envelope with endosomal membrane that forms a pore through which viral RNPs are released into host cell cytoplasm while the M2 channel disrupts internal protein-protein interactions. The synthesis of vRNA occurs in the nucleus. The viral RNP is trafficked into the host cell nucleus via the viral nuclear localization signals where it either makes genetic material for new virions or forms polyadenylated, capped mRNA for host cell translation of viral proteins. Since influenza RNA is negative sense, it can only make one complimentary copy of its own which must be copied again to get the original copy transcribed. Incapable of driving its own viral protein synthesis due

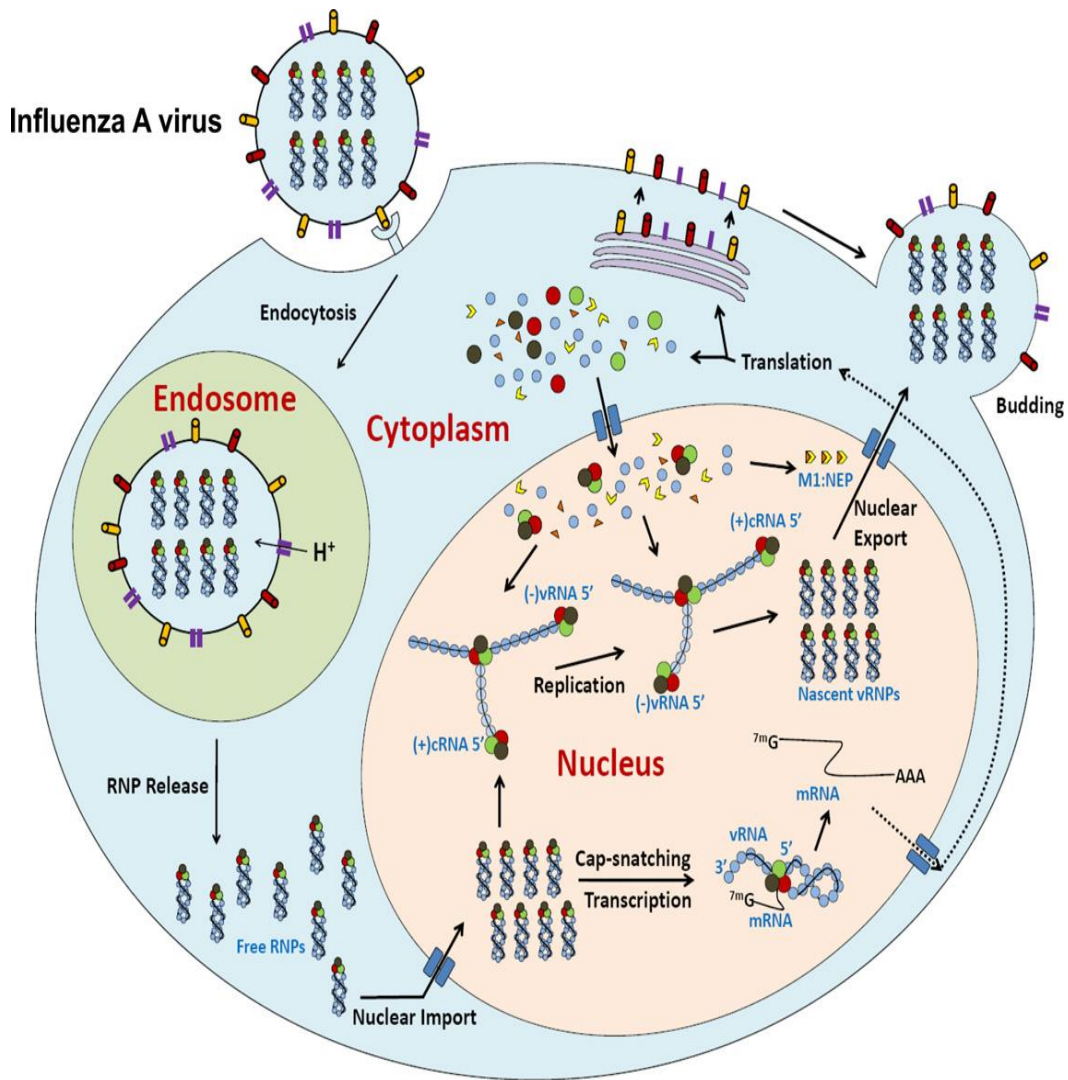


Figure 1.3. Life cycle of influenza A virus. Helical hairpins represent RNPs, polymerase subunits are coloured in red, brown and green, and NP is represented by blue. After endocytosis, the released nucleoproteins are trafficked into the nucleus for viral RNA synthesis which is then exported to the cytoplasm for the translation of other viral proteins. (Adapted from Zheng & Tao, 2013).

to the absence of capped mRNA, the viral RNP hijacks the host mRNA translation system on its way to translate a host protein. The heterotrimeric polymerase consists of PA1, PA2 and PB subunits. The PB subunit binds to the host's capped pre-mRNA at 5' end while the PA subunit possesses an endonuclease that cleaves the cap and attaches it to its own vRNA in a process

called ‘cap snatching’ (Dias et al., 2008). Once the viral mRNA is capped, it can be exported like the host mRNA. The vRNA segments are exported via nucleoporins through M1 channel and NEP (Figure 1.3).

The viral protein translation occurs in the host cell cytoplasm where HA, NA and M2 are translated and trafficked from endoplasmic reticulum to Golgi apparatus for post-translational modifications and thereafter are packed into the new progeny virions through self-sorting signals. The M1 channel brings the RNP-NEP complex into close contact with the lipid envelope containing glycoproteins, through signaling mechanisms. The new progeny are released in the cytoplasm through membrane budding whereby NA cleaves the terminal sialic acid to detach the virions from cell surface. (Reviewed in (Bouvier & Palese, 2008; Zheng & Tao, 2013)).

1.6 Influenza pathophysiology

The clinical presentation of influenza infection includes abrupt febrile onset, cough, headache, malaise and inflammation of upper respiratory tract. The infection typically lasts for 7-10 days (reviewed in (Taubenberger & Morens, 2008)). At histopathological level, the lungs show very minor damage up to 2 days post-viral encounter with focal inflammation of alveolar septa, mild infiltration and septal thickening (Fukushi et al., 2011). The virus is actively replicating but undetectable at this stage; a mechanism not yet clearly understood but could be due to a NS1-dependent delay of type-I interferon response and the subsequent delay in priming of dendritic cells and naïve T-cells leading to a

‘stealth phase’ that could help the virus evade host immune system (Molledo et al., 2009).

At day 3 post-viral encounter, the virus titre in the lungs increases along with host cytokine response in the form of a ‘cytokine storm’. Serial histopathologic analyses of severe viral pneumonia revealed that the infection affects the entire lung parenchyma with multi-focal destruction and desquamation of tracheal and bronchial epithelium, oedema, mixed inflammatory cellular infiltration, formation of fibrin and pulmonary exudates along with alveolar collapse. The viral replication reaches its peak around day 5 or 6 when the entire alveolar structure is collapsed along with hyaline membrane formation and vascular thrombosis leading to diffused alveolar damage (DAD). Sustained infection together with the cytokine storm can further lead to squamous cell metaplasia, pneumocyte hyperplasia and interstitial fibrosis. (Fukushi et al., 2011); (reviewed in (Damjanovic et al., 2012; Taubenberger & Morens, 2008)).

1.7 Secondary bacterial infections

Within the first two weeks of influenza infection, the host is susceptible to numerous bacterial superinfections which are the leading cause of influenza-related morbidity (Morens et al., 2008). Superinfections with bacteria like *Streptococcus pneumoniae* can cause massive neutrophil infiltration in the lungs leading to suppurative bronchopneumonia (Grabowska et al., 2006; Kadioglu et al., 2000). A lot of the influenza-related research has been directed towards

understanding the mechanism behind the viral-bacterial synergism in causing respiratory distress.

1.8 Inflammation and cellular infiltration

Influenza infection often culminates in acute inflammation of the lung parenchyma characterized by edema, pulmonary exudates and cellular infiltration as discussed earlier in section 1.6. Mild inflammation is considered beneficial to the host as it activates the immune system to bring in regulatory cytokines that drive immune cells into the lung and in turn activate the infiltrating cells to secrete more cytokines via a positive feedback loop (Tumpey et al., 2005). Normally, this mechanism is kept in check by regular clearance of cellular debris from the site of infection to avoid hyperactivation. Neutrophils and macrophages are the two main type of infiltrating cells along with lymphocytes (reviewed in (Damjanovic et al., 2012)). The neutrophils first reach the site of infection and stimulate cytokine response to drive macrophages into the lungs. Neutrophils are short-lived and undergo apoptosis once they have finished phagocytosing a pathogen or secreting cytokines. These apoptotic cells are cleared by the resident alveolar macrophages (Savill et al., 1989). However, during fatal influenza infections, the system gets overpowered by the hyperstimulation resulting in over-accumulation of cytokines in the form of a ‘cytokine storm’ (Kobasa et al., 2004; Perrone et al., 2008). As a result, the lung gets overburdened with cytotoxic leukocyte components and ROS that can lead to acute lung injury (ALI) and acute respiratory distress syndrome (ARDS). Cytokine storm has been attributed to be

the main cause of death during the lethal 1918 ‘Spanish flu’ (Kobasa et al., 2004; Tumpey et al., 2005).

1.9 Neutrophil

Neutrophils are the most abundant white blood cells that are grouped under granulocytes together with eosinophils and basophils because of their granular components. These cells are also known as polymorphonuclear leukocytes (PMN) since their nucleus can occur in varying shapes. They are terminally differentiated cells that play an active role in the innate immunity along with macrophages. They are the first line of defense for the host immune system and are the first to reach the site of injury. Once there, they undergo cytokine signaling to bring in other immune cells; meanwhile trying to control the invading pathogens. The average half-life of neutrophils in circulation is 6.7 hours whereas in tissue, they can live upto 1 to 2 days. (Reviewed in (Squier et al., 1995)).

1.9.1 Neutrophil granules

Granules are stores of proteins in granulocytes that are responsible for killing microbes and digesting tissues. They are formed during the various stages of neutrophil maturation from hematopoietic stem cells in bone marrow in varying amounts. The primary granules are formed during the promyelocyte stage; the secondary granules during the myelocyte stage whereas the tertiary granules are formed during the metamyelocyte stage (reviewed in (Borregaard, 2010)).

The neutrophil granules are categorized into three groups:

- a) Primary or azurophil granules, e.g. myeloperoxidase (MPO), serine proteases like neutrophil elastase (NE), bacterial permeability index proteins (BPI), defensins, proteinase 3 and cathepsin G.
- b) Secondary or specific granules, e.g. lactoferrin, NADPH oxidase, cathelicidin and lysozyme.
- c) Tertiary granules, e.g. gelatinase and cathepsin B.

These granules are released dependent on their time of formation, usually those that are formed the latest are released first. Tertiary granules are released during the transmigration through the endothelium while the primary and secondary granules are released at the site of inflammation. Many of these granules such as cytotoxic MPO, iron-binding lactoferrin, pore forming BPI and cathelicidin possess antimicrobial properties. Tissue degrading proteases like gelatinases and collagenases are also abundant e.g. matrix metalloproteinases like MMP9. (Reviewed in (Faurischou & Borregaard, 2003)).

1.9.2 Modes of bacterial killing by neutrophil

Neutrophils possess a variety of pattern recognition receptors (PRRs) that can recognize certain molecular patterns of a pathogen once the pathogen invades a tissue. One such example is the Toll-like receptor (TLR) that recognizes pathogen associated-molecular patterns (PAMPs) on infectious agents. Once the receptor recognizes a pathogen, it leaves the circulation and enters the site of infection via a process called 'chemotaxis'. Through this process, neutrophils are guided by an

array of cytokines, such as interleukin 8 (IL-8) and tumour necrosis factor-alpha (TNF- α), via cell surface receptor recognition to the site of invasion by a pathogen. (Reviewed in (Mantovani et al., 2011)).

Once neutrophils encounter a pathogen, they employ both oxidative and non-oxidative mechanisms to kill them.

1.9.2.1 Phagocytosis

Neutrophils have the ability to engulf bacteria through amoeba-like pseudopods. Neutrophils recognize bacteria through PAMPs or coating with IgG antibody or complement C3b for which receptors are present in neutrophils. Engulfment of bacteria happens upon binding of the receptors to the pathogen after which the pathogen is trapped in a membrane-bound vesicle called 'phagosome'. Inside the phagosome, the granule proteins fuse with the bacteria and release their cytotoxic contents, a process known as 'degranulation'. Proteases such as NE and cathepsin degrade bacterial proteins thereby killing and digesting the bacteria. (Reviewed in (Pruchniak et al., 2013)).

Neutrophils also use oxidative killing mechanism called 'the respiratory burst' using molecular oxygen. During the phagosome formation, molecular oxygen gets trapped inside. This oxygen is converted through a series of chemical reaction into toxic compounds such as hydrogen peroxide (H_2O_2), which are thought to be the main mechanism behind bacterial death. Neutrophils possess NADPH oxidase complex, assembled at the phagosome membrane, which generates superoxide that can be converted to H_2O_2 by superoxide dismutases (SODs). The H_2O_2 is

utilized by MPO to generate hypochlorous acid which is a potent bactericidal agent. (Reviewed in (Hampton et al., 1998; Mayer-Scholl et al., 2004)).

1.9.2.2 Extracellular killing of bacteria

Neutrophils have been shown to trap bacteria and other microbes onto a web-like DNA structure that brings the pathogen into close contact with cytotoxic neutrophil granules and other antimicrobial proteins thereby killing the bacteria extracellularly. These DNA traps are called neutrophil extracellular traps (Brinkmann et al., 2004).

1.10 Neutrophil extracellular traps

Unlike phagocytosis and degranulation, NETs are a relatively recent discovery, an alternative mechanism of neutrophil-mediated microbial killing. In 2004, a chance yet keen observation of neutrophils activated with *Shigella flexneri* by a team of German scientists revealed complex nucleic acid structures emanating from lysed neutrophils with entrapped bacilli (Brinkmann et al., 2004). This phenomenon was later studied and verified by various laboratories and is now known as 'NETosis'. Later this phenomenon was seen in other leucocytes as well like mast cells, eosinophils and macrophages (reviewed in (Brinkmann & Zychlinsky, 2007)).

1.10.1 Components

The primary components of NETs are DNA and histone proteins along with various intracellular proteins attached to the structure. High resolution scanning

electron microscopy (SEM) has shown smooth threads of unfolded chromatin of about 15 nm diameter released from the dead cells that is studded with globular structures of about 30-50 nm diameter (Figure 1.4). The threads can collectively form cables of various lengths that appear as webs in 3-dimensional space. NETs are degradable by treatment with DNases but not proteases. (Reviewed in (Brinkmann & Zychlinsky, 2007)).

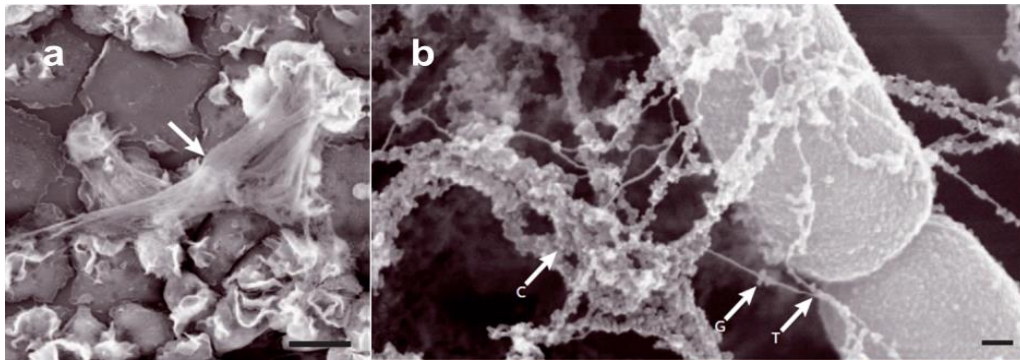


Figure 1.4. SEM micrographs showing (a) DNA traps (white arrows) emerging out of stimulated neutrophils, scale bar = 10 μm and (b) NETs trapping *Shigella flexneri*, scale bar = 100 nm. The threads, globular domains and the cables are indicated as T, G and C respectively (white arrows). (Adapted from Brinkmann & Zychlinsky, 2007).

1.10.2 Mechanism of NETs formation

NETs have been shown to be released by activated neutrophils upon stimulation with IL-8, lipopolysaccharide (LPS), activated platelets, TLR activators, bacteria and other microbes (reviewed in (Brinkmann & Zychlinsky, 2007)). Many different receptors are believed to be involved in NETs generation that basically activate protein kinase C (PKC) initiating a signal transduction cascade leading up to NADPH oxidase complex assembly and activation (Gray et al., 2013).

1.10.2.1 ROS are generally required for NETosis

ROS are believed to play an important role in NETs formation. Fuchs et al. (2007) have demonstrated that physiological levels of H₂O₂ can stimulate NETs generation that can be inhibited by catalase that breaks down H₂O₂ to water and oxygen. NETs were found to be highly inducible with catalase inhibitor, 3-amino-1,2,4-triazole. NETs generation upon stimulation with PKC activator phorbol 12-myristate 13-acetate (PMA) could be inhibited by NADPH oxidase inhibitor, DPI. Finally, neutrophils from chronic granulomatous disease patients with inactive NADPH oxidase failed to generate NETs stressing on the importance of NADPH oxidase complex and ROS in NETs generation. However, a *Staphylococcus aureus*-induced model of NETosis was shown to be independent of oxidants where neutrophils secrete vesicles filled with DNA and proteases into extracellular space (Pilszczek et al., 2011). Moreover, neutrophils from neonates were shown to be incapable of generating NETs even though they generate sufficient ROS implying that ROS alone may not be sufficient to induce NETs (Yost et al., 2009). Nevertheless, most NET-induction models were shown to be oxidative in nature (reviewed in (Parker & Winterbourn, 2013)).

1.10.2.2 NETosis is distinct from apoptosis and necrosis

Using time-lapse microscopy, Fuchs et al. (2007) have demonstrated that NETosis is a cell death process quite distinct from apoptosis and necrosis. Upon stimulation of human neutrophils with PMA, the nucleus gradually starts losing its lobular structure and the chromatin undergoes decondensation segregating into

transcriptionally active euchromatin and inactive heterochromatin, thus forming an amorphous chromatin. Later, the membranes of the nuclear envelope separate and eventually disintegrate bringing the chromatin in close contact with cytoplasm wherein the granules start to dissolve (Figure 1.5 a-c).

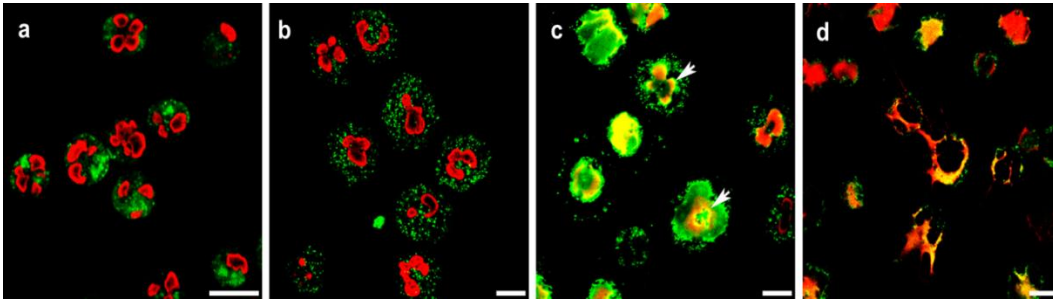


Figure 1.5. Confocal microscopy images of neutrophils that are (a) unstimulated for 180 min showing clearly lobulated nuclei of neutrophils with granules forming a patchy configuration close to the nucleus; or stimulated with 20 nM PMA for (b) 60 min when granules become distinct from the nucleus (c) 120 min when the granules co-localise with the chromatin and (d) 180 min when some neutrophils have already released NETs. Red indicates histone-DNA complex and green indicates neutrophil elastase. Scale bar = 10 μm . (Adapted from Fuchs et al., 2007).

Roughly about 3 to 4 hours from initial stimulation, all the cellular contents mix and NETs are released (Figure 1.5 d). However, the process has been shown to occur much earlier, starting from 5 minutes upon stimulation, by stimulants such as *Staphylococcus aureus* and LPS-stimulated platelets (Clark et al., 2007; Pilszczek et al., 2011).

In contrast to the systematic release of NETs from activated neutrophils (Figures 1.5 and 1.6 c), necrosis involves rapid disintegration of nuclear lobules without any clear distinction between eu- and hetero-chromatin while the nuclear envelope and proteins remain intact (Figure 1.6 b). Stimulation with pore-forming toxins of *S.aureus* led to necrosis in 15 minutes but not NETosis even after

prolonged incubation. The cells stained TUNEL-negative ruling out apoptosis as well. On the other hand, apoptotic neutrophils undergo DNA fragmentation while the membrane and organelles remains intact (Figure 1.6 a). Treatment with anti-Fas antibody for 18 hours led to apoptosis but not necrosis or NETosis as revealed by TUNEL analysis and extracellular DNA concentration (Brinkmann et al., 2004; Fuchs et al., 2007). These studies have confirmed that NETosis is a distinct cell death event along with apoptosis and necrosis. However, NETs have also been demonstrated to be generated by granulocyte-macrophage colony stimulating factor (GM-CSF)-primed live neutrophils in a ROS-dependent manner upon stimulation with LPS and complement factor C5a. Moreover, the DNA was found to be mitochondrial in origin in contrast to the genomic DNA released by dying neutrophils which is the case with most stimulants of NETosis (Yousefi et al., 2009).

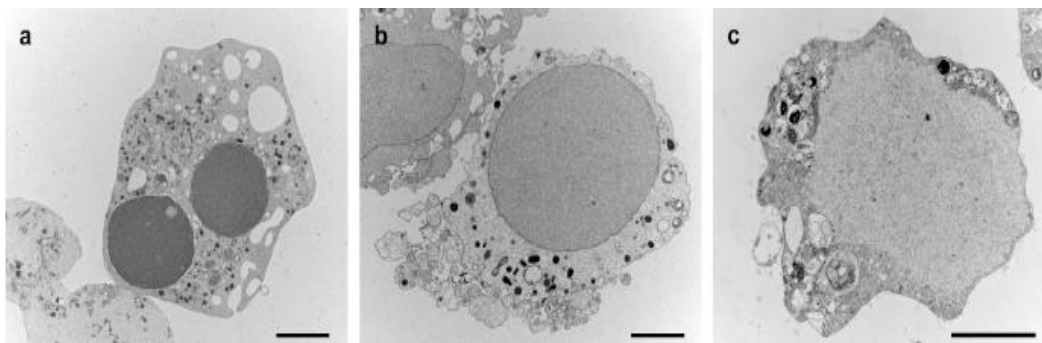


Figure 1.6. Transmission electron micrographs of neutrophils (a) treated with 20 ng/ml anti-Fas antibodies for 18 h to induce apoptosis showing nuclear condensation, fragmentation, cytoplasmic vacuolisation and other characteristic apoptotic morphology (b) incubated with 25 µg/ml of *S. aureus* pore-forming toxin for 15 minutes to induce necrosis showing loss of segregation into eu- and heterochromatin while the nuclear envelope and granules remain intact (c) stimulated with 10 nM PMA for 4 h to induce NETs that show clear fragmentation of nuclear membrane allowing direct mixing of nuclear, cytoplasmic and granular components as the granules too dissolve. Scale bar = 2 µm. (Adapted from Fuchs et al., 2007).

1.10.2.3 Histone hypercitrullination mediates chromatin decondensation and NETosis

Histone citrullination or deimination is the conversion of amino acid arginine into amino acid citrulline as part of post-translational modification of proteins. The replacement of positively charged arginine to neutral citrulline under neutral pH conditions increases hydrophobicity of proteins thereby affecting protein folding. Citrullination is known to be mediated by a group of enzymes called peptidyl argininedeiminases (PADs), namely PAD4 which specifically deiminates the arginine residues at R2, R8, R17 and R26 positions on histone H3 tail (Cuthbert et al., 2004). Various studies have reported the PAD4-mediated citrullination of histones H3 and H4 during NETosis albeit not necessary for the process as such (Neeli et al., 2008; Wang et al., 2009). Specific isoforms of PKC were shown to influence PAD4-mediated NETosis (Neeli & Radic, 2013). Different stimuli activated different PKC for instance, calcium ionophore-mediated stimulation which is common in bacterial and fungal infection activated PKC-zeta (PKC- ζ), an inducer of PAD4 while PMA stimulation activates PKC-alpha (PKC- α), an inhibitor of PAD4. This suggests differential regulation of PAD4 activation by PKC that controls the extent of NETosis as well as affects the basic characteristics of NETs dependent on the stimulant. This study establishes NETosis as a highly evolved mechanism that depends on critical balancing of histone citrullination. Mice deficient in PAD4 have shown remarkable reduction of NETs generation however, their involvement in disease pathogenesis is not yet clearly defined. In a viral infection model of influenza, PAD4-mediated NETs did

not affect the outcome of disease *in vivo* while in a bacterial infection model of *S. flexneri* and necrotizing fasciitis, PAD4-mediated NETs played a crucial role in the bactericidal activity (Hemmers et al., 2011; Li et al., 2010).

1.10.2.4 MPO and NE synergistically enhance chromatin decondensation

Papayannopoulos et al. (2010) have shown that neutrophil granules like NE and MPO are crucial for the formation of NETs. NE knock-out mice were found to be deficient in pulmonary NETs generation. Neutrophils from MPO-deficient human donors failed to generate NETs (Metzler et al., 2011). MPO synergizes with NE in a ROS-dependent manner that allows NE translocation into nucleus and subsequent degradation of histones to cause chromatin decondensation (Figure 1.7) (Papayannopoulos et al., 2010).

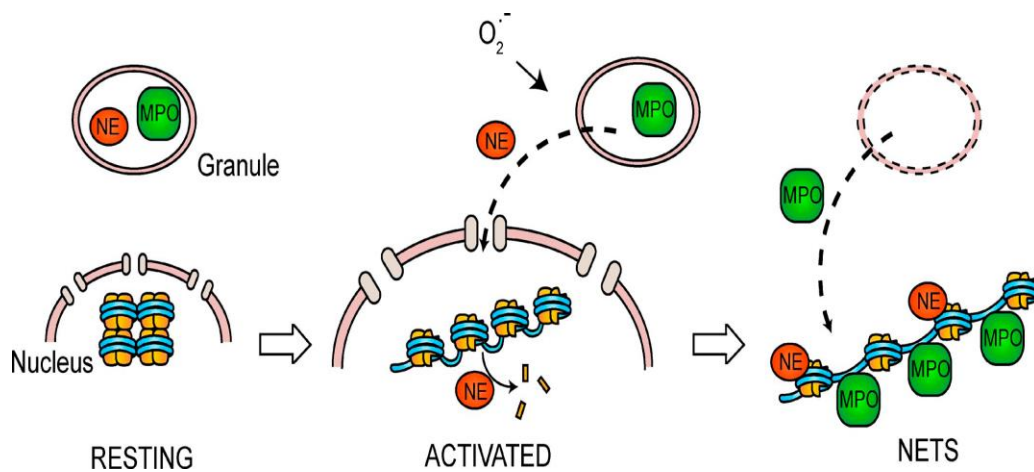


Figure 1.7. Model of MPO and NE synergism during NETs formation. NE and MPO are stored in the azurophilic granules in resting neutrophils. Upon activation and ROS production, NE translocates to the nucleus from granules where it cleaves histones and promotes chromatin decondensation. At later stages, MPO binds to the chromatin as well; further enhancing the decondensation synergistically with NE that eventually leads to cell rupture and NET release. (Adapted from Papayannopoulos et al., 2010).

Upon oxidative burst in a *Candida albicans* model of NETosis, H₂O₂ caused dissociation of NE into cytosol in a MPO-dependent manner (Metzler et al., 2014). The NE forms a complex called azurosome together with cathepsin G and azurocidin that can localize on the granule membrane. Only a subset of azurophilic granules has the ability to localize on the membrane. The azurosome dissociates along with MPO, lactotransferrin, proteinase 3 and lysozyme to cytosol. Once in cytosol, the enzymatic activity of NE is activated in a MPO-dependent manner. The NE binds to and degrades F-actin to arrest actin dynamics which promotes the proteases to enter nucleus and thus, the NE translocates to nucleus. The mechanism by which ROS causes dissociation of NE and by which MPO regulates the process is not clear yet. In another *Candida* model of stimulation, phagocytosis was shown to adversely affect NETosis in a NE-dependent way (Branzk et al., 2014). Phagocytic neutrophils sense microbial size via a dectin-1 mediated process that prevents NETs release by downregulating NE translocation to nucleus. These experiments prove the importance of MPO and NE in the formation of NETs.

1.10.2.5 Other pathways involved in NETosis

Recent studies using human neutrophils have identified the involvement of cell signalling pathways like p38 MAP kinase and Raf-MEK-ERK pathways that are oxygen-dependent. Using a chemical genetic screen, the involvement of some proteins from the Raf-MEK-ERK were elucidated that induce the expression anti-apoptotic proteins suggesting that neutrophils might block apoptosis to allow

NETosis (Behnen et al., 2014; Hakkim et al., 2011; Keshari et al., 2013). Such preference may or may not be stimuli-dependent and needs further investigation.

1.10.3 Antimicrobial function of NETs

Neutrophils carry various proteins that are antimicrobial in nature. They possess antimicrobial peptides (AMPs) like LL-37 and defensins while other proteins like MPO, NE, proteinase 3, BPI, S100s, lactotransferrin, pentraxin 3 as well as histones are known to possess antimicrobial properties (reviewed in (Rogan et al., 2006; Wiesner & Vilcinskas, 2010)). The presence of these proteins in extracellular space along with improved contact with pathogens is thought to play a key role in NETs-mediated microbial killing. Histones contribute to the major part of antimicrobial action of NETs (Saffarzadeh et al., 2012).

1.10.3.1 Bacterial infections

Several bacteria have been shown to bind to NETs but not all of them were killed by such interactions. It is not clear why microbes bind to NETs but electrostatic interactions between cationic components of NETs and anionic surface components of microbes are thought to play a role (reviewed in (Brinkmann & Zychlinsky, 2007)). *Shigella flexneri*, *Salmonella typhimurium* and suspension cultures of *Pseudomonas aeruginosa* were shown to be killed by NETs (Brinkmann et al., 2004; Young et al., 2011). However, others such as *Streptococcus pneumoniae*, Group A Streptococcus (GAS) and *Staphylococcus aureus* were shown to evade NETs-mediated killing by secreting DNases (Beiter et al., 2006; Berrends et al., 2010; Buchanan et al., 2006).

Mycobacterium tuberculosis, *Haemophilus influenzae* also bind to NETs but do not get killed (Juneau et al., 2011; Ramos-Kichik et al., 2009).

Probably as an evolutionary response to massive threat from host immune system, bacteria employ several tactics to evade killing by NETs. A few mechanisms have been characterised by which bacteria evade NETs-mediated killing.

1.10.3.1.1 Secretion of nucleases

DNA being the backbone of NETs is the most important component that is involved in disseminating AMPs to a larger surface area and trapping bacteria to bring them in closer contact with the AMPs.

Many bacteria have been shown to secrete nucleases which could degrade NET strands and help the bacteria escape entrapment and subsequent killing. A surface endonuclease encoded by *endA* gene helps *S. pneumoniae* in escaping entrapment by NETs (Beiter et al., 2006). Though *endA* mutant of TIGR serotype was as equally efficient as wild type TIGR in colonizing the upper respiratory tract, it failed to cause invasive infection in lower respiratory tract and diffusion in blood when compared to the wild type. In a murine model of necrotizing fasciitis, a potent DNase, *sda1*, was shown to be crucial for resistance towards neutrophil-mediated killing of GAS (Buchanan et al., 2006). Similarly, nuclease secretion was shown to be associated with delayed bacterial clearance and increased mortality in murine model of *S. aureus* infection (Berrends et al., 2010). The nuclease deficient bacteria were unable to escape NETs-mediated killing.

Furthermore, *S. aureus* was shown to convert NETs to deoxyadenosine via nucleases and adenosine synthase that triggers the caspase-3 mediated immune cell death (Thammavongsa et al., 2013). For years, scientists have wondered why certain bacteria express nucleases on their surface; since the discovery of NETosis, the underlying reason and its importance in the pathogenesis of bacteria are now comprehensible.

1.10.3.1.2 Expression of capsules

Polysaccharide capsules have been shown to be crucial for pathogenesis of many bacteria. Capsules have been used for serotyping pathogenic bacteria like *S. pneumoniae* of which 94 capsular types have been described so far (reviewed in (Song et al., 2013)). Even the pneumococcal vaccines are raised against the capsular antigens of 23 selected serotypes (Cox & Link-Gelles, CDC⁸). Using capsular mutants for comparison, wild type *S. pneumoniae* were shown to evade entrapment by NETs but were not protected from NET-mediated killing (Wartha et al., 2007). Nevertheless, capsule mutants have been shown to be severely impaired in causing lethal infections in murine models of *S. pneumoniae* and *K. pneumoniae* where capsule has been shown to promote anti-inflammatory responses in the host to facilitate better bacterial survival (Lawlor et al., 2006; Morona et al., 2004; Yoshida et al., 2001).

1.10.3.1.3 Inhibition/Repulsion of AMPs

NETs provide high local concentration of AMPs to enhance microbicidal action of these peptides. Certain bacteria like GAS contain M1 protein that is

directly involved in higher virulence of the bacteria. M1 protein has been shown to induce NETosis while at the same time protecting the bacteria from NET-killing through inhibition of LL-37 (cathelicidin), an important AMP of extracellular traps (Lauth et al., 2009). In the same study, strains isolated from patients with invasive necrotizing fasciitis were found to be highly resistant to LL-37. On the other hand, certain strains of *S. aureus* possessed modified anionic lipid membranes through inclusion of L-lysine via *MprF* gene that facilitates repulsion of AMPS such as defensins and cationic AMPs (CAMPs) (Kristian et al., 2003). Similarly, D-alanylation of lipoteichoic acid via *dltA* operon creates a positive surface charge on *S. pneumoniae* which helps in evading NETs- and AMP-mediated killing (Wartha et al., 2007). Mice infected with *dltA* mutant showed enhanced survival and decreased bacterial load in lungs and blood.

1.10.3.2 Fungal and parasitic infections

Even though NETs were first identified as antibacterial entities, they were later implicated in many non-bacterial infections as well. Urban et al. (2009) identified calprotectin, a dimer between S100A8 and S100A9, as a key antifungal secretion of neutrophils via NETosis. *Candida albicans* is an opportunistic microbe that can cause highly invasive disease with colossal inflammation and tissue damage. Calprotectin chelates Mn^{2+} and Zn^{2+} which are required for *C. albicans* growth. Calprotectin-deficient neutrophils were unable to kill the fungus. *In vivo* murine infections also revealed that calprotectin-deficient mice have difficulty in clearing fungal load from their system. Similar effect was observed with *Aspergillus nidulans* that showed high susceptibility to calprotectin

via Zn^{2+} chelation (Bianchi et al., 2011). However, conidia were less susceptible to killing by NETs than hyphal forms of fungus since the conidia promoted phagocytosis. This was the case too with the highly invasive fungus, *Aspergillus fumigatus*. Bruns et al. (2010) demonstrated that a hydrophobic protein, *RodA* makes the conidia immunologically inert and hence less prone to NETs-mediated killing.

NETs were also shown to be effectively induced by parasites such as *Toxoplasma gondii*, *Leishmania* species and *Plasmodium falciparum*. It is not very clear how extracellular traps can contain intracellular parasitic infections but the proposed hypothesis is that ETs entrap the emerging parasites from lysed cells before they could infect other cells (reviewed in (Abi Abdallah & Denkers, 2012)). *T. gondii*-induced NETs were shown to be dependent of extracellular signal regulated kinases (ERK) pathway through inhibition studies (Abi Abdallah et al., 2012). Intranasal infection with *T. gondii* tachyzoites released NETs in the lungs of infected mice. *P. falciparum* induced NETs were measured as circulating dsDNA in the blood of infected children in Nigeria (Baker et al., 2008). Like bacteria, parasites also seem to be evolving in NETs evasion by mechanisms such as secretion of nuclease by *Leishmania infantum*. Nuclease-deficient promastigotes were easily killed by NETs via a lipophosphoglycan-dependent mechanism (Guimarães-Costa et al., 2014). Moreover, *Leishmania* promastigotes and amastigotes have been shown to be susceptible to histone proteins H2A and H2B, key microbicidal proteins of NETs (Wang et al., 2011).

1.10.3.3 Viral infections

Viruses are generally not known to infect neutrophils although they can stimulate the cells by eliciting higher pro-inflammatory cytokine response via oxidative signaling from infected cells. However, neutrophils infected with H3N2 influenza virus exhibited early cell death and upregulated Type I interferon signalling (Ivan et al., 2013). A few viruses, both DNA- and RNA-based, have been associated with NETs. Human immunodeficiency virus (HIV)-1 has been shown to be entrapped and neutralized by NETs in TLR7- and TLR8-dependent manner (Saitoh et al., 2012). MPO and α -defensins were identified as key viricidal components of NETs. In addition, HIV-1 was shown to engage CD209 on dendritic cells with envelope protein gp120 that enhances IL-10, an anti-inflammatory cytokine thereby reducing NETs. Similarly another single stranded-retrovirus, feline leukemia virus (FeLV), was shown to regulate NETs in a feline infection model (Wardini et al., 2010). FeLV inhibits neutrophil activation by inhibition of PKC activation to reduce ROS production. Neutrophils from chronic FeLV-infected felines show reduced responsiveness to secondary stimulation with *Leishmania* promastigotes. This alludes to another regulatory mechanism of NETs by viruses. Intravenous challenge of mice with double-stranded DNA Myxoma virus and its analogs led to excessive NETs generation which were entangled with circulating platelets. Here, the platelets were shown to enhance activation of neutrophils during adhesion (Jenne et al., 2013).

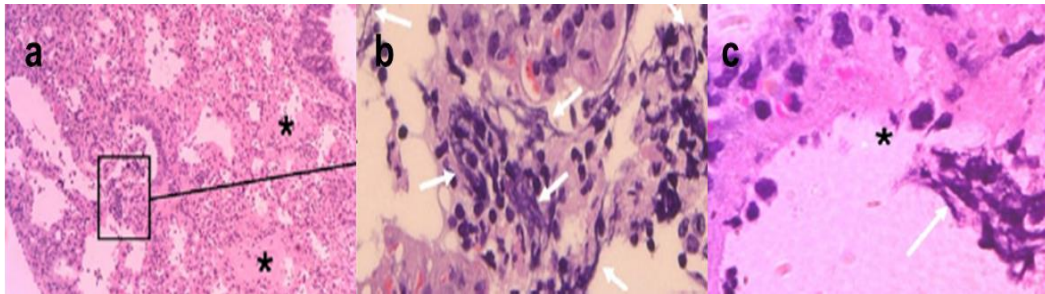


Figure 1.8. Haematoxylin and eosin stained-lung sections showing NETs present on day 10 post-infection in macrophage-depleted mice infected with influenza A virus. (a) Alveolar spaces show proteinaceous exudates (asterix) indicating diffused alveolar damage together with interstitial thickening. (b) Extensive NETs formation at the terminal bronchioles opening into alveoli (white arrows). (c) Bundles of NETs were observed in the large blood vessels showing endothelial damage (asterix). Magnification a=200x, b and c=1000x. (Adapted from Narasaraju et al., 2011).

NETs have also been described during influenza A infection. Excessive neutrophil accumulation and NETosis during acute influenza infection were shown to cause lung injury (Narasaraju et al., 2011). Bundles of NETs were seen near the terminal bronchioles and large blood vessels (Figure 1.8). Though the virus itself could not generate enough NETs, virus-infected alveolar epithelial cells could generate significant NETs. Hemmers et al. (2011) demonstrated that PAD4-deficient mice had impaired NETs generation but this did not affect the outcome of the disease thereby making PAD4-mediated NETs dispensable in influenza infection. Another study by Garcia *et al.* (2013) demonstrated that NETs could be inhibited by blocking C5a activation using chemical inhibitors. Using Omcl, a lipocalin protein from the salivary glands of the tick *Ornithodoros moubata*, C5a activation was blocked that reduced overall neutrophil accumulation and NETs generation in mice infected with influenza A virus.

1.10.4 NETs and tissue injury

NETs like ROS are non-specific in causing cell death. The cytotoxic components of NETs which have microbicidal properties could also be toxic to the host cells in the surrounding tissue. Their non-specific nature could be implicated in various non-infectious conditions like pre-eclampsia, deep vein thrombosis and systemic lupus erythematosus (SLE) ((reviewed in (Brinkmann & Zychlinsky, 2007)); (Fuchs et al., 2010; Leffler et al., 2012). Excessive NETosis have been shown to be associated with ALI during influenza A infection (Narasaraju et al., 2011). NETs can induce endothelial and epithelial cell damage *in vitro* mainly mediated by histones and MPO (Saffarzadeh et al., 2012). Histones have been implicated in many models of tissue injury like sepsis where antibodies to histones or activated protein C abrogate septic death (Xu et al., 2012). During deep vein thrombosis in mice, citrullinated H3 were found to be in close association with von Willebrand factor, a platelet adhesion molecule crucial for thrombus development. Treatment with DNase I protected the mice from thrombosis (Brill et al., 2012). In SLE, the complement C1q was shown to inhibit NET degradation by inhibiting DNase I in serum and these undegraded NETs led to enhanced complement activation thereby exacerbating tissue injury (Leffler et al., 2012). Liu et al. (2012) found acetyl-modified H2B as a key post-translational histone modification during SLE but could not induce sufficient immune response by passive transfer of NETs in mice. A low-density granulocyte subset was identified in SLE patients which had enhanced propensity to generate NETs and

thus could cause increased endothelial damage and tissue infiltration (Villanueva et al., 2011).

Other NETs proteins like MPO and MMPs have also been implicated in tissue damage. MPO was shown to induce DNA strand breakage and increased levels of haemoxygenase-1 in alveolar and bronchial epithelial cells *in vitro* (Haegens et al., 2008). It was also found to be directly cytotoxic to endothelial cells (Saffarzadeh et al., 2012). Ng et al. (2012), have shown the importance of gelatinases like MMPs in causing lung tissue damage by using doxycycline to inhibit MMPs in mice infected with influenza virus. MMP2 and MMP9 were found to be associated with elevated levels by T1- α and thrombomodulin, indicators of epithelial and endothelial cell damage.

Due to the extracellular nature of NET components, they are bound to activate host immune response against themselves. Circulating anti-neutrophil cytoplasmic antibodies (ANCA) and anti-nuclear antibodies (ANA) as well as ribonucleic acids have been measured in various models of tissue injury like rheumatoid arthritis (RA) and SLE (Nakazawa et al., 2014; Pratesi et al., 2013). ANCA can be generated against either MPO or proteinase-3 though MPO-ANCA are the most-studied ones during NETs generation. In conditions like RA, the extracellular ANA against histones were used as diagnostic markers (Pratesi et al., 2013). ANA were also observed in blood of children infected with *Plasmodium falciparum* (Baker et al., 2008). Type I interferons have been shown to prime neutrophils to respond to autoimmune complexes formed by NETs (Garcia-Romo et al., 2011). Thus, NETs-mediated ANA and ANCA contribute to

heightened immune response which is detrimental to the host. Circulating free double-stranded DNA (cf-ds DNA) has been suggested as an important prognostic marker for sepsis and other autoimmune disorders (Margraf et al., 2008).

Since NETosis is an oxidative process, it is dependent on ROS released from neutrophils which by itself can cause tissue injury. Activated neutrophils undergo respiratory burst which releases reactive oxygen radicals in the surrounding tissue that can cause DNA, protein or lipid damage (reviewed in (Almyroudis et al., 2013)). In addition, radicals like hypochlorous acid generated by MPO are also extremely cytotoxic. Inhibition of ROS generation by blocking NADPH oxidase activity has been shown to be beneficial in some conditions (Vlahos et al., 2011; Wang et al., 1994).

1.10.5 Techniques used for studying NETs

Due to a lack of reliable assay markers for detection of NETs in live subjects, NETs are mostly studied morphologically on autopsy samples and in animal models or *in vitro* using neutrophils isolated from blood or bone marrow (Ermer et al., 2009). However in recent times, citrullinated histone 3 detection by ELISA has been employed as a surrogate for NETs (Hirose et al., 2014). For laboratory experiments, extracellular DNA quantification using Sytox dye or picogreen dsDNA quantification reagent is being employed but microscopic detection of NETs by immunolabelling remains the gold standard (Berends et al., 2010; Saffarzadeh et al., 2012). However, there is a dire need for development of better assay techniques for rapid and reliable detection of NETs in clinical environment.

1.11 Aims and objectives

NETosis is an oxygen-dependent process that depending on the circumstances is either a beneficial antimicrobial phenomenon or it can cause injury to surrounding tissues (Brinkmann et al., 2004; Narasaraju et al., 2011). The outcome of influenza infection is often complicated by comorbidities such as secondary bacterial infections and underlying chronic disorders like obesity (risk factor during 2009 pandemic influenza) as discussed in the previous sections.

So far, most studies on NETs have concentrated on the induction of NETs induced using primary stimuli. Alluding to the importance of bacterial superinfections in worsening influenza outcome, this project aims to characterise and evaluate the role of NETs generated during secondary pneumococcal infection with *S. pneumoniae* which has not been done so far.

Furthermore, only few studies have tried to observe NETosis from the host's point of view such as in the context of complement-activation and toll-like receptor stimulation (Brinkmann et al., 2004; Leffler et al., 2012). Even though obesity is known to influence the outcome of influenza infection, no study has been done till now on the effect of high adiposity on NETs generated during influenza infection.

Hence, this project aims at studying NETs induction from a combination of microbial and host factors both with primary and secondary microbial stimuli.

The main objectives of the thesis are,

- a) To evaluate the generation of NETs in the lungs during secondary pneumococcal infection after influenza infection [Chapter 3].
- b) To compare different serotypes of *S. pneumoniae* with respect to their ability to induce NETs and to assess the role of the pneumococcal capsule in pulmonary NETosis [Chapter 4].
- c) To assess the impact of high fat diet-induced adiposity on pulmonary NETosis after influenza infection [Chapter 5].
- d) To evaluate the effect of chemical inhibition of oxidants namely NADPH oxidase on influenza-induced lung injury [Chapter 6].

CHAPTER TWO

MATERIALS AND METHODS

2.1 Propagation of influenza virus [Chapters 3-6]

Influenza virus A/Puerto Rico/8/34 (H1N1) or PR8 obtained from the American Type Culture Collection (ATCC; VA, U.S.A.) was propagated in embryonated eggs at 37°C for 72 hours, and the allantoic fluid was harvested and stored at -80°C. Viral titres (Plaque forming units, PFU) were determined by plaque assay (Section 2.5.4.1). For experimental usage, the virus stock was freshly diluted to desired concentration in 1x PBS (1st Base).

2.2 Propagation of bacteria and fungi

2.2.1 *Streptococcus pneumoniae* [Chapters 3 and 4]

S. pneumoniae serotype 19F (clinical isolate), serotype 3 (Xen 10; Perkin Elmer, MA, U.S.A.), serotype 4 (TIGR; a gift from Professor Andrew Camilli, Tufts University, U.S.A.) and serotype 4cps4D- capsule mutant strain (TIGRcps4D-; a gift from Professor Hiroshi Watanabe, Kurume University, Japan) were grown in brain heart infusion (BHI; Fluka, Buchs, Switzerland) broth supplemented with 5% foetal bovine serum (FBS; Biowest, France) until mid-logarithmic phase ($\text{O.D.}_{600\text{nm}} = 0.4\text{-}0.6$) at 37°C with 5% CO₂. The culture was then pelleted, centrifuged at 5,000 rpm for 5 minutes, washed twice with 1x PBS

and re-suspended with 1x PBS to desired volume. Serial dilutions were made from the stock to desired concentration and samples were plated (spread plate or Miles & Misra techniques) on 5% sheep blood agar plates (Becton Dickinson, NJ, U.S.A.) to determine the number of colony forming units (CFU).

2.2.2 *Klebsiella pneumoniae* [Chapter 3]

K. pneumoniae serotype 15 (K15; clinical isolate) was grown in Luria-Bertani (LB; Sigma, MO, U.S.A.) broth until mid-logarithmic phase at 37°C. The culture was then washed twice with 1x PBS and re-suspended with 1x PBS to the desired volume. Serial dilutions were plated on LB agar plates (1.5% agar-agar; Oxoid, Hampshire, U.K.) for CFU determination.

2.2.3 *Candida albicans* [Chapter 3]

C. albicans (clinical isolate) was grown on Sabouraud dextrose agar (SDA; Oxoid, Hampshire, U.K.) slants supplemented with 1.5% agar-agar at 28°C (yeast growth) overnight. Colonies were scraped and re-suspended with 1x PBS, washed twice and re-suspended again in 1x PBS to desired volume. Serial dilutions were plated on SDA plates and incubated at 37°C (hyphal growth) for CFU determination.

2.2.4 Estimation of CFU/ml in a culture sample [Chapters 3 and 4]

Bacteria were grown from a single colony overnight, diluted 1:100 with fresh broth and re-grown for 5-7 hours (Neat). *C. albicans* was cultured on SDA slants overnight and colonies were scraped and re-suspended in 1x PBS (Neat). 2-fold

and 10-fold serial dilutions from 'Neat' were made with 1x PBS after washing the pellets. Optical density (O.D.) at 600 nm was recorded (Beckman Coulter, CA, U.S.A.) for the 2-fold dilutions while the 10-fold dilutions were plated and incubated overnight to determine the colony count. Based on the colony count of 'Neat', the CFU/ml was calculated for the 2-fold dilutions. A graph was plotted with O.D. on the x-axis and CFU/ml on the y-axis and the slope was obtained which would predict the value of 'y' (CFU/ml) based on 'x' (O.D.). An R^2 value between 0.97 and 1.0 was considered ideal. The growth curve equation was verified at least three independent times by diluting an unknown sample based on the equation and verifying the colony count.

2.3 Bacterial assays

2.3.1 PCR amplification of *cps4D* gene to confirm deletion [Chapter 4]

Five colonies of *S. pneumoniae* serotype 4 wild type and *cps4D*- mutant were re-suspended with 50 μ l nuclease-free water and boiled at 95°C for 5 minutes to extract DNA. 2 μ l of lysate was mixed with 23 μ l PCR master mix comprising 1x GoTaq[®] green buffer in H₂O, 10 mM dNTP, 1.25 U GoTaq[®] Polymerase, 10 μ M primers and 25 mM MgCl₂ (Promega, WI, U.S.A.). The mixture was then subjected to PCR amplification in the Mastercycler Personal (Eppendorf, Germany) under the following conditions - denaturation at 95°C for 1 min, followed by 35 cycles of denaturation at 95°C for 20 sec, annealing at 55°C for 20 sec, extension at 72°C for 20 sec, and a final extension at 72°C for 10 min.

The primers (IDT, U.S.A.) used were - forward primer sequence 5'-ATA ACC GGA CCT TCTGAA TC-3' and reverse primer sequence 5'-GAA TAT ACG AGT ACC ACG CGA-3'. To visualise the product of amplification (1728 bp), the samples were subjected to 1.2% agarose gel electrophoresis and stained with ethidium bromide. Absence of amplification product was considered as confirmation of gene deletion.

2.3.2 FITC-Dextran exclusion assay to measure capsule thickness [Chapter 4]

S. pneumoniae were grown to mid-logarithmic phase and 500 μ l of the cultures were aliquoted and washed with 1x PBS. 10 μ l of the bacteria was mixed with 2 μ l of 2000 kDa FITC-Dextran (10 mg/ml in d.H₂O; Sigma, MO, U.S.A.) on a glass slide. A coverslip was mounted and the preparations were visualised using a confocal microscope (Olympus IX81, Japan) equipped with FV-10 ASW 3.0 viewer under 1000x magnification. Images were captured with FITC channel and DIC at 3000x magnification using a built-in zoom option. The FITC images were exported to greyscale in JPEG format and analysed using ImageJ software (U.S.A.) – Set scale << '2 μ m' << Image << Adjust << Threshold << 'Set threshold/cover cell area' << Analyze << Tools << ROI manager << 'Click' Magic Wand << 'Choose cells to analyse' << Add in ROI manager << 'Select the cells in ROI manager' << Measure area.

The area of 100 bacterial cells were measured based on the zone of exclusion under the FITC channel and mean area (μ m²) was calculated to represent capsule thickness.

2.3.3 DNase activity assay [Chapter 3]

Supernatant and cell pellet of *S. pneumoniae* 19F and *K. pneumoniae* K15 cultures were collected. 2 µg of Salmon sperm DNA (Invitrogen, MA, U.S.A.) was treated with either the bacterial pellet (10^7 cells) or double-filtered supernatant (3 µl) at 37°C for 1 hour in a DNase buffer (10 mM Tris, 3 mM MgCl₂, 5 mM CaCl₂, pH 7.4). Salmon sperm DNA with 10 U recombinant DNase I (Roche, Basel, Switzerland) and buffers alone served as controls. The reaction was stopped with 0.5 M EDTA (Biological industries, Israel) and the samples were then subjected to 1% agarose gel electrophoresis. Smearing in place of intact DNA bands or absence of any DNA indicated DNase activity.

2.4 *In vitro* assays using murine neutrophils

2.4.1 Isolation and purification of bone marrow-derived neutrophils [Chapters 3 and 4]

Mature neutrophils were isolated from bone marrow of healthy mice by density gradient separation method using a previously established protocol (Ermert et al., 2009). Bone-marrow was collected from the tibia and femur of 6-10 weeks old female BALB/c mice by flushing the bones with 1x Dulbecco's PBS without Ca²⁺/Mg²⁺ (Biowest, France) until they turn white. The bone marrow was then homogenised using a 22G needle and passed through a 70 µm cell strainer (Thermo Fisher Scientific, U.K.) to obtain a single cell suspension. The cell suspension was centrifuged at 500 g for 10 minutes, re-suspended in 2 ml 1x

Dulbecco's PBS and then layered on the top 52% layer of a discontinuous Percoll™ gradient (GE Healthcare, Amersham, U.K.) – from bottom, 2 ml of 78%, 69% and 52% v/v Percoll in Dulbecco's PBS. The gradient was centrifuged for 30 minutes at 1,500 g without breaks. Mature neutrophils were recovered from the interphase between 69% and 78% Percoll after washing the cells thrice with Dulbecco's PBS. The cell numbers and viability were determined using a Neubauer chamber and trypan blue staining. The purity of mature neutrophils was morphologically assessed by modified Giemsa staining (Sigma, MO, U.S.A.) and was found to be more than 85%.

2.4.2 Stimulation of neutrophils to induce NETs [Chapters 3 and 4]

Neutrophils were re-suspended in RPMI-1640 medium without HEPES (ATCC, VA, U.S.A.) and serum. $1-2 \times 10^5$ cells were seeded onto poly-L-Lysine (Sigma, MO, U.S.A.) coated 8-well chamber slides (Lab-tek™, ThermoScientific, U.S.A. and SPL Lifesciences, Korea) and incubated at 37°C for 30 minutes in a CO₂ incubator. Stimulants were added at the desired concentration in 100-200 µl volume per well and incubated for various time-points as mentioned in the figures. For stimulation with influenza virus, cells were incubated with bronchoalveolar lavage fluid (FLU-BALF) from mice infected with 500 PFU PR8 virus or as mentioned in the figures. BALF from uninfected animals (CON-BALF) or just RPMI-1640 medium were used as controls. 10 µM H₂O₂ (Sigma, MO U.S.A.) has been used in some experiments as positive control. For representing secondary bacterial stimulation, neutrophils were first incubated with FLU-BALF for 2-2.5 hours and then bacteria at the desired multiplicity of

infection (MOI) were added and incubated for 2 hours. In other experiments, capsule polysaccharide from *S. pneumoniae* serotype 4 (ATCC, VA U.S.A.) was diluted to desired concentration with RPMI-1640 medium and incubated for 2 hours.

2.4.3 Visualisation of NETs and scoring [Chapters 3 and 4]

Immunostaining of NETs was performed for morphological identification. After the desired stimulation and incubation period, supernatant from the wells were gently removed and the cells were fixed with 4% (w/v) paraformaldehyde in PBS (PFA; Sigma, MO, U.S.A.) for 30 minutes. The PFA was then discarded and the cells were washed 2-3 times with 1x PBS. The chambers were removed and the cells were permeabilised with 0.5% TritonX-100 (Sigma, MO, U.S.A.) in 1x TBS (Section 2.8.1) for 5 minutes and then blocked with bovine serum albumin (BSA; Santa Cruz biotechnology, TX, U.S.A.) in 1x TBS for 1-2 hours. Mouse monoclonal anti-histone2B and rabbit polyclonal anti-myeloperoxidase antibodies (Abcam, Cambridge, U.K.) were diluted 1:500 with 1x TBS and incubated for 1 hour at room temperature. 1:250 dilutions of anti-mouse Alexafluor 488 and anti-rabbit Alexafluor 555 (Molecular Probes, U.S.A.) were used as secondary antibodies along with 300 nM DAPI (Life technologies, U.S.A.) for 45 minutes at room temperature in dark. The slides were mounted with slow-fade mounting medium (Life technologies, U.S.A.) and observed under Olympus IX81 microscope or BX60 microscopes (Japan) under 4000x magnification. At least 10 fields were captured and NETs were represented as percentage NETs over total number of cells.

2.4.4 Effect of inhibition of redox enzymes on NETs [Chapter 3]

Neutrophils were pre-incubated with 10 μ M Diphenyleneiodonium chloride (DPI; Sigma, MO, U.S.A.), 100 μ M 4-amino benzoic acid hydrazide (ABAH; Sigma, MO, U.S.A.) and 100 μ M Diethyldithiocarbamate (DETC; Sigma, MO, U.S.A.) for 15 minutes prior to stimulation with FLU-BALF or CON-BALF to inhibit NADPH oxidase, MPO and SOD activity respectively. After 2 hours, NETs were stained and percentage NETs was determined as mentioned in section 2.4.3. DPI and ABAH were dissolved in 1% DMSO (MP Biomedicals, CA, U.S.A.) while DETC was dissolved in RPMI-1640 medium.

2.4.5 mRNA gene expression of bactericidal proteins during NETs generation [Chapter 3]

1.5×10^6 neutrophils were incubated with 150 μ l of FLU-BALF or CON-BALF in several wells for 15 or 30 minutes, 1, 1.5 or 2 hours. The samples were later pooled for each time point and RNA was extracted using the RNeasy RNA purification kit (Qiagen, Netherlands) according to the manufacturer's instructions. The RNA was eluted in 30 μ l RNase-free water. The RNA concentrations were determined using Nanodrop ND-1000 (Thermo Fisher Scientific, U.K.). 1 μ g RNA in H₂O was heated at 70°C for 5 minutes and later was reverse-transcribed with M-MLV reverse transcriptase (RT) reaction mix (1x M-MLV reaction buffer in H₂O, 10 mM dNTPs, 25 U recombinant RNasin[®] ribonuclease inhibitor, 200 U M-MLV RT and 10 μ M random primers) under the

following conditions – 37°C for 1 hour, 70°C for 15 min and finally at 4°C. The cDNA were stored at -20°C until use.

The cDNA was then utilised for real-time PCR analysis using Light Cycler SYBR[®] Green PCR mix and lightcycler system (Roche, Basel, Switzerland). 1 µl of cDNA and 0.5 µl of primer mixture for relevant genes were used according to the manufacturer's protocol under the following conditions - 95°C for 10 minutes followed by 45 cycles of 95°C for 10 sec, 55-58°C for 5 sec, 72°C for 15 sec and finally 65°C for 1 minute. The primers used in the experiment are listed under table 2.1. Relative gene expression levels were calculated using $2^{-\Delta\Delta C_t}$ method (Livak & Schmittgen, 2001). Specificity of amplification reactions was confirmed by melting curve analysis to check the specificity of primer pairs.

2.4.6 Estimation of bacterial entrapment by NETs [Chapter 3]

For evaluating the entrapment of *S. pneumoniae* by NETs, bacteria were incubated with NETs generated from FLU-BALF at MOI of 0.01, 0.1, 1, 10 and 100 for 2 hours. NETs were fixed and then stained with mouse monoclonal antibody against H2B (1:500, Abcam, Cambridge, U.K.) and rabbit antisera against *S. pneumoniae* serotype 19F (1:200, Statens serum institute, Denmark) and were detected using Alexafluor 488 and 555 secondary antibodies (Molecular Probes, U.S.A.) with DAPI (Life technologies, U.S.A.). To assess the bacterial entrapment of NETs, percentage of total NETs showing entrapment in an average of 10 fields were calculated.

2.4.7 Antimicrobial activity assay using NETs generated during influenza infection [Chapter 3]

5×10^6 neutrophils were stimulated using 150 μ l of FLU- and CON-BALF for 1 or 2.5 hours and *S. pneumoniae* 19F and *K. pneumoniae* K15 were added at the MOI of 0.2, 0.1 or 0.01 for 120, 30 or 90 minutes respectively. Cytochalasin B (10 μ g/ml; Sigma, MO, U.S.A.) was added 15 minutes prior to addition of bacteria to inhibit phagocytosis. For *C. albicans*, 0.1% gelatin-coated (Sigma, MO, U.S.A.) wells were used and the fungus was added at MOI 0.1 and incubated overnight at 37°C. After incubation, the contents of the wells were scraped thoroughly and serial dilutions were plated on blood agar (*S. pneumoniae*), LB agar (*K. pneumoniae*) and SDA (*C. albicans*) for colony counts.

2.4.8 Surface killing assay [Chapter 4]

Surface killing assay was modified from a previously published protocol (Weinberger et al., 2009). Mid-logarithmic *S. pneumoniae* cultures were adjusted to 4×10^3 CFU/ml in RPMI-1640 medium and 10 μ l of the culture were spotted onto the blood agar plates and allowed to dry. At least 4-6 spots were placed per plate. 20 μ l of neutrophils (2×10^6 cells/ml) were overlaid on each spot and allowed to dry. To inhibit phagocytosis, 10 μ g/ml of cytochalasin B was incubated with neutrophils 30 minutes prior to use. The assays were done with replicates for each condition. The plates were then incubated overnight at 37°C under anaerobic conditions. The average number of colonies per condition was calculated and expressed as percentage phagocytic and non-phagocytic killing

over total killing. Neutrophils + Bacteria = Total killing, Neutrophils + Cytochalasin B + Bacteria = Non-phagocytic killing and Total killing - Non-phagocytic killing = Phagocytic killing.

2.5 Animal experiments

2.5.1 Intratracheal instillation of pathogens [Chapters 3-6]

All animal experiments were performed according to the regulations of the Institutional Animal Care and Use Committee, National University of Singapore (protocol numbers 050/11 and 117/10). 6-8 weeks female BALB/c mice were used for all *in vivo* experiments except otherwise stated. Mice were anaesthetised using 75 mg/Kg ketamine and 1 mg/Kg medetomidine (0.1 ml/10 g body weight). Infectious agents in 50 µl 1x PBS were gently forced down the trachea after pulling the tongue aside. The anaesthesia was reversed using Atipamezole hydrochloride (5 mg/ml, 0.1 ml/10 g) and the mice were monitored until they wake up. Mouse lethal dose (MLD₅₀) was determined by using different titres of influenza virus for infection. Mice were monitored for 14 days (or otherwise stated) or 30% loss in initial body weight whichever is earlier. Clinical features of influenza and pneumococcal infections include breathlessness, hunched back, ruffled fur and shivering. Mice were euthanized if any signs of discomfort were found like lethargy, reduced food intake, acute breathlessness and morbidity.

2.5.2 Harvesting and processing of tissues [Chapters 3-6]

At the end of experiment or at specific time points, the mice were sacrificed and cardiac puncture was performed to collect blood. Lungs were excised and the left lobes were immersed in 4% buffered-PFA while the right lobes were cut into pieces and frozen in liquid nitrogen for later assays. Depending on the experiment, other organs like brain, kidneys, heart, liver and spleen were collected.

2.5.3 Harvesting and processing of blood and bronchoalveolar lavage fluid [Chapters 3 and 4]

Blood was allowed to clot at room temperature for 30 minutes and serum was collected by centrifuging at 10,000 rpm for 15 minutes at 4°C. The serum was collected as supernatant and stored at -20°C or -80°C until use. BALF was collected by inserting a 23G blunt-end needle through a hole into the trachea (after exposing it by removing the attached skin) and washing the lungs with 0.5 ml of 1x PBS four times through the needle to collect the lavage. The fluid was then pooled together and centrifuged at 400 g for 10 minutes at 4°C; aliquots of the cell-free supernatants were stored at -80°C until use.

2.5.4 Homogenisation of frozen lung tissues for microbial load and other assays [Chapters 3-6]

Frozen lung tissues were homogenised in M tubes using GentleMACS homogenizer (Miltenyi Biotec, Germany). For influenza infection studies, approximately 10% of right lobe was homogenised in 800 µl 1x PBS under

in-built RNA02 setting for 80 sec and then centrifuged at 10,000 rpm for 10 minutes to collect the supernatant which was aliquoted and stored at -80°C.

For pneumococcal infection studies, the whole of right lobe barring a 10% section for RNA extraction, was homogenised in 3 ml 1x PBS under RNA01 setting for 20 sec and serial dilutions of homogenate were plated on blood agar for colony counting. Aliquots of homogenate were stored in 40% glycerol stock for later CFU assays. The remaining fluid were re-homogenised at RNA02 to collect supernatant for other assays.

2.5.4.1 Plaque assay [Chapters 5 and 6]

Madin-Darby canine kidney (MDCK) cell line (ATCC, U.S.A.) were trypsinised (0.25% Trypsin-EDTA, GE Healthcare, Amersham, U.K.) and 2×10^5 cells were seeded in 24-wells plates and grown overnight at 37°C with 5% CO₂ in EMEM medium (ATCC, U.S.A.) supplemented with 10% FBS. After the cells reached 90% confluency, virus or lung homogenates were serially diluted in EMEM with 1 µg/ml TPCK-Trypsin (Tosyl phenylalanyl chloromethyl ketone, Sigma, MO, U.S.A.). The monolayers were then washed twice with 1x PBS and infected with 100 µl of serially-diluted virus and incubated at 35°C for 1 hour with intermittent shaking after which the inoculum was removed and 1 ml of overlay medium (Section 2.8.2) was added to all wells and incubated at 35°C. After 72 hours, the overlay medium was discarded and the cells were fixed with 4% PFA and stained with 1% crystal violet solution (Section 2.8.3) to observe

plaques. The plaques were counted and expressed as PFU/ml or normalised with protein content as PFU/mg.

2.5.4.2 Amplex red hydrogen peroxide assay [Chapters 4-6]

Fresh aliquots of lung homogenates were used to estimate the concentration of H₂O₂. Amplex red hydrogen peroxide/peroxidase assay kit (Invitrogen A22188, MA, U.S.A.) was used according to the manufacturer's instructions. The values were normalised to lung protein content.

2.5.4.3 Myeloperoxidase activity [Chapters 4-6]

Freshly thawed lung homogenates were assayed for MPO activity by a modification of the method established by Klebanoff et al. (1984). The assay solution was freshly prepared as follows: 26.9 ml d.H₂O, 2.0 ml 0.1 M sodium phosphate buffer (pH 7.0, Section 2.8.4), 0.1 ml 0.1 M H₂O₂ and 0.048 ml Guaiacol (Sigma, MO, U.S.A.), and kept at room temperature. 10 µl of lung homogenate was mixed with 190 µl of assay solution and the absorbance was read immediately at 470 nm for 1 minute using Infinite[®] M200 multimode reader (Tecan, Maennedorf, Switzerland). Samples were assayed in triplicates and the units were calculated as:

$$\text{Units/ml} = (\Delta\text{O.D.} \times V_t \times 4) / (E \times \Delta_t \times V_s) \times 2$$

where, V_t = total volume (ml), V_s = sample volume (ml), $\Delta\text{O.D.}$ = density change, Δ_t = time of measurement (minutes) and 2 is the conversion factor to 1 cm light path-length.

Four moles of H_2O_2 are required to produce 1 mole of tetraguaiacol product which has the extinction coefficient (E) of $26.6 \text{ mM}^{-1}\text{cm}^{-1}$ at 470 nm. The values were normalised to lung protein content.

2.5.4.4 Superoxide dismutase activity [Chapter 6]

SOD determination kit (Sigma 19160, MO, U.S.A.) was used according to the manufacturer's instructions. The values were normalised to lung protein content.

2.5.4.5 Protein concentration [Chapters 3-6]

Protein content in the lung homogenates were determined by modified Bradford method using Protein assay kit (Bio-rad, CA, U.S.A.) according to the manufacturer's instructions.

2.5.5 Extraction of RNA from lung tissues [Chapters 3 and 6]

Lungs were homogenised in 350 μl RNA lysis buffer (Qiagen, Netherlands) using GentleMACS homogenizer under RNA02 similar to section 2.5.4. RNA was extracted, converted to cDNA and subjected to real-time PCR analyses similar to section 2.4.5 using primers listed under table 2.1.

2.5.6 Paraffin-embedding of tissues and Haematoxylin & Eosin staining [Chapters 3-6]

Lungs were fixed in 4% (w/v) PFA for less than 48 hours and transferred into histology cassettes (SPL Lifesciences, Korea) and dehydrated in a tissue processor (Leica Biosystems, IL, U.S.A.) according to the manufacturer's instructions. The dehydrated tissues were embedded in paraffin and 5 μm sections

were cut using a microtome (Leica Biosystems, IL, U.S.A.) and mounted on pre-coated glass slides (Menzel-Gläser, Germany).

The sections were re-hydrated through a series of xylene (2 changes, 5 min each), 100% ethanol (2 changes, 30 sec each), 90% ethanol (30 sec), 70% ethanol (30 sec), 50% ethanol (30 sec) and finally 3 changes in d.H₂O.

Haematoxylin and Eosin staining was performed by immersing the rehydrated sections in Shandon's concentrated haematoxylin for 5 minutes, then differentiating for 30 sec and counter-staining with alcoholic Eosin (Section 2.8.5). The slides were mounted with PermountTM mounting medium (Thermo Fisher Scientific, U.K.).

2.5.7 Immunohistochemistry of lung sections and NETs scoring [Chapters 3-5]

The lung sections were rehydrated and subjected to heat-mediated antigen retrieval in sodium citrate buffer (Section 2.8.6) for 20 minutes. The sections were permeabilised with 0.025% TritonX-100 in 1x TBS for 10 minutes and then blocked with 3% BSA in 1x TBS for 2 hours. Mouse monoclonal anti-H2B and rabbit polyclonal anti-MPO antibodies (Abcam, Cambridge, U.K.) were diluted 1:1000 (confocal microscopy) or 1:250 with 1x TBS and incubated overnight at 4°C. 1:250 dilutions of anti-mouse Alexafluor 488 and anti-rabbit Alexafluor 555 (Molecular Probes, U.S.A.) were used as secondary antibodies along with 300 nM DAPI (Life technologies, U.S.A.) for 1 hour at room temperature in dark. The slides were mounted with slow-fade mounting medium (Life technologies,

U.S.A.) and observed under Olympus IX81 microscope or scanned with a high resolution MIRAX MIDI system (Carl Zeiss, Germany). At least 20 fields from the whole section were captured using Panoramic viewer and NETs were scored using a newly devised scoring system based on their morphological appearance as individual strands or clusters (Refer Figure 3.5 B and C, and Tables 3.1 and 3.2). The areas of the clusters were measured using ImageJ software (U.S.A.).

2.5.8 Analyses used for secondary pneumococcal study [Chapter 4]

2.5.8.1 RNA extraction and real-time PCR analyses

RNA from the tissues was extracted using TRIzol[®] (Invitrogen, U.S.A.). Hydrophobic and aqueous phase were separated by adding 200 μ l of chloroform (Sigma, MO, U.S.A.) per 1ml of TRIzol[®] to the samples and centrifuging at 13,200 rpm for 15 minutes at 4°C. 500 μ l of isopropanol (Sigma, MO, U.S.A.) was added to the aqueous phase to precipitate the RNA and the samples were centrifuged again at 13,200 rpm for 10 minutes at 4°C. The RNA pellet was washed with 750 μ l of cold 75% ethanol (Sigma, MO, U.S.A.) and centrifuged at 13,200 rpm for 5 minutes at 4°C. The RNA pellet was re-suspended in 20 μ l of DEPC-treated water (Invitrogen, U.S.A.) and the concentration of RNA samples were measured by BioTek[®] Microplate Reader (VT, U.S.A.).

1 μ g of RNA diluted in 4 μ l DEPC-treated H₂O was added to 1 μ l of Oligo(dT)15 Primer (Promega, WI, U.S.A.), and the mixture was incubated first at 70°C for 5 minutes and then at 4°C for 5 minutes using the T100[™] Thermo Cycler (Bio-Rad, CA, U.S.A.). The sample mixture was subsequently added to a

reaction mixture consisting of 4.2 µl of H₂O, 4 µl of ImProm-II™ 5X reaction buffer, 4.8 µl of MgCl₂, 1 µl of dNTP mix, and 1 µl of ImProm-II™ Reverse Transcriptase to form a total of 20 µl solution. The solution was then subjected to the following cycling conditions using T100™ Thermal Cycler (Bio-Rad, CA, U.S.A.) - 25°C for 5 min, 42°C for 1 hour, 70°C for 15 min and then hold at 4°C. The cDNA were stored at -20°C until use.

The cDNA were subjected to further analyses in a CFX Connect™ Real-time PCR detection system (Bio-Rad, CA, U.S.A.). SYBR® Green PCR master mix (Bio-Rad, CA, U.S.A.), 1 µl of cDNA and 1 µl of primer mixture for relevant genes were used according to the manufacturer's protocol. The PCR conditions are as follows - 95°C for 3 minutes followed by 40 cycles of 95°C for 10 sec and 60°C for 30 sec and finally at 65°C for 5 seconds. The primers used in the experiment are listed under table 2.1. Relative gene expression levels were calculated as mentioned in section 2.4.5.

2.5.8.2 Enzyme-linked immunosorbant assay

Sandwich ELISA using 96-well MicroWell™ MaxiSorp™ flat bottom plates (Nunc, U.S.A.) was performed to determine the concentrations of TNF-α, IL-6, IL-10 and IL-17. 100 µl of 1µg/ml (diluted in PBS) capture antibodies (BD Pharmingen, U.S.A.) was coated on to the wells at 4°C overnight. After washing once with 0.05% Tween-20 in PBS solution (Sigma, MO, U.S.A.), the wells were blocked using 5% BSA (PAA, Austria) in PBS) at 37°C for 1 hour. The wells were washed again once and 100 µl of standards and samples diluted in 5% BSA

were added to each well and incubated at 37°C for 3 hours. The wells were washed three times and then, 100 µl of 1µg/ml biotinylated detection antibodies (BD Pharmingen, U.S.A.) diluted in 5% BSA were added to each well and incubated at room temperature for 1 hour. After three washes, 100 µl of 1µg/ml streptavidin-HRP (Biolegend, U.S.A.) was added to each well and incubated at room temperature for 1 hour. Thereafter, the plates were washed 6 times. O-phenylenediamine dihydrochloride (OPD) (Sigma, MO, U.S.A.) was dissolved in d.H₂O and added as substrate to the plate and incubated at room temperature for 15 minutes. 4.5 N H₂SO₄ (Merck, Germany) was added to stop the reaction and the absorbance was read at 490 nm with BioTek[®] Synergy H1 Hybrid Multi-Mode Microplate Reader to determine the concentration of the cytokines.

IL-1β concentration was measured using specific ELISA kit (R&D systems, MN, U.S.A.) according to the manufacturer's protocol. The concentration was determined by measuring the absorbance at 450 nm with BioTek[®] Microplate Reader.

The concentration of cytokines were determined using the standard curve and were normalised to total protein concentration.

2.5.9 Special diet course [Chapter 5]

Four weeks old male BALB/c mice were acclimatised for 1 week with standard chow at the animal facility before beginning an 18 weeks schedule on defined diet. Special diets comprising 10% and 45% kcal from fat (Research diets,

NJ, U.S.A.) were provided to the mice categorised as low fat (LFD) and high fat (HFD) groups.

2.5.9.1 Body weight and BMI

Body weight (in g) and nose to anus length (in cm) were measured every week. BMI was calculated as $\text{weight (g)}/[\text{nose to anus length (mm)}]^2$.

2.5.9.2 Food and calorie intake

Weekly food consumption was monitored by subtracting the food remaining (g) from the food consumed (g). Calorie intake was calculated by adjusting for calories gained from fat – 1 g of LFD = 3.85 kcal and 1 g of HFD = 4.73 kcal.

2.5.9.3 Blood glucose level

Glucose levels in the blood were measured by tail vein puncture using Accu-Check[®] Performa glucometer (Roche, Basel, Switzerland) according to the manufacturer's instructions.

2.5.9.4 Harvesting organs and tissues

Infection with influenza virus was done as described in the section 2.5.1. Apart from lungs, other organs like brain, kidneys, heart, liver, spleen and white adipose tissues from gonadal, perirenal and interscapular (iBAT, brown adipose tissue) regions were harvested.

2.6 Statistical analyses [Chapters 3-6]

The statistical analyses were performed using SPSS version 22 (IBM, U.S.A.). Student's *t*-test was used for pairwise comparison, ANOVA with Tukey post-hoc correction (parametric data) and Kruskal-Wallis test with post-hoc Mann-Whitney pairwise comparison and Bonferroni correction (non-parametric data) were used for comparison of more than two groups. *P* values less than 0.05, 0.01, 0.001 and 0.0001 were considered significant as shown in the figures.

2.7 Histopathology scoring systems

All histopathology scoring were done in a blinded manner. Multiple fields were examined under 400x magnification and scores were assigned to specific criteria, weighted according to their relative importance. The individual scores were then added to generate the final lung injury score.

2.7.1 Comparison of influenza with secondary pneumococcal pneumonia [Chapter 3]

Modified from Matute-Bello et al., 2001

$$\text{Total score} = 1 \times (\text{alveolar hemorrhage, 0-3}) + 2 \times (\text{alveolar infiltrate, 0-3}) + 3 \times (\text{fibrin, 0-3}) + 1 \times (\text{alveolar septal congestion, 0-3})$$

where, 0-3 refers to 0 = Absent, 1 = Mild, 2 = Moderate and 3 = Severe.

Highest possible score = 21.

2.7.2 Comparison of different pneumococcal serotypes [Chapter 4]

Modified from McAuley et al., 2007

Total score = Cellular infiltration (0-3) + Necrosis (0-3) + Pleuritis (0-3) + Fibrin (0-3) + Percentage lung involvement (0-3)

where, 0-3 refers to 0 = Absent, 1 = Mild & <10% lung involved, 2 = Moderate & 10-30% lung involved, 3 = Severe & >30% lung involved.

Highest possible score = 15.

2.7.3 Influenza infection [Chapters 5 and 6]

Modified from Matute-Bello et al., 2001

Total score = 1 × (alveolar hemorrhage, 0-3) + 2 × (alveolar infiltrate, 0-3) + 2 × (bronchiolar infiltrate, 0-3) + 2 × (fibrin, 0-3) + 1 × (alveolar septal congestion, 0-3)

where, 0-3 refers to 0 = Absent, 1 = Mild, 2 = Moderate and 3 = Severe.

Highest possible score = 24.

Table 2.1. List of primers used for real time PCR (1st Base, Singapore and IDT, U.S.A.)

Gene	Primers	Sequence (5' – 3')	Usage
NP (H1N1 PR8)	Forward	GGGTGAGAATGGACGAAAAA	Chapter 3
	Reverse	TCCATCATTGCTTTTTGTGC	Chapter 3
Actb	Forward	GGCTGTATTCCCCTCCATCG	Chapter 3 for H1N1 NP
	Reverse	CCAGTTGGTAACAATGCCATGT	Chapter 3 for H1N1 NP
S100a8	Forward	AAATCACCATGCCCTCTACAAG	Chapter 3
	Reverse	CCCACTTTTATCACCATCGCAA	Chapter 3
S100a9	Forward	GCACAGTTGGCAACCTTTATG	Chapter 3
	Reverse	TGATTGTCCTGGTTTGTGTCC	Chapter 3
Ptx3	Forward	CGCAGGTTGTGAAACAGCAAT	Chapter 3
	Reverse	ATGCACGCTTCCAAAAATCTTC	Chapter 3
Ltf	Forward	CCGCTCAGTTGTGTCAAGAAA	Chapter 3
	Reverse	CATGGCATCAGCTCTGTTTGT	Chapter 3
Mmp9	Forward	GCAGAGGCATACTTGTACCG	Chapter 3
	Reverse	TGATGTTATGATGGTCCCCTTG	Chapter 3
Camp	Forward	GGCTGTGGCGGTCACTATC	Chapter 3
	Reverse	GTCTAGGGACTGCTGGTTGAA	Chapter 3
Gapdh	Forward	CTTCATTGACCTCAACTACA	Chapter 3,6
	Reverse	ATATTTCTCGTGGTTCACAC	Chapter 3,6
Ifnb	Forward	CCCTATGGAGATGACGGAGA	Chapter 4
	Reverse	CTGTCTGCTGGTGGAGTTCA	Chapter 4
Il1b	Forward	CAACCAACAAGTGATATTCTCCATG	Chapter 4
	Reverse	ATCCACACTCTCCAGCTGCA	Chapter 4

Ccl5	Forward	ATATGGCTCGGACACCA	Chapter 4
	Reverse	ACACACTTGGCGGTTTCCT	Chapter 4
Mkp2	Forward	TCTAAAACCAAGGCCCTGGC	Chapter 4
	Reverse	GCCTCCTCCAGCCTCACCCG	Chapter 4
Mkp3	Forward	GAGCTGGGCAACGAACGGCT	Chapter 4
	Reverse	ACCGGGAAGGAAGGCTGGCT	Chapter 4
Mkp5	Forward	GCTGTCCACATTAAGTGTGCCG	Chapter 4
	Reverse	TGGGCGTTAGCTCTGCGTTCTC	Chapter 4
Gapdh	Forward	GACAACCTTTGGCATTGTGG	Chapter 4
	Reverse	ATGCAGGGATGATGTTCTG	Chapter 4
Nox2	Forward	AGTGCGTGTTGCTCGACAA	Chapter 6
	Reverse	GCGGTGTGCAGTGCTATCAT	Chapter 6
Mpo	Forward	GCTGGAGAGTCGTGTTGGAA	Chapter 6
	Reverse	GAGCAGGCAAATCCAGTCCT	Chapter 6
Sod3	Forward	CCTTCTTGTTCTACGGCTTGC	Chapter 6
	Reverse	TCGCCTATCTTCTCAACCAGG	Chapter 6

2.8 Buffer and media preparations

2.8.1 10x Tris-buffered saline (TBS)

Tris base	24.23 g
NaCl	80.06 g
d. H ₂ O	800 ml

The contents were mixed well and the pH was adjusted to 7.6 with 6 N HCl and made up to 1 L.

2.8.2 Overlay medium (1.2% Avicel in 1x MEM) for plaque assay

Avicel (FMC Biopolymer, PA, U.S.A.): 6g in 250 ml d.H₂O. Autoclaved for 15 min and stored at 4°C until use.

2x MEM (Life technologies, U.S.A.): 1 pack MEM powder in 500 ml of d.H₂O with 2% HEPES buffer and 1.5% sodium bicarbonate. Filter-sterilised and stored at 4°C until use.

Avicel and 2x MEM were mixed in equal volumes prior to use.

2.8.3 1% crystal violet solution

Crystal Violet dye	1 g
Ethanol	20 ml
d.H ₂ O	80 ml

2.8.4 1M Sodium phosphate buffer, pH 7.0

1M Dibasic Na₂HPO₄ (100 ml)

Na₂HPO₄ 14.2 g

d.H₂O 100 ml

1M Monobasic NaH₂PO₄ (100 ml)

NaH₂PO₄ 13.8 g

d.H₂O 100 ml

1M Sodium phosphate buffer, pH 7.0

Na₂HPO₄ 57.7 ml

NaH₂PO₄ 42.3 ml

The pH was adjusted with NaH₂PO₄ (decreases pH) and Na₂HPO₄ (increases pH). The stock was autoclaved and stored at room temperature.

2.8.5 Haematoxylin and Eosin staining reagents

Shandon's Haematoxylin (Thermoscientific, U.S.A.)

Differentiation fluid:

HCl 250 µl

70% ethanol 100 ml

Eosin Y Stock Solution (1%):

Eosin Y 10 g

(Sigma, MO, U.S.A.)

d. H₂O 200 ml

95% Ethanol 800 ml

Dissolved and stored at room temperature.

Eosin Y series:

95% Ethanol: Alcoholic Eosin: 95% Ethanol: 100% Ethanol (3 changes):

Clearane (3 Changes).

Clearane (Leica Biosystems, IL, U.S.A.)

2.8.6 10x Sodium Citrate Buffer, pH 6.0 (1x, 10mM Sodium Citrate, 0.05% Tween-20)

Tri-sodium Citrate (dehydrate) 29.4 g

d.H₂O 1000 ml

The powder was dissolved in water and the pH was adjusted to 6.0 with 2 N HCl. 0.25 ml of Tween20 was added to 500 ml of 1x buffer and mixed well before use.

CHAPTER THREE

SECONDARY PNEUMOCOCCAL INFECTION AFTER INFLUENZA INFECTION LEADS TO HIGHER GENERATION OF NEUTROPHIL EXTRACELLULAR TRAPS IN MURINE LUNGS

3.1 Background

3.1.1 Epidemiology

Most complications of influenza infection arise not from the viral infection by itself but due to the onset of bacterial superinfections (Morens et al., 2008). Secondary bacterial infections can either occur as co-infections which involve the interaction between the virus and bacteria together with the host or they can occur after primary viral infections exploiting the virus-induced impaired host defences (Figure 3.1) (reviewed in (van der Sluijs et al., 2010)).

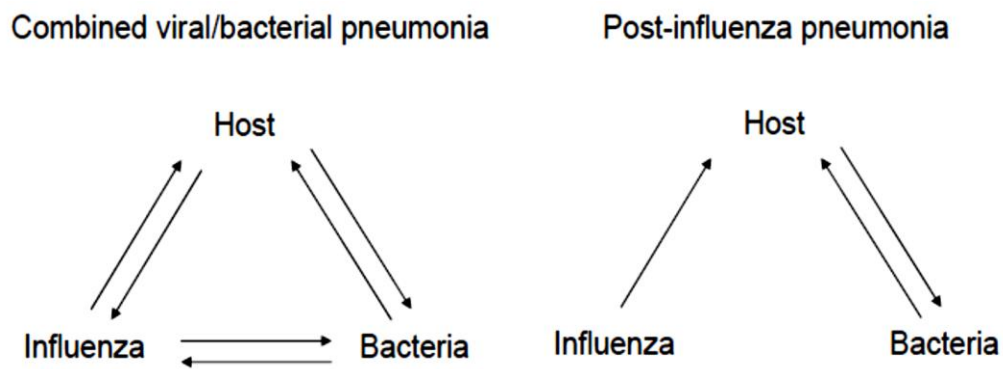


Figure 3.1. Complexity of combined viral/bacterial and post-influenza pneumonia. There is a multi-factorial interaction between the virus, the bacteria and the host during combined viral/bacterial infection whereas in post-influenza bacterial pneumonia, the virus-induced changes to the host affect the course of bacterial infection. (Adapted from van der Sluijs et al., 2010).

Histopathological and bacteriological analyses of 1918 ‘Spanish flu’ and 1957 ‘Asian flu’ have indicated the presence of bacterial infections in severely lethal cases (Hers et al., 1958; Morens et al., 2008). Bacterial co-infection accounted for nearly 30 percent of cases studied during the ‘Asian flu’ (Hers et al., 1958).

The bacteria that are commonly associated with secondary infections are *Staphylococcus aureus*, *Streptococcus pneumoniae*, *Streptococcus pyogenes* and *Haemophilus influenzae*. Among these, *Streptococcus pneumoniae* has been the focus of much research as it has been implicated in many cases of severe invasive pneumonia post-influenza infections including the ‘Spanish flu’ (Grabowska et al., 2006; Walters et al., 2015).

3.1.2 Pneumococcal respiratory infection and pneumonia

Streptococcus pneumoniae or pneumococcus (*S. pneumoniae* or SP) is a Gram positive, alpha-haemolytic, facultative anaerobic coccoid bacterium that occurs as diplococci (Figure 3.2 A) when grown in liquid media (WHO, April 2012⁹). First isolated in 1881 by Louis Pasteur and George Steinberg independently (Austrian, 1999), it has undergone nomenclature change from *Diplococcus pneumoniae* in 1920 to *Streptococcus pneumoniae* in 1974. *S. pneumoniae* is commonly found in the nasopharynx of healthy individuals where it remains asymptomatic. However, in immunocompromised individuals like HIV patients as well as individuals with lower immunity due to age and predisposing conditions like viral infections, it can turn pathogenic (Siemieniuk et al., 2011). It can cause infection in many parts of the body namely middle ear (Otitis media), respiratory tract (acute sinusitis,

bronchitis and pneumonia) or blood (bacteraemia). Once in blood, it can spread to other parts like bones (osteomyelitis), joints (septic arthritis), brain (meningitis) etc. Severe infections involving bacteraemia, meningitis or bacteraemic pneumonia are known as invasive pneumococcal disease (IPD) (WHO, April 2012⁹).

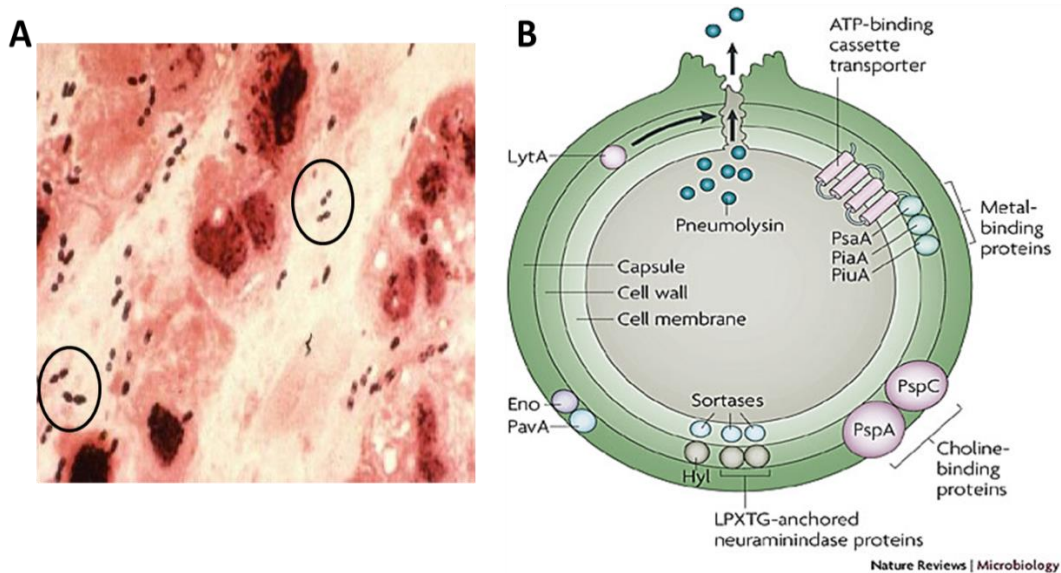


Figure 3.2. *S. pneumoniae* and virulence factors. (A) Gram stained-sputum film from a case of lobar pneumonia showing the presence of *S. pneumoniae* (encircled). (Adapted from Todar's online Textbook of bacteriology¹⁰) (B) Virulence factors of *S. pneumoniae*. Abbreviations: Psp – pneumococcal surface proteins, Hyl - hyaluronate lyase, PavA - pneumococcal adhesion and virulence A, Eno – enolase, LytA - autolysin A, Psa A - pneumococcal surface antigen A, PiaA - pneumococcal iron acquisition A and PiuA - pneumococcal iron uptake A. (Adapted from Kadioglu et al., 2008).

S. pneumoniae possesses various virulence factors that help in infecting host cells and evading host defences. Some of the important virulence factors are (i) the polysaccharide capsule (PS) that inhibits C3b opsonisation of bacteria thus preventing phagocytosis, (ii) pneumolysin (Ply), a pore-forming 53 kDa protein, (iii) autolysin (LytA) that lyses bacterial cells to release the toxic components like

pneumolysin, (iv) pili that helps in colonization and (v) H₂O₂ that is cytotoxic to the cells (Figure 3.2 B) (reviewed in (Mitchell AM & Mitchell TJ, 2010)).

Clinical onset of pneumococcal infection is characterised by sudden fever and chills. Chest pain may follow. Infection usually starts with the nasopharynx and spreads to lungs via bronchial infection. Most of the pneumococcal infections are characterised by lobar infection which develops in the distal airways and spreads to the adjacent lungs creating a homogenous pattern of consolidation. The lungs show progressive oedema and hepatisation of tissue (a liver-like appearance due to infiltration by blood cells from capillaries into lung tissues). Intense inflammatory response follows, predominated by neutrophils, leading to intra-alveolar haemorrhage. The bacterial growth is initially stable till about 4 hours after which it drastically multiplies by 60 hours. Death usually occurs by 72 hours in lethal cases if left untreated. During the final stages of IPD, the bacteria enter the blood stream causing bacteraemia which may progress to sepsis (Bergeron et al., 1998; Kadioglu et al., 2002); (reviewed in (Chiavolini et al., 2008; Reynolds et al., 2010)).

3.1.3 Secondary pneumococcal infection post-influenza infection

While the combined bacterial-influenza infection makes the virus compete with the bacteria to colonise the host and face a stronger host immune response due to simultaneous bacteria-induced inflammation; secondary bacterial infection after influenza infection allows the virus to exploit the lung environment first and thereby, making later bacterial propagation in the lungs conducive. By the time

the bacteria efficiently multiply in the lung, the virus is almost cleared out of the system. Combined viral-bacterial infection is indistinguishable from bacterial pneumonia by radiology alone and hence is very difficult to diagnose. However, the secondary bacterial infections are easier to diagnose due to clear demarcation of timeline between onsets of the two infections. (Reviewed in (van der Sluijs et al., 2010)).

There exists a lethal synergism between viral and pneumococcal infections during secondary infection (McCullers & Rehg, 2002; Smith et al., 2013). The viral load is mostly unaffected by the bacterial multiplication in the lungs, however some researchers have noticed initial rebounding of viral titres soon after bacterial infection due to increased virus release from infected cells (Smith et al., 2013). The pneumococci multiply very fast and remain elevated until the end of the infection period if left unchecked. The bacterial colony forming units required to kill mice in experimental secondary infection with pneumococcus was found to be significantly lower when compared to primary infection by bacteria alone (McCullers & Rehg, 2002). It has also been shown that influenza NA mediates increased adherence of pneumococci to lung epithelium by sialidase activity thereby reducing mucocilliary clearance of pneumococci (Peltola & McCullers, 2004). Pneumococci also possess two types of NA, NanA and NanB, which helps in pneumococcal adherence to lung epithelial cells. Prior influenza infection provides an already cleaved platform for the bacteria and hence aids in enhanced adhesion (Peltola & McCullers, 2004). The correlation between influenza virus-mediated upregulation of platelet-activating factor receptor (PAFr) and

pneumococcal adhesion has also been studied as the bacteria possesses a PAF ligand, phosphorylcholine. Mice deficient in PAFr show better survival due to reduced lung bacterial burden and dissemination of infection (van der Sluijs et al., 2006). Blocking of PAFr however did not affect pneumococcal infection highlighting the complexity of infection dynamics (McCullers & Rehg, 2002). Several studies have reported immune system desensitisation and suppression during secondary pneumococcal infection (Kash et al., 2011; McNamee & Harmsen, 2006; Smith et al., 2013). Impaired lung responses and PMN dysfunction have been observed in mice infected with pneumococci post-influenza infection. While neutrophil accumulation and pro-inflammatory cytokines increase in the lung environment, the neutrophils are unable to clear bacteria from the lungs due to initial increase in bacterial phagocytosis that forces the neutrophils to undergo enhanced respiratory burst and apoptosis and apoptotic clearance by macrophages (Engelich et al., 2001; Speshock et al., 2007). Increases in both type I and II interferon levels suppresses phagocytic activity and leads to impaired clearance of the bacteria (Sun & Metzger, 2008; Shahangian 2009). Enhanced levels of anti-inflammatory cytokine, IL-10 during secondary infection also contributes to neutrophil dysfunction highlighting the importance of coordination between pro-and anti-inflammatory responses in the host (van der Sluijs et al., 2004).

3.1.4 Treatment available

Treatment of secondary infection lies in the effective and timely treatment of primary influenza infection to prevent the occurrence of secondary bacterial

infections. Hence, vaccinations and anti-virals play a major role in averting lethal bacterial infections. Moreover, pneumococcus has also been shown to be partly dependent on NA activity for adhesion and hence neuraminidase inhibitors like oseltamivir and zanamivir may help in treating secondary bacterial infections (reviewed in (van der Sluijs et al., 2010)). In an experimental model of secondary pneumococcal infection, even delayed oseltamivir treatment was shown to be effective in reducing the severity of pneumococcal infection though it may not reduce the mortality by 100 percent unless captured within the crucial active viral replication phase (Peltola & McCullers, 2004). Antibiotics such as fluoroquinolones and macrolides help in treating mild cases. Capsular PS-based vaccinations may prevent secondary infection with some of the *S. pneumoniae* serotypes (WHO, April 2012⁹).

3.1.5 Streptococcus pneumoniae and NETs

Various studies have shown that *S. pneumoniae* is susceptible to many neutrophil granular proteins like MMP 2 and 9, Leukotriene B4 and serine proteases (Hong et al., 2011; Mancuso et al., 2010; Standish et al., 2009). Yet, virulent serotypes of *S. pneumoniae* are successful in causing invasive infections. Studies have shown that *S. pneumoniae* can outcompete other respiratory bacteria including common pathogens like *H. influenzae* and *Neisseria meningitidis*, by secreting H₂O₂ thereby making the shared lung microenvironment toxic for these bacteria to proliferate (Pericone et al., 2000). After overtaking the lung colonisation, *S. pneumoniae* deals with the host immune system by using its capsule to prevent phagocytosis. In fact, all the *S. pneumoniae* serotypes are

characterised by their pathogenicity based on the presence of surface capsule. Thus, an important defence mechanism of neutrophils to tackle pathogens is compromised by *S. pneumoniae* (Hyams et al., 2010).

In the absence of phagocytic killing, NETosis forms a crucial back-up defensive action by the host. Though α -enolase produced by *S. pneumoniae* has been shown to induce NETs *in vitro*, the bacteria have found ways to escape them (Beiter et al., 2006; Mori et al., 2012; Wartha et al., 2007). Wartha *et al.* have shown that capsule and D-alanylation of lipoteichoic acid (LTA) in conjunction with each other help in reducing bacterial entrapment on NETs but capsules as such do not provide resistance to NETs-mediated killing. D-alanylation of LTAs, polymers that are anchored to the cytoplasmic membrane via glycolipids, introduces a positive charge that requires a D-alanine-activating enzyme and a D-alanine-D-alanyl carrier protein ligase; both encoded on the *dlt* operon. Deletion of *dltA* gene rendered non-capsulated strains sensitive to killing by cationic AMPs while there was no effect on the capsulated strains. However, the *dltA* mutant of an encapsulated strain got easily outcompeted by the wild type which spread to the lungs and bloodstream in a murine model of pneumococcal pneumonia. Thus, the authors concluded that D-alanylation of LTA may play an important role in the early stages of pneumococcal invasion when the capsule expression is supposed to be low.

Another important study by Beiter et al. (2006) showed that pneumococci bear surface endonucleases, encoded by *endA* gene that can cleave NET DNA structures thus helping the trapped bacterium to avoid close contact with the

AMPs. *EndA* is a Mn^{2+}/Mg^{2+} -dependent membrane-bound DNA-entry nuclease that functions by introducing single-stranded nicks on the extracellular DNA which is followed by a second nick in the opposite direction that initiates DNA entry (Smith et al., 1985). However, recent studies have shown that *EndA* can be secreted by pneumococci under certain growth conditions, which may have far-reaching impact than just being restricted to local DNA traps (Zhu et al., 2013).

3.2 Specific objectives of the study

Current research has focused on the generation of NETs during primary influenza and primary pneumococcal infections but their significance during bacterial superinfections has not been considered yet. Moreover, there is a lack of quantitative studies on NETs *in vivo* and hence their real importance during an infection is very difficult to enunciate. Based on the current knowledge, we are unable to clearly articulate whether NETs generated during primary influenza infection are further enhanced during secondary bacterial infections *in vivo* and whether they provide any beneficial bactericidal protection against pneumococci. Hence, our study focusses on assessing the generation and importance of NETs during secondary pneumococcal infection after primary influenza infection.

The specific objectives of the study are,

- a) To evaluate the pathology of secondary pneumococcal infection in a murine model and study the generation of NETs in the lungs of infected mice.

- b) To develop a semi-quantitative scoring methodology to analyse NETs *in vivo*.
- c) To assess whether NETs play a harmful role inside the host or whether they provide some beneficial protection against the bacteria.
- d) To study NETs generated by influenza virus and pneumococci in an *in vitro* NETs generation model that mimics primary influenza infection and secondary pneumococcal infections.

3.3 Results and Discussion

3.3.1 Lethal synergism between primary influenza infection and secondary pneumococcal infection leads to increased bacterial persistence in lungs and higher lung pathology

To determine if there exists any lethal synergism between primary influenza infection and secondary pneumococcal infection, mice were challenged with sub-lethal doses of first influenza infection followed by *S. pneumoniae* 19F at day 7 post-infection and the microbial replication in the lungs were analysed.

The lung viral titres remained mostly unaltered until day 5 post-secondary pneumococcal infection when the viral NP RNA levels significantly declined when compared to influenza alone infection (Figure 3.3 A). On the contrary, the bacterial load in the lungs remained persistent post-secondary infection when compared to bacteria alone infection (Figure 3.3 B) indicating that the bacteria was able to exploit the already influenza-damaged lung environment for its

efficient replication. This corresponds to other related studies which showed that secondary infection does not alter viral replication but positively affects bacterial replication probably due to enhanced bacterial adherence to cell membrane (Kash et al. 2011; Peltola & McCullers, 2004).

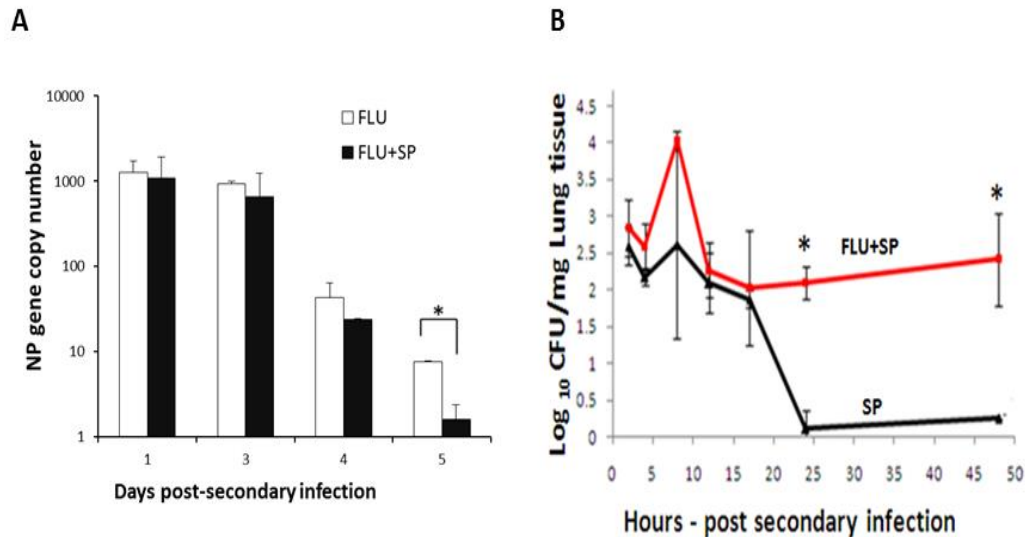


Figure 3.3. Microbial replication in the lungs of dually infected mice. C57BL/6 mice were infected with sub-lethal dose (30 PFU) of influenza PR8 virus (FLU) or mock-infected with PBS (control). Seven days after influenza infection, mice were challenged with sub-lethal doses of *S. pneumoniae* 19F (10^5 CFU) for bacterial infection alone (SP) and dual infection (FLU + SP) experiments. **(A)** Real-time PCR analysis was performed to detect the expression of the viral nucleoprotein gene until 5 days post-secondary infection. **(B)** Lung bacterial load was estimated by colony count method in the tissue homogenates of mice with bacteria only and dual infection until 48 hours post-secondary infection. Values represent the means \pm SE of 3 animals per group (Single experiment). * represents P value < 0.05 , Student's t -test.

To compare NETs at similar severity of infections, mice were challenged with lethal dose of influenza virus followed by sub-lethal challenge with *S. pneumoniae* 19F and monitored until 30% loss from initial body weight. Histopathological analyses revealed severe diffused pulmonary damage in mice infected with virus alone and virus-bacteria dual infection. The lung samples from

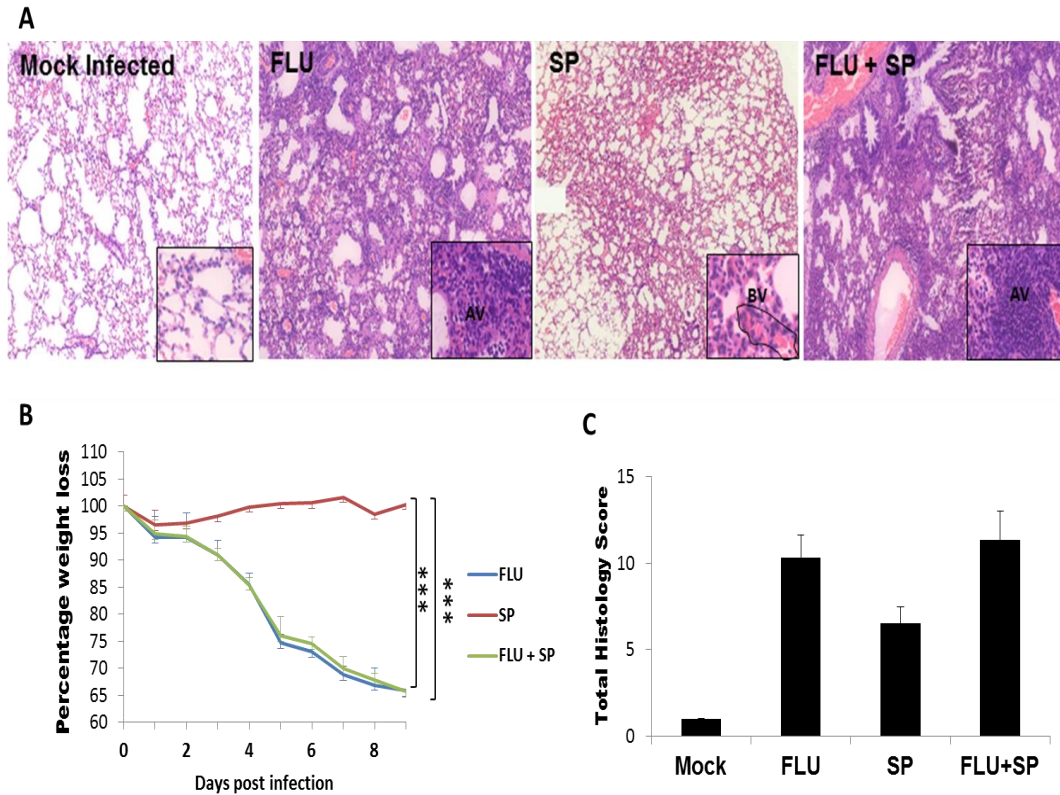


Figure 3.4. Histopathological analyses of lung sections. C57BL/6 mice were infected with lethal doses of influenza virus (250 PFU) or mock-infected with PBS (Mock). Seven days after influenza infection, mice were challenged with sub-lethal doses of *S. pneumoniae* 19F (10^5 CFU) for bacterial infection alone (SP) and dual infection (FLU+SP) experiments. **(A)** Histopathologic analyses of lung sections reveal alveolar-septal congestion and inflammation in the influenza-infected mice, while infection with bacteria alone for 48h did not cause severe pathology with inflammation mainly concentrated in the blood vessels (BV). Dual infection culminated in extensive pulmonary damage and severe pneumonia with inflammation in the alveoli (AV). Mock-infected animals showed normal alveolar architecture. Magnification of images: 100x (main panels) and 400x (inserts). **(B)** Flu alone and Flu+SP showed similar trend in body weight loss post-infection while the bacteria alone group lost very little weight. *** indicates P value < 0.001 . **(C)** Histopathologic scores of lungs were comparable between influenza alone and dual infection groups. P value not significant. Values represent the means \pm SE of 6 animals per group (2 independent experiments), Student's t -test.

these groups showed severe pulmonary consolidation, septal congestion, fibrin deposition and cellular infiltration in the alveoli and large air spaces as well as in blood vessels. Though the dual infection group was almost indistinguishable from the virus alone group based on lung histology and clinical signs like body weight

loss, pockets of proteinaceous exudates and neutrophil infiltration were more pronounced in the former possibly due to enhanced cytokine levels from primary influenza infection that may have gone awry after bacterial infection. In comparison, the bacteria alone group showed focal inflammation with infiltration concentrated more in the small blood vessels and capillaries (Figure 3.4 A and B). The histology scores did not show any significant difference between the three groups though the bacteria alone group had the lowest scores (Figure 3.4 C).

3.3.2 Secondary bacterial infection with pneumococcus leads to enhanced NETs formation in the lungs

To assess the extent of NETs generation in the lungs of infected mice, a scoring system was devised based on immunostaining of NET components. DNA, histone and MPO were detected using antibodies and fluorochromes to locate NETs in the lung sections (Figure 3.5 A). NETs were classified based on their appearance and size (Figure 3.5 B and C) and scores were assigned based on the area occupied with the single strands getting lower scores (1-2) while the clusters were ranked higher (2-10) (Tables 3.1 and 3.2). Based on this scoring system, NETs were found to be highest in the dual infected mice group while being the lowest in the influenza alone infection group. Interestingly, the bacteria alone infection group received an intermediate score higher than influenza alone group despite having the lowest histology score (Figure 3.5 D). The comparatively higher score of NETs after pneumococcal infection could have been due to neutrophil-predominant infiltration with the presence of large NET clusters as opposed to single strands and smaller clusters after only influenza infection.

Hence, it can be said that pneumococcal infection influences NETs formation in the lungs of influenza-infected mice. Neutrophils and other phagocytes recognise different pathogens through different receptor e.g., TLR2 to detect LPS and TLR7/8 to detect influenza virus (reviewed in (Brinkmann & Zychlinsky, 2007)); (Lee et al., 2014; Wang et al., 2008). Hence, the activation pattern of neutrophils is highly dependent on the stimulant. Further studies need to be done based on the receptors engaged by pneumococcus and influenza virus in influencing NETosis. As NETosis involves various receptors, different mechanisms of activation may occur based on the pathogen involved.

Category	Number	Area (μm^2)	Score
None	N.A.	N.A.	0
Single strand	<5	N.A.	1
Single strand	≥ 5	N.A.	2
Cluster, Small	1	<500	2
Cluster, Small + Single strands/clusters	>1	<500	4
Cluster, Medium	1	500-5000	6
Cluster, Medium + small cluster/strands	>1	500-5000	8
Cluster, Large \pm small cluster/strands	N.A.	>5000	10

Table 3.1. Semi-quantitative scoring system for the evaluation of NETs in the lungs of infected mice. Total score = Sum of scores in 20 fields under 400x magnification. Areas of NET clusters were delineated and calculated using the ImageJ software. N.A. = Not available.

1. Attributes :

- Absent/Present
- Single strand/cluster
- Single strand → numbers present
- Cluster → size

2. Weightage for attributes:

- Single strands:
Less area covered → less score
- Clusters & size:
Area covered more than or equal to single strand → increasing scores based on size
- Clusters + Single strands:
Undefined region. Total NETs area not quantifiable.
Considered bigger than the cluster involved → Higher scores

3. Scores for attributes:

- Presence: Absent → 0, Present → ≥1 (Go to next attribute)
- Nature: If, Single strand → Numbers → <5 = 1 or >5 = 2

Else, Clusters →

Small (<500 μm ²)	2	} 2 ^(1,2,3,4,5) increase
Small + Single strands/small clusters	4	
Medium (500 μm ² - 5000 μm ²)	6	
Medium + Single strands/small clusters	8	
Large (>5000 μm ²) ± Single strands/small clusters	10	

4. Calculation: Maximum quantifiable fields of a section suitable for large sample size i.e. 20

Table 3.2. Attributes and corresponding weightage used for NETs scoring. (1) Attributes of NETs were defined based on the appearance and (2) weightage was assigned to each attribute according to the area occupied by the NET structures in the lung tissue. (3) Scores were given to each attribute according to the weightage after sampling multiple sections with varying levels of tissue damage and cellular infiltration (*data not shown*). Finally, (4) a minimum quantifiable number of fields were selected for total NETs calculator.

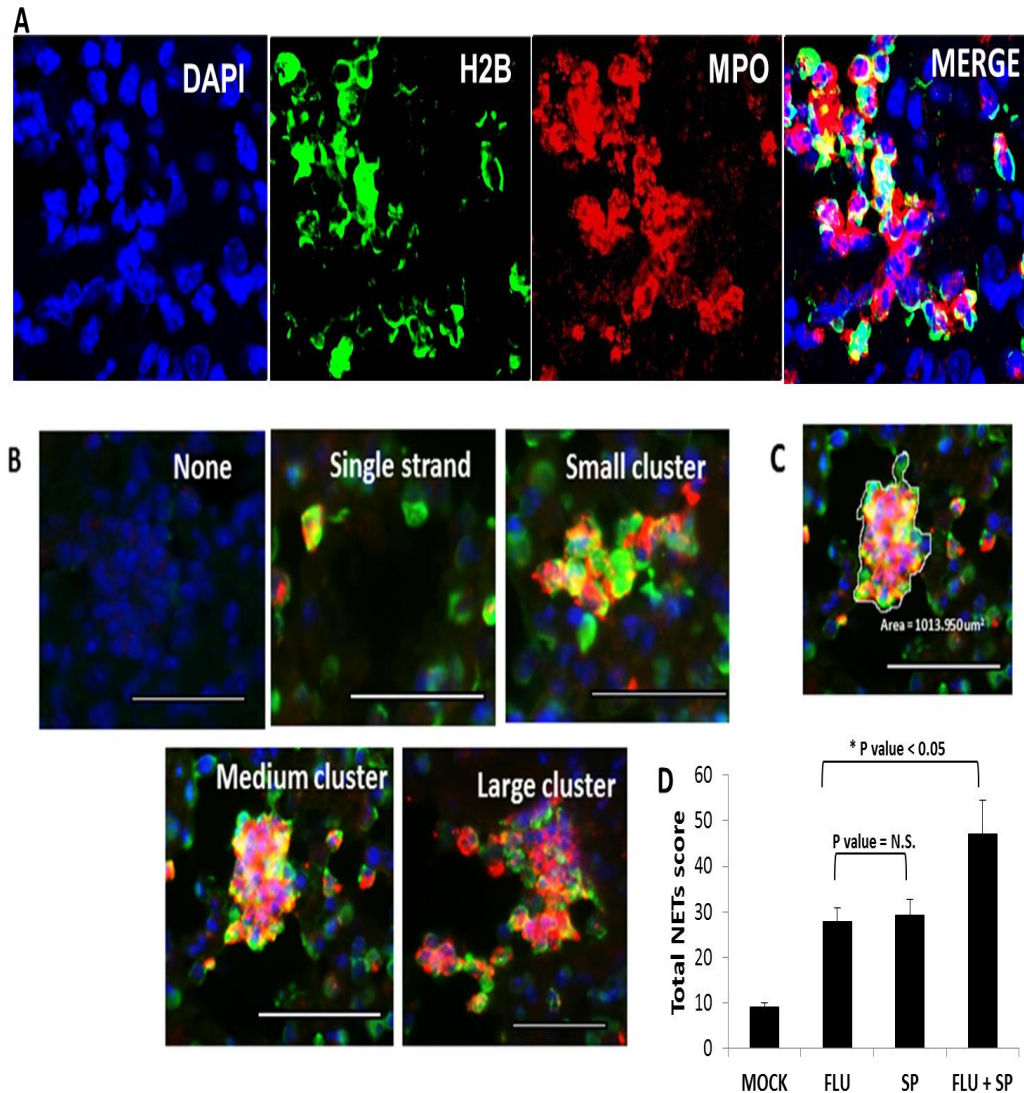


Figure 3.5. Immunofluorescence detection and quantification of NETs in the lungs of infected mice. (A) NETs were identified in 5 μm thin lung tissue sections from mice infected with a lethal dose of influenza virus followed by *S. pneumoniae*, using immunostaining with DAPI (blue) and antibodies for Histone2B (green) & MPO (red). (B) NETs were detected using immunofluorescence technique and categorised as single strands or small to large clusters based on their morphological appearance. Scale bar = 50 μm . (C) An illustrative image of a NET cluster with area demarcated for measurement using imageJ software. (D) A total of 20 fields per lung section were assessed and scores were assigned based on Table 3.1. The total NETs score were estimated as the sum of all 20 fields per section. Values represent the means \pm SE of 6 animals per group (2 independent experiments). * indicates P value < 0.05; N.S. = Not significant, Student's t-test.

3.3.3 NETs induced *in vitro* representing primary influenza-secondary pneumococcal stimulation are influenced by redox enzymes

To assess NETs generation *in vitro*, neutrophils were extracted from bone marrow of healthy donor mice and incubated with various stimulants to mimic primary influenza condition. For the virus-mediated NETs generation, neutrophils were incubated either with virus at MOI 1 or BAL fluid of mice infected with 50 PFU or 500 PFU virus (50 or 500 PFU BALF). The use of BALF represents the lung microenvironment after low and very high lethal doses of virus on day 5 post-infection. Day 5 was chosen as it represents the highest viral replication-active infiltration phase in lungs of lethally infected mice (Fukushi et al., 2011). As controls, neutrophils were incubated with BALF of mice treated with just PBS under the same conditions. 10 μ M H₂O₂ served as positive control while the resting neutrophils were incubated with just PBS. After 2 hours, the cells were fixed, immunostained and NETs were counted (Figure 3.6 A and D). The neutrophils incubated with 500 PFU BALF generated the highest NETs when compared to virus alone or 50 PFU BALF. Both H₂O₂ positive control and 500 PFU-BALF generated significantly higher NETs when compared to uninfected and 50 PFU BALF groups (Figure 3.6 A). This shows that the lung microenvironment after viral infection has potential stimulants for inducing NETs in neutrophils recruited to lungs and the lethality of infection due to initial infectious dose of virus can affect the extent of NETosis.

When neutrophils were incubated with 500 PFU BALF (FLU-BALF) along with control uninfected BALF (CON-BALF) for various time points, NETs could

be induced as early as 30 minutes with 500 PFU BALF signifying NETosis as an early event in influenza infection (Figure 3.6 B). It has been reported that the cytokines and redox state of host microenvironment can influence NETs generation. Neutrophils incubated with various inhibitors of redox enzymes failed to generate significant NETs upon incubation with influenza virus-infected epithelial cells (Narasaraju et al., 2011). Indeed, when we incubated neutrophils with inhibitors of NADPH oxidase, MPO and SOD, NETs were significantly reduced upon inhibition of NADPH oxidase and MPO but not SOD (Figure 3.6 C). This confirms that the redox state of the lung microenvironment influences NETs generation perhaps because NETosis is mostly an oxidative process.

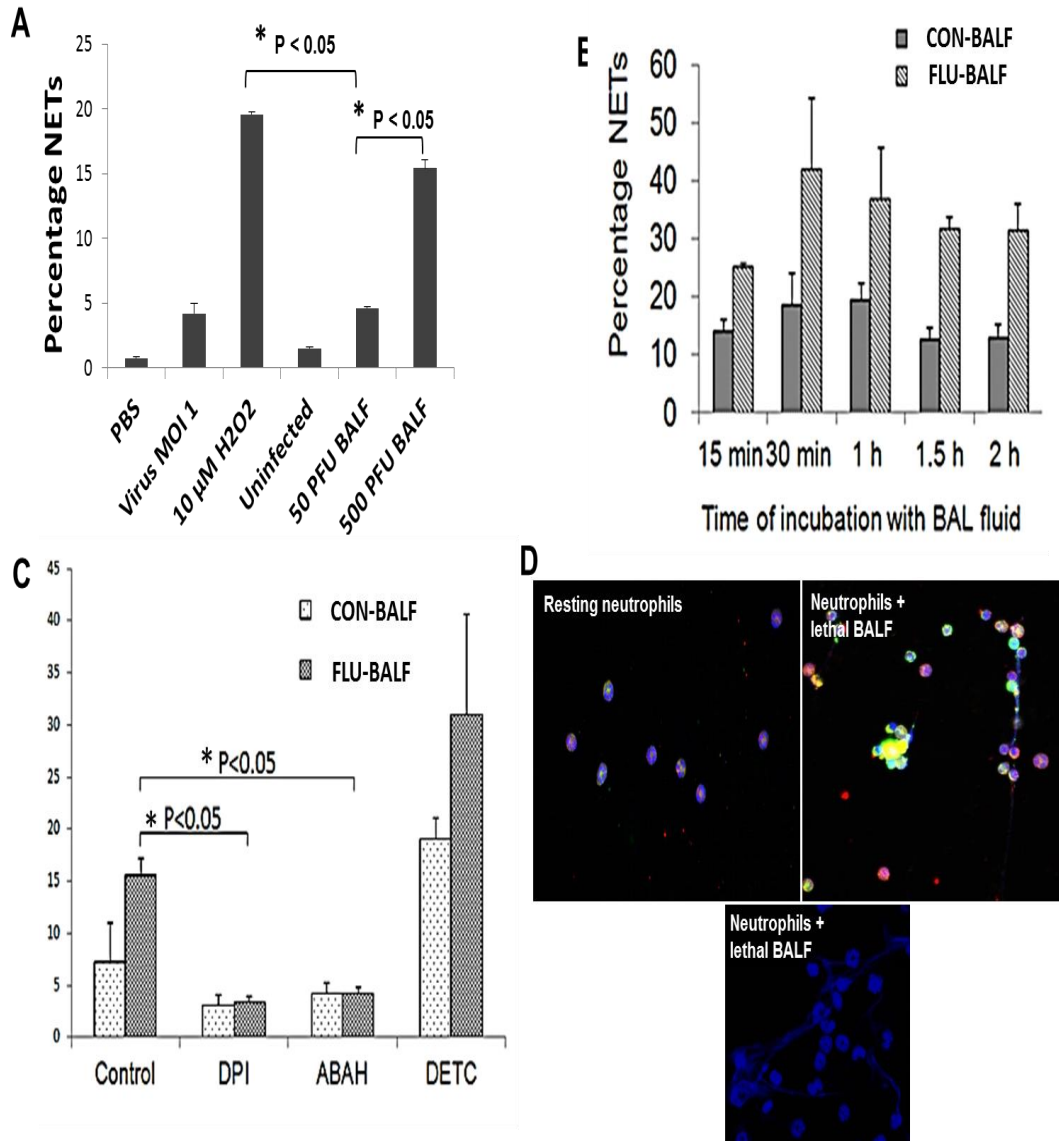


Figure 3.6. Induction of NETs *ex vivo* mimicking primary influenza stimulation. (A) Mature neutrophils from bone-marrow of healthy donor mice were incubated for 2 hours with 10 μ M H₂O₂ or influenza A PR8 virus at MOI 1 or BALF from mice instilled with PBS (CON-BALF) or infected with 50 PFU or 500 PFU PR8 virus on day 5 post infection. Highest NETs were generated with 10 μ M H₂O₂ and 500 PFU BALF (FLU-BALF) stimulation. * indicates *P* value < 0.05, Student's *t*-test. (B) Neutrophils stimulated with FLU-BALF produced high amounts of NETs as early as 30 minutes when compared to stimulation with uninfected mice BALF (CON-BALF). *P* value not significant, ANOVA with tukey post-hoc correction. (C) NETs formation after 2 hours incubation was significantly reduced upon treatment with inhibitors of redox enzymes NADPH oxidase (10 μ M DPI) and MPO (100 μ M ABAH) whereas SOD inhibition (100 μ M DETC) increased NETs generation. * denotes *P*<0.05 vs control (FLU-BALF incubation), Kruskal-Wallis test with Mann-Whitney pairwise comparison and Bonferroni correction. (D) Representative immune-labelled images (DAPI-H2B-MPO as blue-green-red) of resting and FLU-BALF-stimulated neutrophils. Magnification of 600x (top panel) and 1200x (bottom panel). Values represent means \pm SE of at least three independent experiments.

To assess whether NETs generated during influenza infection are influenced by secondary bacterial infections *in vitro*, NETs were generated by incubating neutrophils with lethal FLU-BALF (500 PFU) for 2 hours and then incubated for 2 hours with *S. pneumoniae* serotype 19F at different MOIs. The entrapment of bacteria on NETs increased proportionately to the amount of bacteria added (Figures 3.7 A and B).

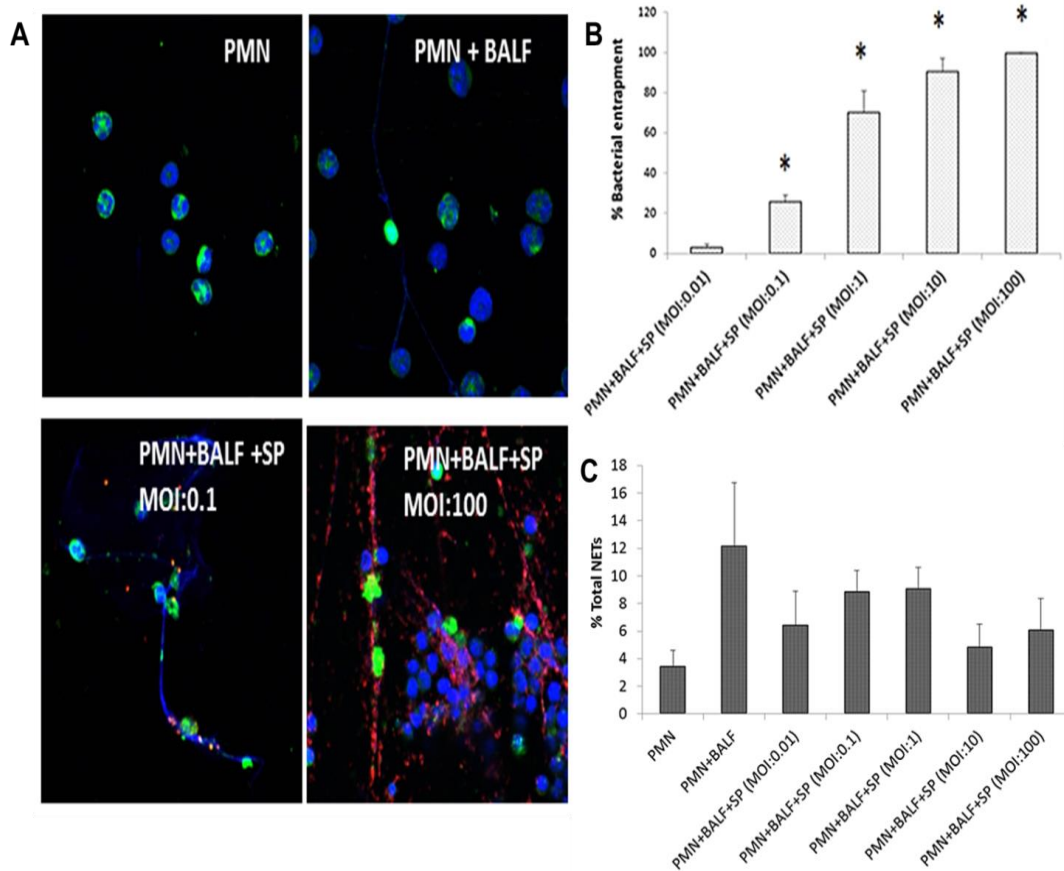


Figure 3.7. Pneumococcal entrapment on NETs released during influenza stimulation. NETs were induced using influenza-infected BALF for 2 hours after which *S. pneumoniae* 19F were added. (A-B) *S. pneumoniae* 19F (red) were found entrapped within the NET fibers (DNA-blue and H2B-green). Bacterial entrapment on NETs progressively increased with increasing multiplicity of infection with higher MOI of 100 displaying greater accumulation and entrapment of bacteria near NETs compared to lower MOI of 0.1. * denotes P value < 0.05 versus MOI of 0.01. (C) Infection with different MOI of bacteria resulted in variation of total NETs implying degradation of NETs by *S. pneumoniae*. P value not significant versus PMN+BALF group. Values represent the means \pm SE of at least 3 independent experiments, Student's t -test.

3.3.4 NETs are partially degraded in the presence of *S. pneumoniae*

As mentioned in section 3.3.2, NETs were seen mainly as clusters in the lungs of dually infected mice. Apart from intact clusters, some apparent degradation of NETs after pneumococcal infection was also noticed (Figure 3.8 A and B). Upon staining for DNA-H2B-MPO complex, the NETs in the lungs of dually infected mice showed scattered staining for histone and MPO surrounding the DNA strands or clusters whereas in the lungs of mice with influenza virus alone infection, the NET strands were found to be intact (Figure 3.8 C and D). Pneumococci generate endonucleases that are known to degrade NETs and DNA *in vitro* (Beiter et al., 2006 and Figure 3.10 D). Due to lack of an effective antibody to detect pneumococcus in tissue samples, this phenomenon could not be confirmed by locating pneumococcus concentrated around the degraded clusters. Nevertheless, the presence of degraded NET clusters could indicate higher possibility of lung damage as cytotoxic proteins scattered from the degraded NETs can spread to nearby tissues or leak into bloodstream. Indeed, NETs have been implicated in deep vein thrombosis in rodents and humans (Fuchs et al., 2010).

However, when pneumococci were incubated at different MOIs with NETs formed by lethal BALF of influenza-infected mice, the final amount of NETs in the samples varied giving inconclusive trend (Figure 3.7 C). Again, due to the lack of a sensitive assay to quantify varying levels of endonuclease activity in smaller bacterial numbers, this observation could not be directly correlated to endonuclease activity of pneumococci.

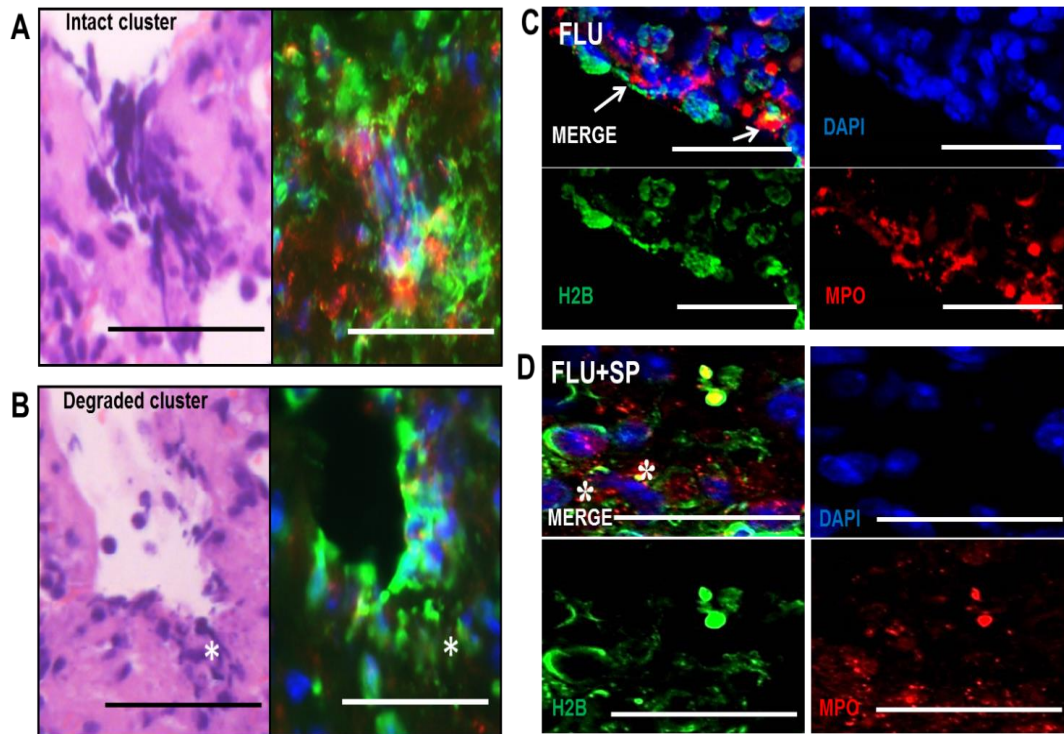


Figure 3.8. Partial degradation of NETs in the lungs of dually infected mice. (A-B) Haematoxylin and eosin stained-image of lung sections from mice with dual viral and bacterial infection that show both (A) large intact clusters as well as (B) degraded NETs. *Scale bar = 50 μm.* (C-D) Immuno-labelled images (DAPI-H2B-MPO as blue-green-red) of lungs sections from influenza alone infection groups revealed intact extracellular NET strands (C, Flu) whereas dual infection group (D, Flu+SP) showed large clusters of NETs often filled with degraded DNA and surrounded by dispersed MPO and histone 2B. Arrows indicate intact NET structures while asterix indicate degraded NETs. *Scale bar = 20 μm.*

3.3.5 NETs do not show antibacterial activity but possess antifungal activity

To assess the expression of antibacterial genes during NETs generation, neutrophils were incubated with FLU-BALF for different time points; after which RNA was extracted for real time PCR analyses. Six antimicrobial proteins were identified from gene expression in the lungs of lethal influenza-infected mice by DNA microarray (data not shown). These were calprotectin dimer-forming S100 proteins A8 and A9, pentraxin 3, lactotransferrin, cathelicidin and MMP9. Real

time PCR analyses of all six genes did not show any significant gene expression up to 2 hours post-incubation (Figure 3.9).

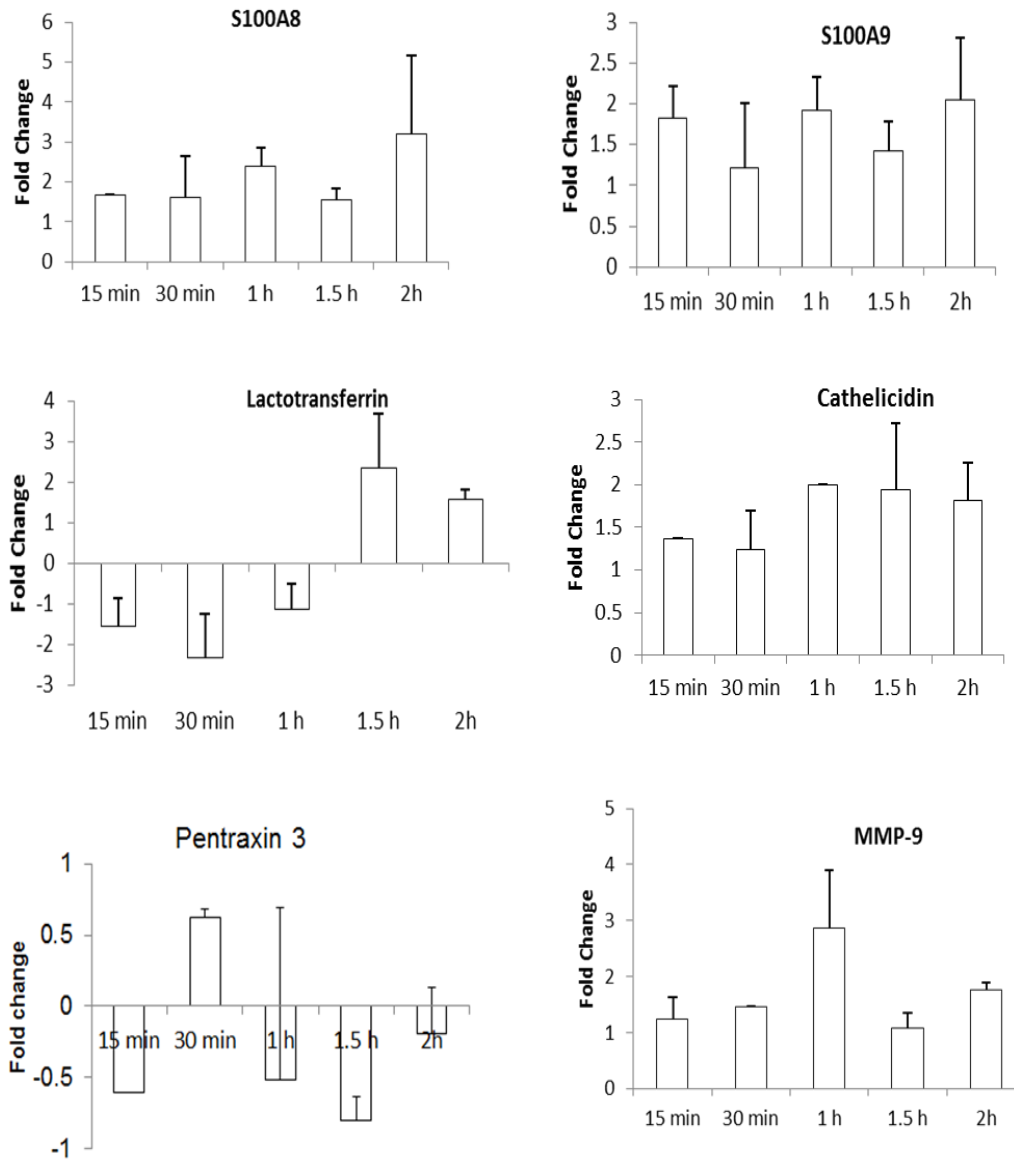


Figure 3.9. Gene expression analyses of antibacterial proteins during NETs release. Real-time PCR analyses for gene expression of selected proteins (including S100A8, S100A9, lactotransferrin, cathelicidin, pentraxin-3 and matrix metalloproteinase-9) in the neutrophils incubated with FLU-BALF for up to 2 hours. Values represent the means \pm SE of two independent kinetics. *P* value = not significant, Student's *t*-test.

Nevertheless, the antibacterial activity was tested to determine if the NETs formed during influenza infection could kill bacteria during secondary bacterial infection. Upon incubation of NETs with *S. pneumoniae* 19F or *K. pneumoniae* K15, no bactericidal activity could be seen. Cytochalasin B was used to inhibit actin polymerisation to prevent phagocytosis in non-NETting neutrophils. Interestingly, even phagocytic activity was not seen under the conditions tested (Figure 3.10 A and B). On the other hand, significant antifungal activity was seen against *C. albicans* when compared to controls without neutrophils. Even though fungal infections are not very common after influenza infection, the moderate gene expression of antifungal calprotectin dimer-forming S100 proteins (Figure 3.9) prompted an inquiry into the antifungal nature of NETs. Moreover, the susceptibility of *C. albicans* to killing by NETs has been shown thus, making it a good positive control for the antimicrobial assay (Urban et al., 2009). The total killing did not vary much when phagocytosis was inhibited indicating mostly NETs-mediated antifungal activity. However, the killing was not very different between neutrophils incubated with BALF from uninfected (CON-BAL) and lethally infected mice (FLU-BAL) implying that NETs formed during primary influenza infection do not provide any additional protection against secondary fungal infections (Figure 3.10 C). The role of endonuclease in the absence of antibacterial activity against *S. pneumoniae* was suspected. Indeed, both *S. pneumoniae* pellets and double-filtered bacteria-free culture supernatant showed endonuclease activity (Figure 3.10 D, lanes 5 and 6). Even though the endonuclease was previously thought to be membrane-bound, recent evidence has

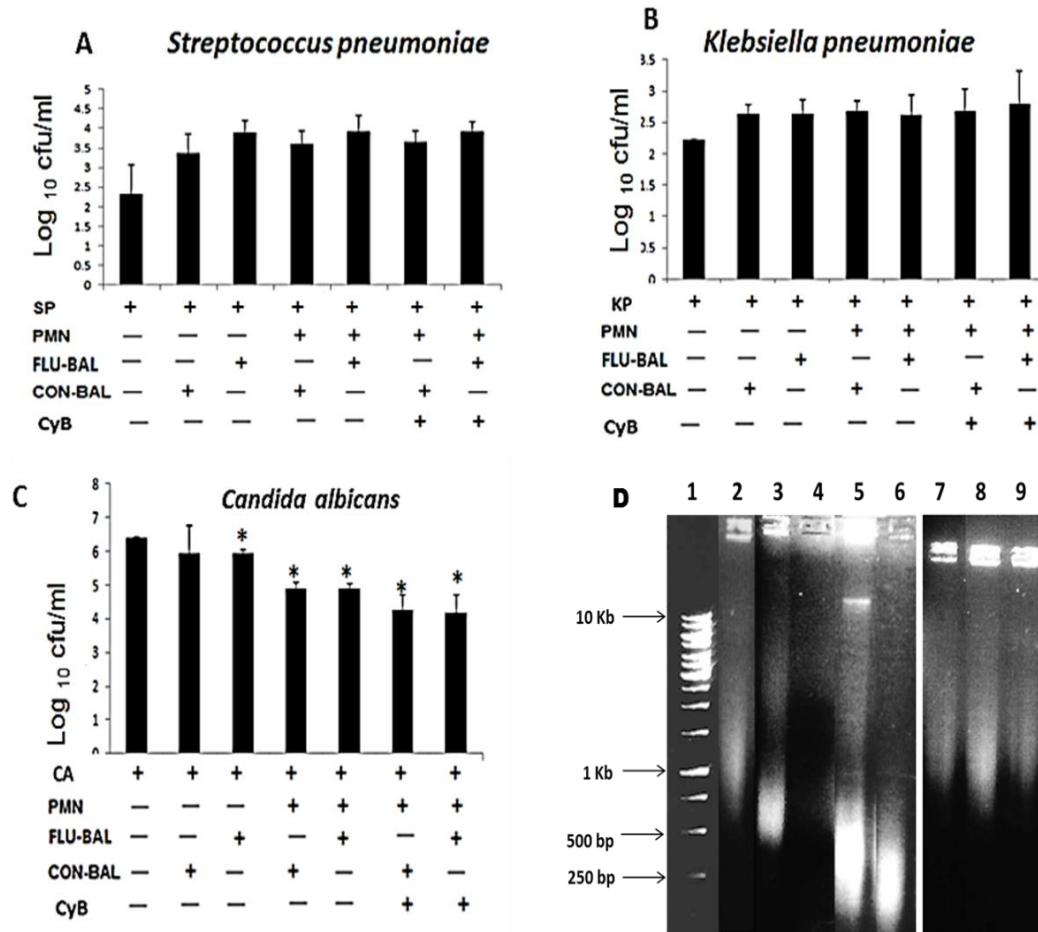


Figure 3.10. Microbicidal activity of NETs generated by influenza stimulation. Neutrophils (PMN) were incubated with influenza-infected (FLU-BAL) or uninfected control (CON-BAL) BALF for 2 hours post which they were incubated with (A) *S. pneumoniae* 19F (SP), (B) *K. pneumoniae* K15 (KP), and (C) *C. albicans* (CA). (A-B) After incubation for 2.5 hours, the contents in the wells were scraped and serial dilutions were plated on sheep blood agar or Luria-Bertani agar, and colonies were counted 24 hours later. (C) *C. albicans* were incubated overnight incubation with neutrophils and serial dilutions were plated on Sabouraud dextrose agar for colony counts. 10 µg/ml cytochalasin B (CyB) was used to inhibit phagocytosis. Values represent the means ± SE of at least three independent experiments. * denotes P value < 0.05 versus untreated fungus only control, Student's t-test. (D) DNase activity in bacterial pellets (10⁷ cells) and double-filtered supernatants of *S. pneumoniae* and *K. pneumoniae* were analysed by incubating with salmon sperm DNA (2 µg) for 1 hour at 37°C. The reaction was stopped using 0.5 M EDTA and the DNA in the samples were visualised with 1% agarose gel electrophoresis. Lanes: (1) DNA ladder. Salmon sperm DNA was incubated with (2) DNase buffer; (3) DNA alone; (4) BHI broth; (5) *S. pneumoniae* pellet; (6) *S. pneumoniae* supernatant; (7) LB broth; (8) *K. pneumoniae* pellet; and (9) *K. pneumoniae* supernatant. The DNA smearing below 500 bp in lanes 5 and 6 revealed that salmon sperm DNA was digested by both pellet and supernatant of *S. pneumoniae*, indicating both cell-bound and secreted DNase activity. However, *K. pneumoniae* did not digest the DNA as shown by relatively intact salmon sperm DNAs.

shown that it could be secreted as well thus potentially damaging NETs away from point of contact with bacteria (Zhu et al., 2013). However, the same could not be applied to the absence of antibacterial activity against *K. pneumoniae* as the Gram-negative bacterium does not produce DNase (Figure 3.10 D, lanes 8 and 9) insinuating other modes of NETs evasion such as capsules that pneumococci possess as well (Lawlor et al., 2006; Yoshida et al., 2001).

3.4 Conclusion

Secondary bacterial infections are the most common complications of influenza infections and are quite frequent during pandemics like the 2009 H1N1 pandemic (Lucas, 2010); (reviewed in (Metersky et al., 2012)). The lethal synergism between the influenza virus and *S. pneumoniae* has been attributed with the causation of severe pathology during secondary pneumococcal infections (McCullers & Rehg, 2002). Indeed, extensive neutrophil infiltration in the airways and blood vessels along with severe lung consolidation, fibrin deposition and epithelial cell necrosis were noticed during the secondary pneumococcal infection in the murine model. Though the viral titre remained largely unaffected, the bacterial load remained persistent up to 48 hours post-bacterial infection indicating failure of clearance of bacteria by host immune system or increased bacterial replication due to increased PAFr-mediated adherence to epithelial basement membrane (McCullers & Rehg, 2002) (Figures 3.3 and 3.4).

Due to the lack of a quantitative assessment of NETs *in vivo*, not many studies report the extent of NETosis inside a host (Bruns et al., 2010; Villanueva et al.,

2011). To address this issue, a semi-quantitative scoring system to quantify NETs in lung sections was formulated to assess whether NETosis is differently influenced during secondary pneumococcal infections (Figure 3.5 and Tables 3.1 and 3.2). NETs were found to be significantly enhanced after secondary infection when compared to primary influenza infection alluding to a possible role in the worsening of lung pathology. Even though the histopathology with the bacteria alone infection was not very significant, NETs were higher than the influenza alone infection. Several possibilities could be explained for the difference in NETosis between *S. pneumoniae* and influenza virus. One possibility could be that the H₂O₂ generated by *S. pneumoniae* may take part in inducing NETs. Low amounts of H₂O₂ can induce NETs (Figure 3.6 A). The generation of H₂O₂ by *S. pneumoniae* is shown to negatively affect other respiratory pathogens (Pericone et al., 2000). Increased NETs-inducing ability may be another mode of virulence exerted by H₂O₂ which is a known and important virulence factor of *S. pneumoniae* (Rai et al., 2015).

Partially degraded NETs were observed that could be due to degradation by pneumococcal endonuclease or could be necrotic cellular debris (Figure 3.8). A good antibody for detecting pneumococcus in lungs would help in confirming the association of bacteria with NET degradation. The antisera (Statens serum institute) used in this study, did not stain *S. pneumoniae* in the lung sections. Considering that NETs were found to be partially degraded when incubated with *S. pneumoniae in vitro* (Figure 3.7 C), the occurrence of such events inside a host becomes more likely. Degradation of NETs could mean that components of NETs

get scattered to a larger surface area in the lungs, some of which like histones are extremely cytotoxic (Kessenbrock et al., 2009; Saffarzadeh et al., 2012; Xu et al., 2009). Histones and other neutrophil proteins like proteinase 3 are frequently used as biomarkers of autoimmune disease (Baker et al., 2008; Nakazawa et al., 2014; Pratesi et al., 2013). This warrants further investigation into the role of NET degradation and NET components in the immunopathology of ALI.

NETs were shown to be induced *in vitro* by incubating neutrophils with BALF from mice lethally challenged with influenza virus (Figure 3.6). Lethally challenged mice possess very high amounts of pro-inflammatory cytokines and chemokines in the lungs like IL-8, TNF- α etc., which have been shown to induce NETs (reviewed in (Brinkmann & Zychlinsky, 2007)). Redox enzymes play a crucial role in regulating these cytokines into the lungs and some of them have been shown to affect NETosis (Gray et al., 2013; Narasaraju et al., 2011). Indeed, NETs were significantly reduced when incubated with inhibitors of NADPH oxidase and MPO; highlighting the oxidative nature of NETosis and the importance of MPO in the whole process as previously reported (Saffarzadeh et al., 2012).

NETs induced during influenza infection did not show any significant antibacterial gene expression *in vitro* (Figure 3.9). Corresponding to the gene expression, NETs generated by lethal BALF incubation did not kill *S. pneumoniae* and *K. pneumoniae in vitro* possibly due to endonuclease activity or capsule expression (Figure 3.10). Even though NETs were first reported as an antibacterial defence system, some later reports have suggested otherwise

(Brinkmann et al., 2004; Menegazzi et al., 2012; Nazareth et al., 2007). In the absence of a common pathway of NETs induction, it becomes extremely difficult to identify a cause and effect mechanism. NETs induced by different stimuli could undergo different pathways at early stages of stimulation which may have impact at the final properties of NETs generated by that stimulant. This area commands a huge focus to ascertain whether there could be a common event occurring in all types of NETosis which would greatly help in studying the phenomenon as it would be possible to control NETs at will and observe its effects in a systematic manner. Nevertheless, further studies could be done using other respiratory pathogens such as *Pseudomonas aeruginosa* in a secondary infection model after influenza infection.

In conclusion, this study for the first time demonstrates that secondary pneumococcal infection after primary influenza infection greatly enhances NETs generation in the lungs of infected mice but these NETs do not participate in the killing of pneumococci. Moreover, partial degradation of NETs by *S. pneumoniae* could play a possible role in the deterioration of lung pathology during secondary infection.

CHAPTER FOUR

CAPSULE PLAYS AN IMPORTANT ROLE IN THE VARIABILITY AMONGST PNEUMOCOCCI IN INDUCING NEUTROPHIL EXTRACELLULAR TRAPS AND LUNG PATHOLOGY DURING MURINE PNEUMONIA

4.1 Background

4.1.1 Clinical prevalence of pneumococcal serotypes

The severity of pneumococcal infection depends on the virulence factors of the bacteria and the health and socio-economic status of the host (Alanee et al., 2007; Sjöström et al., 2006). *S. pneumoniae* IPD-causing strains have been characterised into 94 clinical isolate serotypes based on capsule-specific Quellung reactions (reviewed in (Song et al., 2013)). Globally, there are different circulating strains with varying levels of virulence (Figure 4.1).

In a study involving meta-analysis of several independent clinical studies, the risk of death arising due to IPD was found to be positively associated with serotype variation (Weinberger et al., 2010). Inverse correlation has been found between the carriage prevalence and invasiveness of a serotype meaning that the most commonly carried serotypes do not cause invasive infection and vice versa (Brueggemann et al., 2004; Weinberger et al., 2010). Introduction of immunisation schemes at schools and in the elderly age group has decreased the

circulation of some of the previously prevalent strains in countries like the U.S.A., the U.K. and those in South-East Asia (Grijalva et al., 2007; Jauneikaite et al., 2012; Melegaro et al., 2010). The pneumococcal vaccines currently available in the market are based on the immunogenicity of the polysaccharide capsule. The first formulation known as the pneumococcal polysaccharide vaccine (PPV) 23 has been available since 1983 and consists of polysaccharide components from 23 clinical serotypes. Later formulations during the 2000s were called the pneumococcal conjugate vaccine (PCV). PCV-7 and PCV-13 cover serotypes 4, 6B, 9V, 14, 18, 19F, 23F and serotypes 1, 3, 5, 6A, 7F, 19A. (Cox & Link-Gelles, CDC⁸).

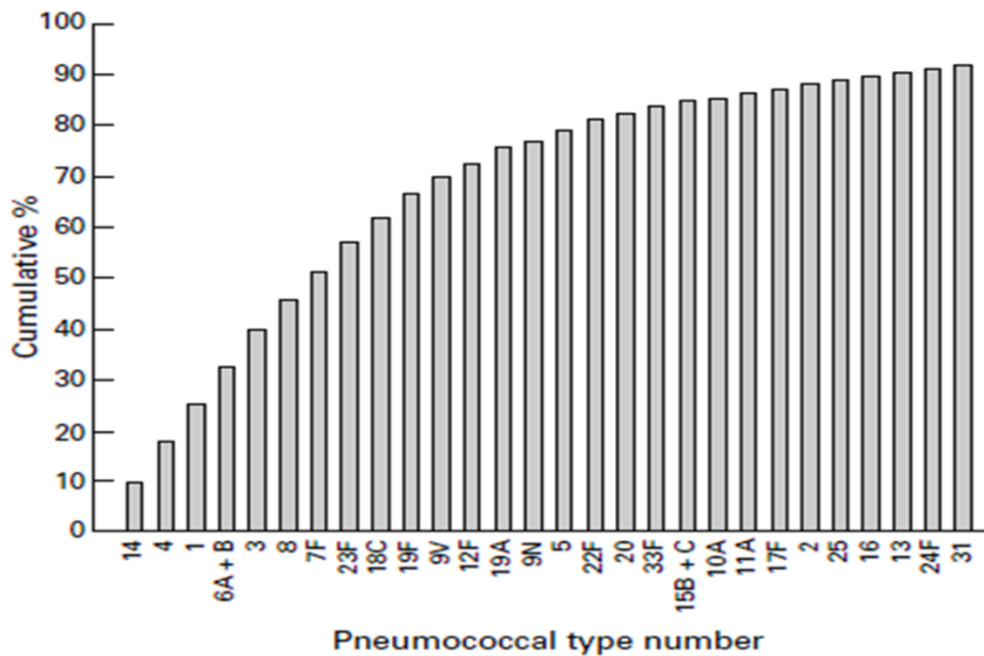


Figure 4.1. World-wide type distribution (WHO multi-center database, 1970-1983) of *S. pneumoniae* strains isolated from invasive clinical cases. (Adapted from Kalin, 1998).

4.1.2 Pneumococcal capsule biosynthesis

Most of the pneumococcal serotypes produce capsule through a *wzy*-dependent mechanism except serotypes 3 and 37 (Figure 4.2). The capsule (*cps*) locus falls between the genes *dexB* and *aliA* (Geno et al., 2015). For most of the serotypes, the *cps* locus of the *S. pneumoniae* genome consists of four conserved genes *wzg*, *wzh*, *wzd* and *wze*, also known as *cpsA*, *cpsB*, *cpsC* and *cpsD* (Morona et al., 2000, 2004). While CpsA has been associated with the transcriptional regulation of the *cps* gene expression levels, CpsB-D take part in the encapsulation and regulation of PS production. CpsB is a manganese-dependent phosphotyrosine-protein phosphatase that regulates the dephosphorylation of CpsD (Morona et al., 2002). CpsC is a membrane protein associated with the PS co-polymerase and hence regulates the PS chain length and export to surface in conjunction with CpsD (Morona et al., 2006). CpsD is an autophosphorylating protein-tyrosine kinase that serves as a negative regulator of PS production as dephosphorylation of CpsD by CpsB is essential for PS production (Morona et al., 2003). However, favourable changes in the atmospheric oxygen has been shown to guide the phenotype change of *S. pneumoniae* colonies from transparent to opaque with the opaque phenotype showing higher PS production and CpsD phosphorylation (Weiser et al., 2001). The contradicting roles of CpsD in PS production have not been clearly addressed yet. An additional role for CpsC in the attachment of PS to the bacterial cell wall and its importance in the progression of pneumonia to bacteraemia has also been described (Morona et al., 2006).

Phosphoglucomutase (Pgm) and glucose-1-phosphate uridyl transferase (GalU) together lead to the formation of uridine diphosphate glucose (UDP-Glc) which a precursor sugar for all pneumococcal serotype capsules as well as teichoic acid (Hardy et al., 2000); (reviewed in (Kadioglu et al., 2008)).

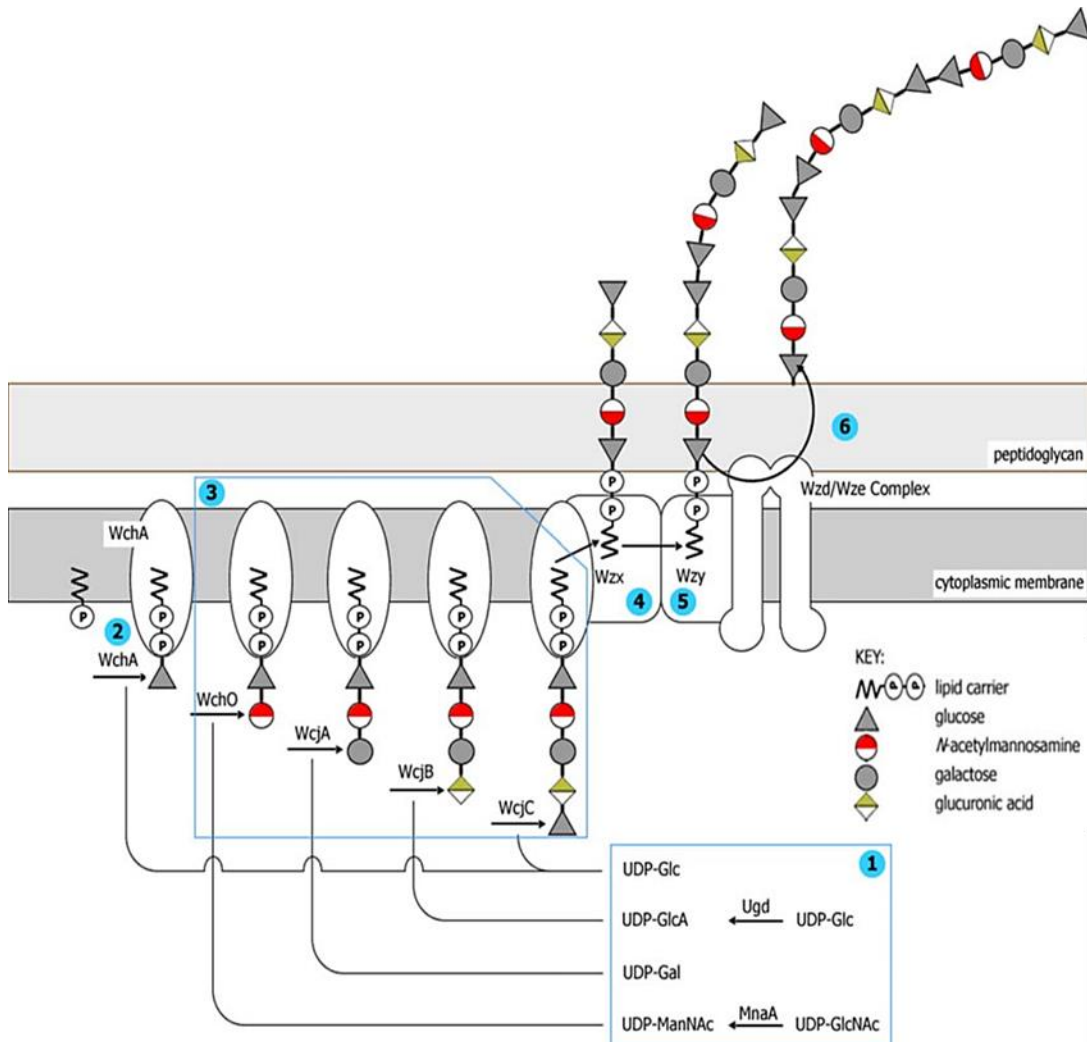


Figure 4.2. Illustration of the Wzx/Wzy-dependent pathway for the biosynthesis of CPS 9A. (Adapted from Bentley et al., 2006). Oligosaccharide repeat units are synthesised through the sequential addition of sugars to a membrane-associated lipid carrier on the inner layer of the cell membrane. (1) Biosynthesis of activated sugar precursors. A glycosyltransferase (WchA for Cps9A) initialises the assembly of the PS (2) by linking the initial sugar as a sugar phosphate (Glc-P) to an undecaprenyl phosphate acceptor. Other glycosyltransferases then sequentially link further sugars to generate repeat units (3) which gets transported across the cytoplasmic membrane to the external face by a flippase (Wzx, 4). A polymerase (Wzy) adds the growing polymer chain to new repeat units forming high molecular weight PS (5). Wzd/Wze (CpsC/CpsD) complex then translocates the mature PS to the cell surface and attaches to the cell wall peptidoglycan (6). The final lipid link to the cell wall is poorly understood but role of CpsC

has been suggested (Aanensen et al., 2007; Bentley et al., 2006; Morona et al., 2006); (reviewed in (Geno et al., 2015; Kadioglu et al., 2008)).

Biosynthesis of serotype 3 PS happens via a much simpler mechanism. In a synthase-dependent process, a single enzyme transfers a sugar to a lipid acceptor thereby initiating the PS synthesis and thereafter keeps on adding to the chain whereas in other serotypes separate glycosyltransferases are needed for this purpose (Geno et al., 2015). The *cps* locus of serotype 3 consists of 4 genes – *cps3S*, *cps3D*, *cps3M* and *cps3U* of which *cps3M* and *cps3U* are not essential for the PS biosynthesis (Cartee et al., 2005).

The type 3 synthase encoded by *cps3S* initialises the PS synthesis by adding glucose (Glc) and glycosaminoglycan (GlcUA) on the non-reducing end of the PS chain which during extension remains tightly associated with the carbohydrate-binding site on the synthase. The UDP-Glc dehydrogenase encoded by *cps3D* oxidises UDP-Glc to form uridine diphosphoglucuronic acid (UDP-GlcUA) which is the second substrate for the type 3 PS formation. A phosphatidylglycerol serves as an anchor on the cell wall for the type 3 PS as the PS does not get covalently bonded to the cell wall. (Cartee et al., 2000, 2005; Dillard et al., 1995).

In the case of serotype 37, only one gene, *tts*, encoding a putative glycosyltransferase is required for PS synthesis that lies outside the *dexB/aliA* locus. *Tts* shows very high sequence similarity to other glycosyltransferases and cellulose synthases of many bacteria and higher plants. *Cps37* is a

homopolysaccharide consisting of repeating units of monosaccharide chains of β -D-Glc (Llull et al., 2001).

4.1.3 Capsule and pneumococcal virulence

S. pneumoniae capsule has been strongly associated with the nasopharyngeal carriage prevalence. While thicker capsule increases the carriage prevalence, the biochemistry of the capsule such as energy spent on capsule biosynthesis can negatively influence the prevalence since the bacteria would find it harder to survive under unfavourable conditions while maintaining their energy-demanding capsules (Hathaway et al., 2012; Weinberger et al., 2009, 2010). Due to the last aspect, *S. pneumoniae* need to lose some of their capsular material to be able to survive inside the host. In a study with a murine model, non-encapsulated pneumococci reached the lungs from the nasopharynx in more numbers even though the capsulated strains colonised the nasopharynx more efficiently (Küng et al., 2014).

Loss of PS has been shown to increase the bacterial adherence levels to the lung epithelial cells. The capsule was found to elicit an anti-inflammatory response from the epithelial cells whereas the pneumolysin elicited strong pro-inflammatory responses (Hammerschmidt et al., 2005). Since high cellular infiltration and inflammation is seen in the lung after virulent pneumococcal infection, it can be inferred that while the capsule helps in evading clearance by host-mediated complement and phagocytic activity in the nasopharynx, its subsequent migration into the lower respiratory tract and the resultant pathology

is due to its pro-inflammatory virulence factors like Ply along with the loss of capsule.

The association of capsule with virulence has been known since 1950 (MacLeod & Kraus, 1950). Since then, several studies have independently confirmed this association (Briles et al., 1992; Hyams et al., 2010; Magee & Yother, 2001; Morona et al., 2004; Melin et al., 2010; Shainheit et al., 2014; Sjöström et al., 2006). Morona et al. (2004) showed that deletion of *cpsA* gene does not have any effect on the virulence whereas deletion of *cpsB* or *cpsD* attenuates the bacterial virulence. Cross-expression of the capsule changes the virulence of a strain (Melin et al., 2010). Differing levels of PS have different effect on the virulence of the bacteria as a minimum amount of PS is needed for the mice to succumb to infection meaning that not all of the polysaccharide may be lost during invasion of the epithelial cells (Magee & Yother, 2001). In a murine study using human isolates, Briles et al. (1992) found that capsular type of pneumococcal strains defined their virulence. Almost all the strains of type 4 were found to be virulent whereas only 40% of type 3 were virulent and all strains from the group 19 were avirulent in mice. The current study uses these strains - type 3, 4 and 19F (Figure 4.3) and it would be interesting to see its correlation with the earlier study.

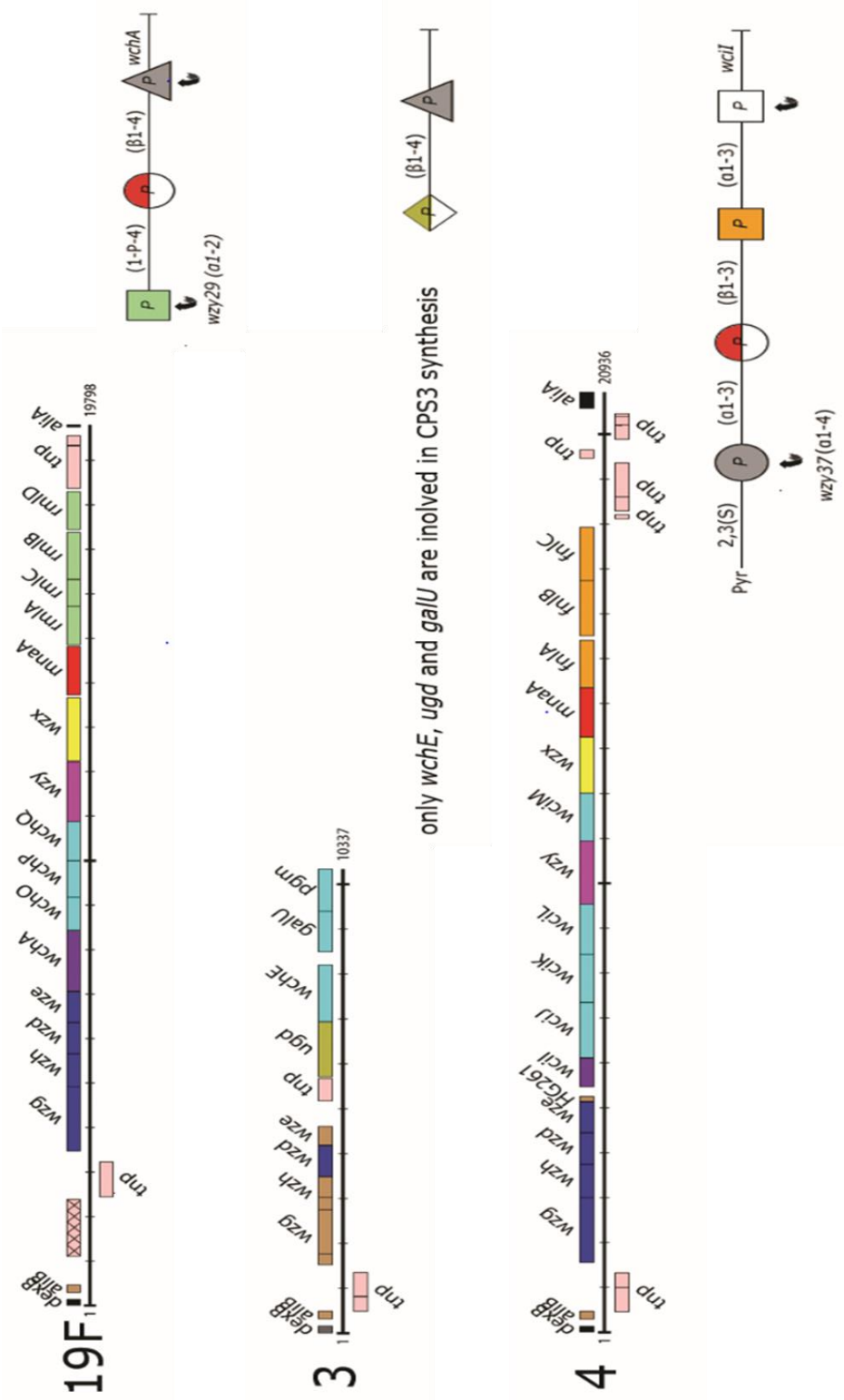


Figure 4.3. Gene clusters (left) and the repeat unit structures (right) of the serotypes used in this study. (Adapted from Bentley et al., 2006).

4.1.4 Capsule and NETs

Pneumococcal capsule is known to direct strong anti-inflammatory cytokine response like IL-10 while suppressing the pro-inflammatory cytokines like IL-6 and impairing recognition of TLR ligands and thus impeding the MyD88-mediated bacterial defence (Hyams et al., 2010; de Vos et al., 2015; van der Poll et al., 1996, 1997). Capsule is known to influence immune cells like neutrophils by encouraging the production of IL-10 (Lawlor et al., 2006; Yoshida et al., 2001). However, studies connecting capsule with NETosis are extremely limited. Wartha et al. (2007) for the first time demonstrated that capsule is essential for the evasion of *S. pneumoniae* from neutrophils but not for escaping the killing by NETs and that the structural biochemistry of cell membrane is important to determine the survival of bacteria inside the host. In the same study, few serotypes of *S. pneumoniae* were compared along with their capsule mutants in their susceptibility to NETs mediated-killing *in vitro*. In both the wild types and the capsule mutants, phagocytic killing predominated leading to the conclusion that capsules do not help in evading NETs-mediated killing.

In recent studies, capsule mutants of *C. albicans* and *Burkholderia pseudomallei* were shown to induce higher NETs compared to wild types supposedly due to increased oxidative burst in the neutrophils (Riyapa et al., 2012; Rocha et al., 2015). In the study involving *C. albicans*, the wild type and the major PS, glucuronoxylomanan were shown to inhibit NETs induction whereas the acapsular variant and a minor PS, glucuronoxylomannogalactan induced NETs (Rocha et al., 2015).

4.2 Specific objectives of the study

Serotype of a pneumococcus influences its virulence through the capsular polysaccharide. Deletion of capsule can have profound impact on the invasiveness of the bacterium. Very few studies have been done to associate the capsule of pneumococci with NETs. There are no hitherto reports on the serotype-specific variations in NETs induction and the role of pneumococcal capsule in it during secondary pneumococcal infection after influenza infection. Since pneumococci were found to induce more NETs during secondary infection (chapter 3), the comparison of pneumococcal serotypes with respect to NETosis was the next step.

The specific objectives of the study are,

- a) To evaluate the induction of NETs using purified pneumococcal capsule polysaccharide.
- b) To compare NETs induction by different serotypes of *S. pneumoniae* in both primary and secondary (after influenza) murine infection models.
- c) To assess the effect of capsule deletion on the NETs induction capability of *S. pneumoniae*.
- d) To evaluate the overall serotype-specific variation in the pathogenesis of *S. pneumoniae*.

4.3 Results and discussion

4.3.1 Purified pneumococcal capsular polysaccharide induces NETs in a dose-dependent manner

To determine if capsulated bacterial polysaccharide by itself can induce NETs, bone-marrow derived neutrophils were incubated with purified capsule PS of serotype 4 (ATCC). NETs were induced by PS in a concentration-dependent manner with 10 µg/ml inducing 3-fold greater NETs than control (Figure 4.4). This indicates that the capsule quantity of *S. pneumoniae* can influence the degree of NETs generation. Previously, LPS has been shown to induce extensive NETs in the presence of certain cytokines (Brinkmann et al., 2004). This study shows the direct role of capsule PS of a bacterium in inducing NETs thereby emphasising its importance in gauging host immune response to bacteria which leads to more potential areas of research, especially in murine models to observe similar effects *in vivo*.

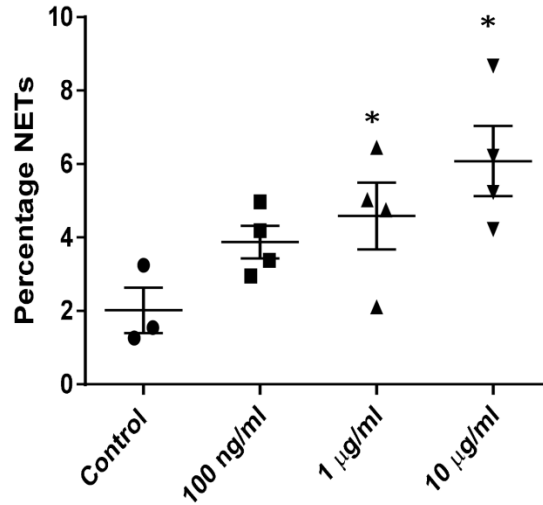


Figure 4.4. Pneumococcal capsular polysaccharide induces NETs in a dose-dependent manner. Bone marrow-derived neutrophils were stimulated for 2 hours with various concentrations of purified capsule polysaccharide from serotype 4 (x-axis). Values represent the means \pm SE of at least three independent experiments. * indicates P value < 0.05 , Student's t -test.

4.3.2 Capsule thickness of pneumococci influences their susceptibility to neutrophil-mediated surface killing

Three clinically prevalent strains of *S. pneumoniae*, serotypes 19F, 3 and 4, were used in the study along with a capsule mutant of serotype 4 (type cps4D-) that lacks the *cps4D* gene required for PS export to bacterial cell surface (Figure 4.5 A). FITC-dextran exclusion assay was performed to assess the capsule thickness. As the presence of capsule would block the diffusion of dextran molecules through the cell wall, capsulated bacteria would appear as a clear zone (zone of exclusion) against a dark background. Serotype 3 possessed the largest capsule as measured by the zone of exclusion followed by serotype 4 and finally by serotype 19F and type cps4D- (Figure 4.5 B and C). All strains of *S. pneumoniae* were compared in their vulnerability towards surface killing by

neutrophils. It is believed that neutrophils show better phagocytic activity on tissue surfaces when compared to conventional *in vitro* assays. This concept has been previously applied to pneumococcal studies as pneumococci show low phagocytic susceptibility *in vitro* (Weinberger et al. 2009). Serotypes 3 and 4 showed no or little susceptibility to killing while serotype 19F was killed in very high numbers (Figure 4.5 D).

Correlation of capsule size with the surface killing assay results showed high association between the thickness of capsule and the susceptibility of *S. pneumoniae* towards neutrophil-mediated killing. The serotype with the largest capsule, type 3, was not at all killed by neutrophils whereas serotype 19F was killed with high efficiency. Serotype 4 was an intermediate in both capsule thickness and susceptibility to killing. Moreover, the capsule mutant of serotype 4, type 4cps4D-, displayed very high susceptibility towards killing while having only about 30% of capsule thickness of wild type (Figure 4.5 B-D). This demonstrates the importance of capsule in evading immune cell-mediated killing. Indeed, the role of PS content of capsule in pneumococcal virulence was first highlighted as early as 1950 (MacLeod & Kraus, 1950). Subsequently many studies have linked capsule to higher virulence and carriage prevalence of *S. pneumoniae* (Hathaway et al., 2012; Morona et al., 2004; Weinberger et al., 2009). An important observation from the surface killing assay is that in all wild type serotypes except serotype 3 which did not get killed, non-phagocytic killing including those by NETs predominated over phagocytic killing (Figure 4.5 D). Phagocytosis was inhibited using cytochalasin B that restricts actin

polymerisation in neutrophils without affecting other functions. Non-phagocytic killing was calculated as the difference between total killing without cytochalasin B and killing with cytochalasin B. Previous studies have reported phagocytosis to be the dominant mode of killing (Genschmer et al., 2013; Wartha et al., 2007). However, those experiments were performed using human neutrophils while the current study used murine ones. The exact effect of different sources of neutrophil on killing efficiency is not clear and is an important area that needs more attention. Interestingly, type 4cps4D- showed a relatively higher tendency towards phagocytic killing when compared to the wild type showing an almost two-fold increase in phagocytic death. Again, this indicates the importance of capsule in determining the fate of bacteria inside the host wherein capsule helps the bacteria in evading phagocytosis by neutrophils and as a result, neutrophils are forced to try other modes of killing like NETosis. Thus, NETs emerge as important defence mechanisms inside the host against some of the virulent serotypes of *S. pneumoniae* and possibly other capsulated bacteria.

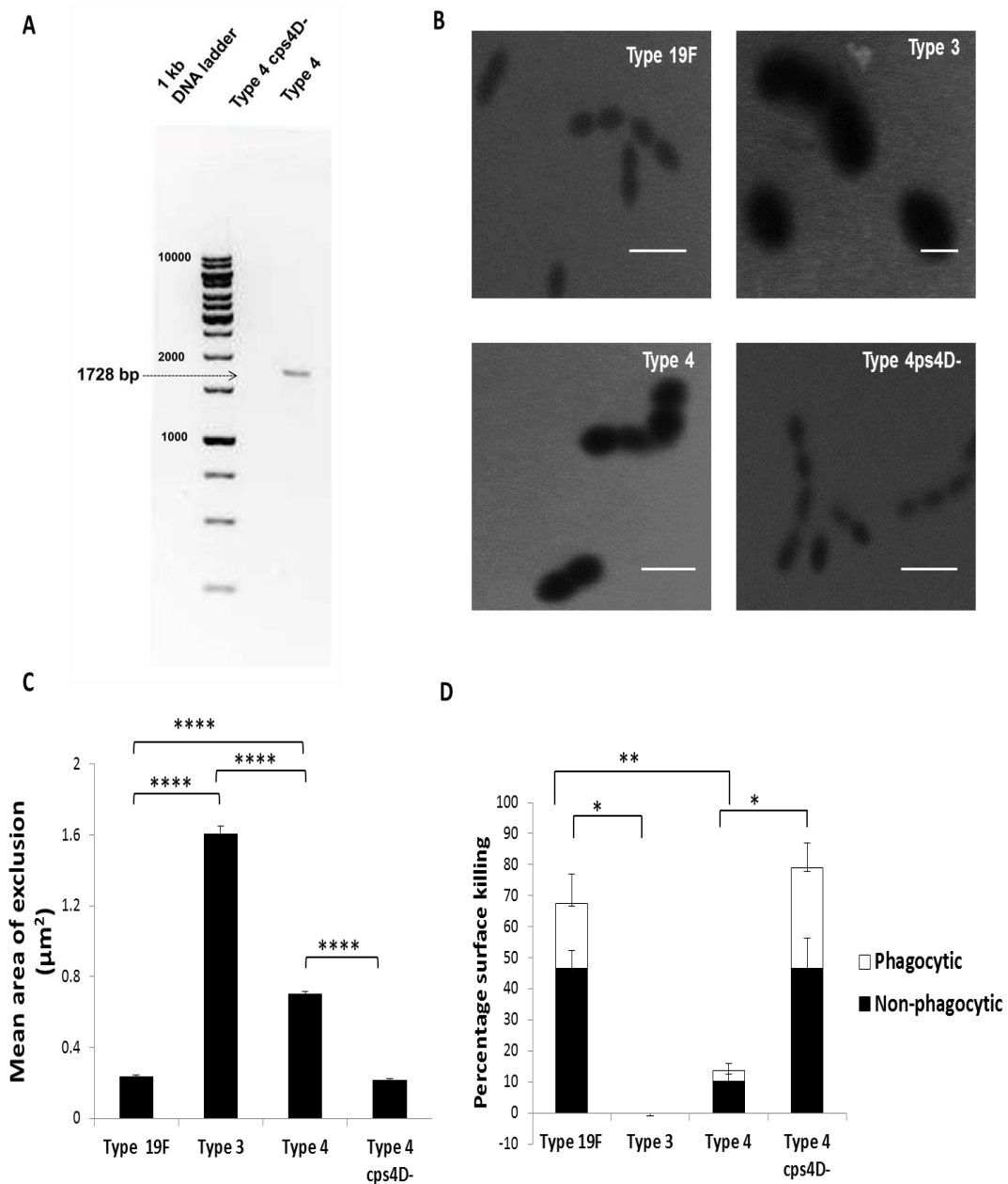


Figure 4.5. Thicker capsule protects pneumococci from neutrophil-mediated surface killing. (A) PCR amplification of *cps4D* gene showed the absence of the gene in the mutant of serotype 4, type 4cps4D-. (B, C) FITC-dextran (2000 kDa) exclusion assay was performed on serotypes 19F, 3 and 4 as well as the capsule mutant type 4cps4D- to estimate the capsule thickness. Type 3 had the largest capsule while type 4cps4D- had significantly smaller capsule than type 4. Values represent mean area \pm SE of 100 bacterial cells. (B) Representative images from dextran-FITC exclusion assay, scale bars = 2 μ m. (D) Surface killing assay was performed on all four strains. 10 μ g/ml cytochalasin B (CyB) was used to inhibit phagocytosis. For all strains, non-phagocytic killing predominated over phagocytic killing. Type 19F and type 4cps4D- were found to be very susceptible to neutrophil-mediated killing. Values represent the means \pm SE of at least three independent experiments. * indicates P value < 0.05 ** P value < 0.01, *** P value < 0.001, **** P value < 0.0001, ANOVA with Tukey post-hoc correction.

4.3.3 Capsule thickness correlates with overall pathogenesis and pulmonary NETosis during primary pneumococcal pneumonia

Mice were infected with a high dose (10^7 CFU) of the four bacterial strains and were sacrificed on three consecutive days. All wild type strains caused illness in the mice as seen by body weight trend while the capsule mutant did not cause any noticeable change (Figure 4.6 A). This is consistent with earlier reports which show that loss of capsular genes or locus affects colonisation and invasion by pneumococcus in mice (Magee & Yother, 2001; Melin et al., 2010; Shainheit et al., 2014). Mice infected with serotypes 3 and 4 presented severe clinical features such as drastic body weight loss, breathlessness, morbidity and even death by day 3 whereas mice infected with serotype 19F showed recovery on day 3. Among the wild types, mice infected with type 3 showed the highest mortality however, infection with type 4 caused similar morbidity by day 3 thus resulting in the end of experiment (Figure 4.6 B). The high virulence of serotype 3 could be attributed to the high bacterial load in the lungs of infected mice (Figure 4.6 C) which corresponds well with the resistance of serotype 3 to surface killing (Figure 4.5 D) suggesting uninhibited replication. Likewise, serotype 4 also flourished well in the lungs albeit two-logs lesser than serotype 3. Serotypes 19F and the capsule mutant serotype 4cps4D- could not be recovered from lungs implying either very low replication rate or clearance by immune cells.

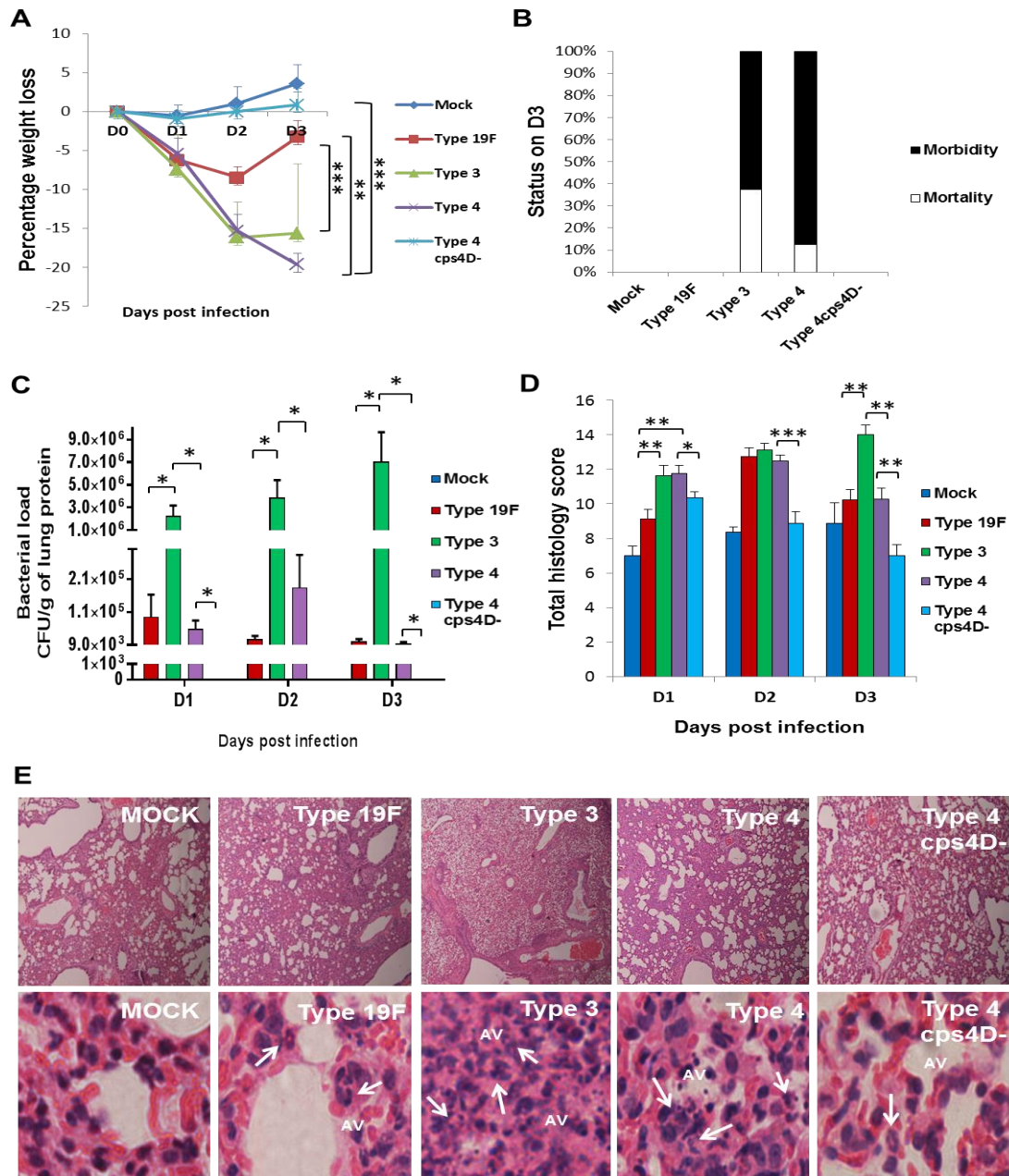


Figure 4.6. Primary infection with serotypes 19F, 3, 4 and 4cps4D-. BALB/c mice were intratracheally infected with 10^7 CFU of serotypes 19F, 3 and 4 as well as a capsule mutant of type 4 (cps4D-). Lungs were harvested on three consecutive days post-infection. **(A)** Both type 3 and type 4 caused significant body weight loss in mice until day 3 while mice infected with type 19F recovered by day 3 and type 4cps4D- failed to cause any clinical symptoms. **(B)** Both type 3 and type 4 induced 100% morbidity with type 3 causing more actual deaths. Type 19F and type 4cps4D- did not cause any morbidity. **(C)** Type 3 replicated very efficiently in the lungs of infected mice with type 4 coming a distant second. **(D)** Histopathology scores showed that type 3 caused the progressively worst lung pathology while type 19F, type 4 and type 4cps4D- induced lesser infiltration by day 3. **(E)** Haematoxylin and eosin staining of lung sections revealed very high neutrophil infiltration (arrows) in the alveolar spaces (AV) from infection with serotypes 3, 4 and 19F while infection with type 4cps4D- showed a relatively lower neutrophil presence in the lungs. Magnification of images: 100x for top panels; 1000x for lower panels. *Values represent the*

means \pm SE of 8 animals per group (2 independent experiments). * indicates P value < 0.05 ** P value < 0.01 , *** P value < 0.001 , ANOVA with Tukey post-hoc correction.

Histopathologically, serotypes 3 and 4 took the lead again in causing severe necrosis, oedema and cellular infiltration in infected lungs. However, there was some difference in the pattern of pathological scores. While initially only mice infected with serotypes 3 and 4 presented high cellular infiltration, by day 2 all wild type groups showed comparable levels of pathology while type 4cps4D- groups showed decrease in lung score. By day 3, only mice infected with serotype 3 showed progressively worse pathology while infection with serotypes 4 and 19F led to decreased pathological scores. On all days, infection with the capsule mutant presented significantly lower pathological scores than the wild type. While all wild types induced very high neutrophil infiltration in lungs the capsule mutant induced a mixed cellular response on day 1 and thereafter caused very minimal infiltration (Figure 4.6 D and E).

Lung hydrogen peroxide has the potential to mediate oxidative damage to tissues. Infection with serotype 4 induced greater levels of H_2O_2 in the lungs followed by serotype 3 infection. Serotype 19F and type 4cps4D- groups had comparatively lower H_2O_2 (Figure 4.7 A). In an *in vitro* study, researchers have shown that serotype 4 generates higher H_2O_2 than serotype 3 under aerobic conditions that may potentially cause more double-stranded breaks in the DNA in lungs (Rai et al., 2015). This could in fact be the reason behind higher H_2O_2 concentration in mice infected with serotype 4 as the bacteria by itself contributes to high amounts of H_2O_2 .

While MPO activity which acts as a surrogate for neutrophil activity did not show any serotype-specific trend, the activities in lung were generally elevated after infection with wild types whereas infection with capsule mutant led to lower MPO activity when compared to the wild type (Figure 4.7 B).

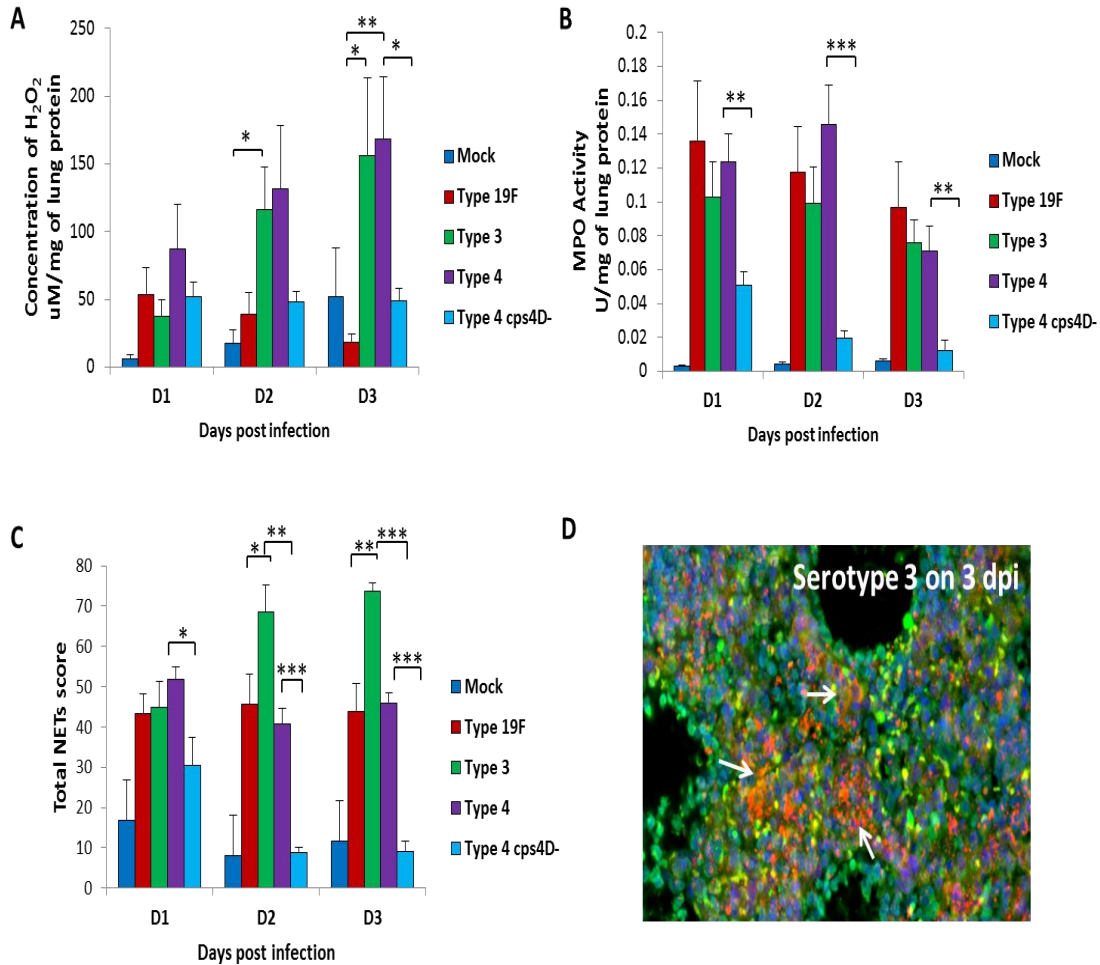


Figure 4.7. NETs and neutrophil activity in lungs after primary pneumococcal infection. (A) Mice infected with type 4 showed the highest H₂O₂ concentration. (B) Infection with all wild types led to higher MPO activity in the lungs. (C, D) Type 3 induced the highest pulmonary NETs (D, white arrows; blue=DAPI, green=H2B and red=MPO). Infection with type 4cps4D- presented significantly lower values in all parameters than wild type. Values represent the means \pm SE of 6-8 animals per group (2 independent experiments). * indicates P value < 0.05 ** P value < 0.01, *** P value < 0.001, ANOVA with Tukey post-hoc correction.

NETs correlated well with clinical presentation, lung bacterial burden and pathology (Figure 4.7 C). Serotype 3 being able to replicate the highest in lungs, caused the highest pathology and NETs generation (Figures 4.6 B-D and 4.7 C-D). Serotypes 4 and 19F which came next in pathology induced NETs at similar levels except on day 1. This suggests some histopathological relevance of NETs in infection. Similar association between NETs and severe pathology was made earlier with influenza virus (Narasaraju et al., 2011). Capsule mutant of serotype 4 was significantly lower than its wild type in both MPO activity and NETs score.

4.3.4 Capsule thickness along with other virulence factors influences the virulence and NETs-inducing ability of *S. pneumoniae* during secondary lung infection following influenza infection

Virulence and NETs-inducing ability of serotypes 19F, 3 and 4 as well the capsule mutant type 4cps4D- were assessed in a secondary pneumococcal infection model. BALB/c mice were first infected with 5 PFU sublethal dose of influenza A/H1N1/PR8 virus followed by 100 CFU sublethal doses of the four bacterial strains and were sacrificed at 24 and 48 hours after pneumococcal infection to harvest lungs. All the influenza-infected mice including those dually infected with *S. pneumoniae* showed similar trend in body weight loss (Figure 4.8 A). However, the mice dually infected with serotypes 3 and 4 showed severe clinical manifestations such as laboured breathing, hunched back and reduced intake of food culminating in the experimental end-point by day 9 (48 hours post-secondary infection). This was evident in a separate experiment done for survival analysis after secondary infection (Figure 4.8 B). Mice challenged with serotypes

3 and 4 after influenza infection showed mortality beginning from day 9 and by day 10, all surviving mice had become moribund. All other groups including those dually infected with serotype 19F survived until the experimental end-point of day 13 and had already started recovering from the illness.

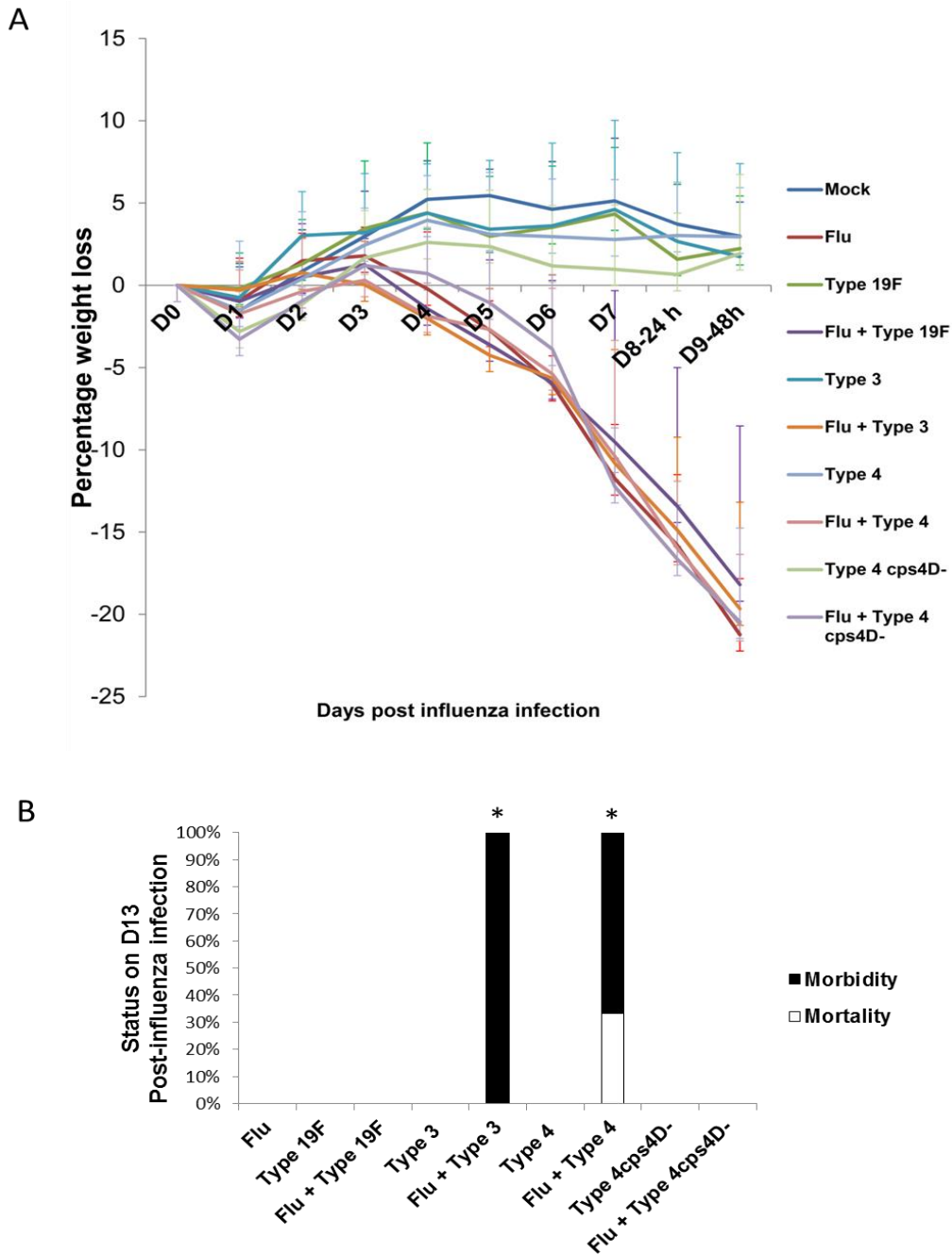


Figure 4.8. Secondary infection with serotypes 19F, 3, 4 and 4cps4D-. BALB/c mice were first intratracheally infected with 5 PFU PR8 virus followed by 100 CFU *S. pneumoniae* on day 7. Mice were monitored daily until they lose 30% of initial body weight or were sacrificed at specific time points. Lungs were harvested at 24 and 48 hours after secondary infection. **(A)** All the influenza infected mice suffered similar body weight loss. *P* value <0.05 between infected and uninfected groups. Values represent the means \pm SE of 6 animals per group (2 independent experiments). **(B)** Secondary infection with both type 3 and type 4 led to 100% morbidity by day 10 while mice infected with types 19F and cps4D- lived until the experimental end point on day 13. The Kaplan-Meier survival analysis revealed the survival of Flu + type 3 and Flu + type 4 groups to be statistically lower than Flu alone, Flu + type 19F and Flu + type 4cps4D-, *P* < 0.05, Kaplan-Meier survival analysis. Animals/group=3 (Single experiment).

Secondary infection with serotype 3 as expected caused the highest lung bacterial load while bacterial load after serotype 4 infection came a close second, different from the primary pneumococcal infection (Figure 4.9 A). Serotype 19F showed a comparatively lower replication in lungs after secondary infection. In all the wild type groups, secondary dual infection greatly enhanced the replicative efficiency of *S. pneumoniae* in lungs, consistent with the previously established studies (McNamee & Harmsen, 2006; Smith et al., 2013; Figure 3.2 B). Interestingly, the capsule mutant type 4cps4D- was again not detected in the lungs implying susceptibility to host immune system or inefficient replication.

Upon histopathological analysis, all influenza and dual-infected groups seem to have higher histology scores when compared to bacteria alone or mock infections (Figure 4.9 B and C). Secondary infection with serotypes 3 and 4 showed the worst pathology. Surprisingly this time, infection with serotype 4 showed higher pathological features such as cellular infiltration, necrosis and pleuritis when compared to serotype 3 despite the latter being at least ten times higher in lung bacterial burden by 48 hours. This indicates the presence of other factors apart from capsule size that may govern the virulence of a serotype during secondary infection.

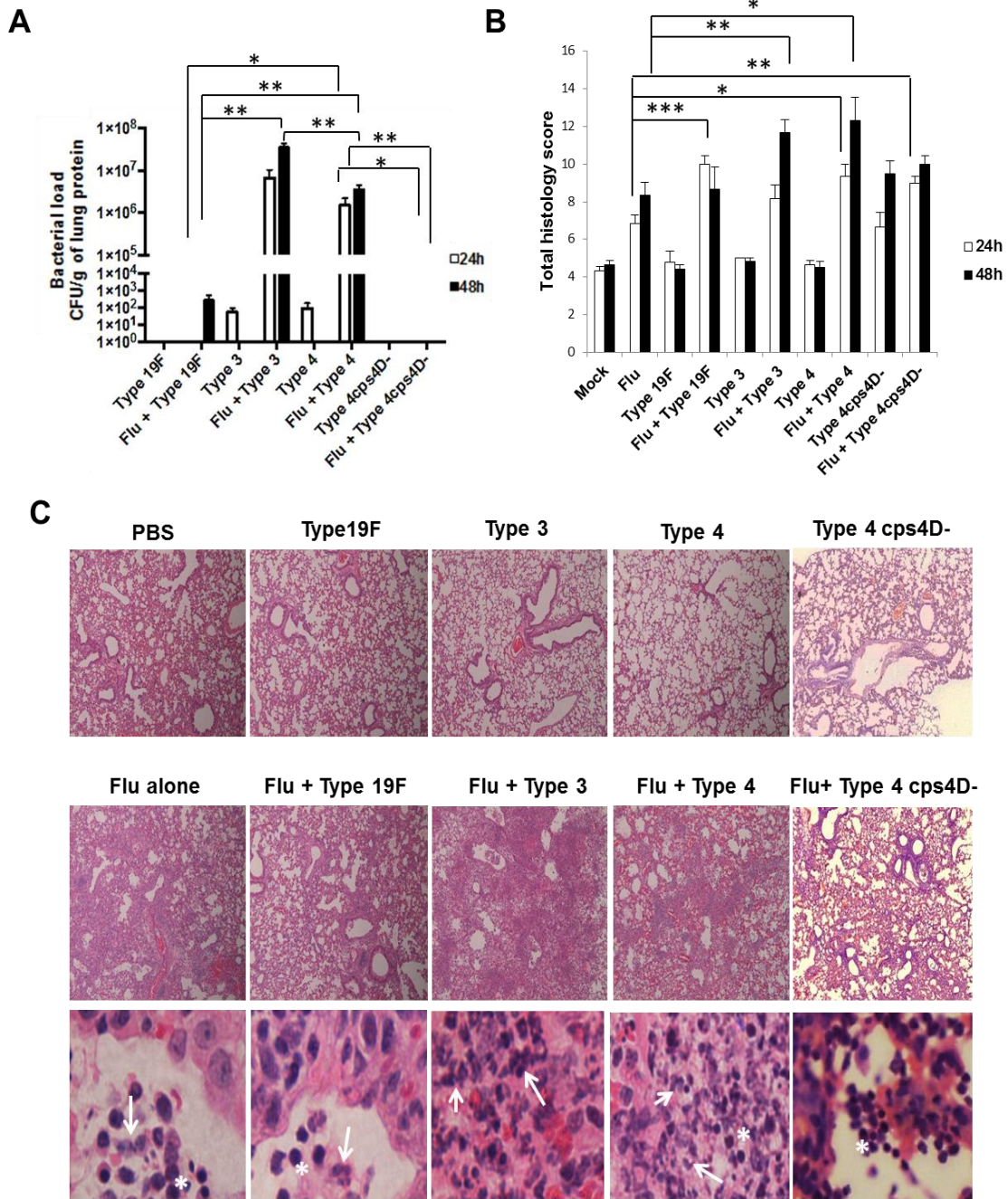


Figure 4.9. Histopathology and lung bacterial load after secondary infection. (A) Secondary pneumococcal infection after influenza infection makes pneumococcal replication in lungs very conducive. All the serotypes replicated efficiently in the lungs after secondary infection (Flu+bacteria) compared to bacteria alone infection. Type 3 followed by type 4 replicated with most efficiency in the lungs of influenza-infected mice. The capsule mutant of type 4, cps4D- was not detected in the lungs. (B, C) Secondary infection with type 4 caused the worst lung pathology followed by type 3. Values represent the means \pm SE of 6 animals per group (2 independent experiments). * indicates P value < 0.05 ** P value < 0.01 , *** P value < 0.001 , ANOVA with Tukey post-hoc correction. (C) Haematoxylin and eosin staining of lung sections revealed very high neutrophil infiltration (arrows) in the alveolar spaces (AV) of dual infected groups of types 3, 4

and 19F while type 4cps4D- groups showed more lymphocyte infiltration (asterix) in lungs. Magnification of images: 100x for top two panels; 1000x for bottommost panel.

As the airways are already damaged due to influenza infection, bacteria can easily exploit the situation and multiply in high numbers. However, each serotype may have its own unique mechanism to utilise the available space, as is evident from the pathological differences between serotypes 19F, 3 and 4 infection groups. Serotype 4 is known to produce the highest hydrogen peroxide levels among the three serotypes and thus can cause the highest DNA damage in the lungs (Rai et al., 2015). Another possibility is the uptake of pneumococci assisted by PAFr receptor as the receptor undergoes rapid internalisation upon binding to a ligand. This property is dependent on the virulence of *S. pneumoniae* as avirulent strains do not adhere efficiently using this mechanism (Cundell et al., 1995). Despite contradictory reports on the efficacy of PAFr-neutralisation approaches in reducing bacterial dissemination in the host, it may still be worthwhile to study the correlation of virulence of a serotype with PAFr binding (McCullers & Rehg, 2002; van der Sluijs et al., 2006).

Further strain dependent variance has been seen with pneumolysin (Ply) which can differ in its cytolytic potential. Both cytolytic and non-cytolytic Ply have been associated with invasive disease however, only the cytolytic Ply-possessing strains can trigger TLR4-mediated activation of NOD-like receptor family, NLRP3 inflammasome that activates IL-1 β secretion from macrophages. Some cytolytic strains stimulate GM-CSF and IFN- β secretion which again can invoke strong immune response. Yet some strains like serotypes 1, 8 and 7F are

not recognised by NLRP3 mechanism and hence can evade clearance by immune system (Harvey et al., 2014; Witzentrath et al., 2011). Thus, virulence factor diversity can potentially influence the invasiveness of *S. pneumoniae* strains. Furthermore, capsule mutant type 4cps4D- also caused significantly higher pathology compared to influenza alone infection, despite being undetectable in the lungs indicating that unencapsulated strains can also prove perilous during secondary infection. A notable feature of strain-dependent variation is the type distribution of infiltrating cells (Figure 4.9 C). While all wild types showed very high neutrophil infiltration in the lungs, the capsule mutant showed high number of lymphocytes infiltrating the lungs. Pneumococcal capsule is known to influence cytokine response in the host immune cells shifting from pro- to anti-inflammatory action (de Vos et al., 2015; van der Poll et al., 1996, 1997). Studies have shown that capsular PS can influence Th1/Th2 cytokine response based on the serotype (Mawas et al., 2000). It is not very clear whether and how capsule can dictate myeloid/lymphoid cell activation by manipulating cytokine signalling and how it ties up with secondary infection after influenza as primary infection with the capsule mutant did not display such strong predilection for lymphocytes. Nevertheless, this observation strengthens the widely held notion that the presence of capsule in *S. pneumoniae* determines the immune response of the host. The ROS content in the lungs of infected mice in the form of H₂O₂ was measured and was found to lack any clear pattern amongst the tested groups (Figure 4.10 A). This could arguably be an effect of intratracheal procedures that was done twice on these mice for secondary infection but one would expect a

clear difference between infected and mock infected groups in any case. Further analysis is required to elucidate the cause of such discrepancies.

MPO activity on the other hand, showed a very clear trend similar to the histopathology (Figure 4.10 B). Groups dually infected with serotype 4 showed the highest MPO activity followed by dually infected serotype 3 groups. Dual infection with serotype 19F led to similar levels of MPO activity to mock and other groups apart from a mild increase at 24 hours post-secondary infection. The MPO activity was lower in the mice infected with capsule mutant following secondary infection when compared to wild type.

NETs formation reflected the trend of MPO activity and histopathology after secondary infection with serotype 4 that showed the highest NETs formation in lungs while infection with serotype 3 came second (Figure 4.10 C). Both serotypes 4 and 3 induced higher NETs formation when compared to serotype 19F in dual infection. The capsule mutant again did not induce NETs as high as its wild type thereby re-stressing on the importance of capsule in inciting efficient host response.

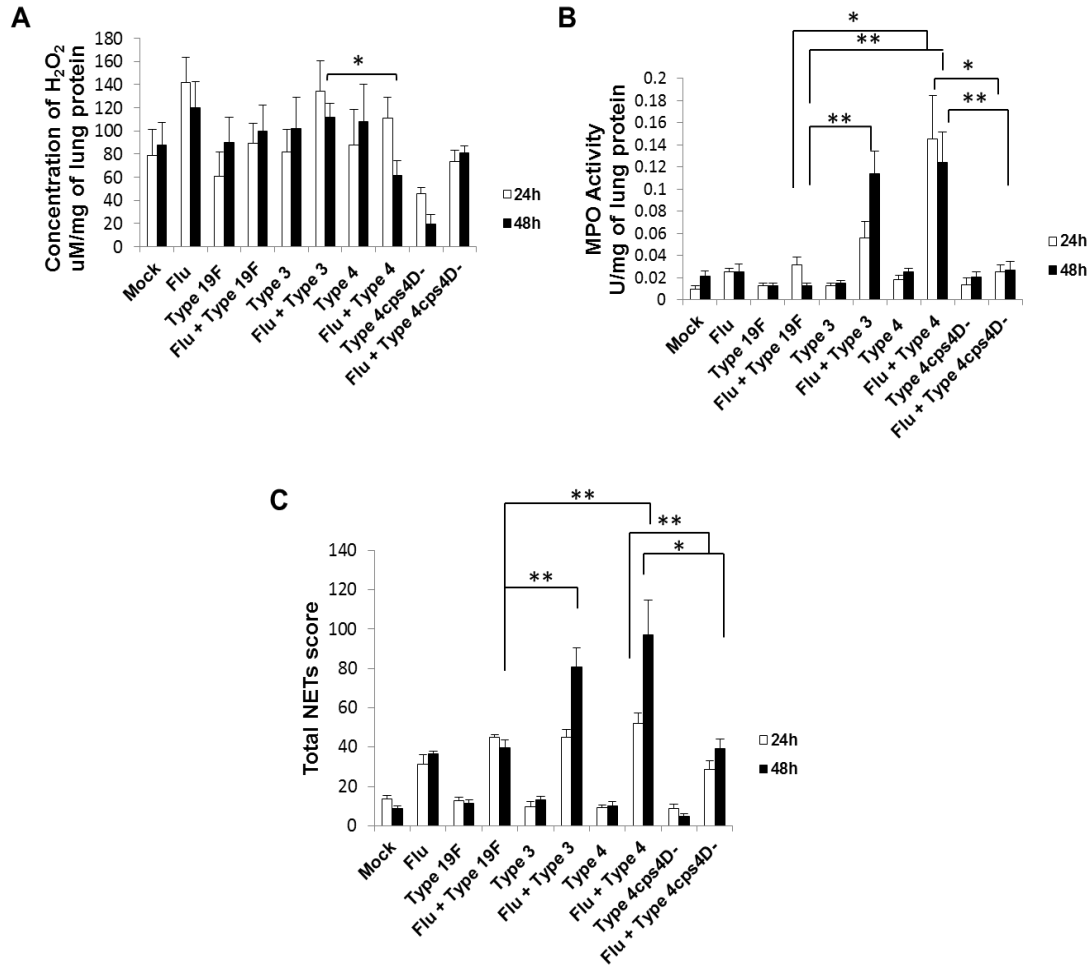


Figure 4.10. NETs and neutrophil activity in lungs after secondary pneumococcal infection. (A) Influenza infection by itself induces high concentrations of H₂O₂. (B) Mice infected with type 4 after influenza infection showed highest MPO activity in lungs followed by serotype 3 infection. (C) Dual infection with type 4 induced the highest NETs followed by type 3. The capsule mutant induced significantly lower NETs than wild type following secondary infection. Values represent the means \pm SE of 6 animals per group (2 independent experiment). * indicates P value < 0.05 ** P value < 0.01 , ANOVA with Tukey post-hoc correction.

mRNA expression of some pro-inflammatory cytokines and cytokine-regulatory factors showed mixed serotype-specific patterns (Figure 4.11 A). While interferon-beta (*IFN- β*) and *IL-1 β* were expressed highly in mice infected with serotype 3 after influenza infection compared serotype 4 infection, the latter group showed higher expression of *RANTES*. Increased expression of *RANTES*

and *IL-1 β* was seen in all influenza-infected groups indicating their importance in host response to influenza virus. Mice infected with capsule mutant of serotype 4 had lower expression profiles than those infected with wild type for all three cytokines. Protein concentrations were much more conclusive (Figure 4.11 B). Levels of IL-6, IL-1 β , TNF- α , IL-17 and IL-10 were measured by ELISA and showed high concentration in the dually infected serotype 4 groups followed by serotype 3 groups. IL-10 was only increased in type 4 dual infection groups and the capsule mutant induced lower levels of all four cytokines than the wild type. IL-17 was not detectable in all samples.

MAP kinase phosphatases (MKPs) are negative regulators of cytokine expression and have profound impact on innate immunity especially after influenza infection (James et al., 2015; Jiao et al., 2015; McCoy et al., 2008). *MKP 5* gene expression was shown to increase during influenza infection and *MKP 5* deficient mice were resistant to influenza infection (James et al., 2015). In this study, while mRNA expression of *MKP 2* and *3* were more or less enhanced after influenza infection, no such change was seen with *MKP 5* (Figure 4.11 A). It is possible that a low sublethal dose of virus (5 PFU) does not invoke a high expression of *MKP 5* in mice since the previous studies had used higher viral doses. Interestingly, *MKP 3* expression was lower at 48 hours after dual infection with serotypes 3 and 4 indicating disruption of cytokine regulation by virulent pneumococci infection (Figure 4.11 A). Considering that dysregulation related-cytokine storm has been implied in severe epidemics of influenza virus such as the 1918 'Spanish flu' (Osterholm, 2005), this finding can have a significant

bearing on the outcome of secondary infection. Although not statistically significant, the lower *MKP 3* gene expression does correlate to statistically significant increase in the protein content of pro-inflammatory cytokines in the serotypes 3 and 4 dual infection groups (Figures 4.11 A and B). Capsule mutant as expected was lower in both mRNA expression and protein concentration of pro-inflammatory cytokines when compared to the wild type. In *MKP* gene expression, the capsule mutant does not show significant dysregulation like wild type for *MKP 3* at 48 hours. However, the *MKP 5* gene expression is lower at 48 hours as an exception.

A

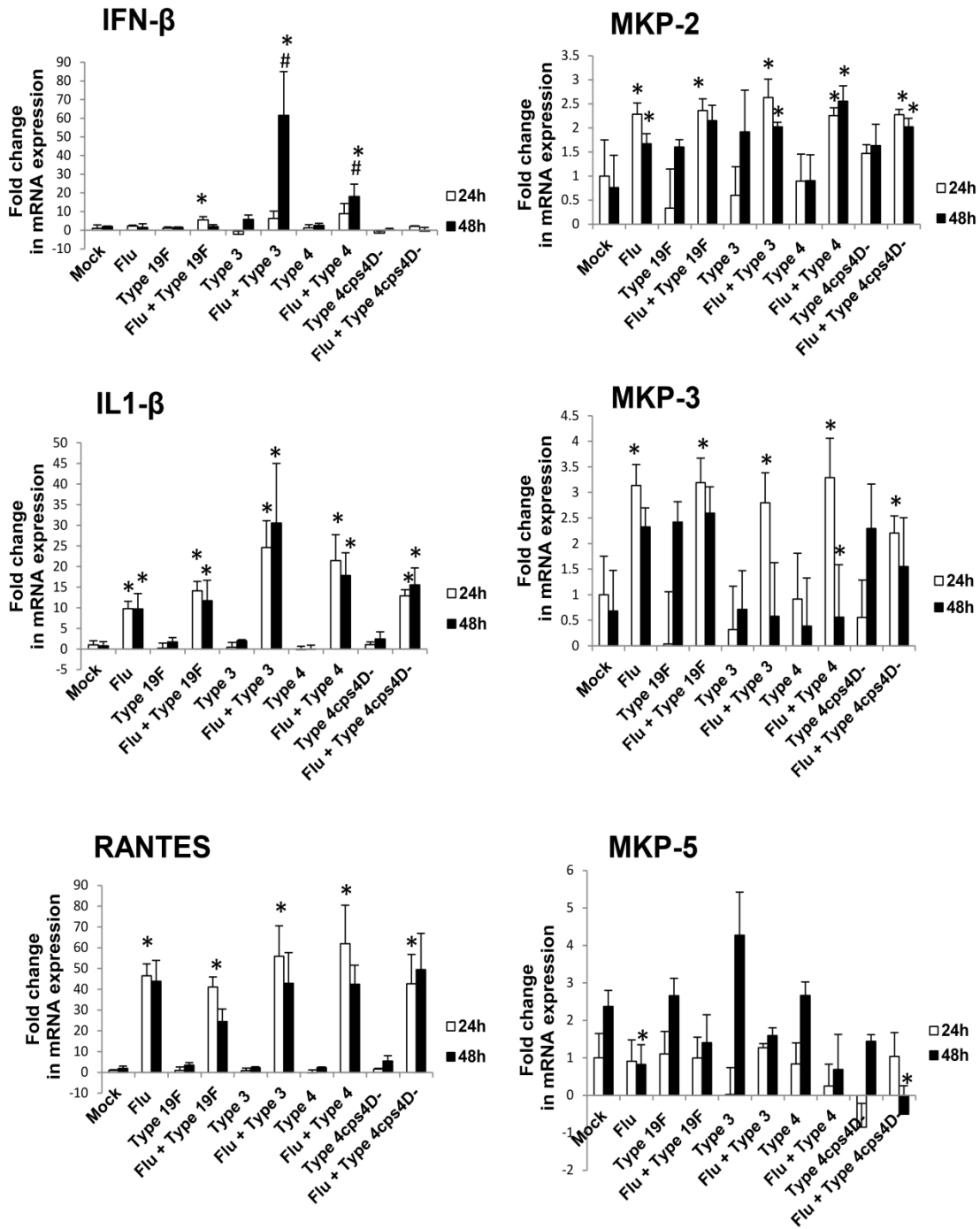


Figure 4.11. (A) mRNA expression of pro-inflammatory cytokines and cytokine-regulatory proteins. Values represent the means \pm SE of 4 animals per group (2 independent experiments). * indicates P value < 0.05 over Mock, # indicates P value < 0.05 over Flu+serotype 19F, ANOVA with Tukey post-hoc correction.

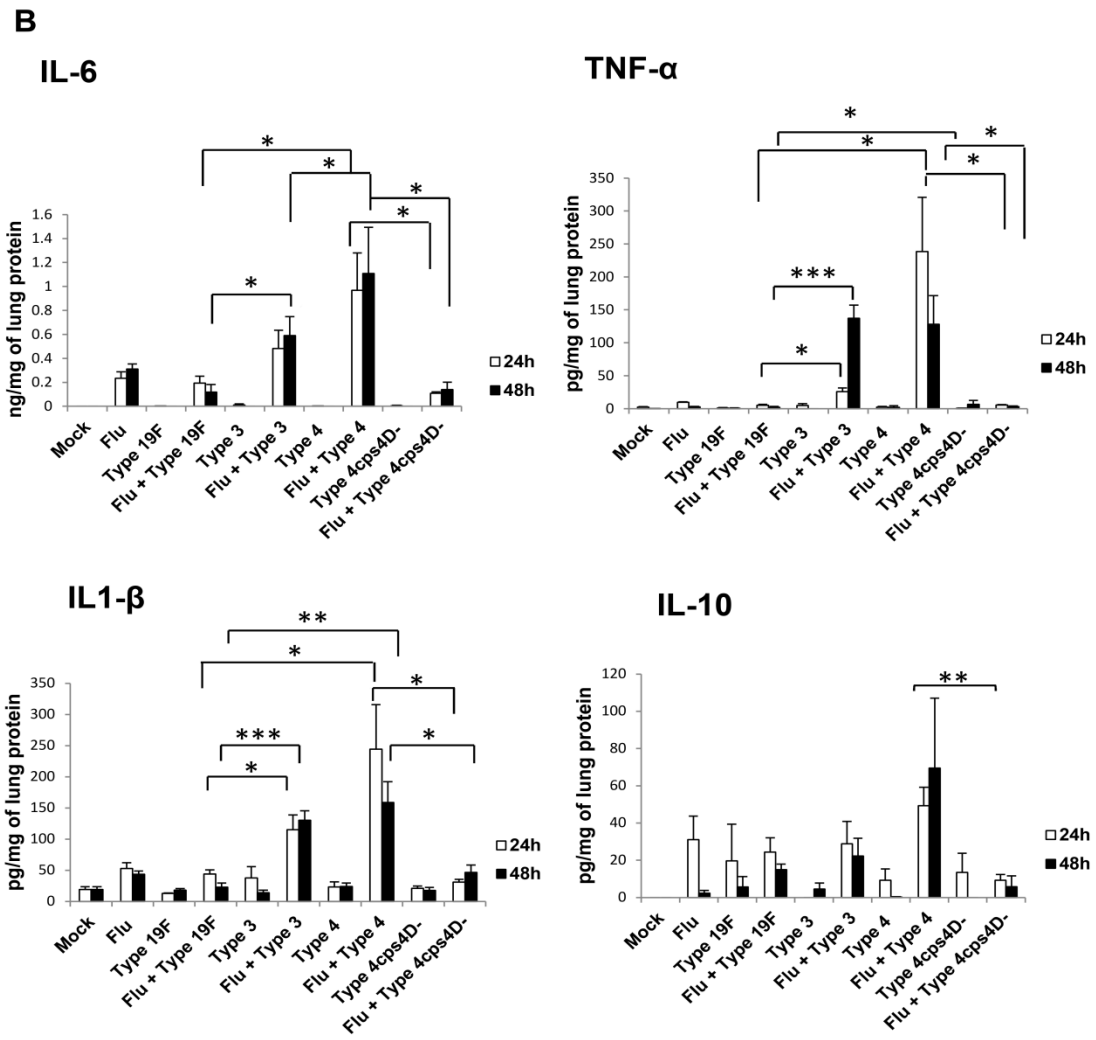


Figure 4.11. (B) Protein levels of pro- and anti-inflammatory cytokines. IL-17 was not detectable in the lung homogenates. Values represent the means \pm SE of 4 animals per group (2 independent experiments). * indicates P value < 0.05 ** P value < 0.01 , *** P value < 0.001 , ANOVA with Tukey post-hoc correction.

4.3.5 NETs induction in bone marrow-derived neutrophils by pneumococci does not reflect *in vivo* patterns of NETosis

Stimulation of bone-marrow derived neutrophils *in vitro* using *S. pneumoniae* serotypes resulted in a pattern of NETs induction different from the *in vivo*

observations (Figure 4.12 A and B). Neutrophils incubated with serotype 4 generated the lowest NETs compared to stimulation with all other strains most notably lower than the capsule mutant *cps4D*-. Serotype 3 induced the highest though not significant NETs generation followed very closely by serotype 19F. Finally, neutrophils were stimulated *in vitro* first with BALF from influenza-infected mice and then with *S. pneumoniae* strains to mimic secondary infection. While all infectious environment including BALF alone (Flu) induced higher amount of NETs than unstimulated neutrophils in media (control), the pattern of NETs formation again did not reflect the *in vivo* findings (Figure 4.12 B). Flu-BALF with Serotypes 19F and 4 induced the highest NETs while the capsule mutant was slightly lower than the type 4 wild type. However, serotype 3 induced lowest NETs amongst all the strains very close to that of flu alone stimulation.

Although it is very hard to speculate the reason behind such discrepancies, the limited bacteria-neutrophil interaction under laboratory conditions could have played some role in it. In an *in vivo* model, neutrophils and bacteria interact in the presence of various overlapping factors such as chemokines and ROS. Both chemokines and ROS are known to be involved in NETosis (Brinkmann et al., 2004; Gray et al., 2013; Figure 3.6 C). During infection, such pro-inflammatory chemokines and ROS are upregulated in lungs which may have provided additional stimulation to the neutrophils as NETosis can occur due to stimulation of different receptors. It is also possible that the neutrophils recruited into the lungs as a result of cell signalling may already have been predestined to form NETs in the peripheral bloodstream itself. The limitation of poor neutrophil yield

from peripheral blood of mice necessitates the use of bone marrow-derived mature neutrophils that may be missing in certain activation features. Use of human peripheral blood neutrophils may address these issues, yet this area warrants more research as most studies on NETs rely solely on *in vitro* examination which may not accurately reflect the *in vivo* scenario.

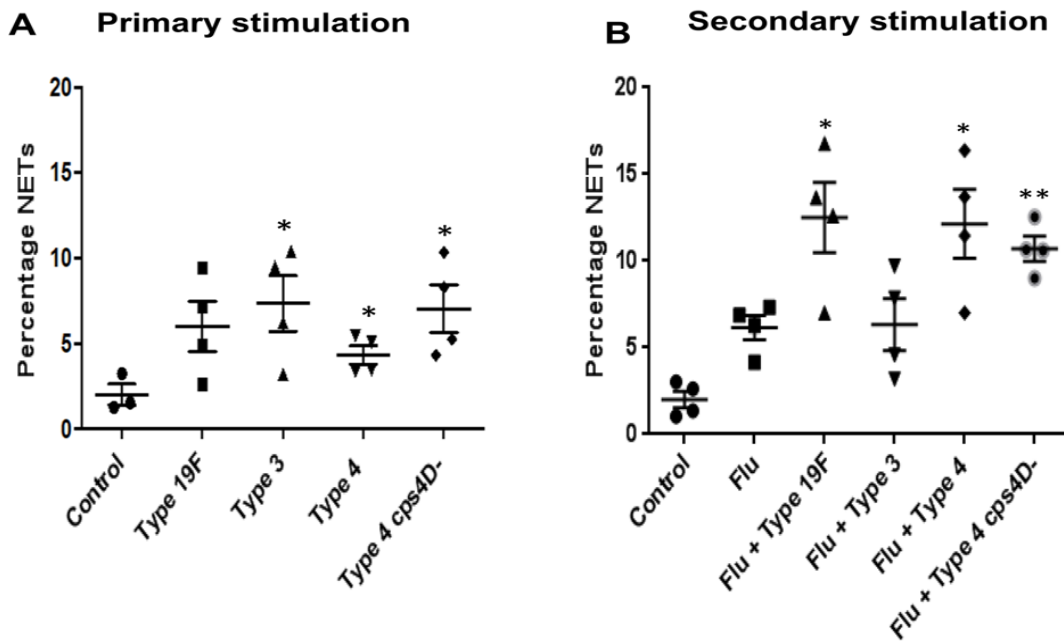


Figure 4.12. Induction of NETs *in vitro* using *S. pneumoniae* do reflect the *in vivo* trend in primary and secondary infection model. Bone marrow-derived neutrophils were stimulated *in vitro* to induce NETs. **(A)** Neutrophils were incubated with pneumococci. At MOI of 1, type 3 induced highest NETs, type 4cps4D- induced more NETs than wild type. **(B)** Neutrophils were stimulated for 2 hours using BALF from influenza-infected animals to induce NETs. *S. pneumoniae* were then added at MOI of 1 and incubated for 2 hours. Flu + type 19F, Flu + type 4 and Flu + type 4cps4D- induced significantly high NETs when compared to Flu alone stimulation. Values represent the means \pm SE of at least three independent experiments. * indicates P value < 0.05 ** P value < 0.01 , Anova with Tukey post-hoc correction.

4.4 Conclusion

The global circulation of infectious strains puts enormous adaptive pressure on the microbes to evolve into more robust beings. Tissue microenvironments can differ from host to host creating ample scope for pathogens like *S. pneumoniae* to re-organise their genome. Sometimes this could lead to enhanced expression of virulence factors that can subdue host immune responses thus leading to invasive disease; at other times the pathogen may downregulate these factors to improve survival under harsh conditions. Thus, various strains of the same pathogen emerge contemporarily and diverge over time from the parent strain with each strain invoking differential immune response from the host they infect.

A total of 94 clinical serotypes of *S. pneumoniae* have been identified so far based on their capsular material (reviewed in (Song et al., 2013)). The pneumococcal conjugate vaccination utilises the immunogenic property of the capsule that is encoded by the *cps* loci of the pneumococcal genome (Melegaro et al., 2010). Variations in the PS composition lead to differences in immunogenicity between serotypes. While serotype 19F represents the most common type of PS structure among *S. pneumoniae* serotypes, serotype 3 has a shorter mechanism of PS biosynthesis which leads to copious amount of PS production. This feature was validated by FITC-dextran exclusion assay which showed serotype 3 to possess the largest capsule when compared to serotypes 19F and 4 (Figure 4.5 B and C). Capsule can negatively affect opsonisation and phagocytosis of bacteria by neutrophils and other phagocytes (Hyams et al., 2010). It can also help the bacteria to evade entrapment by NETs although this aspect was not found to be

very crucial for the virulence of pneumococcus as the diplococci can anyway break the NET structures using DNase (Beiter et al., 2006; Wartha et al., 2007). Though an earlier report on *C. albicans* showed capsular polysaccharide of wild type strains inhibiting NETs (Rocha et al., 2015), the current study for the first time demonstrates that a bacterial capsule polysaccharide by itself can induce NETs. The reason behind the contradiction in findings is not clear at this stage. *In vitro* experiments with isolated neutrophils showed that the PS could induce NETs in a dose-dependent manner (Figure 4.4). Additionally, molecular reduction of PS favoured phagocytosis against NETosis in serotype 4 indicating the manipulative influence of capsule on neutrophil function. NETs apart from antimicrobial action can also cause tissue injury (Narasaraju et al., 2011; Saffarzadeh et al., 2012). While acting as a stimulant for NETs formation, capsule concurrently helps pneumococcus in evading NETs with the help of DNase thereby giving rise to a large number of functionally redundant NET structures in the lung that might lead to higher lung injury.

Serotypes with thicker capsules like type 3 and 4 showed lower susceptibility to neutrophil-mediated killing especially NETs when compared to type 19F (Figure 4.5 D). Upon the development of primary pneumococcal pneumonia in murine lungs, this difference plays a very essential role as the progression of pneumococcal disease along with pulmonary NETs formation correlates with the thickness of the bacterial capsules (Figures 4.6 and 4.7). However, these correlations did not materialise during secondary pneumococcal infection after influenza infection as serotype 4 showed the highest virulence and NETs

induction more than serotype 3 (Figures 4.8, 4.9, 4.10 and 4.11B). This shift in virulence could be attributed to many things as discussed earlier; most notably to the H₂O₂ production and genotoxicity caused by serotype 4 (Rai et al., 2015). While a robust host immune response may permit only those serotypes that can survive in high numbers in the lung to cause invasive disease, during secondary infection such requirements could be relaxed due to the compromised lung environment arising from influenza infection selecting for serotypes that can cause maximum damage with their virulence components without needing to be high in numbers. However, no clear trend in H₂O₂ levels in lungs could be established in this study alluding to other virulence mechanisms such as pneumolysin.

Nevertheless, capsule is still very crucial in maintaining the disease-causing ability of pneumococcus. A capsule mutant of serotype 4 producing lesser PS was used to study the immediate effect of loss of capsule PS on lung pathology and NETs during primary and secondary pneumonia. In both cases, the mutant bacteria failed to cause any clinical manifestation of pneumococcal disease while the wild type did (Figures 4.6, 4.7, 4.8, 4.9, 4.10 and 4.11B). With respect to NETosis, the capsule mutant did not induce as much NETs as the wild type *in vivo*. Hence, it can be concluded that while capsule plays a crucial role in the virulence of *S. pneumoniae* in causing pneumonia-associated lung injury and NETosis during primary infection, capsule along with other pneumococcal virulence factors play an important role in the pathogenesis of secondary pneumococcal infections.

CHAPTER FIVE

HIGH FAT DIET-FED MICE SHOW A MARGINAL INCREASE IN THE FORMATION OF NEUTROPHIL EXTRACELLULAR TRAPS IN LUNGS IN RESPONSE TO INFLUENZA INFECTION

5.1. Background

5.1.1 Epidemiology of obesity - impact of a high fat diet (HFD)

Obesity is a growing worldwide epidemic which is a particular cause of concern for developing nations that have to simultaneously deal with high under-nutrition in its poorer sections as well as increasing obesity in the burgeoning middle and upper class. Clinically, obesity is defined as abnormal accumulation of adipose tissues or fat in the body that may impair health. WHO defines a body mass index (BMI, weight in kilograms divided by square of height in metres) of more than 25 as overweight and more than 30 as obese (WHO Fact sheet, January 2015¹¹). Consumption of high calorie food like fast food, trans-fatty acids and fructose together with a sedentary lifestyle has been identified as the main cause of increasing obesity rates (reviewed in (Hurt et al., 2010)). The prevalence of obesity has doubled since 1980 and in 2013, about 42 million children under the age of five were found to be overweight or obese (WHO Fact sheet, January 2015¹¹, Flegal et al., 2005). Obesity has been associated with cardiovascular diseases like heart disease or stroke, diabetes, osteoarthritis, hypertension, certain cancers like that of breast or colon and even psychological conditions (WHO Fact

sheet, January 2015¹¹). Fears are rampant about the possibility that obesity and related diseases might soon overtake smoking as the leading cause of preventable death in the United States of America (Office of Surgeon General, US, 2001¹²). Similar concerns have been raised in other parts of the world as well.

5.1.2 Inflammation and oxidative stress during obesity

Obesity has been associated with chronic low grade inflammation (Hotamisligil et al., 1993). Adipose tissue possesses a mix of adipocytes, preadipocytes, immune cells and endothelium. Alterations in nutrient excess can lead to adipocyte hypertrophy and hyperplasia that can restrict blood supply to adipocytes leading to hypoxia (reviewed in (Trayhurn & Wood, 2004; Wellen & Hotamisligil, 2005)). Hypoxia can incite necrosis and macrophage infiltration of adipose tissue which in turn leads to over secretion of pro-inflammatory cytokines. Adipocytes are similar to macrophages and express receptor of macrophage proteins like TNF- α , IL-6 and MMPs. Furthermore, lipids themselves can induce inflammation. Macrophages can absorb the excess lipids and store them to become atherosclerotic foam cells. Thus, the localised inflammation of adipose tissue can promulgate systemic inflammation that may lead to the development of obesity-related comorbidities (reviewed in (Trayhurn & Wood, 2004; Wellen & Hotamisligil, 2005)). Among the adipokines secreted during obesity, TNF- α , IL-6 and adiponectin have been found to be of most significance (Hotamisligil et al., 1993; Stenl f et al., 2003); (reviewed in (Liu & Liu, 2009)). Both TNF- α and IL-6 are pro-inflammatory cytokines that elicit higher recruitment of immune cells into the adipose tissues and are upregulated during

obesity. It is suggested that TNF- α inhibits insulin receptor signalling pathway and thus promotes insulin resistance (Hotamisligil et al., 1993, 1996). IL-6 is involved in regulation of inflammation and its receptor is expressed in the regions of brain like hypothalamus that controls appetite (Stenl f et al., 2003). Adiponectin, on the other hand, is downregulated during obesity and is linked to regulation of glucose and lipid metabolism, food intake and body weight and it also protects against chronic inflammation (reviewed in (Liu & Liu, 2009)).

Another crucial adipokine is leptin, a polypeptide hormone that helps to regulate appetite and also functions as immune modulator. It gets elevated during obesity due to over secretion by adipocytes which may lead to leptin-resistance as seen in type II diabetes patients. In addition, it also induces the T-lymphocytes and monocytes to produce proinflammatory cytokines like TNF- α , IL-6 and IL-1 β as well as ROS. Leptin also protects the T-lymphocytes from apoptosis and regulates T-cell proliferation and activation. Leptin has a structural similarity to other cytokines, such as IL-6, which is known to serve a pro-inflammatory role. In endothelial cells, leptin induces oxidative stress and upregulation of adhesion molecules. (Reviewed in (Fantuzzi, 2005; McCallister et al., 2009)).

5.1.3 Obesity and neutrophils

Increases in peripheral neutrophil activity have been reported in healthy obese subjects (Brotfain et al., 2015; Trelakis et al., 2012). Along with increased superoxide generation in response to various stimuli, comparatively lower levels of adiponectin were found in obese subjects when compared to lean subjects.

These increases in neutrophil activity are believed to be due to the production of pro-inflammatory cytokines like IL-8 from the adipocytes (Trellakis et al., 2012). Increased superoxide production is also reported to be due to leptin receptors present on neutrophils which behave like pro-inflammatory cytokines and augment the respiratory burst (Caldefie-Chezet et al., 2001). Acute neutrophil infiltration has been known to precede macrophage infiltration in tissues where they may initiate the inflammatory signalling cascade leading to chronic macrophage infiltration (Strissel et al., 2007). In a diet-induced obesity (DIO) model, researchers found increased neutrophil recruitment into the intra-abdominal adipocytes peaking at day 3-7 since the start of HFD and declining thereafter (Elgazar-Carmon et al., 2008). The neutrophils from HFD-fed mice also demonstrated increased adherence to adipocytes upon stimulation with PMA that was mediated by protein complex formation between CD11b of neutrophils and intercellular adhesion molecule (ICAM) 1 of adipocytes. Ligation of ICAM-1 by itself is known to provide pro-inflammatory effects which can lead to increase in the infiltration of adipose tissues.

5.1.4 Obesity and respiratory health

Obesity has been shown to affect pulmonary competence due to excessive fat deposition in the chest wall, increased pulmonary blood volume and extrinsic mechanical pressure on the thoracic cavity by compression from the excess soft tissue. This alters the lung mechanics by affecting gas exchange and respiratory muscle control (reviewed in (McCallister et al., 2009)). In a cross sectional study, researchers found high correlation of lower circulating levels of lung-derived

innate immune protein, surfactant protein D (SP-D) with obesity and type II diabetes (Fernández-Real et al., 2010). Obesity can lead to increased dyspnoea thereby reducing exercise capacity and also augments respiratory resistance (reviewed in (Falaglas & Kompoti, 2006; McCallister et al., 2009)).

Abdominal obesity is associated with gastro-oesophageal reflux due to increased gastric volumes and gastric pressure from visceral fat tissues that affect the lower oesophageal sphincter closure. In such cases, the gastric fluid may get aspirated into the respiratory tract causing aspiration pneumonia (reviewed in (Mancuso, 2013)). Additionally, obesity can also predispose one to increased risks of community-acquired respiratory tract infections. In a large population study of over 26,000 men aged 44-79 years and 78,000 women aged 27-44 years in the U.S.A., significant weight gain during adulthood and high BMI were shown to correlate with higher risks of community-acquired pneumonia (CAP) in women and to a smaller extent in men (Baik et al., 2000). Other respiratory conditions shown to be influenced by obesity are asthma, chronic bronchitis and chronic obstructive pulmonary disorder (Akerman et al., 2004; Guerra et al., 2002; Schols et al., 2005).

5.1.5 Obesity and influenza

During the 2009 H1N1 pandemic, obesity was for the first time established as an independent risk factor for severe influenza cases (Louie et al., 2009, 2011). Reports suggested that morbidly obese patients i.e. those having BMI more than 40 were more likely to be hospitalised due to influenza-related complications. The

situation gets worse with the presence of comorbidities like type II diabetes, coronary heart conditions and hypertension. Later these findings were extended to increased admission to intensive care units, morbidity and death (reviewed in (Mancuso, 2013)).

Even before the 2009 pandemic, obesity was suspected to be a cause behind acute influenza pneumonitis in many instances. In 2007, Smith et al. (2007) had observed a correlation of severe influenza infection with increased fat mass in a DIO model. Lean and obese mice infected with influenza A/PR8/34 virus showed higher mortality rate and lung pathology in the DIO group. Several cytokines were found dysregulated in the DIO model like delayed but higher expression of pro-inflammatory TNF- α and IL-6, decreased expression of MCP-1 and RANTES as well as reduced expression of interferons- α and β . NK cell cytotoxicity was also found to be reduced in the DIO group.

Subsequent studies found impaired T-cell responses to influenza infection in the DIO mice. Mice sequentially infected with two different strains of the virus – H3N2 and H1N1/PR8 showed increased mortality rates, lung pathology and lung viral titres along with reduced pro-inflammatory and antiviral cytokines most notably IFN- γ in the obese groups when compared to the lean groups. The memory CD8⁺ T-cells of obese group failed to elicit a strong immune response during secondary viral infection (Karlsson et al., 2010). Similar trend was seen in another DIO study using H1N1/PR8 virus for primary infection and pandemic H1N1 virus for secondary infection. Again, there was a reduced cross-protection in the obese group along with higher clinical manifestations. The researchers

found higher regulatory T-cells (Tregs) in the obese mice but the Tregs were 40% less suppressive than those of the lean mice (Milner et al., 2013). These findings indicate a possible reduction in the efficiency of influenza vaccines in protecting obese patients due to weakened T-cell response. Indeed, a 2012 clinical study found that BMI has a negative correlation with vaccine efficiency. A year after receiving trivalent influenza vaccine, obese individuals showed greater decline of antibody titres and decreased *ex vivo* CD8⁺ T-cell activation (Sheridan et al., 2012).

5.2 Specific objectives of the study

Ever since obesity was found to be an independent risk factor for morbidity during influenza infection, a lot of research has been directed towards finding the underlying cause and pathological implications in obese individuals. We now know that the immune system of obese individuals is dysfunctional which causes them to succumb faster or with higher severity to respiratory infections. There are no hitherto reports on the extent of NETs generated in the lungs of these individuals during or after an infection. Hence, this study focuses on analysing NETosis in the lungs of influenza-infected mice fed with HFD.

The specific objective of this study is to evaluate the effect of consumption of high fat diet on NETosis in the lungs of infected host animals.

5.3 Results and Discussion

5.3.1 Prolonged consumption of HFD leads to increased adiposity in mice

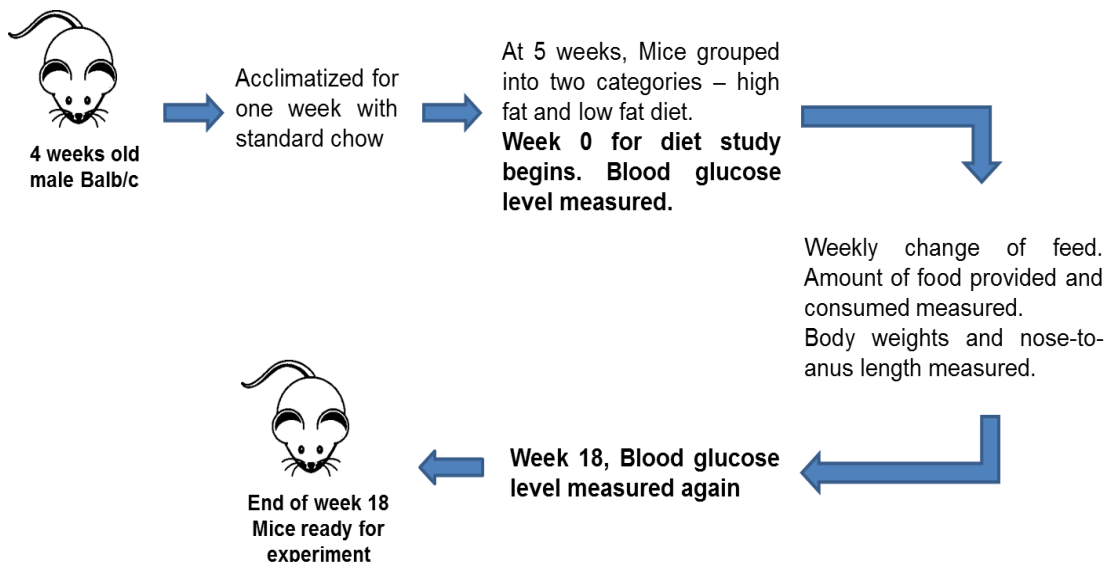


Figure 5.1. Time course for mice on low and high fat diets.

Mice were randomly grouped at 5 weeks of age into two groups and each group was fed with either low fat diet (LFD, 10% kcal from dietary fat) or high fat diet (HFD, 45% kcal from dietary fat) for a period of 18 weeks (Figure 5.1). The weights were comparable between the two groups at the start of the diet (Figure 5.2 A).

Due to higher amount of fat in HFD, the calories consumed are higher when compared to LFD. 1g of LFD amounts to 3.85 kcal while 1g of HFD has 4.73 kcal. Due to this difference, the HFD mice ended-up consuming more calories than the LFD which reflects on their body weight and BMI patterns (Figure 5.2 A-D). The blood glucose levels did not show any significant difference (Figure 5.2 E). Due to randomisation, initial blood glucose levels could not be matched

and hence, the average blood glucose level of HFD group was slightly lower than that of LFD group at the start of the experiments.

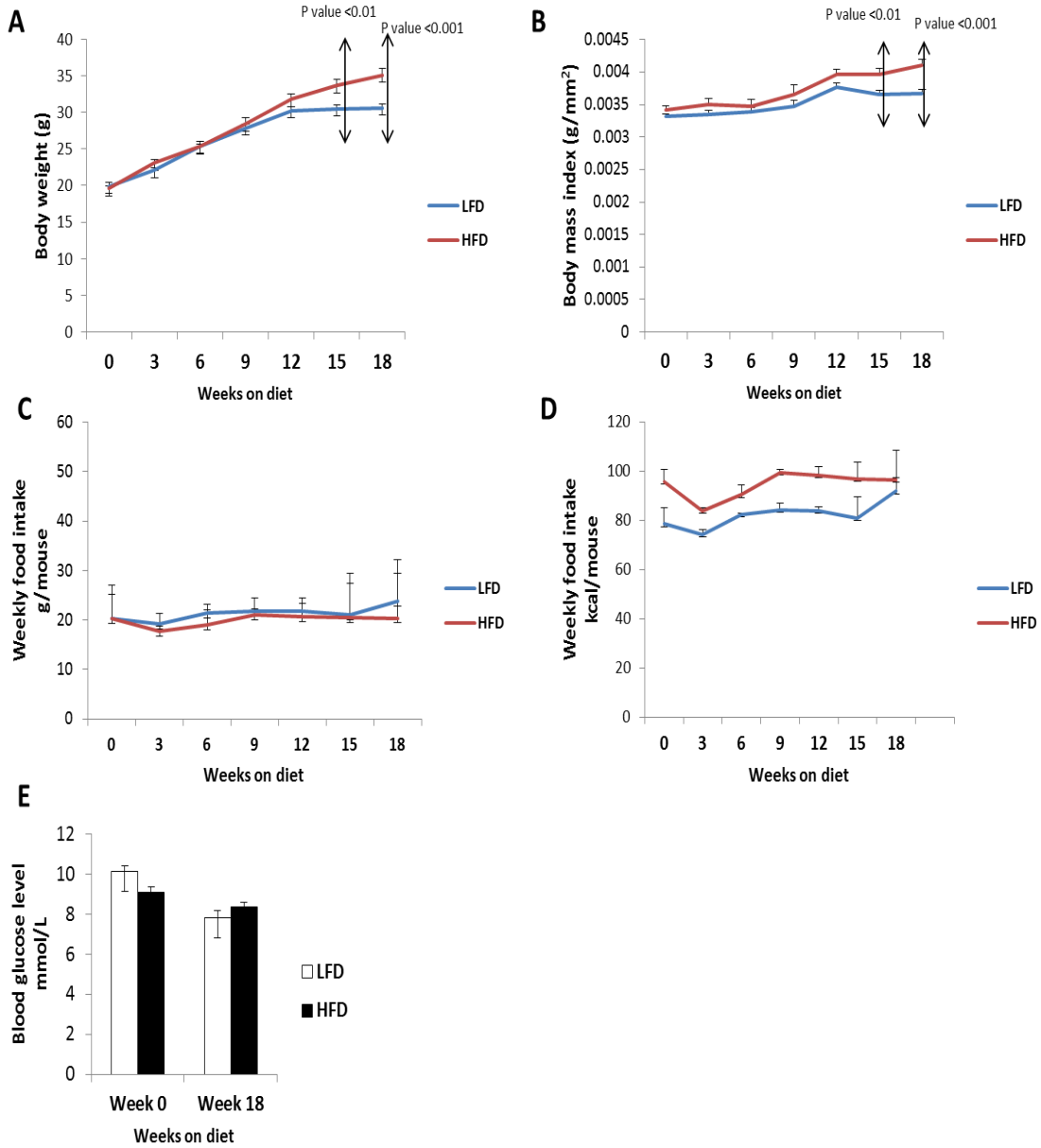


Figure 5.2. HFD mice show higher body weight gain and body mass index compared to LFD mice. After 18 weeks on the respective diets, HFD mice showed significantly higher (A) weight gain and (B) BMI. Even though the (C) weekly consumption of food per mice was comparable between the two groups, the (D) actual calories consumed were different due to higher dietary fat content. (E) Blood glucose levels were not significantly different between the two groups. Values represent the means \pm SE of 15 mice per diet group (3 independent batches), Student's *t*-test.

However after 18 weeks on diet plan, the HFD mice showed slightly higher glucose levels than LFD mice. Whether this later difference would have been more prominent if the initial levels were comparable is not clear.

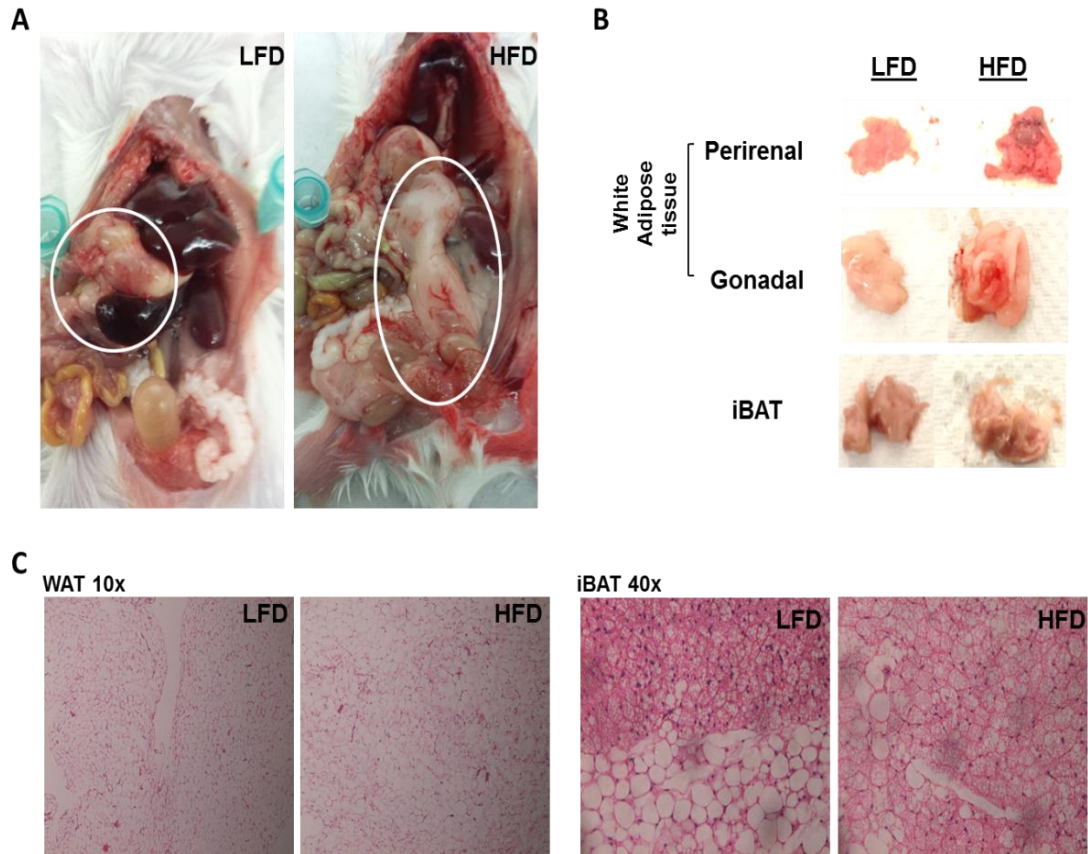


Figure 5.3. HFD mice show increased adiposity compared to LFD mice. (A) After 18 weeks on diet, the HFD mice showed greater accumulation of abdominal fat (white circle) than the LFD mice. (B) Gross anatomy of white (WAT) and brown adipose tissues (BAT) from LFD and HFD mice. The fat pads especially gonadal look larger in the HFD group. (C) Haematoxylin and eosin-stained sections of WAT and iBAT did not show any significant difference in morphology.

The HFD mice also showed higher accumulation of WAT in the gonadal and perirenal fat pads near the abdomen when compared to LFD (Figure 5.3 A and B). Organs like heart and kidneys along with fat pads also showed increased weights while spleen and lungs showed decreased weights in the HFD mice. The weights

of liver and brain were comparable between the two groups (Table 5.1). The adipose tissue sections were analysed by experienced pathologists and it was found that the increase in fat did not lead to any structural difference of the adipose tissue between the groups (Figure 5.3 C).

	LFD	HFD
Heart (mg)	165.93 ± 9.33	174.60 ± 19.33
Left kidney (mg)	292.40 ± 7.99	323.77 ± 21.78
Right Kidney (mg)	286.97 ± 8.22	320.60 ± 20.37
Spleen (mg)	177.33 ± 27.22	126.13 ± 11.23
Lungs (mg)	202.03 ± 23.22	192.03 ± 13.29
Liver (mg)	1330.90 ± 31.97	1319.67 ± 206.59
Brain (mg)	397.83 ± 13.96	397.97 ± 12.99
Gonadal WAT (mg)	245.50 ± 60.41	645.97 ± 137.12
Perirenal WAT (mg)	99.50 ± 35.19	291.07 ± 69.53
Interscapular Brown adipose tissue (iBAT) (mg)	157.57 ± 18.17	250.03 ± 26.66

Table 5.1. Weights of different organs and fat pads of LFD and HFD mice after 18 weeks on diet. Values represent the means ± SE of 3 mice per diet group (Single batch). P value = not significant, Student's t-test.

5.3.2 HFD and LFD mice show similar disease progression upon influenza A infection

After 18 weeks on selected diet, the mice were infected with a lethal dose of influenza A virus. Upon infection with influenza A virus, both the LFD and HFD mice showed similar body weight loss (Figure 5.4 A). Histopathological analyses also showed no significant difference however, there was a non-significant

decrease of overall score in the HFD mice on day 6 post-infection which becomes comparable with the LFD group by day 10 (Figure 5.4 B and D). This

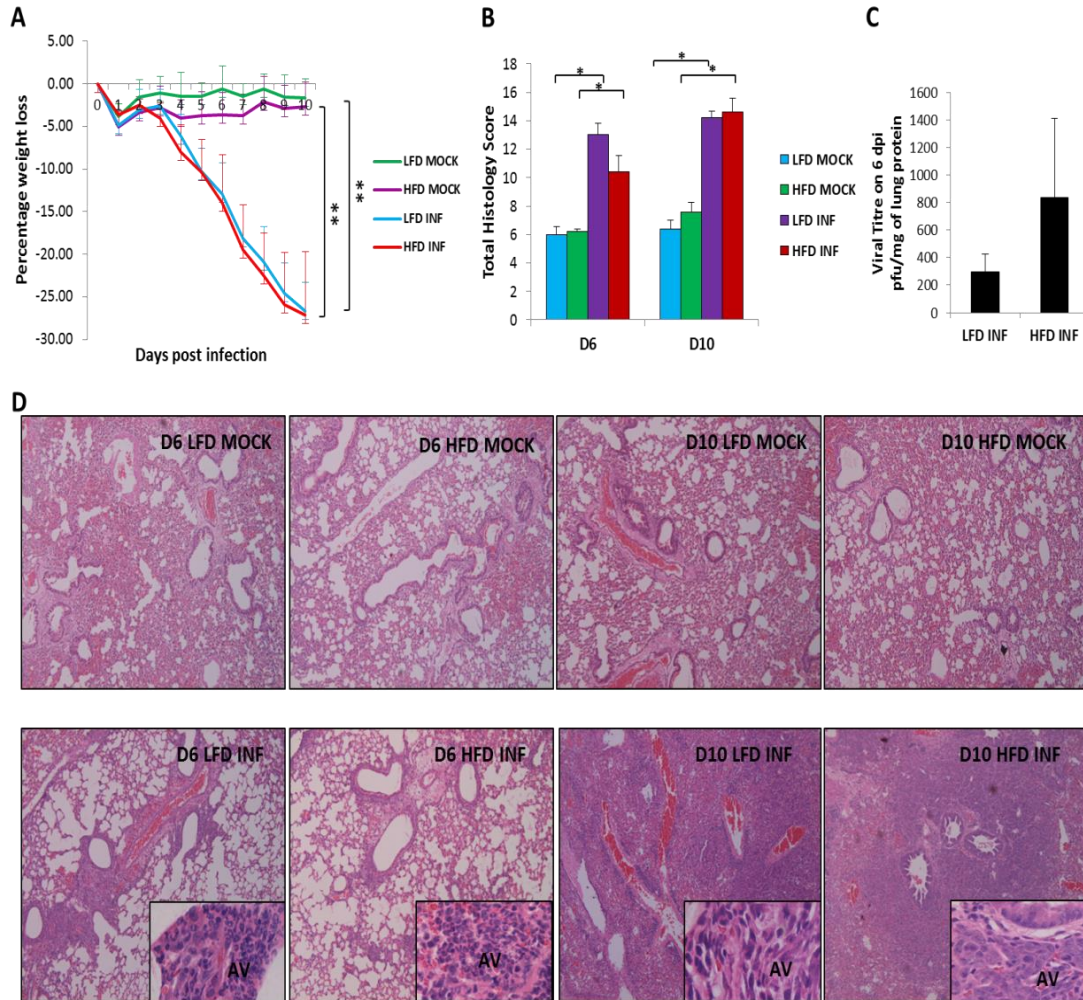


Figure 5.4. HFD and LFD mice show similar body weight loss patterns and histopathology upon lethal influenza A infection. (A) Both HFD and LFD mice showed similar levels of body weight loss upon infection with lethal dose of influenza A virus. (B, D) Histopathological differences among the groups were not significant as revealed by histology score and haematoxylin and eosin staining. AV- alveoli. (C) The viral titre was marginally higher in the HFD group on day 6 post-infection but is non-significant. No virus was detected on day 10. Values represent the means \pm SE of 5 mice per diet group (2 independent experiments). * indicates P value < 0.05 ** P value < 0.01 , ANOVA with Tukey post-hoc correction.

could perhaps indicate either some level of protection offered by increased fat deposits in HFD mice, which might keep the mice warm during the course of

infection or a more robust immune response in LFD mice. Both groups of mice showed thickening of alveolar septae, increased cellular infiltration in the alveolar and bronchiolar space and by day 10, increased alveolar fibrin deposition. The viral titres were not significantly different between both groups; however the titres tend to be higher in the HFD group. Further studies are required to determine if HFD modulates virus replication and/clearance over the course of influenza infection (Figure 5.4 C). Smith et al. (2007) also found similar but non-significant increase in the virus titre in a DIO study with influenza virus showing that obesity exerts only marginal influence on the viral replication inside host.

5.3.3 HFD mice show marginal increase in NETs formation despite lower MPO activity

The H₂O₂ concentration and MPO activity of both LFD and HFD groups were not significantly different. However, the H₂O₂ concentration in lungs was slightly higher in the HFD mice on day 6 indicating slight increase in oxidative stress in the lungs compared to LFD group. The levels of H₂O₂ were similar in both groups by day 10 as both groups reached their end-point of 30% loss in initial body weight (Figure 5.5 A). Previous reports have indicated increased PMN activity in obese individuals and murine DIO models (Brotfain et al., 2015; Elgazar-Carman et al., 2008; Trellakis et al., 2012). Surprisingly, our results showed that the MPO activity is lower albeit not significant in the HFD mice when compared to the LFD mice despite relatively higher H₂O₂ in lungs (Figure 5.5 B). However, this corresponds well with the histology scores where we saw slightly lower score in the HFD group on day 6. This implies a more functionally robust neutrophil

response in the lean mice (LFD). However, more research needs to be done regarding this as the observed differences were statistically insignificant.

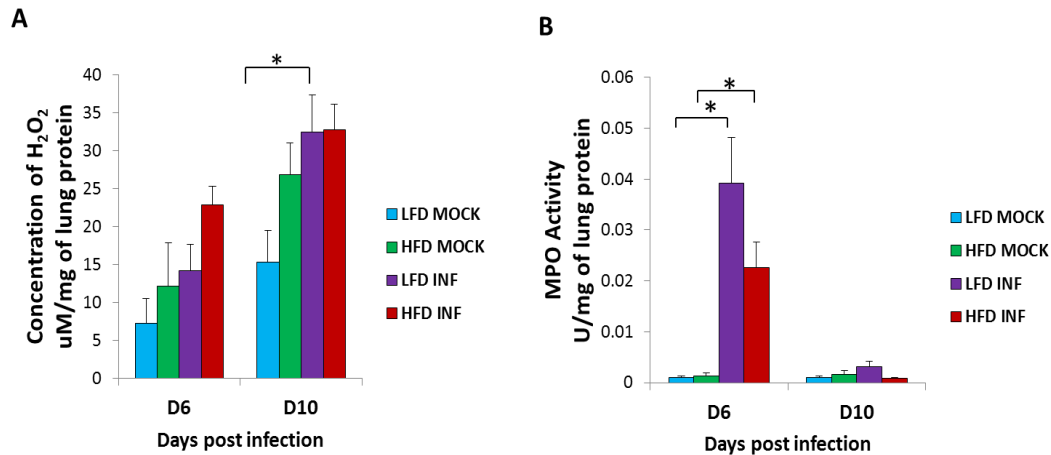


Figure 5.5. Marginal increase in ROS and decrease in MPO activity in the lungs of infected HFD mice. (A) The concentration of hydrogen peroxide in the lungs of infected HFD mice (HFD-INF) was comparatively higher on day 6 but non-significant. By day 10, the H₂O₂ concentrations in both the groups were similar in levels. (B) The MPO activity in the lungs of infected LFD mice (LFD-INF) was slightly higher on day 6 but non-significant. By day 10, the activity went down in both LFD and HFD infected groups but the LFD-INF mice still showed slight increase in activity. Values represent the means \pm SE of 5 mice per diet group (2 independent experiments). * indicates *P* value < 0.05, ANOVA with Tukey post-hoc correction.

The NETs showed a tendency to be increased, although not significant, in lungs on both days in the HFD mice despite lower MPO activity (Figure 5.6). This indicates a possible role of non-viral factors like higher cytokine response in inducing NETs and oxidative stress in the lungs of HFD mice. Again, further research is required to validate the effect of HFD on neutrophil activation and NETosis.

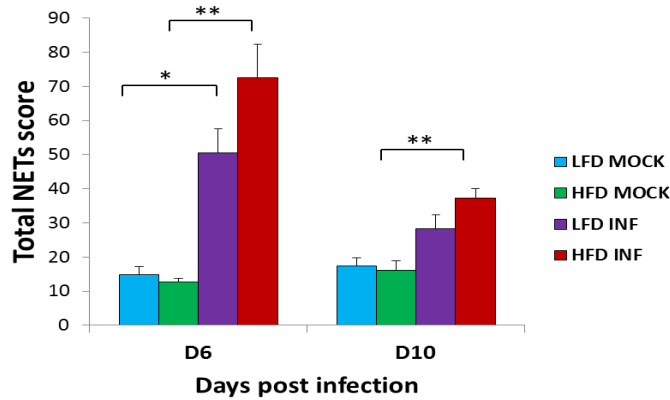


Figure 5.6. Infected HFD mice have marginally higher NETs formation in the lungs. The lungs of HFD-INF mice showed slight increase in NETs formation compared to LFD-INF mice on both day 6 and day 10 post-infection. Values represent the means \pm SE of 5 mice per diet group (2 independent experiments). * indicates P value < 0.05 , ** P value < 0.01 , ANOVA with Tukey post-hoc correction.

5.4 Conclusion

The widespread prevalence of obesity is a cause of concern for health authorities across the globe. With processed high fat-high sugar ‘fast’ food costing cheaper than healthy options, this epidemic is here to stay for quite some time. Apart from leading to a number of metabolic conditions like type II diabetes, atherosclerosis etc., obesity is known to have implications on respiratory health as well (reviewed in (McCallister et al., 2009)). Obesity increases susceptibility to influenza-related complications and CAP (Baik et al., 2000; Louie et al., 2009). Some researchers recommend obese individuals to be given priority for vaccinations against seasonal influenza to minimize fatalities in case of an epidemic thus, emphasising on the need to recognise obesity as a chronic medical condition by public health officials (reviewed in (Mancuso, 2013)).

While earlier studies on DIO and influenza infection concentrated mostly on the function of immune cells like T-cells, macrophages and neutrophils, there are no reports on the extent of NETs generated in obese subjects. Since NETs have been implicated in many pathological conditions, their importance in obesity especially during influenza infection commands more research into this area (Leffler et al., 2012; Narasaraju et al., 2011).

Due to difficulty in studying NETs in human subjects, animal models make an excellent alternative to help us elucidate the possible implications of NETs in disease pathogenesis. Hence, a high fat diet was used to increase adiposity in BALB/c mice. Though these mice are not considered obese in a strict sense, there is sufficient difference in the amount of adipose tissue to create significant difference in BMI and body weights (Figure 5.2 A and B) which are the factors employed during clinical studies in humans (Louie et al., 2009, 2011).

The data in this study reveal that even if both high and low fat diet-fed mice look clinically similar after influenza infection, there may be subtle non-significant differences in the lung physiology and immune response. Generally, there was a tendency to observe higher viral titre, ROS concentration and NETs score in HFD mice post-influenza infection when compared to LFD mice indicating the subtle influence exerted by higher adiposity on these pathological factors (Figures 5.4 - 5.6). One odd factor was the MPO activity which was expected to be higher as well in HFD mice but was found to be lower (Brotfain et al., 2015; Elgazar-Carman et al., 2008; Trellakis et al., 2012). Similarly, the histology scores were also slightly lower in HFD mice earlier in the infection

course. It is possible that the higher neutrophil activity and inflammation in general help in controlling the viral infection resulting in lower viral titre in the LFD mice. Similar results with increased titre in the HFD group were found during pH1N1 infection in a DIO model which was associated with high leptin levels in HFD mice that got abrogated by an anti-leptin antibody (Zhang et al., 2013). However, it is to be noted that the differences in H₂O₂, MPO activity and NETs between LFD and HFD were not statistically significant. Mouse strains show varying levels of obesity when fed with HFD (Montgomery et al., 2013). BALB/c mice are known to be resistant to DIO. There are other mouse strains like C57BL/6 that gain weight more rapidly when fed with HFD and become morbidly obese in 17-20 weeks. Even using transgenic mice such as ob/ob mice which have leptin deficiency that contributes to increased appetite may make these differences more pronounced. Nevertheless, there was indeed some degree of higher NETs and H₂O₂ concentration in the HFD fed-BALB/c mice in this study.

This study shows that increased adiposity due to prolonged consumption of HFD may lead to marginal increase in the formation of NETs in murine lungs in the absence of genetic factors such as leptin deficiency. This suggests that in morbidly obese individuals, NETs may form significantly in the lungs in response of influenza infection that might contribute to increased lung injury and complications of influenza.

CHAPTER SIX

CHEMICAL INHIBITION OF NADPH OXIDASE DOES NOT PREVENT INFLUENZA-INDUCED LUNG INJURY IN MICE

6.1 Background

6.1.1 Reactive oxygen species and oxidative stress

Reactive oxygen species or ROS are by-products of various cellular metabolic processes. Small amounts of ROS can be beneficial during cell signalling, cytokine and hormone regulation as well as in immunomodulation (reviewed in (Dupré-Crochet et al., 2013; Hildeman, 2004; Lander, 1997; Ray et al., 2012)). In addition, ROS is generated by phagocytes such as neutrophils and macrophages that are toxic for microbes and viruses (Fang, 2011). Natural antioxidants like SOD, catalase and glutathione peroxidase (GPx) help to convert ROS into less toxic compounds which can be removed by the host system (Dringen & Hamprecht, 1997). Oxidative stress occurs in case of any imbalance in this process leading up to build-up of toxic radicals that can cause tissue damage (reviewed in (Reshi et al., 2014)).

6.1.2 ROS from neutrophils and other phagocytes

Phagocytes upon activation by appropriate stimuli undergo respiratory burst releasing free radicals in the surrounding environment (Baldrige & Gerard, 1932). Both phagocytosis and ETosis involve respiratory burst that occurs through the activation of nicotinamide adenine dinucleotide phosphate-oxidase

(NADPH oxidase or Nox) complex (Brinkmann et al., 2004; Fang, 2011). The NADPH oxidase is a membrane-bound enzyme complex that transports electrons across biological membranes. It occurs in various isoforms from Nox 1-5 and Duox 1-2. In neutrophils, the complex (Nox2) remains inactive and upon activation assembles to release superoxide (Figure 6.1) (reviewed in (Bedard & Krause, 2007)).

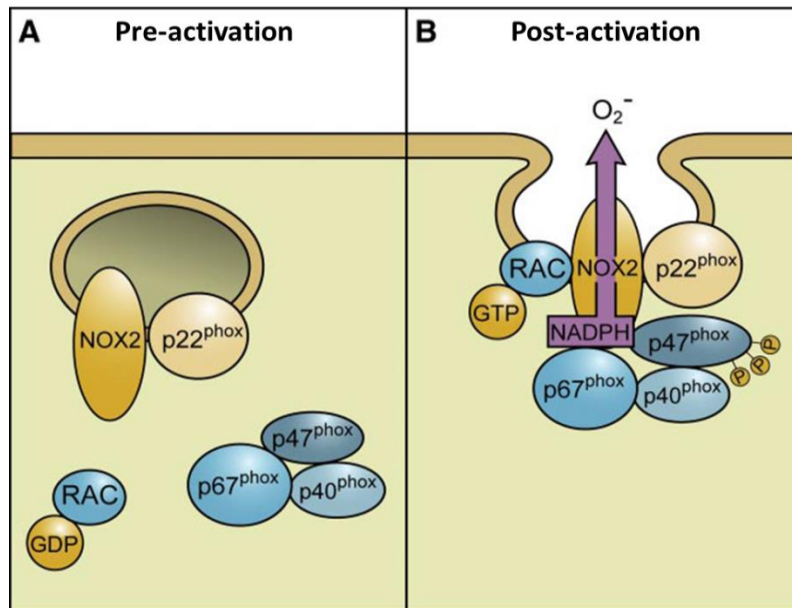


Figure 6.1. Assembly of NADPH complex upon activation. The NADPH oxidase complex comprises 6 subunits – Nox2/gp91-phox (Neutrophil oxidase, Cytochrome b245- α), p22phox (Cytochrome b245- β), p40phox (Neutrophil cytosolic factor, Ncf4), p47phox (Neutrophil cytosolic factor, Ncf1), p67phox (Neutrophil cytosolic factor, Ncf2) and Rho guanosine triphosphatases (GTPase) Rac1/Rac2. Nox2 and p22phox are found in the intracellular vesicle membrane under resting conditions. Activation is initiated at Rac by GDP to GTP exchange. The cytosolic p47phox subunit undergoes phosphorylation and interacts with p22phox along with p67phox and p40phox to form an active Nox2 enzyme complex. The Nox2-containing vesicle fuses with the phagosomal membrane helping the Nox2 to transport electrons from cytoplasmic NADPH to phagosomal oxygen to generate superoxide. (Adapted from Bedard & Krause, 2007).

Several micro-organism including viruses stimulate ROS generation from phagocytes (Kim et al., 2013; Peterhans et al., 1987); (reviewed in (Jones et al., 2012; Peterhans, 1997)). Neutrophils via Nox2 activation generate unstable superoxide (O_2^-) that undergoes spontaneous or SOD-mediated reduction into less toxic H_2O_2 which in turn gets converted into water by catalase (Figure 6.2). The H_2O_2 thus produced can interact with other neutrophil components and radicals such as MPO and reactive nitrogen species (RNS) (reviewed in (Tkaczyk & Vízek 2007)). MPO is another crucial radical-forming component of neutrophil as it generates hypochlorous acid (HOCl) upon interaction with H_2O_2 . HOCl can further react with H_2O_2 to generate singlet oxygen and other ROS (Held et al., 1978); (reviewed in (Arnhold, 2004)).

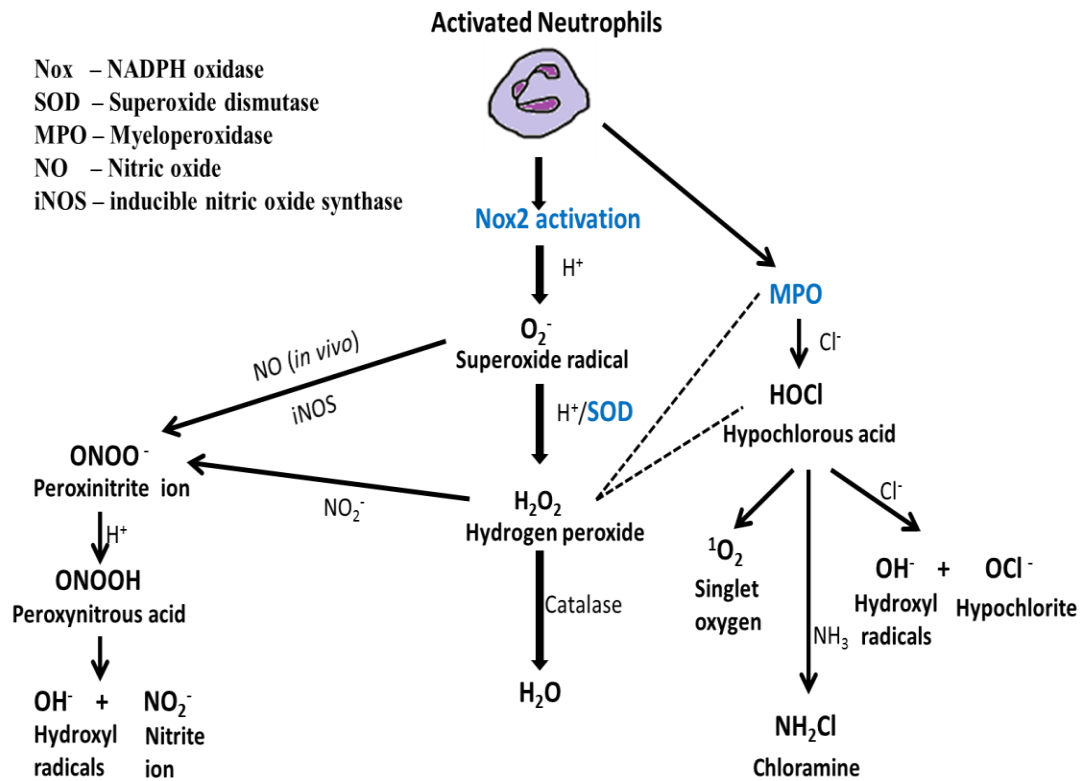


Figure 6.2. Generation of reactive oxygen-nitrogen species by activated neutrophils.

6.1.3 ROS and tissue injury

Free oxygen radicals have been shown to help in clearing pathogens. Neutrophils deficient or defective in active Nox2 were unable to clear fungal infections in patients with chronic granulomatous disease (Urban et al., 2009); (reviewed in (Segal, 1996)). Similarly MPO-deficient patients and transgenic mice were very susceptible to *C. albicans* infection (Kutter et al., 2000); (reviewed in (Klebanoff et al., 2013)). H_2O_2 and HOCl can cause polyunsaturated lipid peroxidation at cell membranes and also react with sulphur-containing amino acids. H_2O_2 especially can cross membranes and thus, is the most available and cytotoxic radical inside the phagocytes. O_2^- undergoes self-reduction to form H_2O_2 . H_2O_2 along with O_2^- react with nitrogen compounds to release RNS. The HOCl reacts with other proteases inside neutrophils to form chloramines which are also cytotoxic. Extracellular H_2O_2 is generated when the pathogens are too large to be handled and during NETosis (Chapman et al., 2002; Fang, 2011; Parker et al., 2012); (reviewed in (Dupré-Crochet et al., 2013; Klebanoff et al., 2013; Reshi et al., 2014)).

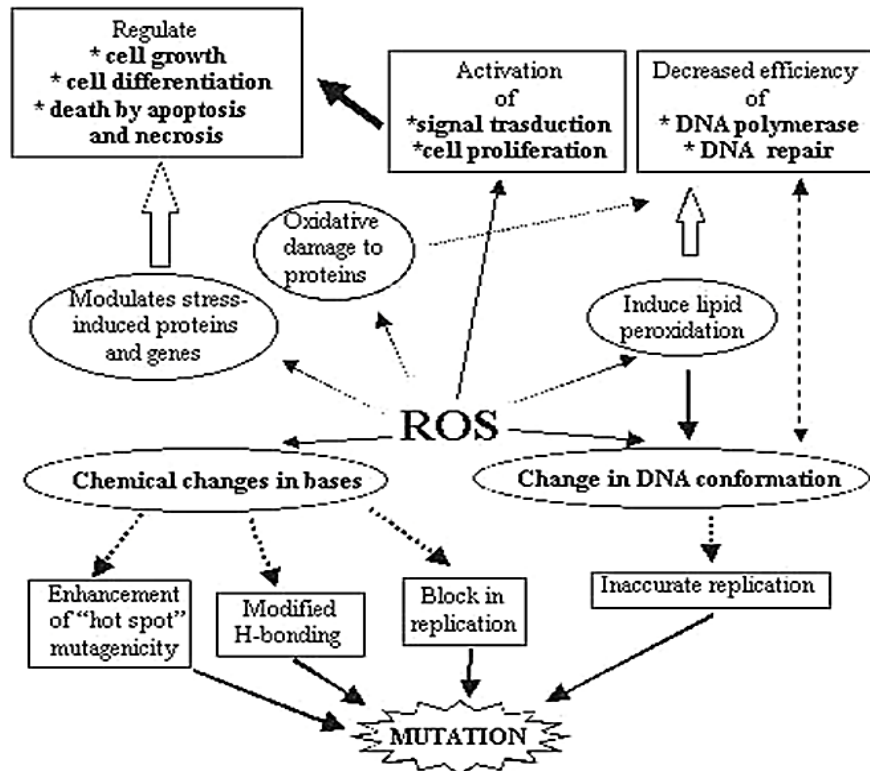


Figure 6.3. Effects of ROS on host. Adapted from (Matés & Sánchez-Jiménez, 1999).

Despite their beneficial actions, oxygen radicals can also cause grave injury to the host. Due to their non-specificity, ROS target both the pathogens and host cells. Many infectious and non-infectious pathological conditions have been attributed to ROS-induced damage (Hurtado-Nedelec et al., 2013; Tsukimori et al., 2005); (reviewed in (Pace & Leaf, 1995; Paracha et al., 2013)). Of these, phagocytic contribution of ROS during inflammation has also been observed (Carp & Janoff, 1980; van Berlo et al., 2010; Vlessis et al., 1995). ROS-induced host damage include cellular apoptosis and necrosis, lipid peroxidation, DNA damage, oxidative damage to amino acids and proteins (Figure 6.3) (reviewed in (Matés & Sánchez-Jiménez, 1999)).

6.1.4 Influenza-induced oxidative stress in lungs and antioxidant-based therapeutic approaches

Oxidative stress has been implicated in influenza pathogenesis (Buffinton et al., 1992); (reviewed in (Reshi et al., 2014)). When influenza virus infects the host, the lung epithelial cells and alveolar macrophages generate ROS via Nox2&4 and Duox 1&2 activation to start signalling cascade (Amatore et al., 2015); (reviewed in (Bedard & Krause, 2007; Fidone & Kennedy, 2003)). ROS have also been believed to possess anti-influenza activity thereby controlling viral burden in the lungs but no conclusive evidence has been reported so far (reviewed in (Reshi et al., 2014)). In fact, contradictory reports claim that ROS actually increases viral titre in the lungs (Hennet et al., 1992); (reviewed in (Peterhans, 1997)). For the influenza virus to be infectious, the initial HA needs to be cleaved into HA1 and HA2 which are done by cellular proteases in the lungs. Lung surfactant proteins help in inhibiting these proteolytic activities thereby reducing the viral titre. However, ROS damages the surfactant proteins and reduces their numbers thereby letting the virus replicate uncontrollably. In another study, incubation of activated neutrophils with human BALF during the culture of influenza virus increased the clearance of the virus possibly via ROS activity whereas pre-incubation led to depletion of SP-D from BALF and hence the antiviral activity also reduced (White et al., 2007). The last study explains the contradictory findings related to antiviral activity of ROS.

Severe inflammation in the lung epithelium following influenza infection indicates possible ROS-induced tissue damage and oxidative stress. Indeed,

influenza infection causes reduction of lung antioxidant expressions like catalase while certain antioxidants like MnSOD and GPx increased in expression probably as compensatory mechanisms (Jacoby & Choi, 1994; Yamada et al., 2012). Increases in neutrophil-induced Nox2 and xanthine oxidase (XO) activities in the lungs have been reported after influenza infection. The mechanism of XO activation in lung epithelial cells involves neutrophil elastase which mediates the conversion of xanthine dehydrogenase to XO (Akaike et al., 1990; Phan et al., 1992); (reviewed in (Vlahos et al., 2012)). In one study, absence of ROS mainly Nox2 led to improved resolution of influenza lung injury (Snelgrove et al., 2006).

Due to several independent studies associating ROS with worsened influenza pathology and oxidative damage, antioxidant therapies have been a favourite topic of research in the past few decades. Strategies include inhibition of oxidants or oxidant-generating mechanisms, increasing the expression or instillation of lung antioxidants as well as other chemical antioxidants therapies either alone or in combination with known antiviral agents (Garozzo et al., 2007; Geiler et al., 2010; Ling et al., 2012); (reviewed in (Uchide & Toyoda, 2011; Vlahos et al., 2012)). Increased expression of extracellular SOD in transgenic mice and treatment with pyran polymer-conjugated Cu/ZnSOD or recombinant MnSOD ameliorated influenza induced-lung injury (Oda et al., 1989; Sidwell et al., 1996; Suliman et al., 2001). Pharmacological inhibition of Nox2 using apocynin improved influenza-induced lung pathology (Vlahos et al., 2011; Ye et al., 2014).

Despite many promising reports, antioxidant therapy has not been very successful (Kamgar et al., 2009; Siriwardena et al., 2012); (reviewed in (Sgarbanti

et al., 2014)). As antioxidants are generally non-specific, they can affect some crucial cellular metabolisms and hence can be detrimental to the host (reviewed in (Selemidis et al., 2008; Vlahos & Selemidis, 2014)). Thus, any interference with oxidative mechanisms in the host requires extensive study and careful deliberation.

6.1.5 Inhibitors of redox enzymes used in the study

Diphenylene iodonium chloride (DPI) is a non-specific inhibitor of NADPH oxidase. It inhibits Nox by accepting an electron from flavin adenine dinucleotide (FAD) to form phenyl radicals. These radicals then attach to the flavin group by covalent bonding leading to irreversible phenylation of FAD (O'Donnell et al., 1993, 1994). Though Nox-inhibitory effect of DPI has been known since 1986, it has not been extensively studied *in vivo* possibly due to its toxic nature (LD₅₀ approx. 6-8 mg/kg in rodents) (Cross & Jones, 1986); (reviewed in (Selemidis et al., 2008)). A few studies have used a lower dose (0.05–5 mg/kg) with positive results for conditions such as hypoglycaemia, arthritis and subarachnoid haemorrhage (reviewed in (Selemidis et al., 2008)).

4-amino benzoic acid hydrazide (ABAH) is a powerful inhibitor of MPO that functions as a suicide substrate for the enzyme. MPO oxidizes it to free radical intermediates that reduce ferric MPO to the ferrous enzyme. In the presence of H₂O₂ and oxidised ABAH, the haeme groups of MPO are destroyed whereas in the presence of oxygen, the ferrous enzyme is converted to oxymyeloperoxidase or compound III and thus is protected from inactivation. Additionally ABAH also

inhibits MPO activation product, HOCl, by competitive binding. Thus, ABAH inhibits both MPO activity and oxidant generated by MPO (Kettle et al., 1995, 1997). ABAH has been used previously in murine models of stroke (Forghani et al., 2015).

Diethyldithiocarbamate (DETC) is a copper-chelating chemical that causes reversible inactivation of SOD and is used in studies involving SOD activity (Cocco et al., 1981; Makino et al., 2003; Misra, 1979; Nemeč et al., 2009). DETC has been tested as a therapeutic for certain intracellular microorganisms to increase oxidative killing (Khouri et al., 2010).

6.2 Specific objectives of the study

ROS can be both beneficial and harmful in infection and inflammation. Several strategies to control ROS have been tested with mixed results. In case of influenza infection, inhibition of oxidant-producing enzyme as well as therapy with antioxidants has been tested. The present study analyses the effect of different redox enzymes particularly the inhibition of NADPH oxidase on lung pathology arising from lethal influenza infection. Inhibitors of NADPH oxidase, MPO and SOD that govern most of the oxygen radical formation by neutrophils (Figure 6.2, highlighted in blue) were tested. These inhibitors (mentioned in section 6.1.5) have not been tested as treatment to reduce lung injury during influenza infection.

The specific objectives of the study are,

- a) To assess the ROS and redox enzyme fluctuations during lethal influenza infection.
- b) To evaluate the effect of inhibition of NADPH oxidase, MPO and SOD on influenza-induced lung injury.
- c) To evaluate the efficacy of DPI in alleviating influenza-induced lung injury.

6.3 Results and discussion

6.3.1 High cellular infiltration phase after influenza infection correlates with increased oxidative activities in the lungs

6 weeks old BALB/c mice were infected with a lethal dose of influenza virus (100 PFU, approx. $6.7 \times \text{MLD}_{50}$) and sacrificed at various time points to assess the expression and generation of ROS and the regulatory enzymatic activities and their relevance with the histopathological progression of the disease. Serial histopathological analyses revealed minimal morphological changes in the lungs until day 2 followed by a phase of high cellular infiltration into the alveoli and bronchioles as well as large air spaces. By day 5, high cellular necrosis could be seen in the bronchioles signifying the end of infiltration phase. By day 7, infiltrating cells have been reduced to the minimum and haemorrhagic patches were seen near alveoli (Figure 6.4 A). Correlating with this trend, the mRNA expression of oxidative enzyme, Nox2 went up at day 3 and lasted until day 5-7 covering the infiltration phase, after which the expression levels came down. The

expression of extracellular *SOD3* gene also followed the same pattern but was not significant, similar to MPO gene expression (Figure 6.4 B). Amongst the lung enzymatic activity levels, MPO activity peaked around day 5 and reduced by day 7 while the SOD activity decreased at day 4 and started regaining during day 5-7 indicating resumption of antioxidant generation in the lungs (Figure 6.4 C). While reduced SOD activity should imply lower conversion of superoxide to H_2O_2 , the H_2O_2 concentration actually increased by day 5. As low levels of SOD activity is enough to catalyse the peroxidase reaction, it is still possible to generate H_2O_2 with reduction of SOD activity in lungs, and moreover H_2O_2 by itself can negatively regulate SOD activity thus increasing oxidative stress (Gardner et al., 2002; Gottfredsen et al., 2013).

Cellular infiltration is known to peak around day 4-6 after influenza infection (Fukushi et al., 2011); (reviewed in (Taunbenberger et al., 2008)). It is preceded by an asymptomatic phase and runs concurrently with an active viral replication phase (days 3-5). Since phagocytes particularly neutrophils are known to contribute oxidants upon activation, acute infiltration by these cells can possibly affect the redox balance of a host system (Vlessis et al., 1995); (reviewed in (Ward, 2010)). As expected, some of the redox enzymes underwent changes in gene expression and activity levels after influenza infection that correlated with the increase in cellular infiltration (Figure 6.4). Increased H_2O_2 and MPO activity-induced HOCl can contribute greatly to oxidative stress in the lung microenvironment and is possibly why intraalveolar haemorrhage and fibrin deposits are seen at the end of infiltration phase (day 7).

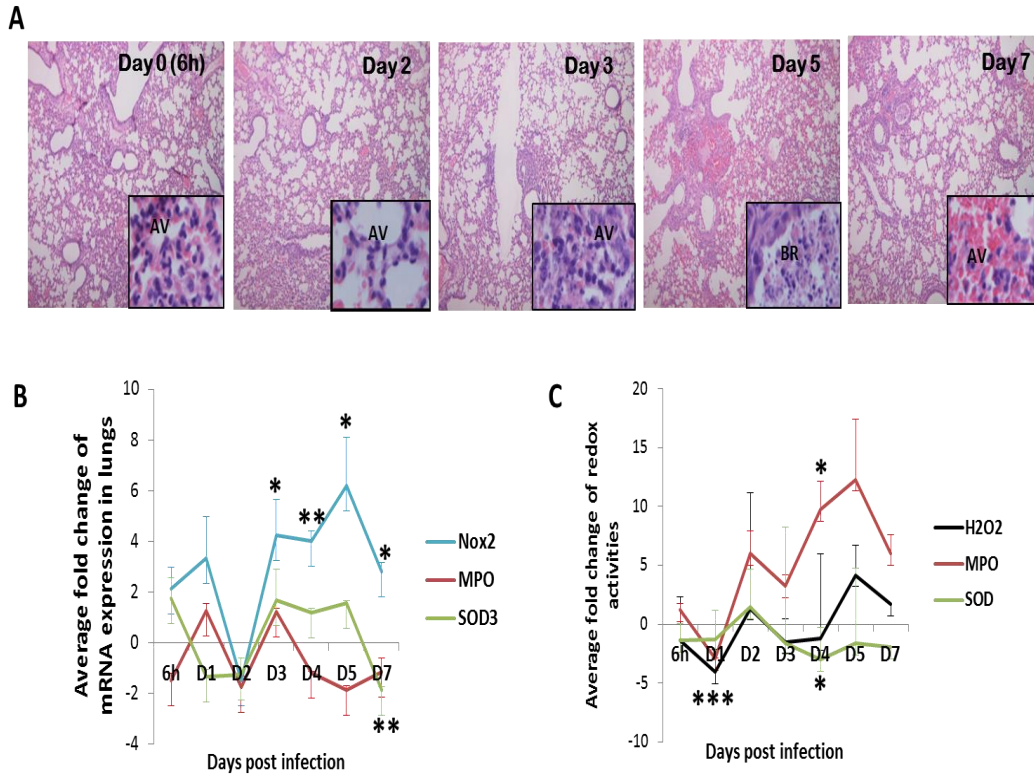


Figure 6.4. Serial histopathology and redox mechanisms after lethal challenge with influenza A virus. BALB/c mice were infected with 100 PFU of influenza A H1N1/PR8 virus and were sacrificed at various time points starting from 6 hours after challenge up to day 7. (A) Haematoxylin and Eosin staining showed changes in histopathology as the infection progressed. Day 3-5 marked the cellular infiltration phase while by day 7, haemorrhagic lesions appeared in small clusters even as the infiltrates slowly disappeared. AV – alveoli, BR – bronchioles. (B) mRNA expression of redox enzymes NADPH oxidase (*Nox 2*), Myeloperoxidase (*MPO*) and Superoxide dismutase, extracellular (*SOD3*) in lung homogenate showed increasing trend of oxidative mechanisms via *nox2* activity. (C) Lung homogenate levels of hydrogen peroxide (H_2O_2), MPO activity and SOD activity showed increases in ROS mechanisms (H_2O_2 & MPO activity) in the lung while antioxidant activity (SOD) dropped as the disease progressed. Values represent the average fold change \pm SE over respective mock-infected groups of 3 mice per time point (Single experiment). * indicates P value < 0.05, ** P value < 0.01 and *** P value < 0.001, Student's *t*-test.

A peculiar occurring is that before the beginning of infiltration at day 3, the oxidant levels dip and then recover the very next day. While the gene expressions of *Nox2* and *MPO* plunged and *SOD3* stagnated on day2, the actual MPO activity and H_2O_2 declined on day 1 while the SOD activity increased on day 2. There is

not much information in the current literature that explains this observation however, the asymptomatic phase (time of infection to day 2) is also the preparatory phase for viral replication and it is possible that influenza virus could manipulate the oxidative machinery to facilitate its replication as ROS can hinder the process. More research is required to find a promising explanation in this regard.

6.3.2 Mild improvement in the appearance of lung consolidation was observed with the inhibition of NADPH oxidase

Mice were infected with 100 PFU virus and later were treated with inhibitors of NADPH oxidase, MPO and SOD namely DPI, ABAH and DETC via the intraperitoneal route starting on day 3 and every 48 hours thereafter. A few doses of DPI, DETC and ABAH with therapy beginning either at day 1 or 3 were tested of which the only best data have been represented in figure 6.5. There was no significant difference in the survival and body weight patterns between all infected and treated animals. However, slightly higher numbers of deaths were observed upon SOD inhibition with DETC. The groups with inhibition of NADPH oxidase and MPO were similar to the infection alone group in all parameters (Figure 6.5 A and B). Histopathological analyses showed slightly lesser pulmonary consolidation in DPI-treated animals while others remained similar to infection alone group (Figure 6.5 C). Although there was no significant improvement in the survival of the mice after any of the treatments, a slightly better lung architecture with reduced consolidation after DPI treatment prompted further study with modifications in the treatment approach.

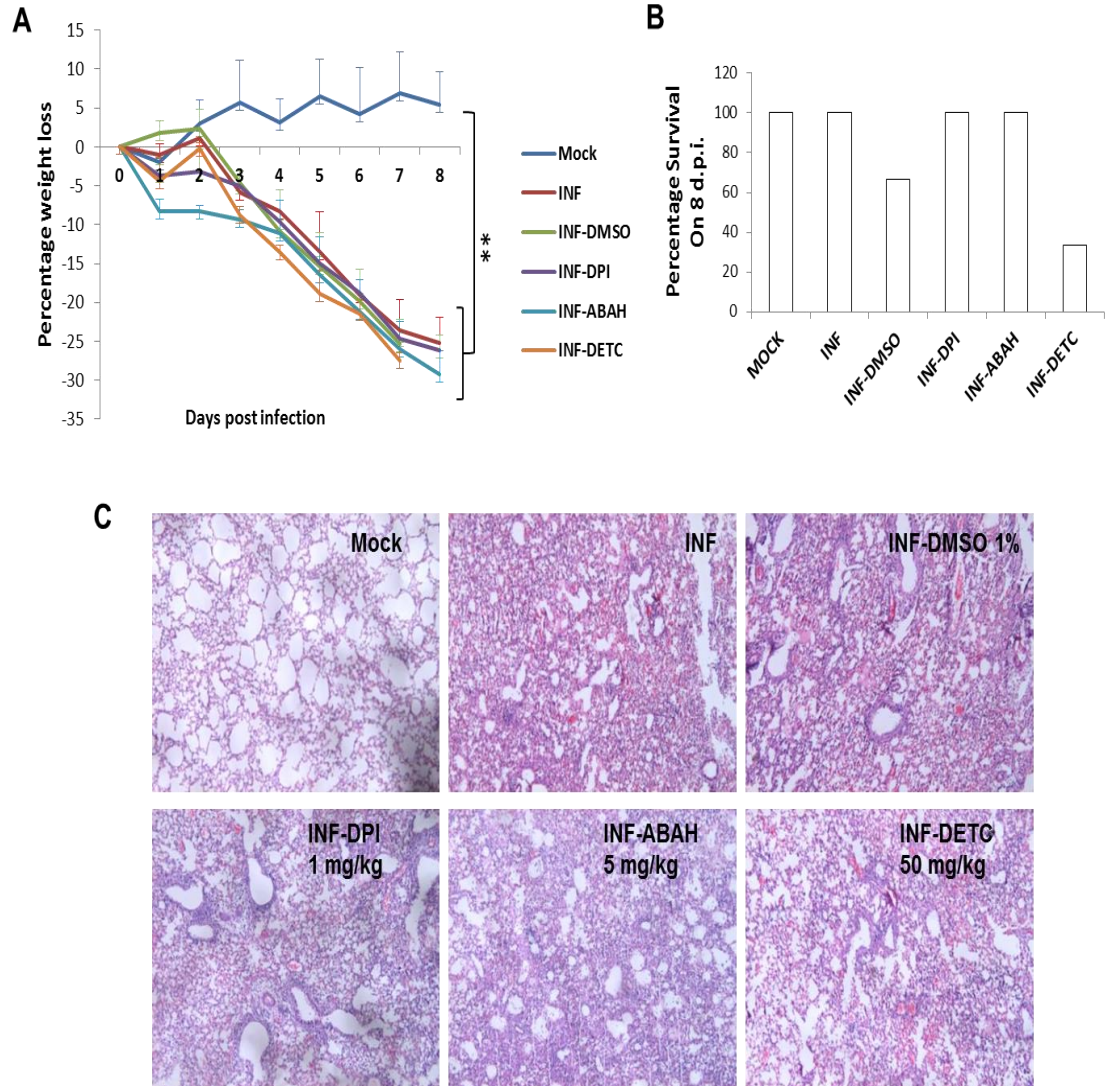


Figure 6.5. Inhibition of NADPH oxidase, MPO and SOD in lungs of infected mice. Mice were infected with 100 PFU of influenza virus and from day 3, inhibitors of redox enzymes were given intra-peritoneally every 48 hours- 1 mg/kg Diphenyleneiodonium chloride, DPI (NADPH oxidase), 5 mg/kg 4-amino benzoic acid hydrazide, ABAH (MPO) and 50 mg/kg Diethyldithiocarbamate, DETC (SOD). DPI and ABAH were dissolved in 1% DMSO which was included as a control (INF-DMSO) (A) All the infected mice showed similar body weight loss and reached the end point of 30% on day 8. ** represents P value < 0.01 , ANOVA with Tukey post-hoc correction. (B) Kaplan-Meier survival analyses showed no significant difference until 8 days post-infection (d.p.i.) in survival even though deaths were seen only in the DETC and DMSO treated groups. P value not significant, Kaplan-Meier survival analysis. (C) Haematoxylin and Eosin staining revealed lesser consolidation in the lungs after DPI treatment while all other ABAH- and DETC-treated groups showed similar levels of lung pathology to untreated group (INF). All infected mice had moderate levels of cellular infiltrates and septal thickening. Magnification of images: 10X. Values represent the means \pm SE of 3 mice (Single experiment).

6.3.3 Inhibition of NADPH oxidase by flavin-binding DPI does not improve lung pathology after lethal influenza challenge.

To improve the efficacy of DPI in alleviating lung injury, increased frequency of treatment was assessed. After the lethal challenge of animals with 100 PFU virus, DPI treatment (1 mg/kg) was given intra-peritoneally either every 24 hours or 48 hours starting from day 3. Again, there was no significant difference in the body weights and histopathology of treated and untreated mice (Figures 6.6 A, C and D). The viral titres were also unaffected by DPI treatment (Figure 6.6 B).

There was some significant reduction in lung H₂O₂ levels and MPO activity with treatment given respectively at every 48 hours and 24 hours (Figure 6.7 A and B). SOD activity also showed decrease (not significant) after DPI treatment with both treatment regimens (Figure 6.7 C). However, these effects were seen even with DMSO treatment which was used as a vehicle control since DPI was dissolved in 1% DMSO suggesting that the effects seen are due to DMSO rather than DPI. Only MPO activity was lower in DPI-treated group than DMSO-treated group implying that a possible additional action by DPI on NADPH oxidase suppression can control phagocyte activation *in vivo*.

Dimethyl sulfoxide or DMSO is an organosulfur by-product of the paper pulp industry which is known to possess antioxidant property. Its efficacy as antioxidant has been shown in inflammatory genito-urinary disorders and hence, its use as antioxidant or drug solvent has been suggested with caution (Sanmartin-

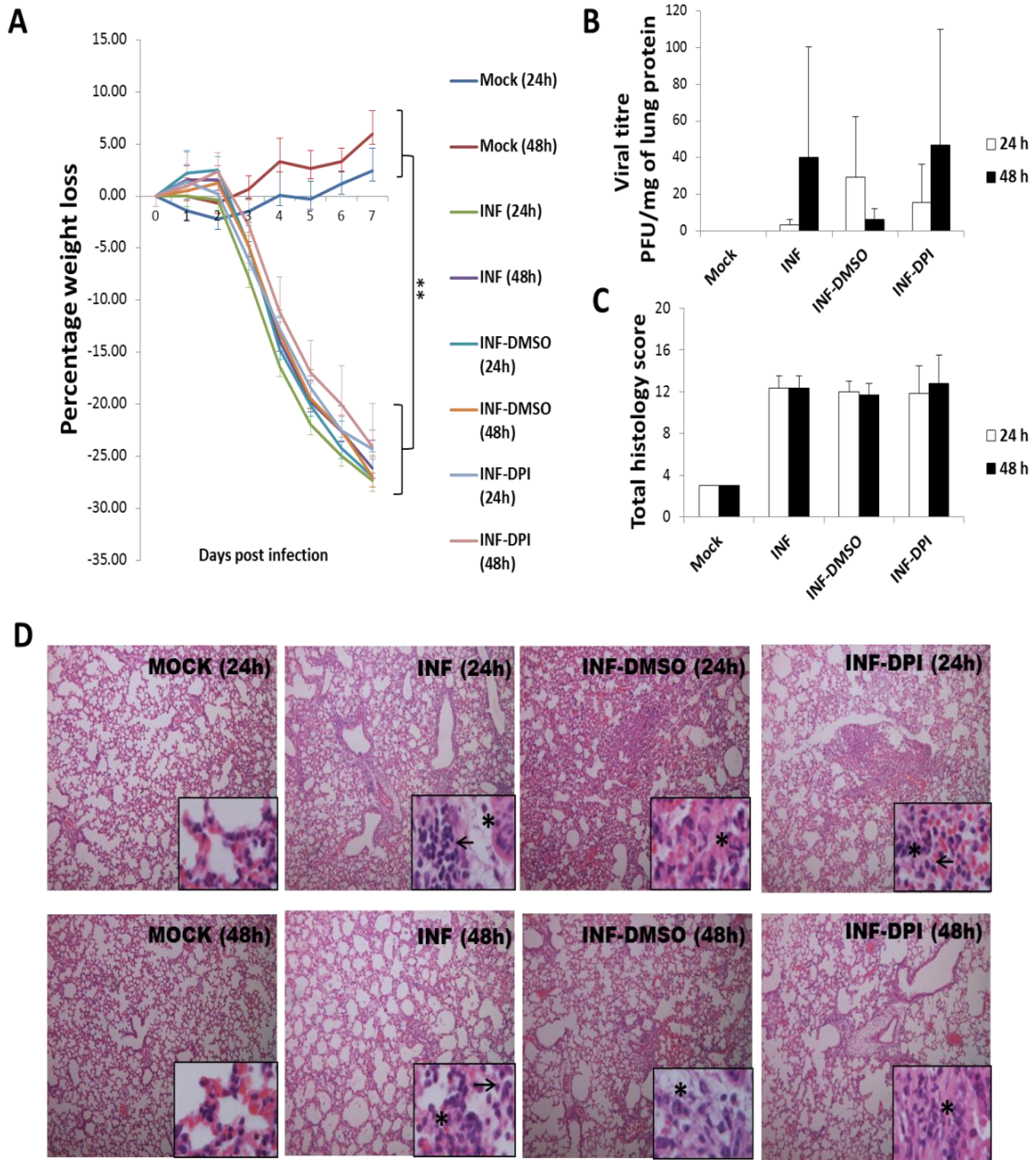


Figure 6.6. DPI treatment of mice infected with 100 PFU influenza virus. Mice were infected with 100 PFU of influenza virus and DPI treatment was given intra-peritoneally every 24 or 48 hours starting from day 3. Lungs were harvested at day 7 post-infection. DPI-treated groups (both 24h and 48h) showed no difference in (A) body weight loss. ** represents P value < 0.01 , ANOVA with Tukey post-hoc correction, (B) lung viral titre. (P value not significant, ANOVA with Tukey post-hoc correction) and (C) Histology scores when compared to untreated (INF) group. (D) Haematoxylin and Eosin staining revealed moderate infiltration in the alveolar space and septal thickening in all infected mice. Asterix indicates neutrophils, arrow indicates lymphocytes. Magnification of images: 100x (main panels) and 1000x (inserts). Values represent the means \pm SE of 3-5 animals per group (Single experiment).

Suárez et al., 2011; Shirley et al., 1978). Since DPI was dissolved in 1% DMSO, the latter might have influenced the outcome due to its antioxidant property and hence, both the DMSO- and DPI(+DMSO)-treated groups showed decrease in H₂O₂ and SOD activity.

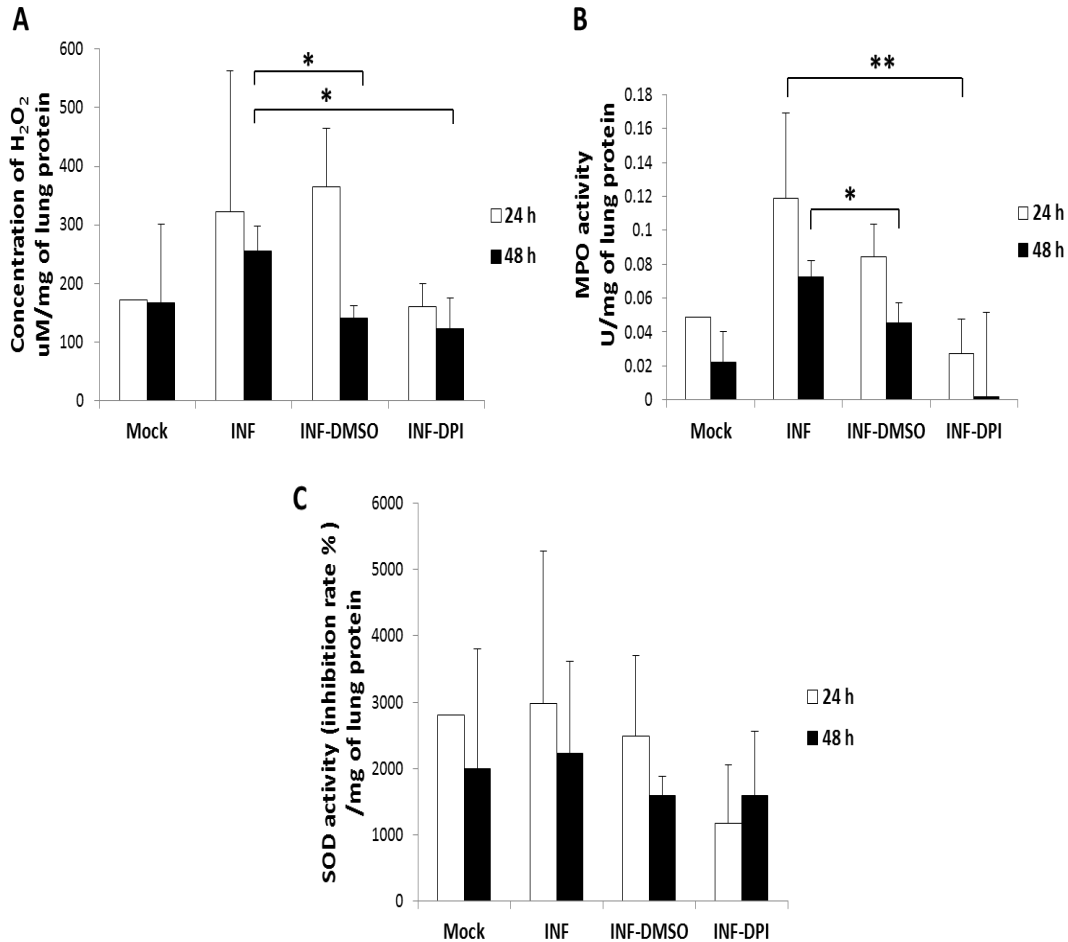


Figure 6.7. Redox enzyme activities in the lungs after DPI treatment of lethally challenged mice. Lungs were homogenised in PBS and assayed for enzymatic activities and ROS concentration. (A) DPI-treated groups showed reduced H₂O₂ concentration in the lungs with both 24 and 48 hours schedule compared to untreated (INF) group; however DMSO control group also showed decreased H₂O₂ at 48 hours. (B) DPI-treated groups showed reduced MPO activity in the lungs with both 24 and 48 hours schedule compared to INF and INF-DMSO groups. (C) DPI-treated groups showed reduced (but non-significant) SOD activity in the lungs with both 24 and 48 hours schedule compared to INF group; however DMSO control group also showed decreased SOD activity at 48 hours. Values represent the means \pm SE of 3-5 animals per group (Single experiment). * indicates *P* value < 0.05 ** *P* value < 0.01, ANOVA with Tukey post-hoc correction.

6.3.4 Inhibition of NADPH oxidase does not improve lung pathology even with lower dose of influenza challenge.

To assess if the effect of DPI treatment could be made better and clear, the challenge dose of influenza virus was lowered to 20 PFU (approx. 1.3 x MLD₅₀). At this dose, the virus induces mortality around day 10 after infection which gives a longer time period for treatment and lesser pathological effect of virus-induced lung damage. The mice were infected with 20 PFU virus and the DPI treatment (1 mg/kg) was commenced on day 3 and continued every day till end-point of 30% weight loss. The mice were either sacrificed on day 6 or at reaching the endpoint defined as time of death (TOD) as some animals died before reaching the experimental end-point. Again, there was no difference in body weight loss between DPI-treated and untreated mice (Figure 6.8 A). The DPI-treated animals showed slightly higher survival until day 10 after which all the infected animals reached the experimental end-point; however the difference was not significant (Figure 6.8 B).

The viral titres were unaffected by the DPI treatment (Figure 6.9 A). However, at the experimental end-point (TOD), slightly lower titres were observed (not significant) in the group after DPI treatment compared to infection alone group. Further studies are required to validate this observation. Some studies have suggested compensatory action by non-oxidative antiviral mechanisms in the host (Droebner et al., 2011; Li et al., 2013). Histology scores were also not different in DPI- and DMSO-treated animals thus confirming the previous observation in figure 6.6 C. Acute infiltration by neutrophils,

macrophages and lymphocytes were seen in the alveoli and bronchioles leading to intra-alveolar haemorrhage and fibrin deposition in all the infected animals (Figure 6.9 B and C).

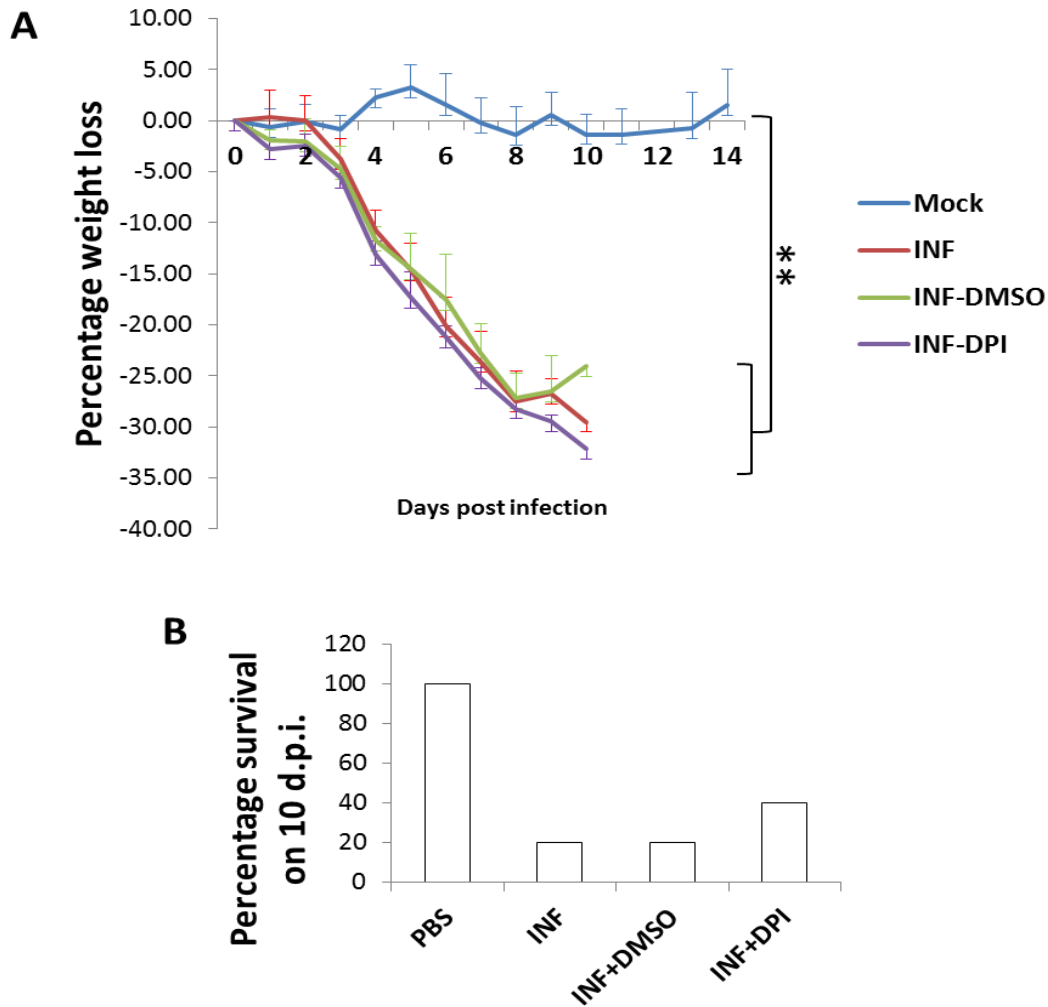


Figure 6.8. DPI treatment of mice infected with 20 PFU influenza virus. Mice were infected with a low lethal dose (20 PFU) of influenza virus and DPI treatment was given intra-peritoneally every 24 hours starting from day 3. **(A)** No difference in weight loss was seen between DPI-treated group and untreated group. All the infected mice reached the end-point of 30% weight loss by day 9-10. ** represents P value < 0.01 , ANOVA with Tukey post-hoc correction. **(B)**. DPI-treated group had a slightly higher but not significant survival rate on day 10 relative to INF and INF-DMSO groups, Kaplan-Meier survival analysis. Values represent the means \pm SE of 5 animals per group (Single experiment).

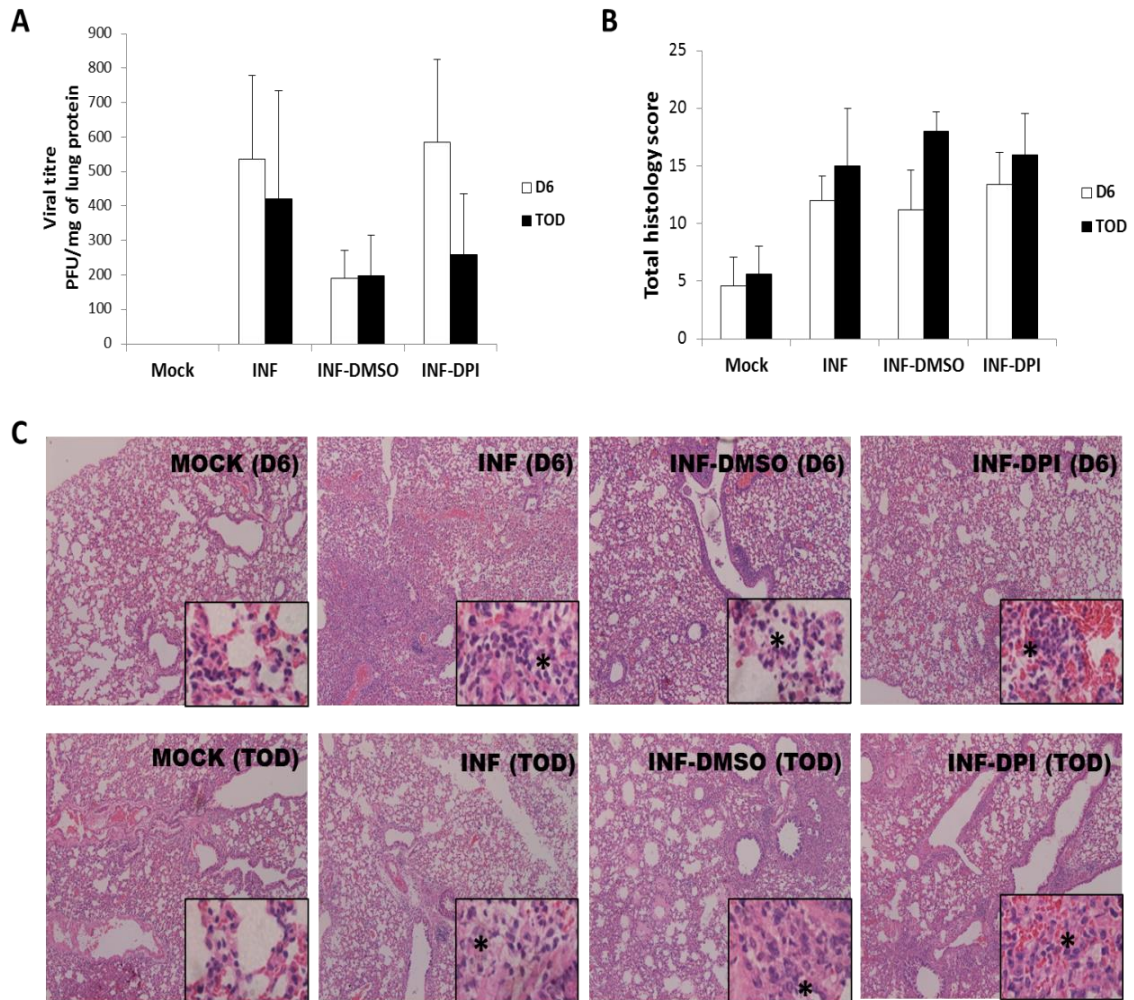


Figure 6.9. Viral titre and histopathology after DPI treatment of mice infected with low lethal dose of influenza virus. Lungs were harvested either at day 6 post-infection or at the time of death (TOD). DPI-treated groups showed no difference in (A) lung viral titre. *P* value not significant, ANOVA with Tukey post-hoc correction and (B) Histology scores. *P* value not significant, ANOVA with Tukey post-hoc correction. (C) Haematoxylin and Eosin staining revealed mild to moderate infiltration (asterix) in the alveolar and bronchiolar space as well as mild septal thickening in all infected mice. Magnification of images: 100x (main panels) and 1000x (inserts). Values represent the means \pm SE of 3-5 animals per group (Single experiment).

Enzymatic activities of MPO and SOD dropped to comparable levels in both DPI- and DMSO-treated groups relative to infection alone but were not significant (Figure 6.10 B and C). The same was observed with H₂O₂ concentration in lungs (Figure 6.10 A). Thus, it was concluded that reduction in

enzymatic activities after DPI treatment could be attributed to the antioxidant property of its solvent i.e. DMSO. In either case, the reduction of lung ROS and redox activity did not reflect in the lung histopathology or significant clinical survival.

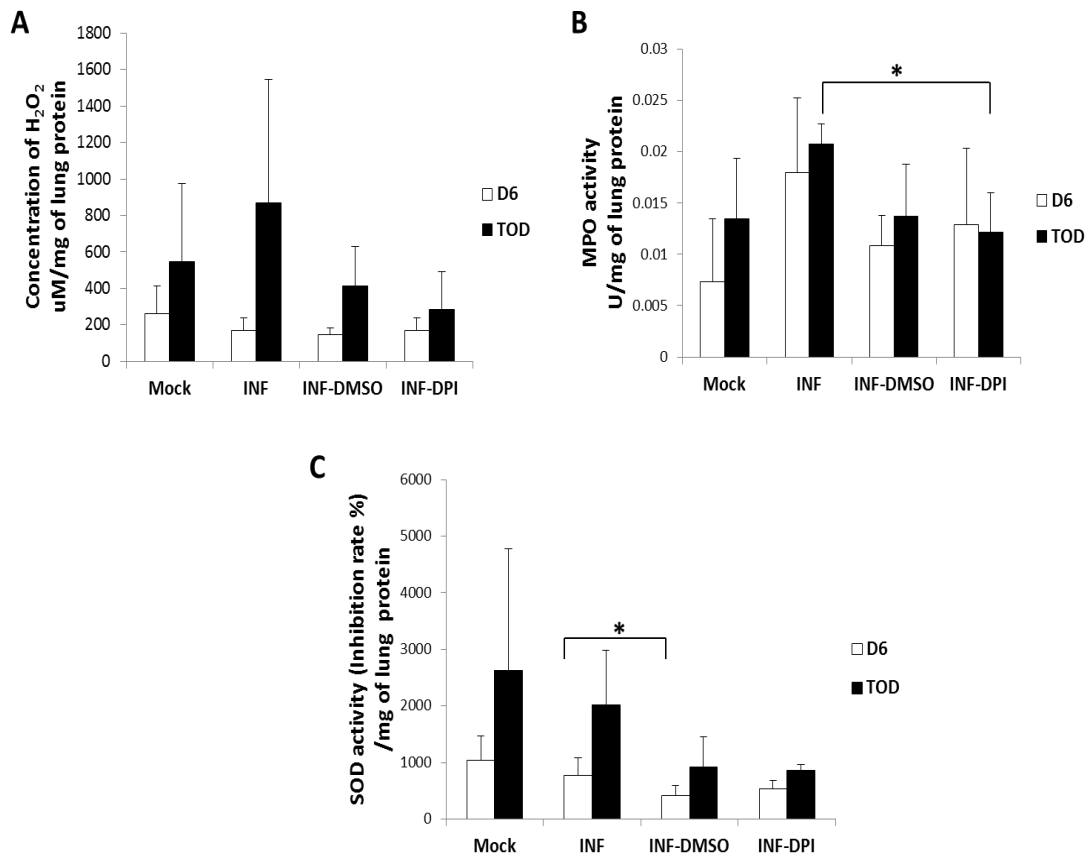


Figure 6.10. Redox enzyme activities in the lungs after low lethal challenge and DPI treatment. Lungs were homogenised in PBS and assayed for enzymatic activities and ROS concentration. (A) H_2O_2 concentrations in the lungs were comparable in all infected groups on day 6 after infection. (B) DPI-treated groups showed reduced MPO activity in the lungs in general compared to infection alone group. However, even INF-DMSO showed reduced MPO activity. (C) SOD activity is slightly reduced (not significant) with both DPI and DMSO treatment. Values represent the means \pm SE of 3-5 animals per group (Single experiment). * indicates P value < 0.05 , ANOVA with Tukey post-hoc correction.

6.4 Conclusion

ROS have been attributed in many pathological conditions (reviewed in (Johnson & Koval, 2009; MacNee & Rahman, 1995)). Free oxygen radicals can be produced from host cells, but most of the ROS comes from phagocytes such as neutrophils that are laden with volatile proteases that can contribute to lung injury by degranulation or NETosis (Vlessis et al., 1995); (reviewed in (Parker & Winterbourn, 2013)). Free oxygen radicals can cause tissue damage by inducing lipid peroxidation, DNA damage and chemical changes to protein (reviewed in (Matés & Sánchez-Jiménez, 1999)).

Antioxidants therapies have been tested for many years for various conditions like cardiac surgery-related complications and renal conditions with mixed results (Castillo et al., 2011; Kamgar et al., 2009); (reviewed in (Kinnula et al., 2005)). Overexpression of antioxidants like SOD or use of mimetics has been shown to work in certain cases of tissue injury (Hassett et al., 2011; Laukkanen et al., 2001). Overexpression of extracellular SOD has been shown to prevent influenza-induced lung injury (Sidwell et al., 1996; Suliman et al., 2001). However, the issue of chemical and pharmacokinetic stability as well as target accessibility has limited research on SOD therapy. On the other hand, suppression of oxidants has also yielded promising results. MPO inhibition has been shown to improve cigarette smoke-induced lung injury (Thatcher et al., 2013). Inhibition of NADPH oxidase using apocynin has been advocated for influenza therapy (reviewed in (Vlahos et al., 2012)). While apocynin showed both antiviral and oxidant-suppressing properties, the NADPH oxidase inhibitor used in this study is

not known to have any antiviral actions thereby allowing the examination of ROS-suppression property alone.

Since NETosis is an oxidative process, it can contribute to the oxidative stress-mediated lung injury. In the present study, chemical inhibitors of three redox enzymes – NADPH oxidase, MPO and SOD were first analysed for their efficacy in reducing lung injury. These enzymes are part of the neutrophil-mediated ROS production (Figure 6.2). The baseline levels of these enzymes underwent changes after influenza infection inclining towards an oxidative environment which would support pro-inflammatory reactions (Figure 6.4 C). While suppression of NADPH oxidase caused some improvement in pulmonary consolidation, suppression of MPO and SOD had no apparent effect on the lungs (Figure 6.5). Thus, inhibitor of NADPH oxidase (DPI) was used for further analysis.

Upon further analysis with high and low lethal doses of influenza virus, it was found that some of the effects of DPI on the enzymatic activities in the lungs could also be seen in the DMSO controls thereby casting shadow on the reliability of DPI for treatment of lung injury (Figure 6.6 - 6.10). Furthermore, no differences were observed in the clinical body weight loss, survival, histopathology and viral titres after DPI treatment.

Intraperitoneal route of treatment was preferred as it has been used previously to deliver DPI in mouse models (Hecker et al., 2009; Pazhanisamy et al., 2011) and is a preferred mode of treatment even in patients with certain

conditions (reviewed in (Chaudhary et al., 2010)). However, other routes such as intravenous could also be used in future. Moreover, these experiments need to be repeated with more mice number for statistical significance. Before that, more optimisations are required to find the best timeframe and dose regimen for DPI treatment during influenza infection.

Iodonium compounds such as DPI are very potent inhibitors of NADPH oxidase that act by binding to the flavin redox centre (O'Donnell et al., 1993). DPI has been shown to prevent tissue injury caused by bleomycin and irradiation (Hecker et al., 2009; Pazhanisamy et al., 2011). However, it is also known to render neutrophil defective in microbial killing efficiency thereby hindering the immune-mediated clearance of pathogens from the host (Ellis et al., 1988). Walking a fine line, suppression of NADPH oxidase activity by DPI after influenza infection could potentially go either way. Indeed, DPI treatment was found to be ineffective in preventing lung injury or reducing oxidant activity significantly even as most of its effect was attributed to its diluent (DMSO). Thus, it can be concluded that chemical suppression of NADPH oxidase activity by DPI in mice is not enough to prevent lung injury after influenza infection.

CHAPTER SEVEN

CONCLUDING REMARKS AND FUTURE SCOPE

Often complications due to influenza infection come from comorbidities like secondary bacterial infections or weakened host immune system due to obesity, chronic lung and coronary disorders or similar conditions (Louie et al., 2011; Smith et al., 2013). Oxidative stress and cytokine storm are characteristic features of lethal influenza infection leading to ALI and ARDS as observed during the 1918 ‘Spanish flu’ pandemic (Kobasa et al., 2004; Osterholm, 2005). However, the unusually high mortality rate in the young adult age group during the 1918 pandemic casts doubt over the causal attribution to oxidative stress and cytokine storm alone (reviewed in (Palese, 2004)). Hence, other mechanisms of morbidity need to be investigated. Despite the reservations, complications arising out of seasonal and recent pandemic influenza have largely been attributed to host-related factors (Le et al., 2012).

Unrestricted inflammation during influenza infection causes lung tissue injury (Buffinton et al., 1992). Although inflammation helps to prime the immune cells to fight against invading pathogens, certain non-specific consequences can arise of which neutrophil-induced tissue injury could be a possibility. Several studies have confirmed neutrophil’s role in worsening the host system either directly by releasing cytotoxic proteases or by contributing to oxidative stress (Muruve et al., 1999; Ng et al., 2012; Perrone et al., 2008; Vlahos et al., 2011).

NETs engender both means of injury in that the DNA fibres carry toxic neutrophil proteins like NE, MPO and histones as well as the mechanism of NETosis involve extensive oxidant generation (Kessenbrock et al., 2009; Narasaraaju et al., 2011; Saffarzadeh et al., 2012; Xu et al., 2012).

7.1 NETs and secondary pneumococcal pneumonia after influenza infection

Since their discovery, much of the research on NETs has focused on elucidating the mechanism of NETosis and identifying NETs generation with various infectious and non-infectious stimuli. Few studies have highlighted the role that NETs play inside the host and how they interact with pre-existing conditions inside the host. One part of the current project tried to assess NETs generation upon secondary infection with *S. pneumoniae* after influenza infection and how the two stimuli contribute to overall NETosis and pathogenesis of the disease. Next, it was seen how various strains of *S. pneumoniae* can differently influence NETosis and how much say does a bacterial virulence factor like capsule has in the entire process. These two studies highlight the importance of pathogen-based factors in determining immune cell response to infection in the form of NETs.

The key findings of these studies are:

- a) NETs are induced in significantly higher numbers in murine lungs during secondary pneumococcal infection after primary influenza infection.
- b) NETs produced during influenza infection do not help in clearing bacteria both *in vivo* and *in vitro* but possess potent antifungal activity. The lack of

antibacterial activity may partly be attributed to minimal alteration in the gene expression of bactericidal proteins after influenza infection.

- c) NETs generated *in vitro* by influenza stimulation are strongly influenced by redox enzymes like NADPH oxidase, MPO and SOD. Blocking of these enzymatic activities in the cell culture system reduced NETs release from stimulated neutrophils.
- d) Secondary pneumococcal infection leads to the presence of many clusters of degraded NET structures in the lungs, possibly due to the bacterial endonuclease activity, that may take part in causing tissue damage.
- e) Serotype of pneumococcus determines the extent of NETs generation and the pathological implications in the lungs of infected mice.
- f) Capsule of *S. pneumoniae* plays a crucial role in determining NETs induction. The capsule polysaccharide by itself can induce NETs potently.
- g) Pathogenicity and NETs-inducing ability of *S. pneumoniae* is serotype-specific in part due to the degree of capsule thickness during primary infection.
- h) Capsule-based serotype specificity is not the sole determinant of extensive NETosis as there is a pattern shift from primary to secondary infection by pneumococci. During secondary infection after influenza infection, other bacterial virulence factors may also exert influence on the disease outcome, inflammatory response and NETs.

The above findings establish the stimuli-specific mechanism of NETs induction. NETs induction can occur due to stimulation of various different

receptors (Parker et al., 2012). The way a virus would stimulate neutrophils may differ from that of a bacteria depending on the receptor involved. Most bacteria interact with neutrophils through the cell's toll-like receptors like TLR2 and TLR4 (Clark et al., 2007; Yipp et al., 2012); (reviewed in (Brinkmann & Zychlinsky, 2007)). LPS is known to stimulate NETs induction through TLR2 (reviewed in (Brinkmann & Zychlinsky, 2007)) while influenza virus mainly stimulates via TLR7/8 & 10 (Lee et al., 2014; Wang et al., 2008). Some recent evidence shows the involvement of p38 MAP kinase and Raf-MEK-ERK pathways in NETosis (Hakkim et al., 2011; Keshari et al., 2013). In this study, the capsule polysaccharide was able to induce NETs by itself. It would thus be interesting to study the mechanism of such induction. Similar to LPS, capsule PS can stimulate neutrophils through the TLRs that might affect downstream processes like complement activation and cytokine release. However, a recent report suggests that the pneumococcal capsule impairs recognition of TLR ligands of *S. pneumoniae* by neutrophils and thereby moderately hampers MyD88-mediated immunity during pneumonia in mice (de Vos et al., 2015).

Apart from receptors, intra-species difference in NETs induction could arise due to different biochemistry of the bacterial capsule. Positive charge provided by D-alanylated LTA on *S. pneumoniae* helps in evading NETs but does not protect from AMP-mediated killing (Wartha et al., 2007). Another study with *C. albicans*, found that the *Candida* PS composition plays a crucial role in determining the induction of NETs where the major PS found on invasive strains actually inhibited NETosis while a minor PS probably found in avirulent strains

could induce NETs (Rocha et al., 2015). Finally, the capsule PS itself could be instilled inside the lungs of a host animal to see if NETs could be induced *in vivo* at certain PS concentration that matches the actual bacterial-induced NETs.

The next area of interest could be NET-induced lung injury in pneumococcal primary and secondary infection models. As degraded clusters of NETs were seen, the possibilities of injury to surrounding tissues arise. The role of some of the NETs components in tissue injury could be studied. Although some *in vitro* research has been done in this regard (Saffarzadeh et al., 2012), not many studies are done to clearly establish the effect *in vivo*. Histones and MPO were found to be the main cytotoxic agents while NE did not have any role to play in causing injury to endothelial cells. Xu et al. (2012) have demonstrated that extracellular histones can mediate death during sepsis. Likewise HOCl generated from MPO enzymatic activity is also shown to cause tissue injury (Wahn & Hammerschmidt, 1998). However, NE has also been implicated in tissue injury emphasising the importance of *in vivo* studies (reviewed in (Chua & Laurent, 2006)). To link pneumococcus with degradation of NETs, further experiments are needed. One such technique is the immunostaining of lung sections to locate pneumococci near the degraded clusters. However, this may not still be very conclusive and only be a qualitative assay. During the present study, an antisera for serotype 19F (Statens serum institute) was used to stain the bacteria in *in vitro* samples but pneumococci could not be stained in formalin-fixed lungs. In one study, NET structures were identified in the plasma of mice during deep vein thrombosis (Fuchs et al., 2010). Such techniques could also be applied to study digested NETs that may enter

blood stream during endothelial injury caused by pneumococci especially when the bacteria also enters the bloodstream during bacteraemia. Alternatively, ANA or ANCA detection can be used to evaluate the immune reaction to circulating NETs components. These kinds of study may give us more insight on host tissue injury caused by pathogen-induced NETs.

7.2 High fat diet, NETs and influenza infection

The other parts of the dissertation focus on the host factors. Host adiposity and dietary fat composition can play a huge role in the way the host responds to a pathogen. HFD- and LFD-fed mice were compared to assess NETs formation in the lungs after influenza infection. The following are the key findings of the study,

- a) High fat diet has a tendency to predispose mice to higher NETosis in lungs when compared to low fat diet although further experiments are required to confirm this observation.
- b) HFD-fed mice also show a tendency to support higher levels of lung viral replication and to exhibit higher ROS levels in the lungs while MPO activity is somewhat lower suggesting inefficient leukocyte response that leads to increased oxidative burst without offering any protective benefits.

The above data were mostly not significant owing to the lower degree of adiposity in BALB/c mice (Montgomery et al., 2013). This is different from other DIO models of influenza infections (Easterbrook et al., 2011; Karlsson et al., 2010; Smith et al., 2007; Zhang et al., 2013) where significant differences in

mortality were observed between high and low fat diet groups. Further studies could be done using the C57BL/6 mice similar to the above studies as they show signs of clinical obesity when fed with HFD. Nevertheless, there indeed was a marginal albeit non-significant increase in NETs in the HFD mice during influenza infection.

This study was based on a HFD model which would apply to subjects with bad dietary habits. However, some individuals are genetically susceptible to gain weight and succumb faster to influenza infection. To address this issue, leptin-deficient knock-out (ob/ob) mice could be used to study the effect of obesity and leptin on NETs generated during influenza infection. Leptin is a negative regulator of appetite and a deficiency in leptin may help us to understand the hormone's association with neutrophils since leptin receptor is present in neutrophils (Caldefie-Chezet et al., 2001). Extending the present study further, NETosis could be correlated to cytokine dysregulation in HFD mice as a general dysregulation has been found in the ob/ob mice (reviewed in (Moreno-Navarrete & Fernández-Real, 2011)). Isolation of neutrophils from HFD mice may reveal mechanistic changes inside neutrophils during NETosis which may shed some light on the differential activation of neutrophils during influenza infection in obese individuals.

7.3 Neutrophil NADPH oxidase and influenza-induced oxidative stress

Infections induce oxidative imbalance inside the host that may be reflected in the way the illness takes shape. ROS are crucial immune defence factors,

however, if they remain uncontrolled they can cause havoc to the system. Hence, inhibition of excess oxidant generation has been the focus of many of the current pharmaceutical and therapeutic research.

The key findings from this study are,

- a) Lethal influenza challenge causes variation in the expression of redox enzymes. While oxidants levels are increased after infection, the expression and activity of anti-oxidant goes down almost concurrently.
- b) Inhibition of key neutrophil redox enzymes, NADPH oxidase, MPO and SOD, has very mild impact on the lung injury of which blocking of NADPH oxidase suggests a modest but not significant improvement in lung pathology.
- c) At the concentrations and inoculation regimens used in this study, the NADPH oxidase inhibitor, DPI, does not alleviate lung injury. In fact, its carrier DMSO reproduces similar results to that of DPI.

The above study was done with one set of mice for each treatment regimen and infection dose. Since no difference was observed after DPI treatment in terms of lung improvement, the treatment methodology was changed for every experiment. More repeats are needed with consistently similar results to confirm the above mentioned observations.

Even though DPI at the tested regimens and doses failed to reduce lung injury, there could be other specific inhibitors of NADPH oxidase that may hold promise (reviewed in (Kim et al., 2011)). Chemicals like apocynin and some others have

shown promise either alone or in combination with antivirals (reviewed in (Selemidis et al., 2008)). In fact, apocynin itself showed some effect on the viral burden in the lungs of treated mice indicating dual properties as an antioxidant and an antiviral (Vlahos et al., 2011). Novel chemicals targeting the redox enzymes may offer more potential probably in combination with antivirals (reviewed in (Vlahos et al., 2012; Vlahos & Selemidis, 2014)).

Moreover, this study was mostly done with single experiments, changing certain parameters each time to improve the efficacy of DPI treatment. More experimental repeats with a wider range of treatment doses and time periods during infection are required. Other routes of injection such as intravenous treatment can also be tested especially in combination with an antiviral.

7.4 Conclusion

The above results demonstrate how various factors from both host and pathogen affect NETs generation after influenza infection (Figure 7.1). This places NETs at the intersection of host-pathogen interactions and more research is warranted to further enhance the knowledge in this area especially the clinical application of the findings. More research is needed for the diagnostic detection of NETs in live subjects as the correlation between NETs and severity of disease has not been clearly established until now. NETs have been detected in the sputum of patients suffering from acute respiratory infections as well as from bloodstream of critically-ill patients (Hirose et al., 2012, 2014). Also, individuals

may vary in their immune response to a stimulus and hence, more focus should be directed towards finding a common factor that occurs in all cases of NETosis.

In conclusion, these studies help us understand the complex interactions of host, viral and bacterial systems in the process leading up to neutrophil oxidative burst and NETosis inside lungs as summarised in the figure 7.1.

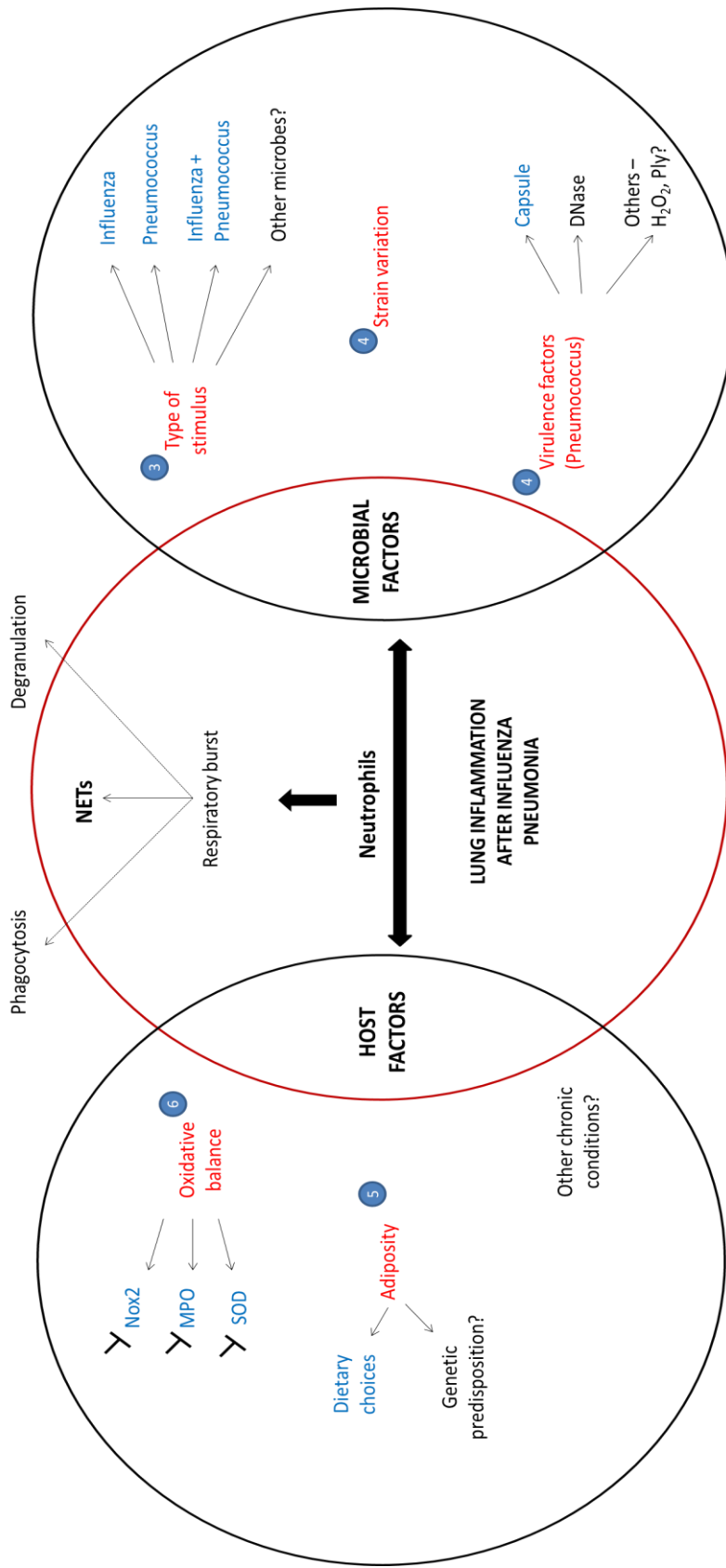


Figure 7.1 Schematic representation of NETs-Host-Pathogen interactions in influenza-pneumococcal pneumonia model. ● indicates work covered under the particular chapter number in the dissertation. √ indicates chemical blocking of the particular enzyme activity.

CHAPTER EIGHT

BIBLIOGRAPHY

8.1 Journal references

Aanensen, D.M., A. Mavroidi, S.D. Bentley, P.R. Reeves and B.G. Spratt. 2007. Predicted functions and linkage specificities of the products of the *Streptococcus pneumoniae* capsular biosynthetic loci. *J Bacteriol.* 189(21):7856-76.

Abi Abdallah, D.S. and E.Y. Denkers. 2012. Neutrophils cast extracellular traps in response to protozoan parasites. *Front Immunol.* 3:382.

Abi Abdallah, D.S., C. Lin, C.J. Ball, M.R. King, G.E. Duhamel and E.Y. Denkers. 2012. *Toxoplasma gondii* triggers release of human and mouse neutrophil extracellular traps. *Infect Immun.* 80(2):768-77.

Akaike, T., M. Ando, T. Oda T. Doi, S. Ijiri, S. Araki and H. Maeda. 1990. Dependence on O₂-generation by xanthine oxidase of pathogenesis of influenza virus infection in mice. *J Clin Invest.* 85(3):739-45.

Akerman, M.J., C.M. Calacanis and M.K. Madsen. 2004. Relationship between asthma severity and obesity. *J Asthma.* 41(5):521-6.

Alanee, S.R., L. McGee, D. Jackson, C.C. Chiou, C. Feldman, A.J. Morris, A. Ortqvist, J. Rello, C.M. Luna, L.M. Baddour, M. Ip, V.L. Yu, K.P. Klugman and International Pneumococcal Study Group. 2007. Association of serotypes of *Streptococcus pneumoniae* with disease severity and outcome in adults: an international study. *Clin Infect Dis.* 45(1):46-51.

Almyroudis, N.G., M.J. Grimm, B.A. Davidson, M. Röhm, C.F. Urban and B.H. Segal. 2013. NETosis and NADPH oxidase: at the intersection of host defense, inflammation, and injury. *Front Immunol.* 4:45.

Amatore, D., R. Sgarbanti, K. Aquilano, S. Baldelli, D. Limongi, L. Civitelli, L. Nencioni, E. Garaci, M.R. Ciriolo and A.T. Palamara. 2015. Influenza virus replication in lung epithelial cells depends on redox-sensitive pathways activated by NOX4-derived ROS. *Cell Microbiol.* 17(1):131-45.

Arnhold, J. 2004. Free radicals - Friends or foes? - Properties, functions, and secretion of human myeloperoxidase. *Biochem.* 69(1): 4-9.

Austrian, R. 1999. The pneumococcus at the millennium: not down, not out. *J Infect Dis.* 179 Suppl 2:S338-41.

Baik, I., G.C. Curhan, E.B. Rimm, A. Bendich, W.C. Willett and W.W. Fawzi. 2000. A prospective study of age and lifestyle factors in relation to community-acquired pneumonia in US men and women. *Arch Intern Med.* 160(20):3082-8.

Baker V.S., G.E. Imade, N.B. Molta, P. Tawde, S.D. Pam, M.O. Obadofin, S.A. Sagay, D.Z. Egah, D. Iya, B.B. Afolabi, M. Baker, K. Ford, R. Ford, K.H. Roux and T.C. Keller,

- 3rd. 2008. Cytokine-associated neutrophil extracellular traps and antinuclear antibodies in *Plasmodium falciparum* infected children under six years of age. *Malar J.* 7:41.
- Baldrige, C.W. and R.W. Gerard. 1932. The extra respiration of phagocytosis. *Am J Physiol.* 103: 235-36.
- Bastien, N., N.A. Antonishyn, K. Brandt, C.E. Wong, K. Chokani, N. Vegh, G.B. Horsman, S. Tyler, M.R. Graham, F.A. Plummer, P.N. Levett and Y. Li. 2010. Human infection with a triple-reassortant swine influenza A (H1N1) virus containing the hemagglutinin and neuraminidase genes of seasonal influenza virus. *J Infect Dis.* 201(8):1178-82.
- Bedard, K. and K.H. Krause. 2007. The NOX family of ROS-generating NADPH oxidases: physiology and pathophysiology. *Physiol Rev.* 87(1):245-313.
- Behnen, M., C. Leschczyk, S. Möller, T. Batel, M. Klinger, W. Solbach and T. Laskay. 2014. Immobilized immune complexes induce neutrophil extracellular trap release by human neutrophil granulocytes via FcγRIIIB and Mac-1. *Immunol.* 193(4):1954-65.
- Beiter, K., F. Wartha, B. Albiger, S. Normark, A. Zychlinsky and B. Henriques-Normark. 2006. An endonuclease allows *Streptococcus pneumoniae* to escape from neutrophil extracellular traps. *Curr Biol.* 16(4):401-7.
- Bentley, S.D., D.M. Aanensen, A. Mavroidi, D. Saunders, E. Rabinowitsch, M. Collins, K. Donohoe, D. Harris, L. Murphy, M.A. Quail, G. Samuel, I.C. Skovsted, M.S. Kalltoft, B. Barrell, P.R. Reeves, J. Parkhill and B.G. Spratt. 2006. Genetic analysis of the capsular biosynthetic locus from all 90 pneumococcal serotypes. *PLoS Genet.* 2(3):e31.
- Berends, E.T., A.R. Horswill, N.M. Haste, M. Monestier, V. Nizet and M. von Köckritz-Blickwede. 2010. Nuclease expression by *Staphylococcus aureus* facilitates escape from neutrophil extracellular traps. *J Innate Immun.* 2(6):576-86.
- Bergeron, Y., N. Ouellet, A.M. Deslauriers, M. Simard, M. Olivier and M.G. Bergeron. 1998. Cytokine kinetics and other host factors in response to pneumococcal pulmonary infection in mice. *Infect Immun.* 66(3):912-22.
- Bianchi, M., M.J. Niemiec, U. Siler, C.F. Urban and J. Reichenbach. 2011. Restoration of anti-*Aspergillus* defense by neutrophil extracellular traps in human chronic granulomatous disease after gene therapy is calprotectin-dependent. *J Allergy Clin Immunol.* 127(5):1243-52.e7.
- Borregaard, N. 2010. Neutrophils, from marrow to microbes. *Immunity.* 24;33(5):657-70.
- Bouvier, N.M. and P. Palese. 2008. The biology of influenza viruses. *Vaccine.* 12;26 Suppl 4:D49-53.
- Branzk, N., A. Lubojemska, S.E. Hardison, Q. Wang, M.G. Gutierrez, G.D. Brown and V. Papayannopoulos. 2014. Neutrophils sense microbe size and selectively release neutrophil extracellular traps in response to large pathogens. *Nat Immunol.* 15(11):1017-25.

- Bright, R.A., D.K. Shay, B. Shu, N.J. Cox and A.I. Klimov. 2006. Adamantane resistance among influenza A viruses isolated early during the 2005-2006 influenza season in the United States. *JAMA*. 295(8):891-4.
- Briles, D.E., M.J. Crain, B.M. Gray, C. Forman and J. Yother. 1992. Strong association between capsular type and virulence for mice among human isolates of *Streptococcus pneumoniae*. *Infect Immun*. 60(1):111-6.
- Brill, A., T.A. Fuchs, A.S. Savchenko, G.M. Thomas, K. Martinod, S.F. De Meyer, A.A. Bhandari and D.D. Wagner. 2012. Neutrophil extracellular traps promote deep vein thrombosis in mice. *J Thromb Haemost*. 10(1):136-44.
- Brinkmann, V. and A. Zychlinsky. 2007. Beneficial suicide: why neutrophils die to make NETs. *Nat Rev Microbiol*. 5(8):577-82.
- Brinkmann, V., U. Reichard, C. Goosmann, B. Fauler, Y. Uhlemann, D.S. Weiss, Y. Weinrauch and A. Zychlinsky. 2004. Neutrophil extracellular traps kill bacteria. *Science*. 303(5663):1532-5.
- Brotfain, E., N. Hadad, Y. Shapira, E. Avinoah, A. Zlotnik, L. Raichel and R. Levy. 2015. Neutrophil functions in morbidly obese subjects. *Clin Exp Immunol*. 181(1):156-63.
- Bueggemann, A.B., T.E. Peto, D.W. Crook, J.C. Butler, K.G. Kristinsson and B.G. Spratt. 2004. Temporal and geographic stability of the serogroup-specific invasive disease potential of *Streptococcus pneumoniae* in children. *J Infect Dis*. 190(7):1203-11.
- Bruns, S., O. Kniemeyer, M. Hasenberg, V. Aimanianda, S. Nietzsche, A. Thywissen, A. Jeron, J.P. Latgé, A.A. Brakhage and M. Gunzer. 2010. Production of extracellular traps against *Aspergillus fumigatus* *in vitro* and in infected lung tissue is dependent on invading neutrophils and influenced by hydrophobin RodA. *PLoS Pathog*. 6(4):e1000873.
- Buchanan, J.T., A.J. Simpson, R.K. Aziz, G.Y. Liu, S.A. Kristian, M. Kotb, J. Feramisco and V. Nizet. 2006. DNase expression allows the pathogen group A *Streptococcus* to escape killing in neutrophil extracellular traps. *Curr Biol*. 16(4):396-400.
- Buffinton, G.D., S. Christen, E. Peterhans and R. Stocker. 1992. Oxidative stress in lungs of mice infected with influenza A virus. *Free Radic Res Commun*. 16(2):99-110.
- Caldefie-Chezet, F., A. Poulin, A. Tridon, B. Sion and M.P. Vasson. 2001. Leptin: a potential regulator of polymorphonuclear neutrophil bactericidal action? *J Leukoc Biol*. 69(3):414-8.
- Carp, H. and A. Janoff. 1980. Potential mediator of inflammation. Phagocyte-derived oxidants suppress the elastase-inhibitory capacity of alpha 1-proteinase inhibitor *in vitro*. *J Clin Invest*. 66(5):987-95.
- Cartee R.T., W.T. Forsee and J. Yother. 2005. Initiation and synthesis of the *Streptococcus pneumoniae* type 3 capsule on a phosphatidylglycerol membrane anchor. *J Bacteriol*. 187(13):4470-9.

- Cartee, R.T., W.T. Forsee, J.S. Schtuzbach and J. Yother. 2000. Mechanism of type 3 capsular polysaccharide synthesis in *Streptococcus pneumoniae*. *J. Biol. Chem.* 275:3907–14.
- Castillo, R., R. Rodrigo, F. Perez, M. Cereceda, R. Asenjo, J. Zamorano, R. Navarrete, E. Villalabeitia, J. Sanz, C. Baeza and R. Aguayo. 2011. Antioxidant therapy reduces oxidative and inflammatory tissue damage in patients subjected to cardiac surgery with extracorporeal circulation. *Basic Clin Pharmacol Toxicol.* 108(4):256-62.
- Chapman, A.L., M.B. Hampton, R. Senthilmohan, C.C. Winterbourn and A.J. Kettle. 2002. Chlorination of bacterial and neutrophil proteins during phagocytosis and killing of *Staphylococcus aureus*. *J. Biol.Chem.* 277, 9757–62.
- Chaudhary, K., S. Haddadin, R. Nistala and C. Papageorgio. 2010. Intraperitoneal drug therapy: an advantage. *Curr Clin Pharmacol.* 5(2):82-8.
- Chiavolini, D., G. Pozzi and S. Ricci. 2008. Animal models of *Streptococcus pneumoniae* disease. *Clin Microbiol Rev.* 21(4):666-85.
- Chua, F. and G.J. Laurent. 2006. Neutrophil elastase: mediator of extracellular matrix destruction and accumulation. *Proc Am Thorac Soc.* 3(5):424-7.
- Clark, S.R., A.C. Ma, S.A. Tavener, B. McDonald, Z. Goodarzi, M.M. Kelly, K.D. Patel, S. Chakrabarti, E. McAvoy, G.D. Sinclair, E.M. Keys, E. Allen-Vercoe, R. Devinney, C.J. Doig, F.H. Green and P. Kubes. 2007. Platelet TLR4 activates neutrophil extracellular traps to ensnare bacteria in septic blood. *Nat Med.* 13(4):463-9.
- Cocco, D., L. Calabrese, A. Rigo, E. Argese and G. Rotilio. 1981. Re-examination of the reaction of diethyldithiocarbamate with the copper of superoxide dismutase. *J Biol Chem.* 256(17):8983-6.
- Couceiro, J.N., J.C. Paulson and L.G. Baum. 1993. Influenza virus strains selectively recognize sialyloligosaccharides on human respiratory epithelium; the role of the host cell in selection of hemagglutinin receptor specificity. *Virus Res.* 29(2):155-65.
- Cross, A.R. and O.T. Jones. 1986. The effect of the inhibitor diphenylene iodonium on the superoxide-generating system of neutrophils. Specific labelling of a component polypeptide of the oxidase. *Biochem J.* 237(1):111-6.
- Cundell, D.R., N.P. Gerard, C. Gerard, I. Idanpaan-Heikkila and E.I. Tuomanen. 1995. *Streptococcus pneumoniae* anchor to activated human cells by the receptor for platelet-activating factor. *Nature* 377:435–438.
- Cuthbert, G.L., S. Daujat, A.W. Snowden, H. Erdjument-Bromage, T. Hagiwara, M. Yamada, R. Schneider, P.D. Gregory, P. Tempst, A.J. Bannister and T. Kouzarides. 2004. Histone deimination antagonizes arginine methylation. *Cell.* 118(5):545-53.
- Damjanovic, D., C-L Small, M. Jeyanthan, S. McCormick and Z. Xing. 2012. Immunopathology in influenza virus infection: Uncoupling the friend from foe. *Clin Immunol.* 144(1):57-69.

Dawood, F.S., A.D. Iuliano, C. Reed, M.I. Meltzer, D.K. Shay, P.Y. Cheng, D. Bandaranayake, R.F. Breiman, W.A. Brooks, P. Buchy, D.R. Feikin, K.B. Fowler, A. Gordon, N.T. Hien, P. Horby, Q.S. Huang, M.A. Katz, A. Krishnan, R. Lal, J.M. Montgomery, K. Mølbak, R. Pebody, A.M. Presanis, H. Razuri, A. Steens, Y.O. Tinoco, J. Wallinga, H. Yu, S. Vong, J. Bresee and M.A. Widdowson. 2012. Estimated global mortality associated with the first 12 months of 2009 pandemic influenza A H1N1 virus circulation: a modelling study. *Lancet Infect Dis.* 12(9):687-95.

de Vos, A.F., M.C. Dessing, A.J. Lammers, A.P. de Porto, S. Florquin, O.J. de Boer, R. de Beer, S. Terpstra, H.J. Bootsma, P.W. Hermans, C. van 't Veer and T. van der Poll. 2015. The polysaccharide capsule of *Streptococcus pneumoniae* partially impedes MyD88-mediated immunity during pneumonia in mice. *PLoS ONE.* 10(2):e0118181.

Dias, A., D. Bouvier, T. Crépin, A.A. McCarthy, D.J. Hart, F. Baudin, S. Cusack and R.W.H. Ruigrok. 2009. The cap-snatching endonuclease of influenza virus polymerase resides in the PA subunit. *Nature.* 458, 914-18.

Dillard, J., M. Vandersea and J. Yother. 1995. Characterization of the cassette containing genes for type 3 capsular polysaccharide biosynthesis in *Streptococcus pneumoniae*. *J. Exp. Med.* 181:973-83.

Dringen, R and B. Hamprecht. 1997. Involvement of glutathione peroxidase and catalase in the disposal of exogenous hydrogen peroxide by cultured astroglial cells. *Brain Res.* 759(1):67-75.

Droebner, K., S. Pleschka, S. Ludwig and O. Planz. 2011. Antiviral activity of the MEK-inhibitor U0126 against pandemic H1N1v and highly pathogenic avian influenza virus *in vitro* and *in vivo*. *Antiviral Res.* 92(2):195-203.

Dupré-Crochet, S., M. Erard, and O. Nüße. 2013. ROS production in phagocytes: why, when, and where? *J Leukoc Biol.* 94(4):657-70.

Easterbrook, J.D., R.L. Dunfee, L.M. Schwartzman, B.W. Jagger, A. Sandouk, J.C. Kash, M.J. Memoli and J.K. Taubenberger. 2011. Obese mice have increased morbidity and mortality compared to non-obese mice during infection with the 2009 pandemic H1N1 influenza virus. *Influenza Other Respir Viruses.* 5(6):418-25.

Elgazar-Carmon, V., A. Rudich, N. Hadad and R. Levy. 2008. Neutrophils transiently infiltrate intra-abdominal fat early in the course of high-fat feeding. *J Lipid Res.* 49(9):1894-903.

Ellis, J.A., S.J. Mayer and O.T. Jones. 1988. The effect of the NADPH oxidase inhibitor diphenyleneiodonium on aerobic and anaerobic microbicidal activities of human neutrophils. *Biochem J.* 251(3):887-91.

Engelich, G., M. White and K.L. Hartshorn. 2001. Neutrophil survival is markedly reduced by incubation with influenza virus and *Streptococcus pneumoniae*: role of respiratory burst. *J Leukoc Biol.* 69(1):50-6.

- Ermert, D., C.F. Urban, B. Laube, C. Goosmann, A. Zychlinsky and V. Brinkmann. 2009. Mouse neutrophil extracellular traps in microbial infections. *J Innate Immun.* 1(3):181-93.
- Falagas, M.E. and M. Kompoti. 2006. Obesity and infection. *Lancet Infect Dis.* 6(7):438-46.
- Fang, F.C. 2011. Antimicrobial actions of reactive oxygen species. *MBio.* 2(5). pii: e00141-11.
- Fantuzzi, G. 2005. Adipose tissue, adipokines, and inflammation. *J Allergy Clin Immunol.* 115(5):911-9
- Faurischou, M. and N. Borregaard. 2003. Neutrophil granules and secretory vesicles in inflammation. *Microbes Infect.* 5(14):1317-27.
- Fernández-Real, J.M., S. Valdés, M. Manco, B. Chico, P. Botas, A. Campo, R. Casamitjana, E. Delgado, J. Salvador, G. Fruhbeck, G. Mingrone and W. Ricart. 2010. Surfactant protein D, a marker of lung innate immunity, is positively associated with insulin sensitivity. *Diabetes Care.* 33(4):847-53.
- Fidone, S. and T.P. Kennedy. 2003. The role of endogenous NADPH oxidases in airway and pulmonary vascular smooth muscle function. *Antioxid Redox Signal.* 5: 751–8.
- Flegal, K.M., B.I. Graubard, D.F. Williamson and M.H. Gail. 2005. Excess deaths associated with underweight, overweight, and obesity. *JAMA.* 293(15):1861-7.
- Forghani, R., H.J. Kim, G.R. Wojtkiewicz, L. Bure, Y. Wu, M. Hayase, Y. Wei, Y. Zheng, M.A. Moskowitz and J.W. Chen. 2015. Myeloperoxidase propagates damage and is a potential therapeutic target for subacute stroke. *J Cereb Blood Flow Metab.* 35(3):485-93.
- Fuchs, T.A., A. Brill, D. Duerschmied, D. Schatzberg, M. Monestier, D.D. Myers Jr, S.K. Wroblewski, T.W. Wakefield, J.H. Hartwig and D.D. Wagner. 2010. Extracellular DNA traps promote thrombosis. *Proc Natl Acad Sci.* 107(36):15880-5.
- Fuchs, T.A., U. Abed, C. Goosmann, R. Hurwitz, I. Schulze, V. Wahn, Y. Weinrauch, V. Brinkmann and A. Zychlinsky A. 2007. Novel cell death program leads to neutrophil extracellular traps. *J Cell Biol.* 176(2):231-41.
- Fukushi, M., T. Ito, T. Oka, T. Kitazawa, T. Miyoshi-Akiyama, T. Kirikae, M. Yamashita and K. Kudo. 2011. Serial Histopathological Examination of the Lungs of Mice Infected with Influenza A virus PR8 Strain. *PLoS ONE.* 6(6): e21207.
- Garcia, C.C., W. Weston-Davies, R.C. Russo, L.P. Tavares, M.A. Rachid, J.C. Alves-Filho, A.V. Machado, B. Ryffel, M.A. Nunn and M.M. Teixeira. 2013. Complement C5 activation during influenza A infection in mice contributes to neutrophil recruitment and lung injury. *PLoS ONE.* 8(5):e64443.
- Garcia-Romo, G.S., S. Caielli, B. Vega, J. Connolly, F. Allantaz, Z. Xu, M. Punaro, J. Baisch, C. Guiducci, R.L. Coffman, F.J. Barrat, J. Banchereau and V. Pascual. 2011. Netting neutrophils are major inducers of type I IFN production in pediatric systemic lupus erythematosus. *Sci Transl Med.* 3(73):73.

- Gardner, R., A. Salvador and P. Moradas-Ferreira. 2002. Why does SOD overexpression sometimes enhance, sometimes decrease, hydrogen peroxide production? A minimalist explanation. *Free Radic Biol Med.* 32(12):1351-7.
- Garozzo, A., G. Tempera, D. Ungheri, R. Timpanaro and A. Castro. 2007. N-acetylcysteine synergizes with oseltamivir in protecting mice from lethal influenza infection. *Int J Immunopathol Pharmacol.* 20(2):349-54.
- Ge, H., Y.F. Wang, J. Xu, Q. Gu, H.B. Liu, P.G. Xiao, J. Zhou, Y. Liu, Z. Yang and H. Su. 2010. Anti-influenza agents from Traditional Chinese Medicine. *Nat Prod Rep.* 27(12):1758-80.
- Geiler, J., M. Michaelis, P. Naczki, A. Leutz, K. Langer, H.W. Doerr and J. Cinatl Jr. 2010. N-acetyl-L-cysteine (NAC) inhibits virus replication and expression of pro-inflammatory molecules in A549 cells infected with highly pathogenic H5N1 influenza A virus. *Biochem Pharmacol.* 79(3):413-20.
- Geno, K.A., G.L. Gilbert, J.Y. Song, I.C. Skovsted, K.P. Klugman, C. Jones, H.B. Konradsen and M.H. Nahm. 2015. Pneumococcal Capsules and Their Types: Past, Present, and Future. *Clin Microbiol Rev.* 28(3):871-99.
- Genschmer, K.R., M.A. Accavitti-Loper and D.E. Briles. 2013. A modified surface killing assay (MSKA) as a functional *in vitro* assay for identifying protective antibodies against pneumococcal surface protein A (PspA). *Vaccine.* 32(1):39-47.
- Gottfredsen, R.H., U.G. Larsen, J.J. Enghild and S.V. Petersen. 2013. Hydrogen peroxide induce modifications of human extracellular superoxide dismutase that results in enzyme inhibition. *Redox Biol.* 1:24-31.
- Grabowska, K., L. Högberg, P. Penttinen, A. Svensson and K. Ekdahl. 2006. Occurrence of invasive pneumococcal disease and number of excess cases due to influenza. *BMC Infect Dis.* 6:58.
- Gray, R.D., C.D. Lucas, A. Mackellar, F. Li, K. Hiersemenzel, C. Haslett, D.J. Davidson and A.G. Rossi. 2013. Activation of conventional protein kinase C (PKC) is critical in the generation of human neutrophil extracellular traps. *J Inflamm.* 21;10(1):12.
- Gregg, M.B., A.R. Hinman and R.B. Craven. 1978. The Russian flu. Its history and implications for this year's influenza season. *JAMA.* 240(21):2260-3.
- Grijalva, C.G., J.P. Nuorti, P.G. Arbogast, S.W. Martin, K.M. Edwards and M.R. Griffin. 2007. Decline in pneumonia admissions after routine childhood immunisation with pneumococcal conjugate vaccine in the USA: a time-series analysis. *Lancet.* 369(9568):1179-86.
- Guerra, S., D.L. Sherrill, A. Bobadilla, F.D. Martinez and R.A. Barbee. 2002. The relation of body mass index to asthma, chronic bronchitis, and emphysema. *Chest.* 122(4):1256-63.
- Guimarães-Costa, A.B., T.S. DeSouza-Vieira, R. Paletta-Silva, A.L. Freitas-Mesquita, J.R. Meyer-Fernandes and E.M. Saraiva. 2014. 3'-nucleotidase/nuclease activity allows

Leishmania parasites to escape killing by neutrophil extracellular traps. *Infect Immun.* 82(4):1732-40.

Haegens, A., J.H. Vernooy, P. Heeringa, B.T. Mossman and E.F. Wouters. 2008. Myeloperoxidase modulates lung epithelial responses to pro-inflammatory agents. *Eur Respir J.* 31(2):252-60.

Hakkim, A., T.A. Fuchs, N.E. Martinez, S. Hess, H. Prinz, A. Zychlinsky and H. Waldmann. 2011. Activation of the Raf-MEK-ERK pathway is required for neutrophil extracellular trap formation. *Nat Chem Biol.* 7(2):75-7.

Hammerschmidt, S., S. Wolff, A. Hocke, S. Rosseau, E. Müller and M. Rohde. 2005. Illustration of pneumococcal polysaccharide capsule during adherence and invasion of epithelial cells. *Infect Immun.* 73(8):4653-67.

Hampton, M.B., A.J. Kettle and C.C. Winterbourn. 1998. Inside the neutrophil phagosome: oxidants, myeloperoxidase, and bacterial killing. *Blood.* 1;92(9):3007-17.

Hardy, G.G., M.J. Caimano and J. Yother. 2000. Capsule biosynthesis and basic metabolism in *Streptococcus pneumoniae* are linked through the cellular phosphoglucosyltransferase. *J Bacteriol.* 182(7):1854-63.

Harvey, R.M., C.E. Hughes, A.W. Paton, C. Trappetti, R.K. Tweten and J.C. Paton. 2014. The impact of pneumolysin on the macrophage response to *Streptococcus pneumoniae* is strain-dependent. *PLoS ONE.* 9(8):e103625.

Hassett, P., G.F. Curley, M. Contreras, C. Masterson, B.D. Higgins, T. O'Brien, J. Devaney, D. O'Toole and J.G. Laffey. 2011. Overexpression of pulmonary extracellular superoxide dismutase attenuates endotoxin-induced acute lung injury. *Intensive Care Med.* 37(10):1680-7.

Hathaway, L.J., S.D. Brugger, B. Morand, M. Bangert, J.U. Rotzetter, C. Hauser, W.A. Graber, S. Gore, A. Kadioglu and K. Mühlemann. 2012. Capsule type of *Streptococcus pneumoniae* determines growth phenotype. *PLoS Pathog.* 8(3):e1002574.

Hecker, L., R. Vittal, T. Jones, R. Jagirdar, T.R. Luckhardt, J.C. Horowitz, S. Pennathur, F.J. Martinez and V.J. Thannickal. 2009. NADPH oxidase-4 mediates myofibroblast activation and fibrogenic responses to lung injury. *Nat Med.* 15(9):1077-81.

Held, A.M., D.J. Halko and J.K. Hurst. 1978. Mechanisms of chlorine oxidation of hydrogen peroxide *J. Am. Chem. Soc.* 100 (18), 5732-40.

Hemmers, S., J.R. Teijaro, S. Arandjelovic and K.A. Mowen. 2011. PAD4-mediated neutrophil extracellular trap formation is not required for immunity against influenza infection. *PLoS ONE.* 6(7):e22043.

Hennet, T., E. Peterhans and R. Stocker. 1992. Alterations in antioxidant defences in lung and liver of mice infected with influenza A virus. *J Gen Virol.* 73 (Pt 1):39-46.

Hers, J.F., N. Masurel and J. Mulder. 1958. Bacteriology and histopathology of the respiratory tract and lungs in fatal Asian influenza. *Lancet.* 2(7057):1141-3.

- Hildeman, D.A. 2004. Regulation of T-cell apoptosis by reactive oxygen species. *Free Radic Biol Med.* 36(12):1496-504.
- Hirose, T., S. Hamaguchi, N. Matsumoto, T. Irisawa, M. Seki, O. Tasaki, H. Hosotsubo, K. Tomono and T. Shimazu. 2012. Dynamic changes in the expression of neutrophil extracellular traps in acute respiratory infections. *Am J Respir Crit Care Med.* 185(10):1130-1.
- Hirose, T., S. Hamaguchi, N. Matsumoto, T. Irisawa, M. Seki, O. Tasaki, H. Hosotsubo, N. Yamamoto, K. Yamamoto, Y. Akeda, K. Oishi, K. Tomono and T. Shimazu. 2014. Presence of neutrophil extracellular traps and citrullinated histone H3 in the bloodstream of critically ill patients. *PLoS ONE.* 9(11):e111755.
- Hollenbeck, J.E. 2005. An Avian Connection as a Catalyst to the 1918-1919 Influenza Pandemic. *Int J Med Sci.* 2(2): 87–90.
- Hong, J.S., K.J. Greenlee, R. Pitchumani, S.H. Lee, L.Z. Song, M. Shan, S.H. Chang, P.W. Park, C. Dong, Z. Werb, A. Bidani, D.B. Corry and F. Kheradmand. 2011. Dual protective mechanisms of matrix metalloproteinases 2 and 9 in immune defense against *Streptococcus pneumoniae*. *J Immunol.* 186(11):6427-36.
- Hotamisligil G.S., N.S. Shargill and B.M. Spiegelman. 1993. Adipose expression of Tumor Necrosis Factor- α : Direct role in obesity-linked insulin resistance. *Science.* 259(5091): 87-91.
- Hotamisligil, G.S., P. Peraldi, A. Budavari, R. Ellis, M.F. White and B.M. Spiegelman. 1996. IRS-1-mediated inhibition of insulin receptor tyrosine kinase activity in TNF- α and obesity-induced insulin resistance. *Science.* 271(5249):665-8.
- Hurt, R.T., C. Kulisek, L.A. Buchanan, and S.A. McClave. 2010. The Obesity Epidemic: Challenges, Health Initiatives, and Implications for Gastroenterologists. *Gastroenterol Hepatol.* 6(12): 780–92.
- Hurtado-Nedelec, M., M.J. Csillag-Grange, T. Boussetta, S.A. Belambri, M. Fay, B. Cassinat, M.A. Gougerot-Pocidallo, P.M. Dang and J. El-Benna. 2013. Increased reactive oxygen species production and p47phox phosphorylation in neutrophils from myeloproliferative disorders patients with JAK2 (V617F) mutation. *Haematologica.* 98(10):1517-24.
- Hyams, C., E. Camberlein, J.M. Cohen, K. Bax and J.S. Brown. 2010. The *Streptococcus pneumoniae* capsule inhibits complement activity and neutrophil phagocytosis by multiple mechanisms. *Infect Immun.* 78(2):704-15.
- Ivan, F.X., K.S. Tan, M.C. Phoon, B.P. Engelward, R.E. Welsch, J.C. Rajapakse and V.T. Chow. 2013. Neutrophils infected with highly virulent influenza H3N2 virus exhibit augmented early cell death and rapid induction of type I interferon signaling pathways. *Genomics.* 101(2):101-12.
- Jacoby, D. and A.M. Choi. 1994. Influenza virus induces expression of antioxidant genes in human epithelial cells. *Free Radic Biol Med.* 16, 821-24.

- James, S.J., H. Jiao, H.Y. Teh, H. Takahashi, C.W. Png, M.C. Phoon, Y. Suzuki, T. Sawasaki, H. Xiao, V.T. Chow, N. Yamamoto, J.M. Reynolds, R.A. Flavell, C. Dong and Y. Zhang. 2015. MAPK Phosphatase 5 Expression Induced by Influenza and Other RNA Virus Infection Negatively Regulates IRF3 Activation and Type I Interferon Response. *Cell Rep.* pii: S2211-1247(15)00176-X.
- Jauneikaite, E., J.M. Jefferies, M.L. Hibberd and S.C. Clarke. Prevalence of *Streptococcus pneumoniae* serotypes causing invasive and non-invasive disease in South East Asia: a review. *Vaccine.* 30(24):3503-14.
- Jenne, C.N., C.H. Wong, F.J. Zemp, B. McDonald, M.M. Rahman, P.A. Forsyth, G. McFadden and P. Kubes. 2013. Neutrophils recruited to sites of infection protect from virus challenge by releasing neutrophil extracellular traps. *Cell Host Microbe.* 13(2):169-80.
- Jiao, H., P. Tang and Y. Zhang. 2015. MAP kinase phosphatase 2 regulates macrophage-adipocyte interaction. *PLoS ONE.* 10(3):e0120755.
- Johnson, L.N. and M. Koval. 2009. Cross-talk between pulmonary injury, oxidant stress, and gap junctional communication. *Antioxid. Redox. Signal.* 11: 355–67.
- Jones, R.M., J.W. Mercante and A.S. Neish. 2012. Reactive oxygen production induced by the gut microbiota: pharmacotherapeutic implications. *Curr Med Chem.* 19(10):1519-29.
- Juneau, R.A., B. Pang, K.E. Weimer, C.E. Armbruster and W.E. Swords. 2011. Nontypeable *Haemophilus influenzae* initiates formation of neutrophil extracellular traps. *Infect Immun.* 79(1):431-8.
- Kadioglu, A., J.N. Weiser, J.C. Paton and P.W. Andrew. 2008. The role of *Streptococcus pneumoniae* virulence factors in host respiratory colonization and disease. *Nat Rev Microbiol.* 6(4):288-301.
- Kadioglu, A., N.A. Gingles, K. Grattan, A. Kerr, T.J. Mitchell and P.W. Andrew. 2000. Host Cellular Immune Response to Pneumococcal Lung Infection in Mice. *Infect Immun.* 68(2): 492–501.
- Kadioglu, A., S. Taylor, F. Iannelli, G. Pozzi, T.J. Mitchell and P.W. Andrew. 2002. Upper and lower respiratory tract infection by *Streptococcus pneumoniae* is affected by pneumolysin deficiency and differences in capsule type. *Infect Immun.* 70(6):2886-90.
- Kalin, M. 1998. Pneumococcal serotypes and their clinical relevance. *Thorax.* 53(3):159-62.
- Kamgar, M., F. Zaldivar, N.D. Vaziri and M.V. Pahl. 2009. Antioxidant therapy does not ameliorate oxidative stress and inflammation in patients with end-stage renal disease. *J Natl Med Assoc.* 101(4):336-44.
- Karlsson, E.A., P.A. Sheridan and M.A. Beck. 2010. Diet-induced obesity impairs the T cell memory response to influenza virus infection. *J Immunol.* 184(6):3127-33.

- Kash, J.C., K.A. Walters, A.S. Davis, A. Sandouk, L.M. Schwartzman, B.W. Jagger, D.S. Chertow, Q. Li, R.E. Kuestner, A. Ozinsky and J.K. Taubenberger. 2011. Lethal synergism of 2009 pandemic H1N1 influenza virus and *Streptococcus pneumoniae* coinfection is associated with loss of murine lung repair responses. *MBio*. 2(5). pii: e00172-11.
- Kawaoka, Y., S. Krauss and R.G. Webster. 1989. Avian-to-human transmission of the PB1 gene of influenza A viruses in the 1957 and 1968 pandemics. *J Virol*. 63(11):4603-8.
- Kessenbrock, K., M. Krumbholz, U. Schönemarck, W. Back, W.L. Gross, Z. Werb, H.J. Gröne, V. Brinkmann and D.E. Jenne. 2009. Netting neutrophils in autoimmune small-vessel vasculitis. *Nat.Med*. 15, 623–25.
- Keshari, R.S., A. Verma, M.K. Barthwal and M. Dikshit. 2013. Reactive oxygen species-induced activation of ERK and p38 MAPK mediates PMA-induced NETs release from human neutrophils. *J Cell Biochem*. 114(3):532-40.
- Kettle, A.J., C.A. Gedge and C.C. Winterbourn. 1997. Mechanism of inactivation of myeloperoxidase by 4-aminobenzoic acid hydrazide. *Biochem J*. 321 (Pt 2):503-8.
- Kettle, A.J., C.A. Gedge, M.B. Hampton and C.C. Winterbourn. 1995. Inhibition of myeloperoxidase by benzoic acid hydrazides. *Biochem J*. 308(Pt 2): 559–63.
- Khouri, R., F. Novais, G. Santana, C.I. de Oliveira, M.A. Vannier dos Santos, A. Barral, M. Barral-Netto and J. Van Weyenbergh. 2010. DETC induces *Leishmania* parasite killing in human *in vitro* and murine *in vivo* models: a promising therapeutic alternative in Leishmaniasis. *PLoS ONE*. 5(12):e14394.
- Kim, H.J., C.H. Kim, J.H. Ryu, M.J. Kim, C.Y. Park, J.M. Lee, M.J. Holtzman and J.H. Yoon. 2013. Reactive oxygen species induce antiviral innate immune response through IFN- λ regulation in human nasal epithelial cells. *Am J Respir Cell Mol Biol*. 49(5):855-65.
- Kim, J.A., G.P. Neupane, E.S. Lee, B.S. Jeong, B.C. Park and P. Thapa. 2011. NADPH oxidase inhibitors: a patent review. *Expert Opin Ther Pat*. 21(8):1147-58.
- Kinnula, V.L., C.L. Fattman, R.J. Tan and T.D. Oury. 2005. Oxidative stress in pulmonary fibrosis: a possible role for redox modulatory therapy. *Am. J. Respir. Crit. Care Med*. 172: 417–22.
- Klebanoff S.J., A.M. Waltersdorff and H. Rosen. 1984. Antimicrobial activity of myeloperoxidase. *Methods Enzymol*. 105:399-403.
- Klebanoff, S.J., A.J. Kettle, H. Rosen, C.C. Winterbourn and W.M. Nauseef. 2013. Myeloperoxidase: a front-line defender against phagocytosed microorganisms. *J. Leukoc. Biol*. 93, 185–98.
- Kobasa, D., A. Takada, K. Shinya, M. Hatta, P. Halfmann, S. Theriault, H. Suzuki, H. Nishimura, K. Mitamura, N. Sugaya, T. Usui, T. Murata, Y. Maeda, S. Watanabe, M. Suresh, T. Suzuki, Y. Suzuki, H. Feldmann and Y. Kawaoka. 2004. Enhanced virulence

of influenza A viruses with the haemagglutinin of the 1918 pandemic virus. *Nature*. 431(7009):703-7.

Kristian, S.A., M. Dürr, J.A. Van Strijp, B. Neumeister and A. Peschel. 2003. MprF-mediated lysinylation of phospholipids in *Staphylococcus aureus* leads to protection against oxygen-independent neutrophil killing. *Infect Immun*. 71(1):546-9.

Küng, E, W.R. Coward, D.R. Neill, H.A. Malak, K. Mühlemann, A. Kadioglu, M. Hilty and L.J. Hathaway. 2014. The pneumococcal polysaccharide capsule and pneumolysin differentially affect CXCL8 and IL-6 release from cells of the upper and lower respiratory tract. *PLoS ONE*. 9(3):e92355.

Kutter, D., P. Devaquet, G. Vanderstocken, J.M. Paulus, V. Marchal and A. Gothot. 2000. Consequences of total and subtotal myeloperoxidase deficiency: risk or benefit? *Acta Haematol*. 104, 10–15.

Lander, H.M. 1997. An essential role for free radicals and derived species in signal transduction. *FASEB J*. 11(2):118-24.

Laukkanen, M.O., P. Leppanen, P. Turunen, T. Tuomisto, J. Naarala and S. Yla-Herttuala. 2001. EC-SOD gene therapy reduces paracetamol-induced liver damage in mice. *J Gene Med*. 3(4):321-5.

Lauth, X., M. von Köckritz-Blickwede, C.W. McNamara, S. Myskowski, A.S. Zinkernagel, B. Beall, P. Ghosh, R.L. Gallo and V. Nizet. 2009. M1 protein allows Group A streptococcal survival in phagocyte extracellular traps through cathelicidin inhibition. *J Innate Immun*. 1(3):202-14.

Lawlor, M.S., S.A. Handley and V.L. Miller. 2006. Comparison of the host responses to wild-type and cpsB mutant *Klebsiella pneumoniae* infections. *Infect Immun*. 74(9):5402-7.

Le T., J. Steel and R. Compans. 2012. Influenza A virus pathogenesis: Identification of host factors that contribute to severe respiratory distress. *J Immunol*. 188, 169.18.

Lee, S.M., K.H. Kok, M. Jaume, T.K. Cheung, T.F. Yip, J.C. Lai, Y. Guan, R.G. Webster, D.Y. Jin and J.S. Peiris. 2014. Toll-like receptor 10 is involved in induction of innate immune responses to influenza virus infection. *Proc Natl Acad Sci*. 111(10):3793-8.

Leffler, J., M. Martin, B. Gullstrand, H. Tydén, C. Lood, L. Truedsson, A.A. Bengtsson and A.M. Blom. 2012. Neutrophil extracellular traps that are not degraded in systemic lupus erythematosus activate complement exacerbating the disease. *J Immunol*. 188(7):3522-31.

Li, H., Z. Xiang, T. Feng, J. Li, Y. Liu, Y. Fan, Q. Lu, Z. Yin, M. Yu, C. Shen and W. Tu. 2013. Human V γ 9V δ 2-T cells efficiently kill influenza virus-infected lung alveolar epithelial cells. *Cell Mol Immunol*. 10(2):159-64.

Li, P., M. Li, M.R. Lindberg, M.J. Kennett, N. Xiong and Y. Wang. 2010. PAD4 is essential for antibacterial innate immunity mediated by neutrophil extracellular traps. *J Exp Med*. 207(9):1853–62.

- Ling, J.X., F. Wei, N. Li, J.L. Li, L.J. Chen, Y.Y. Liu, F. Luo, H.R. Xiong, W. Hou and Z.Q. Yang. 2012. Amelioration of influenza virus-induced reactive oxygen species formation by epigallocatechin gallate derived from green tea. *Acta Pharmacol Sin.* 33(12):1533-41.
- Liu, C.L., S. Tangsombatvisit, J.M. Rosenberg, G. Mandelbaum, E.C. Gillespie, O.P. Gozani, A.A. Alizadeh and P.J. Utz. 2012. Specific post-translational histone modifications of neutrophil extracellular traps as immunogens and potential targets of lupus autoantibodies. *Arthritis Res Ther.* 14(1):R25.
- Liu, M. and F. Liu. 2009. Transcriptional and post-translational regulation of adiponectin. *Biochem J.* 425(1):41-52.
- Livak, K.J. and T.D. Schmittgen. 2001. Analysis of relative gene expression data using real-time quantitative PCR and the 2(-Delta Delta C(T)) Method. *Methods.* 25(4):402-8.
- Llull, D., E. Gracia and R. Lopez. 2001. Tts, a processive-glycosyltransferase of *Streptococcus pneumoniae*, directs the synthesis of the branched type 37 capsular polysaccharide in pneumococcus and other gram-positive species. *J. Biol. Chem.* 276:21053-61.
- Louie, J.K., M. Acosta, K. Winter, C. Jean, S. Gavali, R. Schechter, D. Vugia, K. Harriman, B. Matyas, C.A. Glaser, M.C. Samuel, J. Rosenberg, J. Talarico, D. Hatch and California Pandemic (H1N1) Working Group. 2009. Factors associated with death or hospitalization due to pandemic 2009 influenza A(H1N1) infection in California. *JAMA.* 302(17):1896-902.
- Louie, J.K., M. Acosta, M.C. Samuel, R. Schechter, D.J. Vugia, K. Harriman, B.T. Matyas and California Pandemic (H1N1) Working Group. 2011. A novel risk factor for a novel virus: obesity and 2009 pandemic influenza A (H1N1). *Clin Infect Dis.* 52(3):301-12.
- Lucas, S. 2010. Predictive clinicopathological features derived from systematic autopsy examination of patients who died with A/H1N1 influenza infection in the UK 2009-10 pandemic. *Health Technol Assess.* 14(55):83-114.
- MacLeod, C.M. and M.R. Kraus. 1950. Relation of virulence of pneumococcal strains for mice to the quantity of capsular polysaccharide formed *in vitro*. *J Exp Med.* 92(1):1-9.
- MacNee, W. and I. Rahman. 1995. Oxidants/antioxidants in idiopathic pulmonary fibrosis. *Thorax.* 50(Suppl 1): S53-58.
- Magee, A.D. and J. Yother. 2001. Requirement for capsule in colonization by *Streptococcus pneumoniae*. *Infect Immun.* 69(6):3755-61.
- Makino, A., M.M. Skelton, A.P. Zou and A.W. Cowley Jr. 2003. Increased Renal Medullary H₂O₂ Leads to Hypertension. *Hypertension.* 42: 25-30.
- Mancuso, P. 2013. Obesity and respiratory infections: does excess adiposity weigh down host defense? *Pulm Pharmacol Ther.* 26(4):412-9.

- Mancuso, P., C. Lewis, C.H. Serezani, D. Goel and M. Peters-Golden. 2010. Intrapulmonary administration of leukotriene B4 enhances pulmonary host defense against pneumococcal pneumonia. *Infect Immun.* 78(5):2264-71.
- Mantovani, A., M.A. Cassatella, C. Costantini and S. Jaillon. 2011. Neutrophils in the activation and regulation of innate and adaptive immunity. *Nat Rev Immunol.* 25;11(8):519-31.
- Margraf, S, T. Lögters, J. Reipen, J. Altrichter, M. Scholz and J. Windolf. 2008. Neutrophil-derived circulating free DNA (cf-DNA/NETs): a potential prognostic marker for posttraumatic development of inflammatory second hit and sepsis. *Shock.* 30(4):352-8.
- Matés, J.M. and F. Sánchez-Jiménez. 1999. Antioxidant enzymes and their implications in pathophysiologic processes. *Front Biosci.* 4:D339-45.
- Matrosovich, M.N., T.Y. Matrosovich, T. Gray, N.A. Roberts, H.D. Klenk. 2004. Human and avian influenza viruses target different cell types in cultures of human airway epithelium. *Proc Natl Acad Sci.* 101(13):4620-4.
- Matute-Bello, G., R.K. Winn, M. Jonas, E.Y. Chi, T.R. Martin and W.C. Liles. 2001. Fas (CD95) induces alveolar epithelial cell apoptosis *in vivo*: implications for acute pulmonary inflammation. *Am J Pathol.* 158(1):153-61.
- Mawas, F., I.M. Feavers and M.J. Corbel. 2000. Serotype of *Streptococcus pneumoniae* capsular polysaccharide can modify the Th1/Th2 cytokine profile and IgG subclass response to pneumococcal-CRM(197) conjugate vaccines in a murine model. *Vaccine.* 19(9-10):1159-66.
- Mayer-Scholl, A., P. Averhoff and A. Zychlinsky. 2004. How do neutrophils and pathogens interact? *Curr Opin Microbiol.* 7(1):62-6.
- McAuley, J.L., F. Hornung, K.L. Boyd, A.M. Smith, R. McKeon, J. Bennink, J.W. Yewdell and J.A. McCullers. 2007. Expression of the 1918 influenza A virus PB1-F2 enhances the pathogenesis of viral and secondary bacterial pneumonia. *Cell Host Microbe.* 2(4):240-9.
- McAuley, J.L., K. Kedzierska, L.E. Brown and G.D. Shanks. 2015. Host Immunological Factors Enhancing Mortality of Young Adults during the 1918 Influenza Pandemic. *Front Immunol.* 6:419.
- McCallister, J.W., E.J. Adkins and J.M. O'Brien Jr. 2009. Obesity and acute lung injury. *Clin Chest Med.* 30(3):495-508, viii.
- McCoy, C.E., S. Carpenter, E.M. Pålsson-McDermott, L.J. Gearing and L.A. O'Neill. 2008. Glucocorticoids inhibit IRF3 phosphorylation in response to Toll-like receptor-3 and -4 by targeting TBK1 activation. *J Biol Chem.* 283(21):14277-85.
- McCullers, J.A. and J.E. Rehg. 2002. Lethal synergism between influenza virus and *Streptococcus pneumoniae*: characterization of a mouse model and the role of platelet-activating factor receptor. *J Infect Dis.* 186(3):341-50.

- McNamee, L.A. and A.G. Harmsen. 2006. Both influenza-induced neutrophil dysfunction and neutrophil-independent mechanisms contribute to increased susceptibility to a secondary *Streptococcus pneumoniae* infection. *Infect Immun.* 74(12):6707-21.
- Melegaro, A., Y.H. Choi, R. George, W.J. Edmunds, E. Miller and N.J. Gay. 2010. Dynamic models of pneumococcal carriage and the impact of the Heptavalent Pneumococcal Conjugate Vaccine on invasive pneumococcal disease. *BMC Infect Dis.* 10:90.
- Melin, M., K. Trzciński, S. Meri, H. Käyhty and M. Väkeväinen. 2010. The capsular serotype of *Streptococcus pneumoniae* is more important than the genetic background for resistance to complement. *Infect Immun.* 78(12):5262-70.
- Menegazzi, R., E. Decleva and P. Dri. 2012. Killing by neutrophil extracellular traps: fact or folklore? *Blood.* 119(5):1214-6.
- Metersky, M.L., R.G. Masterton, H. Lode, T.M. File Jr. and T. Babinchak. 2012. Epidemiology, microbiology, and treatment considerations for bacterial pneumonia complicating influenza. *Int J Infect Dis.* 16(5):e321-31.
- Metzler, K.D., C. Goosmann, A. Lubojemska, A. Zychlinsky and V. Papayannopoulos. 2014. A myeloperoxidase-containing complex regulates neutrophil elastase release and actin dynamics during NETosis. *Cell Rep.* 8(3):883-96.
- Metzler, K.D., T.A. Fuchs, W.M. Nauseef, D. Reumaux, J. Roesler, I. Schulze, V. Wahn, V. Papayannopoulos and A. Zychlinsky. 2011. Myeloperoxidase is required for neutrophil extracellular trap formation: implications for innate immunity. *Blood.* 117(3):953-9.
- Milner, J.J., P.A. Sheridan, E.A. Karlsson, S. Schultz-Cherry, Q. Shi and M.A. Beck. 2013. Diet-induced obese mice exhibit altered heterologous immunity during a secondary 2009 pandemic H1N1 infection. *J Immunol.* 191(5):2474-85.
- Misra HP. 1979. Reaction of copper-zinc superoxide dismutase with diethyldithiocarbamate. *J Biol Chem.* 254(22):11623-8.
- Mitchell, A.M. and T.J. Mitchell. 2010. *Streptococcus pneumoniae*: virulence factors and variation. *Clin Microbiol Infect.* 16(5):411-8.
- Moltedo, B., C.B. López, M. Pazos, M.I. Becker, T. Hermesh and T.M. Moran. 2009. Cutting edge: stealth influenza virus replication precedes the initiation of adaptive immunity. *J Immunol.* 183(6):3569-73.
- Montgomery, M.K., N.L. Hallahan, S.H. Brown, M. Liu, T.W. Mitchell, G.J. Cooney and N. Turner. 2013. Mouse strain-dependent variation in obesity and glucose homeostasis in response to high-fat feeding. *Diabetologia.* 56(5):1129-39.
- Moreno-Navarrete, J.M. and J.M. Fernández-Real. 2011. Antimicrobial-sensing proteins in obesity and type 2 diabetes: the buffering efficiency hypothesis. *Diabetes Care.* 34 Suppl 2:S335-41.

- Morens, D.M. and J.K. Taubenberger. 2011. Pandemic influenza: certain uncertainties. *Rev Med Virol.* 21(5):262-84.
- Morens, D.M., J.K. Taubenberger and A.S. Fauci. 2008. Predominant role of bacterial pneumonia as a cause of death in pandemic influenza: implications for pandemic influenza preparedness. *J Infect Dis.* 198(7):962-70.
- Mori, Y., M. Yamaguchi, Y. Terao, S. Hamada, T. Ooshima and S. Kawabata. 2012. α -Enolase of *Streptococcus pneumoniae* induces formation of neutrophil extracellular traps. *J Biol Chem.* 287(13):10472-81.
- Morona, J.K., D.C. Miller, R. Morona and J.C. Paton. 2004. The effect that mutations in the conserved capsular polysaccharide biosynthesis genes *cpsA*, *cpsB* and *cpsD* have on virulence of *Streptococcus pneumoniae*. *J Infect Dis.* 189, 1905-13.
- Morona, J.K., J.C. Paton, D.C. Miller and R. Morona. 2000. Tyrosine phosphorylation of CpsD negatively regulates capsular polysaccharide biosynthesis in *Streptococcus pneumoniae*. *Mol. Microbiol.* 35, 1431-42.
- Morona, J.K., R. Morona and J.C. Paton. 2006. Attachment of capsular polysaccharide to the cell wall of *Streptococcus pneumoniae* type 2 is required for invasive disease. *Proc. Natl Acad. Sci.* 103, 8505-10
- Morona, J.K., R. Morona, D.C. Miller and J.C. Paton. 2002. *Streptococcus pneumoniae* capsule biosynthesis protein CpsB is a novel manganese-dependent phosphotyrosine-protein phosphatase. *J Bacteriol.* 184(2):577-83.
- Morona, J.K., R. Morona, D.C. Miller and J.C. Paton. 2003. Mutational analysis of the carboxy-terminal (YGX)₄ repeat domain of CpsD, an autophosphorylating tyrosine kinase required for capsule biosynthesis in *Streptococcus pneumoniae*. *J. Bacteriol.* 185, 3009-19.
- Muraki, Y. and S. Hongo. 2010. The molecular virology and reverse genetics of influenza C virus. *Jpn J Infect Dis.* 63(3):157-65.
- Muruve, D.A., M.J. Barnes, I.E. Stillman and T.A. Libermann. 1999. Adenoviral gene therapy leads to rapid induction of multiple chemokines and acute neutrophil-dependent hepatic injury *in vivo*. *Hum Gene Ther.* 10(6):965-76.
- Nakazawa, D., H. Shida, U. Tomaru, M. Yoshida, S. Nishio, T. Atsumi and A. Ishizu. 2014. Enhanced formation and disordered regulation of NETs in myeloperoxidase-ANCA-associated microscopic polyangiitis. *J Am Soc Nephrol.* 25(5):990-7.
- Narasaraju, T., E. Yang, R.P. Samy, H.H. Ng, W.P. Poh, A.A. Liew, M.C. Phoon, N. van Rooijen and V.T. Chow. 2011. Excessive neutrophils and neutrophil extracellular traps contribute to acute lung injury of influenza pneumonitis. *Am J Pathol.* 179(1):199-210.
- Nazareth, H., S.A. Genagon and T.A. Russo. 2007. Extraintestinal pathogenic *Escherichia coli* survives within neutrophils. *Infect Immun.* 75(6):2776-85.
- Neeli, I. and M. Radic. 2013. Opposition between PKC isoforms regulates histone deimination and neutrophil extracellular chromatin release. *Front Immunol.* 4:38.

- Neeli, I., S.N. Khan and M. Radic. 2008. Histone deimination as a response to inflammatory stimuli in neutrophils. *J Immunol.* 180(3):1895-902.
- Nemec, A., Z. Pavlica, D.A. Crossley, M. Sentjurc, A. Jerin, D. Erzen, M. Vrecl, G. Majdic, I. Zdovc, M. Petelin and U. Skaleric. 2009. Chronic ingestion of *Porphyromonas gingivalis* induces systemic nitric oxide response in mice. *Oral Microbiol Immunol.* 24(3):204-10.
- Ng, H.H., T. Narasaraju, M.C. Phoon, M.K. Sim, J.E. Seet and V.T. Chow. 2012. Doxycycline treatment attenuates acute lung injury in mice infected with virulent influenza H3N2 virus: involvement of matrix metalloproteinases. *Exp Mol Pathol.* 92(3):287-95.
- Nobusawa, E. and K. Sato. 2006. Comparison of the mutation rates of human influenza A and B viruses. *J Virol.* 80(7):3675-8.
- Oda, T., T. Akaike, T. Hamamoto, F. Suzuki, T. Hirano and H. Maeda. 1989. Oxygen radicals in influenza-induced pathogenesis and treatment with pyran polymer-conjugated SOD. *Science.* 244(4907):974-6.
- O'Donnell, B.V., D.G. Tew, O.T. Jones, and P.J. England. 1993. Studies on the inhibitory mechanism of iodonium compounds with special reference to neutrophil NADPH oxidase. *Biochem J.* 290, 41-9.
- O'Donnell, V.B., G.C. Smith and O.T. Jones. 1994. Involvement of phenyl radicals in iodonium inhibition of flavoenzymes. *Mol Pharmacol.* 46(4), 778-85.
- Osterholm, M.T. 2005. Preparing for the next pandemic. *N Engl J Med.* 352(18):1839-42.
- Pace, G.W. and C.D. Leaf. 1995. The role of oxidative stress in HIV disease. *Free Radic Biol Med.* 19(4):523-8.
- Palese, P. 2004. Influenza: old and new threats. *Nat Med.* 10(12 Suppl):S82-7.
- Papayannopoulos, V., K.D. Metzler, A. Hakkim and A. Zychlinsky. 2010. Neutrophil elastase and myeloperoxidase regulate the formation of neutrophil extracellular traps. *J Cell Biol.* 191(3):677-91.
- Paracha, U.Z., K. Fatima, M. Alqahtani, A. Chaudhary, A. Abuzenadah, G. Damanhour and I. Qadri. 2013. Oxidative stress and hepatitis C virus. *Virol J.* 10:251.
- Parker, H. and C.C. Winterbourn. 2013. Reactive oxidants and myeloperoxidase and their involvement in neutrophil extracellular traps. *Front Immunol.* 3:424.
- Parker, H., A.M. Albrett, A.J. Kettle and C.C. Winterbourn. 2012. Myeloperoxidase associated with neutrophil extracellular traps is active and mediates bacterial killing in the presence of hydrogen peroxide. *J Leukoc Biol.* 91(3):369-76.
- Pazhanisamy, S.K., H. Li, Y. Wang, I. Batinic-Haberle and D. Zhou. 2011. NADPH oxidase inhibition attenuates total body irradiation-induced haematopoietic genomic instability. *Mutagenesis.* 26(3):431-5.

- Peltola, V.T. and J.A. McCullers. 2004. Respiratory viruses predisposing to bacterial infections: role of neuraminidase. *Pediatr Infect Dis J.* 23(1 Suppl):S87-97.
- Pericone, C.D., K. Overweg, P.W. Hermans and J.N. Weiser. 2000. Inhibitory and bactericidal effects of hydrogen peroxide production by *Streptococcus pneumoniae* on other inhabitants of the upper respiratory tract. *Infect Immun.* 68(7):3990-7.
- Perrone, L.A., J.K. Plowden, A. García-Sastre, J.M. Katz and T.M. Tumpey. 2008. H5N1 and 1918 pandemic influenza virus infection results in early and excessive infiltration of macrophages and neutrophils in the lungs of mice. *PLoS Pathog.* 4(8): e1000115.
- Peterhans, E. 1997. Oxidants and antioxidants in viral diseases: disease mechanisms and metabolic regulation. *J Nutr.* 127(5 Suppl):S962-65.
- Peterhans, E., M. Grob, T. Bürge and R. Zanoni. 1987. Virus-induced formation of reactive oxygen intermediates in phagocytic cells. *Free Radic Res Commun.* 3(1-5):39-46.
- Phan, S.H., D.E. Gannon, P.A. Ward and S. Karmiol. 1992. Mechanism of neutrophil-induced xanthine dehydrogenase to xanthine oxidase conversion in endothelial cells: evidence of a role for elastase. *Am J Respir Cell Mol Biol.* 6(3):270-8.
- Pilszczek, F.H., D. Salina, K.K. Poon, C. Fahey, B.G. Yipp, C.D. Sibley, S.M. Robbins, F.H. Green, M.G. Surette, M. Sugai, M.G. Bowden, M. Hussain, K. Zhang and P. Kubes. 2010. A novel mechanism of rapid nuclear neutrophil extracellular trap formation in response to *Staphylococcus aureus*. *J Immunol.* 185(12):7413-25.
- Pratesi, F., I. Dioni, C. Tommasi, M.C. Alcaro, I. Paolini, F. Barbetti, F. Boscaro, F. Panza, I. Puxeddu, P. Rovero and P. Migliorini. 2014. Antibodies from patients with rheumatoid arthritis target citrullinated histone 4 contained in neutrophils extracellular traps. *Ann Rheum Dis.* 73(7):1414-22.
- Pruchniak, M.P., M. Arazna and U. Demkow. 2013. Life of neutrophil: from stem cell to neutrophil extracellular trap. *Respir Physiol Neurobiol.* 187(1):68-73.
- Rai, P., M. Parrish, I.J. Tay, N. Li, S. Ackerman, F. He, J. Kwang, V.T. Chow and B.P. Engelward. 2015. *Streptococcus pneumoniae* secretes hydrogen peroxide leading to DNA damage and apoptosis in lung cells. *Proc Natl Acad Sci.* 112(26):E3421-30.
- Ramos-Kichik, V., R. Mondragon-Flores, M. Mondragon-Castelan, S. Gonzalez-Pozos, S. Muniz-Hernandez, O. Rojas-Espinosa, R. Chacon-Salinas, S. Estrada-Parra and I. Estrada-Garcia. 2009. Neutrophil extracellular traps are induced by *Mycobacterium tuberculosis*. *Tuberculosis.* 89(1):29-37.
- Ray, P.D., B.W. Huang and Y. Tsuji. 2012. Reactive oxygen species (ROS) homeostasis and redox regulation in cellular signaling. *Cell Signal.* 24(5):981-90.
- Reshi, M.L., Y.C. Su and J.R. Hong. 2014. RNA Viruses: ROS-Mediated Cell Death. *Int J Cell Biol.* 2014:467452.
- Reynolds, J.H., G. McDonald, H. Alton and S.B. Gordon. 2010. Pneumonia in the immunocompetent patient. *Br J Radiol.* 83(996):998-1009.

- Riyapa, D., S. Buddhisa, S. Korbsrisate, J. Cuccui, B.W. Wren, M.P. Stevens, M. Ato and G. Lertmemongkolchai. 2012. Neutrophil extracellular traps exhibit antibacterial activity against *Burkholderia pseudomallei* and are influenced by bacterial and host factors. *Infect Immun.* 80(11):3921-9.
- Rocha, J.D., M.T. Nascimento, D. Decote-Ricardo, S. Côrte-Real, A. Morrot, N. Heise, M.P. Nunes, J.O. Previato, L. Mendonça-Previato, G.A. DosReis, E.M. Saraiva and C.G. Freire-de-Lima. 2015. Capsular polysaccharides from *Cryptococcus neoformans* modulate production of neutrophil extracellular traps (NETs) by human neutrophils. *Sci Rep.* 5:8008.
- Rogan, M.P., P. Geraghty, C.M. Greene, S.J. O'Neill, C.C. Taggart and N.G. McElvaney. 2006. Antimicrobial proteins and polypeptides in pulmonary innate defence. *Respir Res.* 7:29.
- Rothberg, M.B., S.D. Haessler and R.B. Brown. 2008. Complications of viral influenza. *Am J Med.* 121(4):258-64.
- Saffarzadeh, M., C. Juenemann, M.A. Queisser, G. Lochnit, G. Barreto, S.P. Galuska, J. Lohmeyer and K.T. Preissner. 2012. Neutrophil extracellular traps directly induce epithelial and endothelial cell death: a predominant role of histones. *PLoS ONE.* 7(2):e32366.
- Saitoh, T., J. Komano, Y. Saitoh, T. Misawa, M. Takahama, T. Kozaki, T. Uehata, H. Iwasaki, H. Omori, S. Yamaoka, N. Yamamoto and S. Akira. 2012. Neutrophil extracellular traps mediate a host defense response to human immunodeficiency virus-1. *Cell Host Microbe.* 12(1):109-16.
- Sanmartín-Suárez, C., R. Soto-Otero, I. Sánchez-Sellero and E. Méndez-Álvarez. 2011. Antioxidant properties of dimethyl sulfoxide and its viability as a solvent in the evaluation of neuroprotective antioxidants. *J Pharmacol Toxicol Methods.* 63(2):209-15.
- Savill, J.S., A.H. Wyllie, J.E. Henson, M.J. Walport, P.M. Henson and C. Haslett. 1989. Macrophage phagocytosis of aging neutrophils in inflammation. Programmed cell death in the neutrophil leads to its recognition by macrophages. *J Clin Invest.* 83(3): 865-75.
- Schols, A.M., R. Broekhuizen, C.A. Weling-Scheepers and E.F. Wouters. 2005. Body composition and mortality in chronic obstructive pulmonary disease. *Am J Clin Nutr.* 82(1):53-9.
- Segal, A.W. 1996. The NADPH oxidase and chronic granulomatous disease. *Mol Med Today.* 2(3):129-35.
- Selemidis, S., C.G. Sobey, K. Wingler, H.H. Schmidt and G.R. Drummond. 2008. NADPH oxidases in the vasculature: molecular features, roles in disease and pharmacological inhibition. *Pharmacol Ther.* 120(3):254-91.
- Sgarbanti, R., D. Amatore, I. Celestino, M.E. Marcocci, A. Fraternali, M.R. Ciriolo, M. Magnani, R. Saladino, E. Garaci, A.T. Palamara and L. Nencioni. 2014. Intracellular redox state as target for anti-influenza therapy: are antioxidants always effective? *Curr Top Med Chem.* 14(22):2529-41.

- Shahangian, A., E.K. Chow, X. Tian, J.R. Kang, A. Ghaffari, S.Y. Liu, J.A. Belperio, G. Cheng and J.C. Deng. 2009. Type I IFNs mediate development of post influenza bacterial pneumonia in mice. *J Clin Invest.* 119(7):1910-20.
- Shainheit, M.G., M. Mulé and A. Camilli. 2014. The core promoter of the capsule operon of *Streptococcus pneumoniae* is necessary for colonization and invasive disease. *Infect Immun.* 82(2):694-705.
- Shanks, G.D. and J.F. Brundage. 2012. Pathogenic responses among young adults during the 1918 influenza pandemic. *Emerg Infect Dis.* 18(2):201-7.
- Sheridan, P.A., H.A. Paich, J. Handy, E.A. Karlsson, M.G. Hudgens, A.B. Sammon, L.A. Holland, S. Weir, T.L. Noah and M.A. Beck. 2012. Obesity is associated with impaired immune response to influenza vaccination in humans. *Int J Obes.* 36(8):1072-7.
- Shirley, S.W., B.H. Stewart and S. Mirelman. 1978. Dimethyl sulfoxide in treatment of inflammatory genitourinary disorders. *Urology.* 11(3):215-20.
- Shope, R.E. 1931. Swine Influenza: III. Filtration experiments and etiology. *J Exp Med.* 54(3):373-85.
- Sidwell, R.W., J.H. Huffman, K.W. Bailey, M.H. Wong, A. Nimrod and A. Panet. 1996. Inhibitory effects of recombinant manganese superoxide dismutase on influenza virus infections in mice. *Antimicrob Agents Chemother.* 40(11):2626-31.
- Siemieniuk, R.A., D.B. Gregson and M.J. Gill. 2011. The persisting burden of invasive pneumococcal disease in HIV patients: an observational cohort study. *BMC Infect Dis.* 11:314.
- Siriwardena, A.K., J.M. Mason, A.J. Sheen, A.J. Makin and N.S. Shah. 2012. Antioxidant therapy does not reduce pain in patients with chronic pancreatitis: the ANTICIPATE study. *Gastroenterol.* 143(3):655-63.e1.
- Sjöström, K., C. Spindler, A. Ortqvist, M. Kalin, A. Sandgren, S. Kühlmann-Berenzon and B. Henriques-Normark. 2006. Clonal and capsular types decide whether pneumococci will act as a primary or opportunistic pathogen. *Clin Infect Dis.* 42(4):451-9.
- Smith, A.G., P.A. Sheridan, J.B. Harp and M.A. Beck. 2007. Diet-induced obese mice have increased mortality and altered immune responses when infected with influenza virus. *J Nutr.* 137(5):1236-43.
- Smith, A.M., F.R. Adler, R.M. Ribeiro, R.N. Gutenkunst, J.L. McAuley, J.A. McCullers and A.S. Perelson. 2013. Kinetics of coinfection with influenza A virus and *Streptococcus pneumoniae*. *PLoS Pathog.* 9(3):e1003238.
- Smith, H., K. Wiersma, G. Venema and S. Bron. 1985. Transformation in *Bacillus subtilis*: further characterization of a 75,000-dalton protein complex involved in binding and entry of donor DNA. *J Bacteriol.* 164(1):201-6.
- Smith, W., C.H. Andrewes and P.P. Laidlaw. 1933. A virus obtained from influenza patients. *Lancet.* 222: 66-8.

- Snelgrove, R.J., L. Edwards, A.J. Rae and T. Hussell. 2006. An absence of reactive oxygen species improves the resolution of lung influenza infection. *Eur J Immunol.* 36: 1364-73.
- Song, J.Y., M.H. Nahm and M.A. Moseley. 2013. Clinical implications of pneumococcal serotypes: invasive disease potential, clinical presentations, and antibiotic resistance. *J Korean Med Sci.* 28(1):4-15.
- Speshock, J.L., N. Doyon-Reale, R. Rabah, M.N. Neely and P.C. Roberts. 2007. Filamentous influenza A virus infection predisposes mice to fatal septicemia following superinfection with *Streptococcus pneumoniae* serotype 3. *Infect Immun.* 75(6):3102-11.
- Squier, M.K., A.J. Sehnert and J.J. Cohen. 1995. Apoptosis in leukocytes. *J Leukoc Biol.* 57(1):2-10.
- Standish, A.J. and J.N. Weiser. 2009. Human neutrophils kill *Streptococcus pneumoniae* via serine proteases. *J Immunol.* 183(4):2602-9.
- Stenlöf, K., I. Wernstedt, T. Fjällman, V. Wallenius, K. Wallenius and J.O. Jansson. 2003. Interleukin-6 levels in the central nervous system are negatively correlated with fat mass in overweight/obese subjects. *J Clin Endocrinol Metab.* 88(9):4379-83.
- Strissel, K.J., Z. Stancheva, H. Miyoshi, J.W. Perfield II, J. DeFuria, Z. Jick, A.S. Greenberg and M.S. Obin. 2007. Adipocyte death, adipose tissue remodeling, and obesity complications. *Diabetes.* 56: 2910-18.
- Suliman, H.B., L.K. Ryan, L. Bishop and R.J. Folz. 2001. Prevention of influenza-induced lung injury in mice overexpressing extracellular superoxide dismutase. *Am J Physiol Lung Cell Mol Physiol.* 280(1):L69-78.
- Sun, K. and D.W. Metzger. 2008. Inhibition of pulmonary antibacterial defense by interferon-gamma during recovery from influenza infection. *Nat Med.* 14(5):558-64.
- Taubenberger, J.K. and D.M. Morens. 2008. The Pathology of Influenza Virus Infections. *Annu Rev Pathol Mech Dis.* 3:499–522.
- Thammavongsa, V., D.M. Missiakas and O. Schneewind. 2013. *Staphylococcus aureus* degrades neutrophil extracellular traps to promote immune cell death. *Science.* 342(6160):863-6.
- Thatcher, T.H., H.M. Hsiao, E. Pinner, M. Laudon, S.J. Pollock, P.J. Sime and R.P. Phipps. 2013. Neu-164 and Neu-107, two novel antioxidant and anti-myeloperoxidase compounds, inhibit acute cigarette smoke-induced lung inflammation. *Am J Physiol Lung Cell Mol Physiol.* 305(2):L165-74.
- Tkaczyk, J. and M. Vízek. 2007. Oxidative stress in the lung tissue - sources of reactive oxygen species and antioxidant defence. *Prague Med Rep.* 108(2):105-14.
- Tong, S., X. Zhu, Y. Li, M. Shi, J. Zhang, M. Bourgeois, H. Yang, X. Chen, S. Recuenco, J. Gomez, L.M. Chen, A. Johnson, Y. Tao, C. Dreyfus, W. Yu, R. McBride, P.J. Carney, A.T. Gilbert, J. Chang, Z. Guo, C.T. Davis, J.C. Paulson, J. Stevens, C.E. Rupprecht, E.C. Holmes, I.A. Wilson and R.O. Donis. 2013. New world bats harbor diverse influenza A viruses. *PLoS Pathog.* 9(10):e1003657.

- Trayhurn, P. and I. S. Wood. 2004. Adipokines: inflammation and the pleiotropic role of white adipose tissue. *Br J Nutr.* 92(3):347-55.
- Trellakis, S., A. Rydleuskaya, C. Fischer, A. Canbay, S. Tagay, A. Scherag, K. Bruderek, P.J. Schuler and S. Brandau. 2012. Low adiponectin, high levels of apoptosis and increased peripheral blood neutrophil activity in healthy obese subjects. *Obes Facts.* 5(3):305-18.
- Tsukimori, K., K. Fukushima, A. Tsushima and H. Nakano. 2005. Generation of reactive oxygen species by neutrophils and endothelial cell injury in normal and preeclamptic pregnancies. *Hypertension.* 46(4):696-700.
- Tumpey, T.M., A. García-Sastre, J.K. Taubenberger, P. Palese, D.E. Swayne, M.J. Pantin-Jackwood, S. Schultz-Cherry, A. Solórzano, N. Van Rooijen, J.M. Katz and C.F. Basler. 2005. Pathogenicity of influenza viruses with genes from the 1918 pandemic virus: functional roles of alveolar macrophages and neutrophils in limiting virus replication and mortality in mice. *J Virol.* 79(23):14933-44.
- Uchide, N. and H. Toyoda. 2011. Antioxidant therapy as a potential approach to severe influenza-associated complications. *Molecules.* 16(3):2032-52.
- Urban, C.F., D. Ermert, M. Schmid, U. Abu-Abed, C. Goosmann, W. Nacken, V. Brinkmann, P.R. Jungblut and A. Zychlinsky. 2009. Neutrophil extracellular traps contain calprotectin, a cytosolic protein complex involved in host defense against *Candida albicans*. *PLoS Pathog.* 5(10):e1000639.
- van Berlo, D., A. Wessels, A.W. Boots, V. Wilhelmi, A.M. Scherbart, K. Gerloff, F.J. van Schooten, C. Albrecht and R.P. Schins. 2010. Neutrophil-derived ROS contribute to oxidative DNA damage induction by quartz particles. *Free Radic Biol Med.* 49(11):1685-93.
- van der Poll, T., A. Marchant, C.V. Keogh, M. Goldman and S.F. Lowry. 1996. Interleukin-10 impairs host defense in murine pneumococcal pneumonia. *J Infect Dis.* 174(5):994-1000.
- van der Poll, T., C.V. Keogh, X. Guirao, W.A. Buurman, M. Kopf and S.F. Lowry. 1997. Interleukin-6 gene-deficient mice show impaired defense against pneumococcal pneumonia. *J Infect Dis.* 176(2):439-44.
- van der Sluijs, K.F., L.J. van Elden, M. Nijhuis, R. Schuurman, S. Florquin, T. Shimizu, S. Ishii, H.M. Jansen, R. Lutter and T. van der Poll. 2006. Involvement of the platelet-activating factor receptor in host defense against *Streptococcus pneumoniae* during postinfluenza pneumonia. *Am J Physiol Lung Cell Mol Physiol.* 290:L194-L199.
- van der Sluijs, K.F., L.J. van Elden, M. Nijhuis, R. Schuurman, J.M. Pater, S. Florquin, M. Goldman, H.M. Jansen, R. Lutter and T. van der Poll. 2004. IL-10 is an important mediator of the enhanced susceptibility to pneumococcal pneumonia after influenza infection. *J Immunol.* 172(12):7603-9.
- van der Sluijs, K.F., T. van der Poll, R. Lutter, N.P. Juffermans and M.J. Schultz. 2010. Bench-to-bedside review: bacterial pneumonia with influenza - pathogenesis and clinical implications. *Crit Care.* 14(2):219.

- Villanueva, E, S. Yalavarthi, C.C. Berthier, J.B. Hodgins, R. Khandpur, A.M. Lin, C.J. Rubin, W. Zhao, S.H. Olsen, M. Klinker, D. Shealy, M.F. Denny, J. Plumas, L. Chaperot, M. Kretzler, A.T. Bruce and M.J. Kaplan. 2011. Netting neutrophils induce endothelial damage, infiltrate tissues, and expose immunostimulatory molecules in systemic lupus erythematosus. *J Immunol.* 187(1):538-52.
- Vlahos, R. and S. Selemidis. 2014. NADPH oxidases as novel pharmacologic targets against influenza A virus infection. *Mol Pharmacol.* 86(6):747-59.
- Vlahos, R., J. Stambas and S. Selemidis. 2012. Suppressing production of Reactive Oxygen Species (ROS) for influenza A virus therapy. *Trends Pharmacol Sci.* 33(1):3-8.
- Vlahos, R., J. Stambas, S. Bozinovski, B.R. Broughton, G.R. Drummond, S. Selemidis. 2011. Inhibition of Nox2 oxidase activity ameliorates influenza A virus-induced lung inflammation. *PLoS Pathog.* 7(2):e1001271.
- Vlessis, A.A., D. Bartos, P. Muller and D.D. Trunkey. 1995. Role of reactive O₂ in phagocyte-induced hypermetabolism and pulmonary injury. *J Appl Physiol* (1985). 78(1):112-6.
- Wahn, H. and S. Hammerschmidt. 1998. Inhibition of PMN- and HOCl-induced vascular injury in isolated rabbit lungs by acetylsalicylic acid: a possible link between neutrophil-derived oxidative stress and eicosanoid metabolism? *Biochim Biophys Acta.* 1408(1):55-66.
- Walters, K.A., F. D'Agnillo, Z.M. Sheng, J. Kindrachuk, L.M. Schwartzman, R.E. Kuestner, D.S. Chertow, B.T. Golding, J.K. Taubenberger and J.C. Kash. 2015. 1918 pandemic influenza virus and *Streptococcus pneumoniae* co-infection results in activation of coagulation and widespread pulmonary thrombosis in mice and humans. *J Pathol.* doi: 10.1002/path.4638
- Wang, J.P., G.N. Bowen, C. Padden, A. Cerny, R.W. Finberg, P.E. Newburger and E.A. Kurt-Jones. 2008. Toll-like receptor-mediated activation of neutrophils by influenza A virus. *Blood.* 112(5):2028-34.
- Wang, W., Y. Suzuki, T. Tanigaki, D.R. Rank and T.A. Raffin. 1994. Effect of the NADPH oxidase inhibitor apocynin on septic lung injury in guinea pigs. *Am J Respir Crit Care Med.* 150(5 Pt 1):1449-52.
- Wang, Y., Y. Chen, L. Xin, S.M. Beverley, E.D. Carlsen, V. Popov, K.P. Chang, M. Wang and L. Soong. 2011. Differential microbicidal effects of human histone proteins H2A and H2B on *Leishmania* promastigotes and amastigotes. *Infect Immun.* 79(3):1124-33.
- Wang, Y.M., M. Li, S. Stadler, S. Correll, P.X. Li, D.C. Wang, R. Hayama, L. Leonelli, H. Han, S.A. Grigoryev, C.D. Allis and S.A. Coonrod. 2009. Histone hyperacetylation mediates chromatin decondensation and neutrophil extracellular trap formation. *J Cell Biol.* 184(2):205-13.
- Ward, P.A. 2010. Oxidative stress: acute and progressive lung injury. *Ann N Y Acad Sci.* 1203:53-9.

- Wardini, A.B., A.B. Guimarães-Costa, M.T. Nascimento, N.R. Nadaes, M.G. Danelli, C. Mazur, C.F. Benjamim, E.M. Saraiva and L.H. Pinto-da-Silva. 2010. Characterization of neutrophil extracellular traps in cats naturally infected with feline leukemia virus. *J Gen Virol.* 91(Pt 1):259-64.
- Wartha, F., K. Beiter, B. Albiger, J. Fernebro, A. Zychlinsky, S. Normark and B. Henriques-Normark. 2007. Capsule and D-alanylated lipoteichoic acids protect *Streptococcus pneumoniae* against neutrophil extracellular traps. *Cell Microbiol.* 9(5):1162-71.
- Weinberger, D.M., K. Trzciński, Y.J. Lu, D. Bogaert, A. Brandes, J. Galagan, P.W. Anderson, R. Malley and M. Lipsitch. 2009. Pneumococcal capsular polysaccharide structure predicts serotype prevalence. *PLoS Pathog.* 5(6):e1000476.
- Weinberger, D.M., Z.B. Harboe, E.A. Sanders, M. Ndiritu, K.P. Klugman, S. Rückinger, R. Dagan, R. Adegbola, F. Cutts, H.L. Johnson, K.L. O'Brien, J.A. Scott and M. Lipsitch. 2010. Association of serotype with risk of death due to pneumococcal pneumonia: a meta-analysis. *Clin Infect Dis.* 51(6):692-9.
- Weiser, J.N., D. Bae, H. Epino, S.B. Gordon, M. Kapoor, L.A. Zenewicz and M. Shchepetov. 2001. Changes in availability of oxygen accentuate differences in capsular polysaccharide expression by phenotypic variants and clinical isolates of *Streptococcus pneumoniae*. *Infect Immun.* 69(9):5430-9.
- Wellen, K.E. and G.S. Hotamisligil. 2005. Inflammation, stress, and diabetes. *J Clin Invest.* 115(5):1111-9.
- White, M.R., T. Tecle, E.C. Crouch and K.L. Hartshorn. 2007. Impact of neutrophils on antiviral activity of human bronchoalveolar lavage fluid. *Am J Physiol Lung Cell Mol Physiol.* 293(5):L1293-9.
- Wiesner, J. and A. Vilcinskas. 2010. Antimicrobial peptides: the ancient arm of the human immune system. *Virulence.* 1(5):440-64.
- Witzenrath, M., F. Pache, D. Lorenz, U. Koppe, B. Gutbier, C. Tabeling, K. Reppe, K. Meixenberger, A. Dorhoi, J. Ma, A. Holmes, G. Trendelenburg, M.M. Heimesaat, S. Bereswill, M. van der Linden, J. Tschopp, T.J. Mitchell, N. Suttorp and B. Opitz. 2011. The NLRP3 inflammasome is differentially activated by pneumolysin variants and contributes to host defense in pneumococcal pneumonia. *J Immunol.* 187(1):434-40.
- Xu, J., X. Zhang, R. Pelayo, M. Monestier, C.T. Ammollo, F. Semeraro, F.B. Taylor, N.L. Esmon, F. Lupu and C.T. Esmon. 2009. Extracellular histones are major mediators of death in sepsis. *Nat Med.* 15(11):1318-21.
- Yamada, Y., G.V. Limmon, D. Zheng, N. Li, L. Li, L. Yin, V.T. Chow, J. Chen and B.P. Engelward. 2012. Major shifts in the spatio-temporal distribution of lung antioxidant enzymes during influenza pneumonia. *PLoS ONE.* 7(2):e31494.
- Ye, S., S. Lowther and J. Stambas. 2015. Inhibition of reactive oxygen species production ameliorates inflammation induced by influenza A viruses via upregulation of SOCS1 and SOCS3. *J Virol.* 89(5):2672-83.

Yipp, B.G., B. Petri, D. Salina, C.N. Jenne, B.N. Scott, L.D. Zbytnuik, K. Pittman, M. Asaduzzaman, K. Wu, H.C. Meijndert, S.E. Malawista, A. de Boisleury Chevance, K. Zhang, J. Conly and P. Kubes. 2012. Infection-induced NETosis is a dynamic process involving neutrophil multitasking *in vivo*. *Nat Med*. 18(9):1386-93.

Yoshida, K., T. Matsumoto, K. Tateda, K. Uchida, S. Tsujimoto and K. Yamaguchi. 2001. Induction of interleukin-10 and down-regulation of cytokine production by *Klebsiella pneumoniae* capsule in mice with pulmonary infection. *J Med Microbiol*. 50(5):456-61.

Yost, C.C., M.J. Cody, E.S. Harris, N.L. Thornton, A.M. McInturff, M.L. Martinez, N.B. Chandler, C.K. Rodesch, K.H. Albertine, C.A. Petti, A.S. Weyrich and G.A. Zimmerman. 2009. Impaired neutrophil extracellular trap (NET) formation: a novel innate immune deficiency of human neonates. *Blood*. 113(25):6419-27.

Young, R.L., K.C. Malcolm, J.E. Kret, S.M. Caceres, K.R. PochR, D.P. Nichols, J.L. Taylor-Cousar, M.T. Saavedra, S.H. Randell, M.L. Vasil, J.L. Burns, S.M. Moskowitz and J.A. Nick. 2011. Neutrophil extracellular trap (NET)-mediated killing of *Pseudomonas aeruginosa*: evidence of acquired resistance within the CF airway, independent of CFTR. *PLoS ONE*. 6(9):e23637.

Yousefi, S, C. Mihalache, E. Kozlowski, I. Schmid and H.U. Simon. 2009. Viable neutrophils release mitochondrial DNA to form neutrophil extracellular traps. *Cell Death Differ*. 16(11):1438-44.

Zhang, A.J., K.K. To, C. Li, C.C. Lau, V.K. Poon, C.C. Chan, B.J. Zheng, I.F. Hung, K.S. Lam, A. Xu and K.Y. Yuen. 2013. Leptin mediates the pathogenesis of severe 2009 pandemic influenza A(H1N1) infection associated with cytokine dysregulation in mice with diet-induced obesity. *J Infect Dis*. 207(8):1270-80.

Zheng, W. and Y.J. Tao. 2013. Structure and assembly of the influenza A virus ribonucleoprotein complex. *FEBS Lett*. 587(8):1206-14.

Zhu, L., Z. Kuang, B.A. Wilson and G.W. Lau. 2013. Competence-Independent Activity of Pneumococcal EndA Mediates Degradation of Extracellular DNA and NETs and is Important for Virulence. *PLoS ONE*. 8(7): e70363.

8.2 Web references

1. Types of Influenza Viruses. Centers for Disease Control and Prevention. <http://www.cdc.gov/flu/about/viruses/types.htm>.
2. Selecting Viruses for the Seasonal Influenza Vaccine. Centers for Disease Control and Prevention. <http://www.cdc.gov/flu/about/season/vaccine-selection.htm>.
3. Pandemic Influenza Risk Management WHO Interim Guidance. World health Organization. June 2013. http://www.who.int/influenza/preparedness/pandemic/influenza_risk_management/en/.

4. Current WHO phase of pandemic alert for Pandemic (H1N1). World health Organization. 2009. <http://www.who.int/csr/disease/swineflu/phase/en/>.
5. U.S. Department of Health & Human Services. <http://www.flu.gov/pandemic/history/> flu.gov.
6. What You Should Know About Flu Antiviral Drugs. Centers for Disease Control and Prevention. <http://www.cdc.gov/flu/antivirals/whatyoushould.htm>.
7. Global Influenza Surveillance and Response System. World Health Organization. 2015. www.who.int/flunet.
8. Cox, C.M. and R. Link-Gelles. Centers for Disease Control and Prevention. <http://www.cdc.gov/vaccines/pubs/surv-manual/chpt11-pneumo.html>.
9. WEEKLY EPIDEMIOLOGICAL RECORD. World Health Organization, Geneva. April 2012. No. 14, 87, 129–144. <http://www.who.int/wer>.
10. Kenneth Todar. Todar's Online textbook of bacteriology. <http://textbookofbacteriology.net/S.pneumoniae.html>.
11. World health Organization. January 2015. Obesity and overweight: Fact sheet N°311. <http://www.who.int/mediacentre/factsheets/fs311/en/>.
12. Office of the Surgeon General (US); 2001 The Surgeon General's Call To Action To Prevent and Decrease Overweight and Obesity Office of the Surgeon General (US); Office of Disease Prevention and Health Promotion (US); Centers for Disease Control and Prevention (US); National Institutes of Health (US). Rockville (MD).